5-1-2009

The role of metnase in DNA replication fork stress response and DNA damage

Leyma De Haro

Leyma Pérez De Haro
Candidate

Biomedical Sciences
Department

This dissertation is approved, and it is acceptable in quality and form for publication:

Approved by the Dissertation Committee:

, Chairperson

Mary Ann Ostey

Elizabeth Williamson

THE ROLE OF METNASE IN DNA REPLICATION FORK STRESS RESPONSE AND DNA REPAIR

BY

LEYMA PÉREZ DE HARO

B.S., Biochemistry, California State University, Los Angeles
2004

DISSERTATION

Submitted in Partial Fulfillment of the
Requirements for the Degree of

Doctor of Philosophy

Biomedical Sciences

The University of New Mexico
Albuquerque, New Mexico

May 2010

DEDICATION

To my husband Sergio with all my love.

ACKNOWLEDGEMENTS

I would like to thank my mentors Dr. Jac Nickoloff and Dr. Robert Hromas for all your help and guidance throughout this process. Your lessons have been very valuable in shaping my career. I would like to thank my dissertation committee, Dr. Mary Ann Osley, Dr. Bryce Chackeryan, Dr. Laurie Hudson, and Dr. Elizabeth Williamson, for your help and support through the years. You have all been wonderful and I appreciate your time and help. I would also like to thank our collaborators: Dr. Amanda Quijas for helping me learn the DNA fiber assay; Dr. Neil Osheroff and Dr. Suk-Hee Lee provided us with valuable reagents. Dr. Justin Wray, Dr. Steven Durant, and Lori Corwin, along with Dr. Elizabeth Williamson, are co-authors in the work I present here. Dr. Toyoko Tsukuda helped me set up the Ad-ISce-I adenovirus system. I would like to thank the members of the Jac Nickoloff and Robert Hromas laboratories for their help, support, and friendship, especially Rosa Sterk and Cheryl Miller for being wonderful technicians and friends.

My dear friends and family helped me through this process, without them, I would not have completed this work. My friends Victor and June Lopez, Wally and Kathy Henderson, and John and Diane Bode, have been my guardian angels. My friends Dr. Isabelle Vergne, Dr. Sharon Master, Drs. Muhammad and Sheema Mir, Dr. Pam Hall, Dr. Monica Delgado-Vargas, Michal Mudd, Jennifer Buntz, Dr. Yuehan (Grace) Wu, and Lisa Dillon have been a great source of support over the years. My parents Leonel Pérez, Maritza Díaz, my sister Maylen, and my tìas Maria and Mariela have believed in my potential and cheered me on always, I love you. I have three loved ones that passed on and were not able to see me finish my Ph.D. my dearest grandmother Abuela Caridad (mi Tata), my cousin Danilo, and my dearest friend Edwin Baca. I miss you all.

Finally, I would like to thank all my teachers, mentors, and friends that have helped me and supported me through my life. I hope I make all of you proud.

THE ROLE OF METNASE IN DNA REPLICATION FORK STRESS RESPONSE AND DNA REPAIR

BY

LEYMA PÉREZ DE HARO

ABSTRACT OF DISSERTATION

Submitted in Partial Fulfillment of the
Requirements for the Degree of

Doctor of Philosophy

Biomedical Sciences

The University of New Mexico
Albuquerque, New Mexico

May 2010

THE ROLE OF METNASE IN DNA REPLICATION FORK STRESS RESPONSE AND DNA REPAIR

Leyma Pérez De Haro

B.S., Biochemistry, California State University, Los Angeles, 2004

ABSTRACT

Metnase is a recently evolved human protein with methylase (SET) and nuclease domains that is widely expressed, especially in proliferating tissues. Metnase promotes plasmid and viral DNA integration, and through an interaction with topoisomerase IIα (TopoIIα) it promotes chromosome decatenation. Metnase interacts with DNA ligase IV, promotes non-homologous end-joining (NHEJ), and repression causes mild hypersensitivity to ionizing radiation. TopoIIα has a proposed role in relaxing positive supercoils in front of replication forks. NHEJ factors have been implicated in the replication stress response. Here we show that Metnase promotes cell proliferation, but does not affect replication fork elongation as measured by cell cycle analysis, BrdU incorporation and DNA fiber analysis. Even though there is no elongation effect, Metnase confers resistance to three replication stress agents, hydroxyurea, UV light, and the topoisomerase I inhibitor, camptothecin. Metnase expression also increases the rate at which H2AX phosphorylation (a marker of stalled or collapsed replication forks) is resolved. There was no difference in formation of gamma-H2AX foci after exposure to these agents. Metnase co-immunoprecipitates (co-IP) with proliferating cell nuclear antigen (PCNA) and

RAD9. Finally, we show that Metnase promotes TopoIIα-mediated relaxation of positively supercoiled DNA, similar to the torsional strain preceding replication forks. These results establish Metnase as an important component of the human replication stress response.

Table of Contents

List of Figures

List of Abbreviations

DSB-double-strand break

DSE-double-stranded end

ssDNA-single stranded DNA

dsDNA-double stranded DNA

HR-homologous recombination

NHEJ-non-homologous end-joining

TopoIIα- Topoisomerase IIα

HU-hydroxyurea

CPT-camptothecin

UV-B-ultraviolet light

HJ-Holliday Junction

PCNA-proliferating cell nuclear antigen

IdU-Iododeoxyuridine

CldU-chlorodeoxyuridine

TLS-translesion synthesis

ATM-Ataxia Telangiectasia mutated

ATR-Ataxia Telangiectasia related

γ-H2AX-phosphorylated histone H2AX

NLS-nuclear localization signal

List of Tables

1. INTRODUCTION

1.1. Cancer epidemiology

Cancer is an important public health concern in the United States, where one out of every four deaths is due to cancer [1-5]. It has been estimated that during 2009 there will be approximately 1.5 million new cancer cases diagnosed, and about 560,000 deaths due to cancer. Recently, the incidence of cancer has decreased at a yearly rate of 1.8% in males and 0.6% in females. This is largely attributed to better screening for the three major sites of cancer in men (lung, prostate, and colorectal) and the two major sites in women (breast and colorectal). However, the probability of a person being diagnosed with cancer in a lifetime is 44% for men and 37% for women [1]. Additionally, cancer is the second leading cause of all deaths in children 1-14 years of age (as of 2006), with acute lymphoblastic leukemia (ALL) being the most common type. However, the five year cancer survival rates have increased from 58% in 1977 to 80% in 2004 in children, and in adults the survival rate is ~90% for some types of cancers, with many exceptions such as pancreatic cancer, some forms of brain tumors, and advanced stages of metastatic cancer [1]. Although there have been many improvements in cancer detection, diagnosis, treatment, and survival over the past few decades. Cancer is nevertheless the second leading cause of all deaths in the US (as of 2006) [1, 6]. Therefore, the study of the molecular basis of cancer is important, and the understanding of the events leading up to the transformation of a normal cell into a cancerous one, imperative.

1.2. Genomic instability and cancer

In 1890, David von Hansemann postulated that aberrant mitotic events were responsible for the abnormal chromosomal content found in cancer cells [7]. In 1914, Theodor Boveri explored this hypothesis in sea urchin eggs, and demonstrated that aberrant mitosis led to unequal distributions of chromosomes, which he postulated would lead to malignant cells with the ability of “unlimited growth”, and that these malignant cells could pass on this information to the next generation of daughter cells [7]. Additionally, Boveri accurately predicted the existence of cell-cycle checkpoints, oncogenes, and tumor suppressor genes. He envisioned that “poisons”, such as radiation and nicotine, could affect mitosis and create chromosomal imbalances in cells [7]. These two scientists formulated the idea that cancer is a genetic disease. Later, work by Schimke provided the first evidence that cancer cells amplified drug resistance genes, and that treatment made cells genetically unstable [8]. Thus, the link between genomic instability and cancer has been established.

1.3. DNA repair

Boveri initiated the idea that cancer can arise from defects in DNA repair mechanisms that protect cells from damage [9]. In seminal work, Alfred Knudson postulated that retinoblastoma arises from two genetic mutations in each allele of the retinoblastoma (Rb) gene [10]. Nordling had concluded earlier that seven mutations fit the range of most cancers [11]. Nordling’s observation still holds today. Importantly, genes associated with cancer such as p53 and Rb were

shown either to be regulated by, or to regulate the cell cycle, and it was demonstrated that p53 is a moderator of the DNA-damage checkpoint [12-16]. Finally, in the 1990s, a clear link was established between several DNA repair pathways, such as nucleotide excision repair (NER), mismatch repair (MMR), and homologous recombination (HR) proteins, and cancer pre-disposition disorders, such as xeroderma pigmentosum (XP), hereditary non-polyposis colon cancer (HNPCC), and familial breast cancer, respectively [9]. This work exploded with the discovery of many more factors involved in DNA repair, cell cycle regulation, and DNA replication, many of which are linked to cancer development or cancer predisposition disorders.

This dissertation focuses specifically on the study of a protein involved in the repair of DNA double-strand breaks, processing of DNA double-strand ends (DSEs), and re-starting stopped or collapsed DNA replication forks. The proper function of DNA repair pathways is necessary for cell viability and for prevention of transformation into cancer. Here are described studies of Metnase, a DNA repair protein with important roles in non-homologous end-joining, DNA integration, and chromosomal decatenation, and its novel role in DNA replication in response to stress. Additionally, two novel interactions between Metnase and the DNA replication proteins, PCNA and Rad9, are identified. This work demonstrates that Metnase is a key component in pathways important for genomic instability.

2. BACKGROUND

2.1. DNA damage

DNA double-strand breaks (DSBs) and DNA double-stranded ends (DSEs) can be seriously damaging to cells, affecting their viability and genome stability. DSBs and DSEs are normally generated during DNA replication, when a replication fork encounters DNA blocking lesions. These lesions are produced by metabolic byproducts of cellular respiration (reactive oxygen species; ROS) which could lead to fork collapse [17]. They can also occur during programmed genome rearrangements induced by nucleases, including yeast mating-type switching [18], V(D)J recombination [19], class-switch recombination [20], and meiosis [21]; and from physical stress when catenated chromosomes are pulled to opposite poles during mitosis [22]. DSBs are also produced when cells are exposed to exogenous DNA damaging agents such as ionizing radiation (IR), which creates DSBs both by direct energy absorption, and indirectly via production of ROS [23]; chemical agents and ultraviolet (UV) light that create replication blocking lesions (alkyl adducts, pyrimidine dimmers, and crosslinks) [24, 25]; and cancer chemotherapeutics that poison topoisomerase I and II, which produce replication-blocking lesions, or which trap the enzyme-DNA complex after DSB induction and can potentially produce DSBs during any phase of the cell cycle [26]. Misrepair, or the failure to repair DSBs, can result in cell death or large-scale chromosome changes that are hallmarks of cancer cells, including deletions, translocations, and chromosome fusions that enhance genome instability. Cells have evolved groups of proteins that function in

signaling networks that sense DSBs or other DNA damage, arrest the cell cycle, and activate DNA repair pathways. These cellular responses can occur at various stages of the cell cycle and are collectively called DNA damage checkpoints. However, when cells suffer damage beyond their ability to repair, signaling pathways can trigger apoptosis and prevent the propagation of cells with highly unstable genomes [27].

2.2. Sources of endogenous double-strand breaks

DSBs arise spontaneously during normal DNA metabolism, including DNA replication and repair, and during programmed genome rearrangements, such as immune cell V(D)J recombination. Many DNA lesions block DNA polymerase, causing replication fork stalling. Stalled forks are stabilized by many factors including the checkpoint kinases ATM and ATR, the DNA repair protein BLM, and the multifunctional single-strand DNA binding protein RPA [28]. In addition, Topoisomerase IIα (TopoIIα) creates DSBs as part of its normal function, and passes double-stranded DNA through the break, decatenating tangled chromosomes before mitosis. If decatenation fails, DSBs may form when catenated chromosomes are pulled toward opposite spindle poles [29]. Endogenous DSBs are also formed during lymphoid development, in B-cells, where V(D)J recombination is initiated by specific DSBs introduced into recombination signal sequences (RSS) sequences by the RAG1/2 endonucleases; these DSBs are subsequently repaired by an error-prone, NHEJ-mediated deletion mechanism that creates novel V(D)J junctions in

antibody coding sequences, a process that is instrumental in generating antibody diversity in mammals [30].

2.3. Sources of exogenous DNA double-strand breaks

DSBs are produced by a wide variety of exogenous DNA damaging agents. Ionizing radiation (IR), including X-rays, γ-rays, β-particles, and α particles, can cause many types of DNA damage. The vast majority of the cytotoxicity associated with IR is due to DSBs. DSBs can also be caused by radiomimetic drugs such as the TopoIIα inhibitors etoposide and adriamycin. TopoIIα is inhibited by the anthracyclines and etoposide, all of which are used in cancer chemotherapy [31]. Topo-II inhibitors induce ATM Ser-1981 phosphorylation and phosphorylation of histone H2AX (γH2AX), both hallmarks of DSB damage [32]. Tobacco smoke is a known carcinogen that induces mutations and DSBs [33]; this damage is mediated through free radicals and is dose dependent [34]. Thus, cells experience many DSBs daily, coming from external and internal sources, which require the proper sensing and repair in order to avoid cell death or genomic instability leading to cancer.

2.4. Syndromes resulting from deficient DNA repair

A key link between DNA repair defects and cancer is the existence of syndromes that have been linked to numerous DNA repair proteins. In humans, mutations in the proteins responsible for DSB repair generate syndromes resulting in a predisposition to cancers, mental retardation and

neurodegenerative disorders. The syndromes identified so far are: Bloom's Syndrome (BLM protein), Werner's Syndrome (WRN protein), Ataxia-Telangiectasia (ATM protein), Seckel syndrome (ATR protein), Cockayne syndrome (CSA and CSB proteins), Li-Fraumeni syndrome (p53 protein), hereditary non-polyposis colon cancer (mismatch repair proteins), Nijmegen Breakage Syndrome (Nbs1 protein), inherited breast cancer (BRCA1 and 2 proteins), Fanconi's Anemia (FA proteins), and Ligase IV syndrome which results in cancer predisposition in people deficient in the proteins Artemis and LigIV (see Table 2-1 for references).

Bloom's Syndrome results from mutations in genes that code for a protein homologous to the E. coli RecQ 3'-5' helicase [38]. This syndrome is a rare autosomal recessive disorder characterized by telangiectases and photosensitivity, growth deficiency, variable degrees of immunodeficiency, and cancer predisposition [39]. Bloom's Syndrome cells in culture are markedly sensitive to HU and UV, but not IR [40, 41]. These studies firmly implicate the Bloom's syndrome protein BLM in replication-associated DSB repair. BLM has recently been demonstrated to play a role in the processing of Holliday Junctions (HJ) resulting from stalled and collapsed replication forks. It has been proposed that BLM associates with Topoisomerase III and functions as a Holiday Junction (HJ) resolvase [42, 43].

Mutations that cause Werner's syndrome occur in the protein WRN, another RecQ family helicase that also possesses an ATP dependent 3'-5' exonuclease motif [44-47]. WRN has the ability to branch migrate HJs during HR

and it has been shown to be important in telomere maintenance and cellular senescence [48].

Ataxia-Telangiectasia has been shown to be the result of mutations in a specific gene named AT-Mutated (ATM). AT is a rare disorder where patients suffer from neurodegeneration, immunodeficiency, and cancer predisposition. ATM is a serine/threonine kinase activated by DNA DSBs [35]. In undamaged cells it is a homo-dimmer which undergoes autophosphorylation in the presence of DNA DSBs [36]. Once phosphorylated on serine 1981, ATM is activated and phosphorylates a number of important DNA repair factors including p53, Chk2, BRCA1, RPAp34, H2AX, SMC1, FANCD2, RAD17, Artemis and Nbs1 [35]. ATM functions as an upstream regulator of both NHEJ and HR [37].

Nijmegen Breakage Syndrome (NBS) is an autosomal recessive disorder known to result from mutations in the protein named Nbs1. Nbs1 is part of a heterotrimeric protein complex consisting of Mre11, Rad50 and Nbs1 (MRN), which is conserved from yeast to mammals and functions in the identification and signaling of DNA DSBs [49]. The MRN complex is important in the activation of ATM, ATR, and the initiation of a proper DSB induced cellular response.

Fanconi's Anemia (FA) is an inherited syndrome where patients display bone marrow failure, developmental abnormalities, and a severe predisposition to cancer. FA consists of 13 complementation groups (FANCA, B, C, D1, D2, E, F, G, I, J, L, and M) each of which represent a specific gene that has been mutated or deleted [50]. FA cells are extremely sensitive to DNA crosslinking

drugs such as MMC and show altered phenotypes comprising abnormal cell cycle regulation (extended G_2), hypersensitivity to oxygen, increased apoptosis, and accelerated telomere shortening [51]. All known FA proteins have functions in DNA repair pathways that are involved in the re-start of stalled replication forks. The majority of these protein products have been shown to form a complex that functions as the E3 specificity enzyme in mono-ubiquitination of FANCD2. Ubiquitinated FANCD2 performs multiple tasks including the recruitment of BRCA2, enhancement of HR, and possibly the promotion of translesion DNA synthesis [52].

Table 2-1. Summary of DNA repair syndromes and the proteins affected.

Condition	Protein	Function	Reference
Familial breast cancer	BRCA1	Involved in HR and NHEJ	[53-55]
Familial breast cancer and Fanconi's anemia	BRCA2	Involved in HR, helps load Rad51	[56-61]
Li-Fraumeni syndrome	p53	Associates with XRCC1	[62, 63]
Li-Fraumeni syndrome	Chk2	Phosphorylated by ATM, activates downstream factors involved in DSB repair	[63-67]
Ataxia Telangiectasia (AT)	ATM	Member of the PI3K family, activates Chk2 and is involved in the DNA DSB response	[68-70]
Seckel Syndrome (SCLK)	ATR	Member of the PI3K family, activates Chk1 and is involved in the DNA replication stress response and the DNA DSB response	[71, 72]
Nijmegen breakage syndrome (NBS)	Nbs1	Member of the MRN complex, involved in sensing DBS and recruiting repair proteins to the break site	[73, 74]
Werner Syndrome	WRN	ATP dependent exonuclease, important for HR and telomere maintenance	[48, 75-90]
Bloom's Syndrome	BLM	Important for repair of stalled or collapsed replication forks and Holiday Junction (HJ) resolution	[42, 43, 91-99]
Fanconi's Anemia	FANC A, B, C, D1 & 2, E, F, G, I, J, L, M	Involved in DNA repair and re-start of stalled replication forks	[100-110]

2.5. DNA double-strand break damage repair in eukaryotic cells

Eukaryotic cells repair DSBs by two mechanisms: homologous recombination (HR) and non-homologous end-joining (NHEJ). Both pathways are able to repair frank DSBs, such as those produced by nucleases and IR. DSBs produced by replication fork collapse are repaired primarily by HR [111, 112]; however there is an emerging body of literature that points to NHEJ also having a role in this repair (discussed in more detail later). Fork collapse produces a one-ended DSB, better described as a “double-strand end” (DSE). Because a DSE at a collapsed fork has no second end with which to rejoin, it has been difficult to imagine how NHEJ can contribute to the repair of collapsed replication forks, although this does not rule out indirect roles for NHEJ proteins in replication fork restart. For a detailed review of the control of pathway choice between HR and NHEJ (see Appendix 6.1) [37].

2.5.1. DNA damage and replication

DNA replication is a process that makes cells particularly vulnerable to DNA damage because many DNA lesions cause replication forks to stall. Cellular responses to replication stress are extremely important in cancer therapy, as a number of chemotherapeutic drugs target DNA metabolism and cause replication stress, including topoisomerase poisons camptothecin (CPT) and hydroxyurea (HU). Cells deal with stalled replication forks in several ways: 1) single-stranded DNA (ssDNA) bound by RPA accumulates at stalled forks and is a major signal for downstream events including fork repair and checkpoint

activation (Table 2-2). 2) The replisome at stalled forks is stabilized by proteins that function in DNA repair and the DNA damage checkpoint response, including RPA, ATR-ATRIP, ATM, TOPBP1, Claspin, 9-1-1 complex, and MDC1 [113-116]; the action of these proteins may preserve the fork structure while the damage is repaired, allowing replication to resume. 3) Alternatively, error-prone translesion synthesis (TLS) polymerases are recruited to monoubiquitinated proliferating cell nuclear antigen (PCNA), allowing lesion bypass in a damage tolerance pathway [117, 118].

Table 2-2. List of all three PIK kinases involved in the repair of DNA DSBs and DNA replication fork damage.

Modified from [119].

Kinase	Target	Activator	Post-translational modification regulation
ATM	Nbs1	Mre11/Rad50 and DNA ends	Phosphorylation
ATR	ATRIP	TOPBP1 and DNA damage	Phosphorylation
DNA-PKcs	Ku70/80	Ku70/80 and DNA ends	Phosphorylation

Type I and type II topoisomerases are very important for normal DNA replication. Topoisomerase I (type I) plays a major role in relaxing positive supercoils produced in front of replication forks during duplex DNA unwinding by the replicative helicase. Topoisomerase IIα (TopoIIα), a type II topoisomerase that has roles in chromosome condensation and decatenation, is present in the replisome, and it has been proposed that it also relaxes positive supercoils ahead of replication forks [120-122]. Although it is known that topoisomerase poisons cause replication stress, specific roles for topoisomerases in response to replication stress have not been defined.

If stalled forks are not restarted in a timely manner, they may be converted to unusual DNA structures and collapse, creating a DSE (see Figure 2-1). Certain types of damage, such as single-strand breaks, may cause direct fork collapse to DSEs. As with double-strand breaks, the checkpoint kinases ATM and ATR are recruited to DSEs and activated, leading to histone H2AX phosphorylation (γ-H2AX) in the vicinity of DSEs [123]. This chromatin modification is important for fork repair and checkpoint activation, and once collapsed forks are repaired, γ-H2AX is replaced by unmodified H2AX [30, 124, 125]. Homologous recombination (HR), involving RAD51-mediated strand invasion, plays a major role in restarting stalled and collapsed forks [115]. NHEJ factors also play a role in cell survival after replication stress [126] (Figure 2-1).

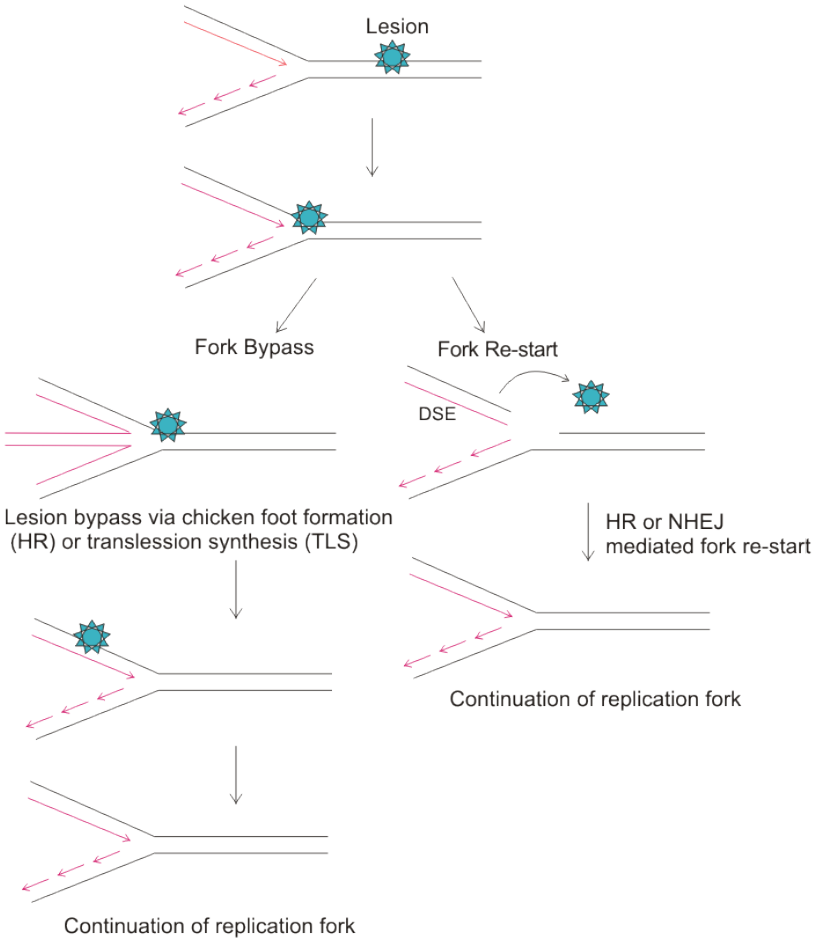

Figure 2-1. Replication fork re-start.

When a replication fork encounters a single stranded lesion cells may take two routes to resolve the problem. The lesion may be bypassed via Chicken foot formation or error-prone translesion synthesis (TLS). Alternatively, the lesion may become a double stranded end (DSE) and be resolved via HR. Although HR is currently believed to be the major repair mechanism for DSEs, there is new evidence suggesting that NHEJ factors may also contribute to this repair. Whether the HR and the NHEJ pathways are mutually exclusive or overlapping remains to be elucidated.

Replication stress activates the intra-S checkpoint, which delays the rate of replication fork progression in order to allow time for DNA repair [115]. ssDNA-RPA at stalled forks is bound by ATRIP leading to activation of its obligate binding partner ATR. ATR activation depends on RAD17 (plus Rfc2-5) loading of the RAD9-HUS1-RAD1 complex (9-1-1; a scaffold and processivity factor structurally related to PCNA) through a RAD9-RPA interaction. RAD9 recruits TopBP1, an essential factor for ATR activation. ATR phosphorylates RAD17, which recruits Claspin to be phosphorylated by ATR, and phosphorylated RAD17-Claspin promotes ATR phosphorylation/activation of Chk1 kinase, which phosphorylates proteins that stabilize the stalled fork and prevent late origin firing (Figures 2-2 and 2-3)

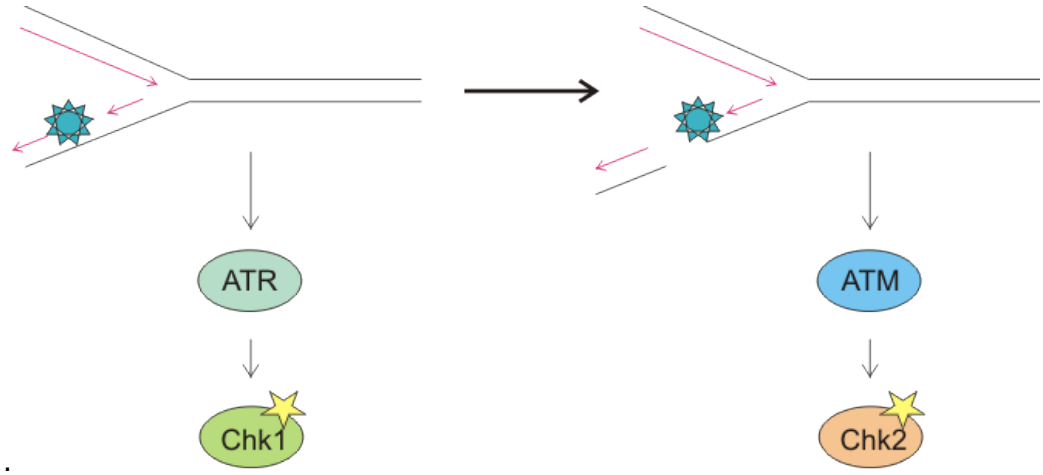

Figure 2-2. Lesions that activate ATM and ATR at a replication fork.

A stalled replication fork activates ATR kinase, which then phosphorylates and activates Chk1. However, nucleases present at the stalled fork can cleave the DNA or the fork can collapse to a DSE. When this happens ATM kinase is activated, and it activates the downstream substrate Chk2 via phosphorylation. Both Chk1 and Chk2 play important roles in activating the cell cycle checkpoints and recruiting DNA repair factors to the stalled/collapsed fork. Modified from [119], star=phosphorylation.

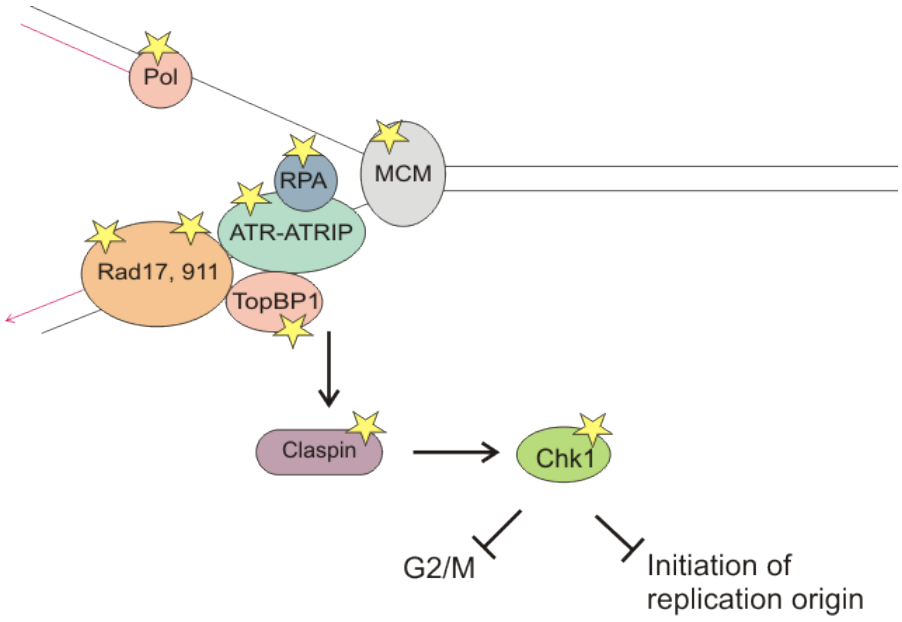

Figure 2-3. ATR mediated activation of cell cycle checkpoint and DNA repair machinery in response to DNA replication fork damage.

When a replication fork encounters DNA damage, the PIK kinase ATR is activated, and it phosphorylates Chk1. Chk1 phosphorylation activates its kinase activity, which then phosphorylates other downstream substrates that negatively regulate cell cycle and DNA replication origin firing. Adapted from [119], star=phosphorylation.

2.5.2. Role of HR in replication fork damage repair

Homologous recombination (HR) is the main repair pathway cells use to repair replication fork damage. Usually a homologous sequence is required to make a copy of damaged DNA; thus making this process more accurate than NHEJ. The proteins involved in HR are Rad51 and its five paralogs (Rad51B, Rad51C, Rad51D, XRCC2, and XRCC3), Rad52, Rad54, BRCA1 and 2, BLM, WRN. Rad51 is the essential protein in this pathway and its absence results in cell and embryonic lethality in mice [127]; which explains why there is no Rad51 cancer defect. However, defects in other HR proteins result in cancer predisposition disorders and premature aging (see Table 2-1). BRCA1 and BRCA2 mutations are particularly severe and result in familial breast cancer, with approximately 60-85% chance of developing breast or ovarian cancer in patients with the mutated proteins. A model of HR is depicted in figure 2-4, a structure similar to those presented in figure 2-1 can be resolved by the Rasd51 coating of the DSE and subsequent invasion of a near-by homologous sequence on the sister chromatid.

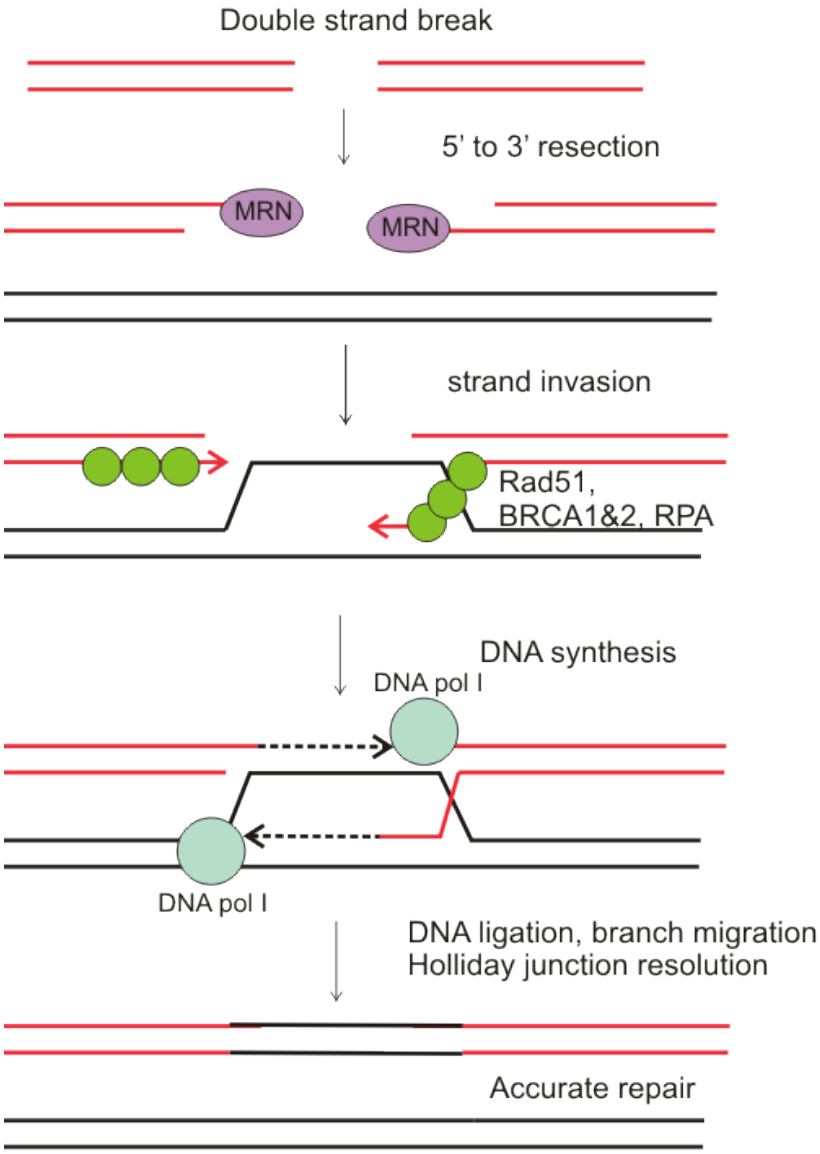

Figure 2-4. Homologous recombination repair of DSBs.

A DSB caused by radiation or other sources mentioned in the text, is recognized by the MRN complex, which regulates end resection from a 5' to 3' direction. This yields a single stranded DNA (ssDNA) section, which is bound by RPA. Subsequently, Rad51 is loaded onto the ssDNA with the help of BRCA2, producing a RAD51-ssDNA nucleoprotein filament that is able to search for

homologous sequences elsewhere in the genome and catalyze strand invasion, producing intermediates termed Holliday junctions. The invading strand can be extended by new DNA synthesis using as a template the sister chromatid (shown here in black). Finally, Holliday Junctions are resolved by helicases, nucleases, and/or topoisomerases, resulting in mature products, and repair of the DSB.

2.5.3. Role of NHEJ in replication fork damage repair

NHEJ is one of two DNA DSB repair pathways in mammalian cells. It is the major repair pathway and plays a role throughout the cell cycle, but is especially important during G_1 phase when sister chromatids are not available to serve as HR repair templates. NHEJ repair factors are recruited to the DSB site though the MRN, complex and in the classical (C-NHEJ) pathway. The Ku70/80 complex binds the free DNA ends, translocates away from broken ends, and this permits DNA-PKcs to contact the DNA end, which then activates the serine/threonine kinase activity of DNA-PKcs. This activation of the kinase permits DNA-PKcs to autophosphorylate and causes a conformational change in DNA-PKcs that enhances access by other NHEJ proteins [128]. Subsequently XRCC4/LigIV ligates the two ends (Figure 2-5). Alternatively, PARP-1 has been shown to compete with Ku for DNA ends and is thought to play a role in alternative, or non-classical, NHEJ (A-NHEJ) pathway [129]. Other proteins such as BLM are also thought to play a role in A-NHEJ during V(D)J recombination, and Ligase3/XRCC1 have been shown to catalyze the ligation reaction in that case, even though the other classical NHEJ factors may also be present [128]. It is possible that the NHEJ pathway functions with much flexibility, so that different factors are recruited depending on the cell cycle stage, cell type (or tissue), or type of end. This would explain the observations stated above since some NHEJ factors would be able to bind certain types of ends, while under different conditions factor recruitment may differ.

NHEJ factors been recently implicated in the repair of replication fork damage. DNA-PK has been shown to be important in the repair of replication fork damage, since cells lacking DNA-PK and treated with replication fork stress had delayed replication [130]. In fission yeast it has been shown that Ku is important in stalled replication forks and that this function is independent of its NHEJ function [131]. A recently identified NHEJ gene, Cernunos/XLF, a gene mutated in patients with microcephaly, has also been shown to be important in replication. Cells lacking Cernunos and exposed to replication stress accumulate in G_2/M and have chromosomal instability. Importantly for this work are the recent findings linking PARP-1, a protein believed to play a role in alternative NHEJ, to replication fork progression. The Helleday laboratory used a DNA fiber assay to show that cells lacking PARP-1 were unable to restart ongoing replication forks, as compared to the control cells [132]. Additionally, the same study showed that PARP-1 co-localized to replication fork-specific foci (labeled with BrdU). Furthermore, they showed direct binding of PARP-1 to stalled replication forks, thus identifying PARP-1 as an important factor in resolving stalled forks. Helleday speculates that PARP-1's function at stalled forks is to stimulate HR repair. Alternatively, it could recruit A-NHEJ components to resolve DSEs at collapsed forks.

Metnase is a novel NHEJ factor that interacts with XRCC4/LigIV and stimulates the efficiency and accuracy of NHEJ (described in more detail later). This dissertation presents evidence that Metnase also plays a role in replication

fork re-start; thus placing it in the same category as the proteins mentioned above.

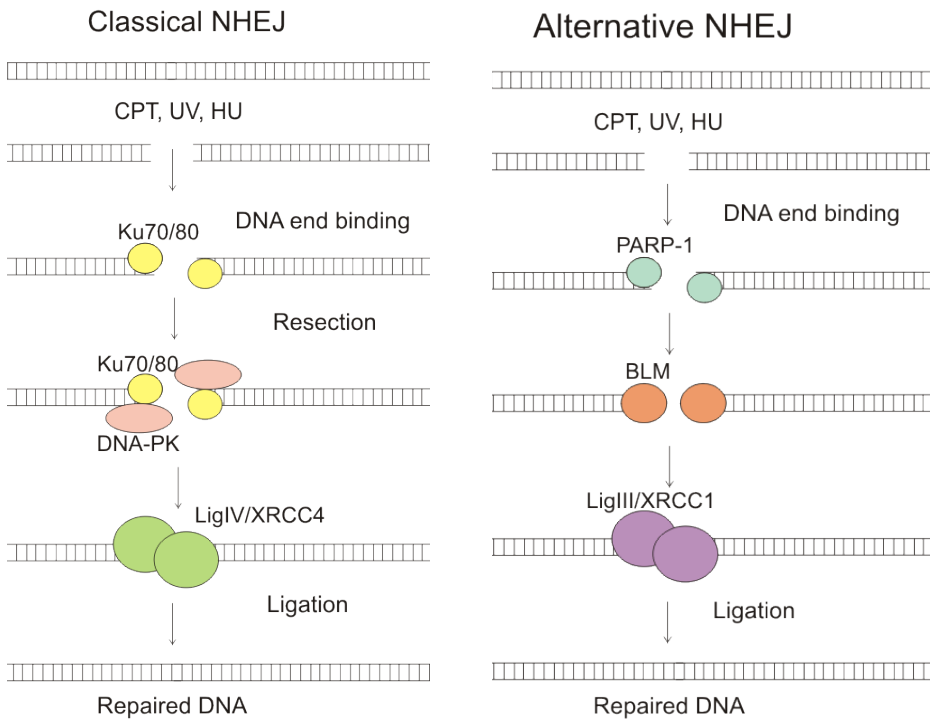

Figure 2-5. Non-homologous end joining of DSBs.

After a DSB is induced by IR or other sources explained in the text, the MRN complex binds the DNA double stranded end (DSE) and initiates end processing. In the classical NHEJ pathway, Ku70/80 binds the free DNA ends and recruits DNA-PKcs. Ligase IV/XRCC4 associates with DNA-PK in a DNA-independent manner, which results in stimulated ligase activity. Subsequently, DNA ligase IV/XRCC3 complex ligate the ends yielding a repaired product. In the non-classical or alternative NHEJ pathway PARP-1, binds the DSE instead of Ku70/80, and DNA ligase III/XRCC1 perform the ligation step. Both processes are considered more error prone than HR because ends are resected to obtain microhomology. This DNA end processing sometimes results in errors such as small deletions.

2.6. Metnase

2.6.1. Evolution of Metnase

Metnase was first identified as a chimeric mRNA transcript that consisted of a SET and a nuclease domain [133]. The SET domain fused with the transposase coding region of the *mariner-like human mariner 1 (Hsmar1)* transposon, in-frame; resulting in a gene that contains three exons [133]. Cordaux and colleagues determined that first an *Hsmar1* transposon was inserted downstream of a SET gene. Then, the transposase domain of the gene was incorporated 40-58 million years ago. Finally, a previously non-coding sequence became an exon and in the process created *de novo* a new intron [134]. Thus, the final functional gene is present only in higher primates (Figure 2-6). Furthermore, the Cordaux group studied the transposase domain and determined that it contains a helix-turn-helix motif and a DDN motif, common in *mariner* transposase domains. These qualities allow Metnase to bind DNA *in vitro,* to the terminal inverted repeats (TIR) of the *Hsmar1* gene [134]. They estimated that there are about 1,500 nearly perfect Metnase binding sites in the human genome [134]. Therefore, Metnase was determined to be a recently evolved protein, containing three exons, and with the capacity to bind DNA in a sequence specific manner.

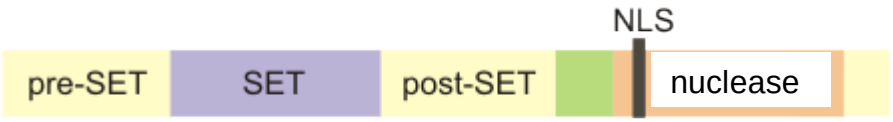

Figure 2-6. Metnase is a 78 kDa protein.

Metnase contains a full SET (methylase) domain containing a pre-SET, SET, and post-SET domains. It also contains a nuclease domain and a nuclear localization sequence (NLS).

2.6.2. Metnase as a possible transposase

The work of Cordaux was followed by a detailed study from the Chalmers group addressing Metnase as a potential human transposase [135]. They cloned full length Metnase and exon3 (transposase domain) from human cDNA and used it in an integration assay with the *Hsmar1* transposon as the integration element. The transposase domain of Metnase showed integration activity through the DDN motif in a Mn^{2+} dependent manner. Although the integration frequency was very low, it was comparable to V(D)J recombination transposition activities of RAG1/2 [135, 136]. However, when they used a pre-cleaved *Hsmar1* transposon, the integration efficiency increased by more than 100 fold, levels comparable to other known transposases such as Mos1. This suggested that full length Metnase and exon3 lacked the biochemical activities necessary for one or more of the transposition reaction preceding the cleaved transposon element integration step [135]. The formation of a paired-end-complex (PEC) is an early

step in the DNA transposition reaction. Liu and colleagues demonstrated using electrophoretic mobility shift assays (EMSA) that Metnase and exon 3 assemble the PEC complex very efficiently, reaching 10% complex assembly, a level of efficiency surpassing any previously established for other *mariner transposases* [135]. The next step of the transposase reaction is the nicking of the 3' end of the transposable element, which generates a 3' hydroxyl group at the end of the element. Metnase exon 3 showed 3' nicking activity as expected, but it also nicked the 5' end of the opposite strand, 3 bp within the element, and this latter activity was much more efficient than the 3' nicking. Thus, Metnase showed a defect in this crucial step of the transposition reaction [135]. The final step of the transposition reaction is the simultaneous integration of the 3' ends of the transposable element into a target site. Metnase and exon 3 were proficient in this step in a Mn^{2+} dependent manner, and this observation was later confirmed by a different group [137]. Further testing of the full length Metnase protein demonstrated that Metnase contained all the *in vitro* activities observed with exon 3 [135]. A study by Roman and colleagues confirmed the DNA binding and nicking activities of Metnase and further implicated the helix-turn-helix (HTH) motif for the interaction between Metnase and terminal inverted repeats (TIR), and the DDN motif in the DNA cleavage reaction [138]. Taken together, their observations demonstrate that although Metnase contains some important biochemical activities of a transposase, it is largely deficient in the *in vitro* transposase reaction and it is therefore not a true human transposase. However,

the DNA binding and nicking activities could be important for other functions of Metnase as described below.

2.6.3. Metnase promotes DNA integration

Metnase evolved from a transposase, which normally has DNA integration activity. Therefore, the Hromas and Nickoloff laboratories investigated whether Metnase could integrate viral DNA into the genome. Metnase integrates viral and plasmid DNA into the genome [139, 140]. When Metnase was overexpressed in human HEK-293 cells, the frequency of plasmid integration increased significantly, in *cis* and *trans* [139]. Additionally, Metnase also integrated Moloney leukemia virus (MLV) DNA into the same cells; suggesting that Metnase also functions as a viral integrase [139]. Williamson and colleagues later investigated whether Metnase functions to promote lentiviral (HIV) integration, and demonstrated that protein expression correlates with lentiviral integration [140]. Thus, Metnase is an integrase with the capacity to integrate DNA, HIV and other retroviruses into the human genome. This is important because Metnase could have roles in viral life cycles and infectivity, but it is also of interest because it can be manipulated to improve the efficiency of gene therapy.

2.6.4. Metnase expression and methylation activity

Our laboratory first characterized Metnase in 2005 and linked it to the NHEJ DNA-DSB repair pathway [139]. In that study, Lee and colleagues cloned

the Metnase gene from cDNA, sequenced the gene, and confirmed that it expresses a full-length protein via Western blot analysis. Metnase contains a full SET domain, including pre-SET and SET domains (Figure 2-6). Metnase was shown to be expressed in all human tissues tested including brain, colon, heart, leukocyte, liver, lung, ovary, placenta, prostate, skeletal muscle, intestine, spleen, and thymus; with placenta having the highest and skeletal muscle the lowest expression levels respectively [139]; suggesting that Metnase expression correlates with proliferative tissues.

One of the most important findings from the Lee study was that Metnase possesses *in vitro* histone H3 methyltransferase activity, demonstrated by an assay in which Metnase catalyzed the transfer of radiolabeled ^{3}H-methyl group from the donor *S*-Adenosyl methionine (SAM) to histone H3. That experiment showed that Metnase dimethylates histone H3 at lysine residue 36, and to a much lesser extent Lysine 4 (but not lysines 9 or 79, which are correlated with transcriptional repression) [139]. It is important to note that dimethylation of lysines 4 and 36 in histone H3 is associated with open (active) chromatin [141-145]. Thus, Metnase histone methylation activity may have important functions in DNA repair, DNA replication, integration of foreign DNA into the genome, or regulation of other aspects of DNA dynamics. Taken together, these observations suggest that Metnase may be important for loosening DNA/histone interactions and thereby increasing access of DNA repair factors to DNA in chromatin through methylation of lysine 36 of histone H3. This hypothesis has

been supported by a study of NHEJ (Appendix 6.4) and our results suggest that it is the case.

Metnase also has automethylation activity that regulates its functional interaction with TopoIIα in chromosomal decatenation [146]. Metnase was shown to interact with TopoIIα and this interaction was important for chromosomal decatenation during the M-phase of the cell cycle [146]. *In vitro* decatenation activity of TopoIIα in the presence of purified Metnase protein was decreased when the methyl donor SAM was added to the reaction. This study also showed that the nuclease defective Metnase mutant D483A is less able to enhance the decatenation activity of TopoIIα [146]. In the presence of TopoIIα inhibitors ICRF-193 and VP-16, the decatenation checkpoint is activated, but this checkpoint arrest could be bypassed by overexpression of Metnase [146]. The enhanced decatenation activity with Metnase overexpression was also demonstrated in leukemia and breast cancer cell lines [147, 148]. Thus, Metnase has an important function in chromosomal decatenation, which is regulated by automethylation and TopoIIα interactions, and Metnase may be an important tumor marker as its expression likely influences cancer cell sensitivity to topoisomerase inhibitors used in cancer chemotherapy.

2.6.5. Metnase roles in DNA repair

Metnase promotes NHEJ *in vitro* and *in vivo*, but not HR [139]. When Metnase was overexpressed, end joining (precise and imprecise) was increased by ~2 fold, and when the protein was knocked-down using siRNA there was a 12

fold reduction in imprecise and 20 fold reduction in precise NHEJ [139]. Additionally, both SET and nuclease domains were shown to be important for this stimulation of NHEJ, as N210S and D248S (SET defective), and D290S (nuclease defective) mutations blocked Metnase NHEJ activity. Interestingly, when Metnase siRNA knock-down cells were exposed to ionizing radiation, whose damage is mainly repaired by NHEJ, there was an eight fold decrease in colony survival. However, Metnase overexpression did not have a significant effect in an HR assay [139]. Thus, Metnase was implicated as a DNA repair protein involved specifically in the NHEJ repair pathway.

In 2008, the Lee laboratory characterized in a series of biochemical experiments the interactions between Metnase and the protein hPso4, a human homolog of the yeast protein PS04, that has been implicated in DNA repair and cell survival through interactions with WRN [149]. Metnase was shown to interact with NBS1, and to co-localize with this protein in IR induced nuclear foci. Furthermore, the NBS1 interaction by co-immunoprecipitation and co-localization in foci was shown to be dependent on hPso4 [149]. Additionally, our laboratory has previously demonstrated that Metnase interacts with the classical NHEJ proteins Ligase IV (LigIV) and XRCC4, in a DNase independent manner, thus Metnase has been shown to interacts with important components of the NHEJ pathway [150].

The Hromas laboratory further characterized the role of Metnase in promoting precise and imprecise NHEJ with different types of ends, namely 4 base 5’ overhangs, 4 base 3’ overhangs, and blunt ends, and in preventing

deletions during NHEJ [150]. In addition, they demonstrated that although Metnase does not have an effect in HR, it does promote resolution of γH2AX foci after IR [150]. Taken together, these findings indicate that Metnase plays a direct role in the NHEJ pathway. Our laboratory has recently conducted a detailed mechanistic study of the role of Metnase in NHEJ. We showed that Metnase promotes recruitment of early NHEJ factors to DSBs by dimethylating histone H3 K36 (Appendix 6.4).

2.7. Hypothesis

Studies have demonstrated that Metnase interacts with TopoIIα *in vivo* and *in vitro*. This interaction is important for chromosomal decatenation during the M-phase of the cell cycle, and cancer cells in which Metnase has been repressed are sensitive to TopoIIα inhibitors. TopoIIα is also involved in DNA replication and it has been isolated as part of the replisome complex [151]. Metnase methylates histone H3 at lysine 36 and this modification is associated with transcriptional complexes [139, 141], which could be important during DNA dynamic processes such as repair and DNA replication. Metnase plays a role in NHEJ and although its specific functions are not fully elucidated, it appears to regulate access of NHEJ factors to DSBs by dimethylating histone H3 Lysine 36 and it interacts with NHEJ proteins such as LigIV, XRCC4, and NBS1. DNA replication fork damage is mostly repaired by the HR pathway; however, recent studies have shown that NHEJ proteins such as DNA-PK and PARP-1 also play a role in replication fork re-start. Therefore, since Metnase enhances TopoIIα function and NHEJ repair, it is **hypothesized that Metnase is involved in replication fork re-start after damage.**

The present study demonstrates that Metnase indeed is important for replication fork re-start after damage as demonstrated by DNA fiber analysis and BrdU incorporation assays. Cell cycle analysis demonstrated that cells lacking Metnase have a delayed S-phase progression and increased sensitivity to replication fork damaging agents. Furthermore, it is demonstrated that Metnase interacts with replication fork factors, PCNA and the RAD9 subunit of the 9-1-1

complex, and that it interacts with TopoIIα. The exact mechanism by which Metnase acts in replication fork re-start is yet to be determined, but these observations demonstrate that Metnase is important for the re-start of stalled and replication forks, and its functions may be mediated by interactions with replication fork components.

3. METHODOLOGY

3.1. Materials and Methods

3.1.1. Cell Lines, RNAi-suppression of Metnase, and Expression of V5-tagged Metnase

Cell lines were cultured in D-MEM with 10% (v/v) fetal bovine serum supplemented with 100 U/mL penicillin and 100 μg/mL streptomycin, or 1× antimycotic/antibiotic (Invitrogen, Carlsbad, CA). Metnase was overexpressed in HEK-293 and HEK-293T cells as described [146]. V5-tagged Metnase expression was confirmed by Western blot with a monoclonal antibody against the V5 tag (Invitrogen). Metnase was downregulated by transfecting cells with a pRNA/U6-Metnase RNAi vector and selecting in growth medium with 150-200 μg/mL hygromycin B (Sigma-Aldrich, St. Louis, MO), or with a Metnase shRNA vector (pRS-shMetnase), and selecting in growth medium with 1 μg/μL puromycin. Control cells were transfected with empty pRNA/U6 or pRS-shGFP vectors. Metnase expression was measured by RT-PCR and by Western blots using antibodies to native Metnase as described [139].

3.1.2. Cell Proliferation and Replication Stress Sensitivity Assays

Cell proliferation was analyzed in triplicate in treated or mock-treated populations incubated in fully supplemented media at 37°C, 5% CO_2. At the indicated times cells were harvested and counted with a Coulter counter. Cell sensitivity to camptothecin (CPT) and hydroxyurea (HU) was determined by seeding 1000 cells per 10 cm (diameter) dish in drug-free medium (to determine plating efficiency, PE), and 100,000 cells per dish in medium with CPT or HU,

incubating for indicated times. Then cells were rinsed with PBS, fresh growth medium was added, and cells were incubated for 12-14 days before colonies were stained with 0.1% crystal violet in methanol and counted. For UV-B sensitivity assays, cells were seeded and incubated for 24 hours as above, rinsed with PBS, exposed to UV-B in a biological safety cabinet equipped with a Phillips UV-B fluorescent bulb, then fresh growth medium was added and cells were incubated and colonies scored. UV doses were determined by using a UVX dosimeter (UVP, Upland, CA). PE was calculated as the number of colonies divided by the number of cells plated without drug or UVB treatment. Percent survival was calculated as the number of colonies formed with drug or UV-B treatment divided by the number of cells plated times the PE.

3.1.3. Analysis of Cell Cycle Distributions and Cell Death

Cell cycle distributions were measured by fixing cells with 70% ethanol and staining with 0.2 mg/mL propidium iodide (PI) in a fresh solution containing 1% (v/v) Triton X-100 and 2 U of DNAse-free RNAse (all from Sigma-Aldrich) for 15 min at 37°C or at 30 min at room temperature. Samples were analyzed using a FACScan or a FACScalibur flow cytometer (Becton Dickinson, Franklin Lakes, NJ). The percentages of cells in G_1, S, or G_2/M phases were calculated by dividing the number of cells in each cell cycle stage by the total number of PI positive cells, normalizing to controls that were not stained with PI, and converting values to percentages). Apoptosis and cell death were analyzed by flow-cytometric measurement of annexin-V expression and PI incorporation by

using the Annexin V-FITC Apoptosis Detection Kit I (BD Pharmingen, San Diego, CA). All flow cytometry data were analyzed with FlowJo software (Ashland, OR, http://www.flowjo.com/).

3.1.4. BrdU Incorporation

Log phase cells, or cells treated with 5 mM HU for 18 h were washed with PBS and released into fully supplemented D-MEM containing 10 μM BrdU. Aliquots were removed at indicated times, cells were fixed, permeabilized, and stained using the FITC BrdU Flow Kit (BD Pharmingen), and analyzed by flow cytometry as above.

3.1.5. DNA Fiber Analysis

DNA fibers were analyzed as described [99]. Briefly, cells were grown to ~50% confluence in six-well tissue culture dishes, 20 μM IdU was added to growth medium (fully supplemented), mixed and incubated for 10 min at 37°C. Media was removed and cells were washed with PBS, followed by a 100 μM thymidine wash. Cells were then either treated with HU, KU55933 (an ATM inhibitor; KuDOS, Cambridge, England), VP16 (etoposide, a TopoIIα inhibitor), ICRF-193 (TopoII inhibitor), NU1025 (a PARP-1 inhibitor; KuDOS, Cambridge, England), or mock treated. The culture medium was then replaced with fresh medium containing 20 μM CldU and cells were incubated for 20 min at 37°C. Cells were harvested, resuspended in PBS, 2500 cells (2 μL) were transferred to a positively charged microscope slide (Superfrost/Plus, Daigger, Vernon Hills,

IL), lysed with 6 µL of 0.5% SDS, 200 mM Tris-HCl, pH 7.4, 50 mM EDTA, and incubated at room temperature for 5-10 min (a longer incubation may be required at lower altitudes or more humid climates). Slides were tilted to allow DNA to spread via gravity, covered with aluminum foil, air-dried for 8 min, fixed for 5 min with 3:1 methanol:acetic acid (prepared fresh), air dried for 8 min, and stored in 70% ethanol at 4°C overnight. Slides were deproteinized in 2.5 N HCl at 37°C for 1 hr, blocked with 5% BSA and labeled sequentially for 1 hr each with mouse anti-BrdU antibody (BD Biosciences, San Jose, CA), secondary goat anti-mouse Alexa-568 (Invitrogen), rat anti-BrdU (Accurate Chemical, Westbury, NY), and secondary donkey anti-rat Alexa-488 (Invitrogen); all antibodies were used at 1:100 dilution and incubated for 1 h at 37°C. Slides were mounted in PermaFluor aqueous, self-sealing mounting medium (Thermoscientific, Waltham, MA). DNA fibers were visualized using an LSM 510 confocal microscope (Zeiss, Thornwood, NY) optimized for each Alexa dye. Images were processed with Zeiss LSM Image Browser software. In some cases, images were further processed with Photoshop (Adobe) and Genuine Fractals (onOne) software. All images in each experiment were identically processed.

3.1.6. Analysis of γ-H2AX Positive Cells

Cells grown to ~50% confluence in six-well tissue culture dishes were treated with 10 mM HU for 18 h in fully supplemented D-MEM, released into fully supplemented D-MEM for indicated times, harvested, cytospun, and fixed with paraformaldehide as described previously [148]. Cells were re-hydrated in PBS

for 5 min at room temperature and blocked with 2% BSA in PBS for 30 min. Primary staining was done with γ-H2AX monoclonal mouse antibody (Merck, Nottingham, UK) and overnight incubation at 4°C. Cells were washed 3 times in TBS-T for 5 min at room temperature and secondary staining was accomplished with an Alexa488-tagged goat anti-mouse antibody (1:500 dilution, Invitrogen) for 1 h at room temperature. The cells were washed 3 times in Tris-buffered saline-tween (TBS-T) for 5 min at room temperature, then covered in Vectashield mounting media containing 4',6-diamidino-2-phenylindole (DAPI [1.5 µg/mL]) (Vector Laboratories, Burlingame, CA) and sealed with clear nail polish. Images were obtained with a Radiance 2100 inverted confocal microscope **(**BioRad, Hercules, CA) fitted with filter sets specific for DAPI and FITC/Alexa488. Images were optimized consistently with ImageJ software (http://rsb.info.nih.gov/ij/).

3.1.7. Protein Immunoprecipitation

Whole cell extracts were obtained using mammalian-protein extraction reagent (M-PER) buffer according to the manufacturer's instructions (Thermo Scientific), and protein concentration was quantified using a standard Bradford assay. Protein samples were pre-treated with 4 U of DNaseI, incubated at 37°C for 10 min, immunoprecipitated using 0.5-5 mg of protein and antibodies to V5 (1:500, Invitrogen), PCNA (1:1000, Abcam, Cambridge, MA), Rad9 (1:1000, Abcam), or TopoIIα (1:500, TopoGEN, Port Orange, FL). Samples were incubated overnight at 4°C, then 25 µL of A/G (1:1) agarose beads (Invitrogen) were added, samples were incubated for 2 h at 4°C, and centrifuged at 300 × g

for 2 min at 4°C. Supernatants were removed and beads were washed four times with M-PER buffer (Thermoscientific) containing 50 mM phenylmethanesulphonylfluoride and 1x protease and phosphatase inhibitor mixture (Invitrogen). Beads were centrifuged at 300 × g for 2 min at 4°C, boiled for 10 min, and centrifuged at 300 × g for 2 min at 4°C. The supernatants were transferred to new tubes; samples were boiled for 10 min, separated by SDS-PAGE, transferred to a PVDF membrane, and analyzed by Western blotting.

3.1.8. Relaxation of Positive Supercoiled DNA

Positively supercoiled DNA was a kind gift from Dr. Neil Osheroff and Amanda Gentry (Vanderbilt University) prepared as described [120]. Positive supercoil relaxation reactions were performed in a total volume of 20 µL in 10 mM Tris-HCl, pH 7.9, 175 mM KCl, 0.1 mM EDTA, 5 mM $MgCl_2$, 2.5% glycerol, 0.5 mM ATP (USB Co., Cleveland, OH), 2 U TopoIIα, 180 ng Metnase (when noted), and 0.3 µg DNA. Aliquots were removed at indicated times and reactions were stopped with 4 µL of 0.77% SDS, 77 mM EDTA. Products were separated on 1% agarose gels and densitometry was performed using Image J software. Background values were subtracted from signals. The resulting values were normalized to signals at initial time points, and plotted as function of time in two independent experiments.

4. RESULTS

4.1. Metnase Promotes Cell Proliferation

Metnase is expressed in a wide variety of human tissues [139] and in all human cell lines tested, except those transformed by T-antigen such as HEK-293T cells (unpublished results). Overexpression of Metnase in HEK-293T increases cell proliferation [146]. HEK-293 cells express Metnase, and stable shRNA knockdown of Metnase in HEK-293 cells significantly reduced the cell proliferation rate compared to control cells (Fig. 4-1A). We confirmed in this study that Metnase overexpression in HEK-293T increases cell proliferation (Fig. 4-1B). Moreover, cells stably transfected with Metnase shRNA vectors either cease to proliferate after 2-3 months, or revert to a normal phenotype, and escape Metnase repression. These results indicate that Metnase promotes proliferation of human cells, and suggest that Metnase is very important for growth of human cells that do not express T antigen.

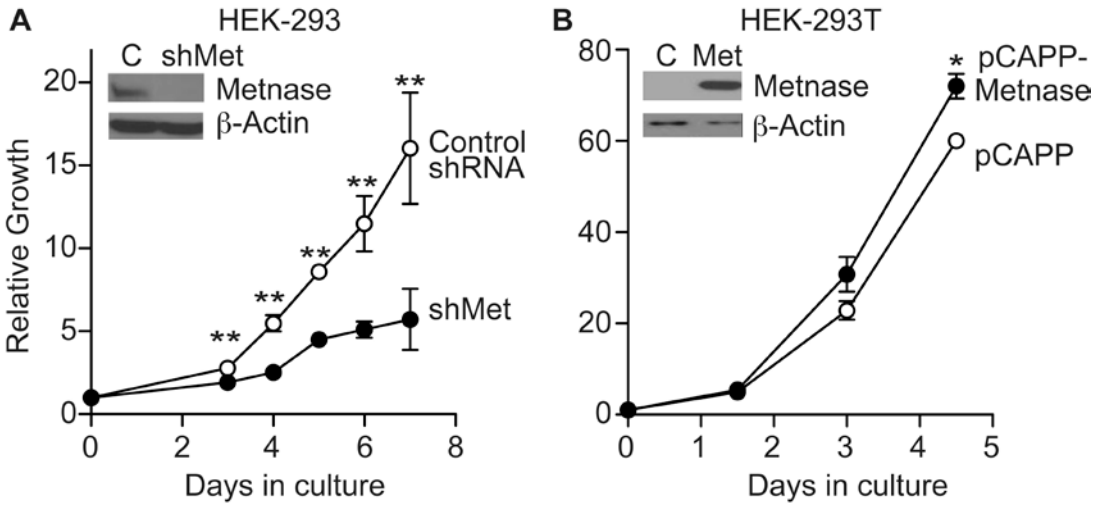

Figure 4-1. Metnase promotes cell proliferation.

A) Cell growth was monitored in HEK-293 cells transfected with shGFP (control) or shMetnase vectors. B) Cell growth was monitored in HEK-293-T cells, which do not normally express Metnase, transfected with the pCAPP-Metnase expression vector or empty pCAPP. Plotted are averages (±SD) of 2-3 determinations per time-point. * indicates P<0.05, ** indicates P<0.01. Metnase expression is shown in representative Western blots with β-actin loading control (insets).

4.2. Metnase Promotes Cell Survival and DNA Replication After Replication Stress

The effect of Metnase on cell proliferation, coupled with its DNA repair properties and functional interaction with TopoIIα [139, 146], suggested that Metnase may have a role in replication and/or in rescuing cells from replication stress at sites of spontaneous or induced DNA damage. We therefore tested whether Metnase regulates sensitivity to replication stress induced by hydroxyurea (HU), camptothecin (CPT), and UV-B (Fig. 4-2). Metnase knockdown sensitized HT1080 cells to 1 mM HU by more than 1000-fold ($p = 0.01$), and to 0.2-0.5 µM CPT by nearly 10-fold ($p \leq 0.011$) (all statistical analyses in this study were performed by using t tests). Metnase knockdown sensitized HEK-293 cells to a UV-B dose of 11.2 J/m^2 by nearly 20-fold ($p = 0.007$). When cultured in a low concentration of HU (0.1 mM), HEK-293 cells proliferated at a slow rate, but Metnase knockdown cells showed almost no proliferative capacity; this effect specifically reflects the Metnase defect since Metnase overexpression in HEK-293T significantly enhanced proliferation under these conditions (Fig.4-3A). The hypersensitivity of Metnase knockdown cells to replication stress reflects, at least in part, enhanced cell death via apoptosis (Fig. 4-3B), as shown by the nearly 30-fold increase in the apoptosis marker annexin V, and >6-fold increase in inviable cells (unable to exclude propidium iodide) (both $p < 0.005$). The marked sensitivity of Metnase knockdown cells to replication stress contrasts with their mild sensitivity to ionizing radiation [139],

perhaps because the replication stressors HU, CPT, and UV-B were continuously present.

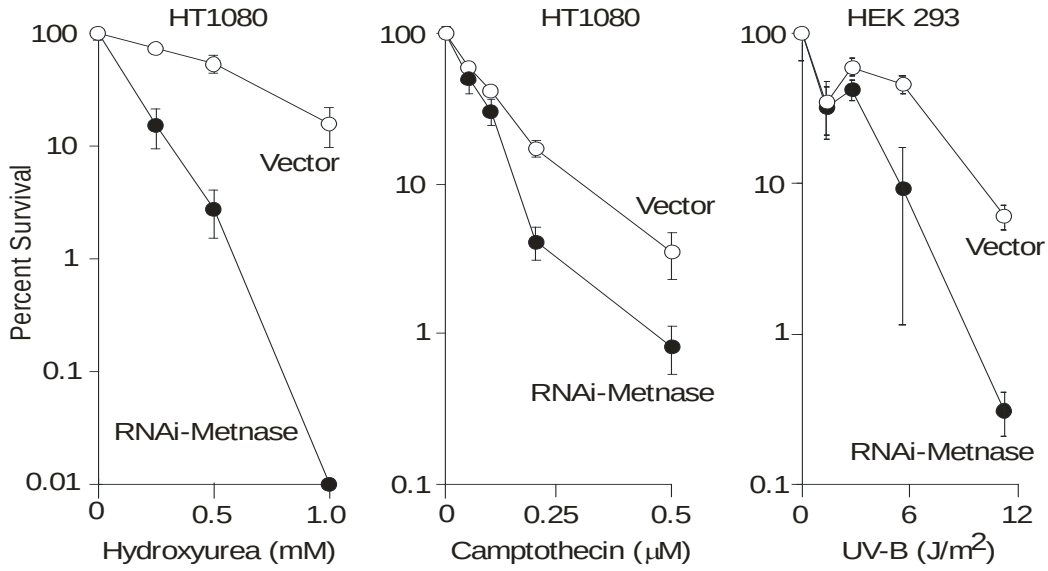

Figure 4-2. Metnase promotes colony survival after DNA replication stress.

Average percent cell survival (± SD) after HU, CPT, or UV-B treatments measured as relative plating efficiency for HT1080 or HEK-293 cells stably transfected with control or shRNA-Metnase vectors. Data are from 2-3 independent experiments per condition; * indicates $p < 0.05$, ** indicates $p < 0.01$. Values are averages (±SD) from 3 independent experiments.

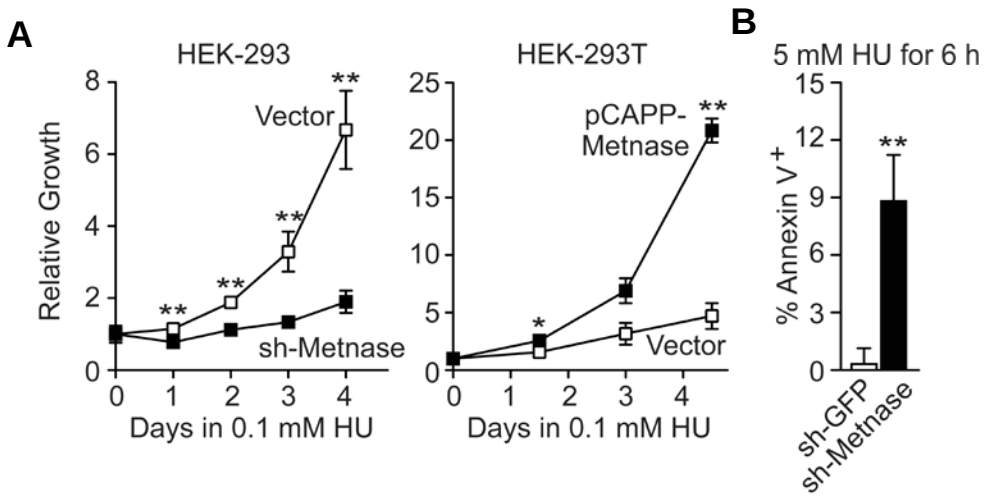

Figure 4-3. Metnase promotes cell growth and prevents apoptosis after DNA replication stress.

A) Average growth rates (±SD) of control HEK-293 and sh-Metnase knockdown cells, and control HEK-293T or Metnase overexpression cells in medium containing 0.1 mM HU; data are from 2-3 independent experiments per cell line. B) HEK-293 control or Metnase knockdown cells were treated with 5 mM HU for 6 h and the percentages of cells expressing annexin V or incorporating propidium iodide were determined by flow cytometry. Data are from 2-3 independent experiments per condition; * indicates $p < 0.05$, ** indicates $p < 0.01$.

To investigate the mechanism by which Metnase promotes cell proliferation and resistance to replication stress, we tested whether Metnase expression level influenced DNA replication by measuring BrdU incorporation and cell cycle distributions by flow cytometry, in unstressed cells and after release from replication stress. In log phase (untreated) HEK-293 cells, Metnase knockdown had no effect on BrdU incorporation during a 30 min incubation (Fig. 4-4A). However, when cells were pretreated with 5 mM HU for 18 h and then released into BrdU, Metnase knockdown in HEK-293 significantly reduced BrdU incorporation (~2-fold), and Metnase overexpression in HEK-293T significantly increased BrdU incorporation (Fig. 4-4B, C). Although neither over- nor underexpression of Metnase significantly affected cell cycle distributions of unstressed cells (Fig. 4-5A), when treated with 5 mM HU for 18 h and released, HEK-293T cells overexpressing Metnase entered S-phase more rapidly than control cells (seen 1 h after release from HU), and entered G2 phase more rapidly (seen 7 h after release from HU (Fig. 4-5B). Somewhat stronger effects were seen when Metnase was overexpressed in HEK-293 cells (Fig. 4-6); this may reflect the fact that HEK-293T cells show robust proliferation even though they do not express Metnase. When HEK-293 Metnase knockdown cells were treated with 5 mM HU for 18 h and released, the opposite effect was seen. In two independent knockdown cell lines, there were marked accumulations of S phase cells 10 and 18 h after release from HU (Fig. 4-7), indicating that Metnase knockdown prolongs S phase after replication stress.

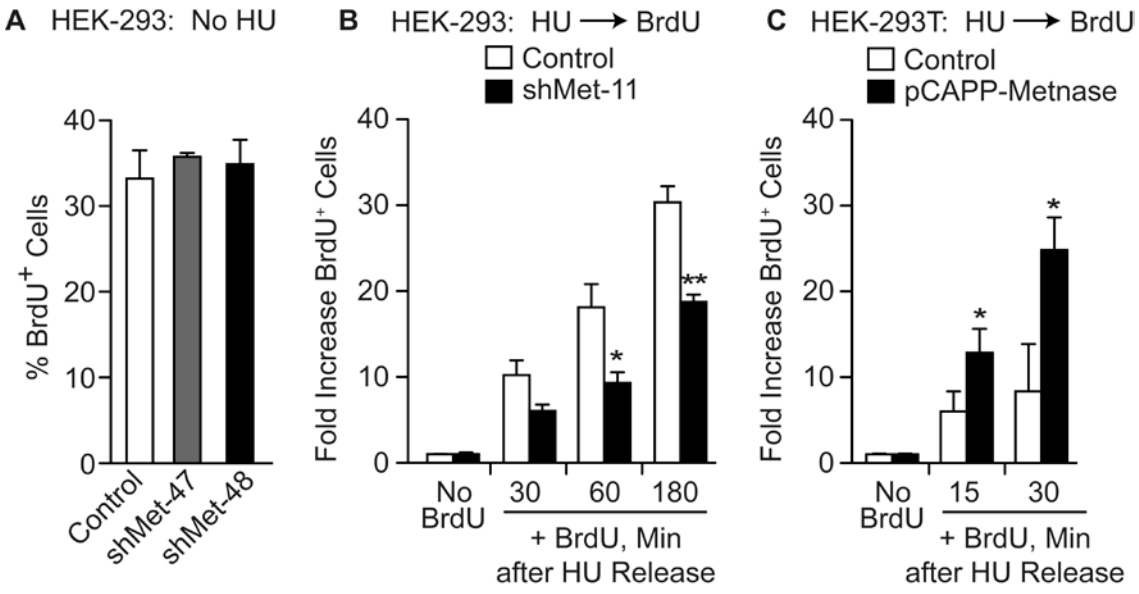

Figure 4-4. Metnase promotes DNA replication after release from replication stress.

A) Log phase HEK-293 cells expressing normal or low levels of Metnase were incubated with 10 μM BrdU for 30 min and average percentages (±SD) of $BrdU^+$ cells are shown for two determinations per strain. B) HEK-293 control and Metnase knockdown cells were treated with 5 mM HU for 3 h and released into medium with 10 μM BrdU. Average fold increases (±SD) in the percentage of $BrdU^+$ cells relative to untreated cells (no HU, no BrdU) are plotted for 3 independent experiments per cell line. C) BrdU incorporation after HU release in HEK-293T control and Metnase overexpression cells as in panel B, except cells were treated with HU for 18 h. For all three panels * indicates $p < 0.05$, ** indicates $p < 0.01$.

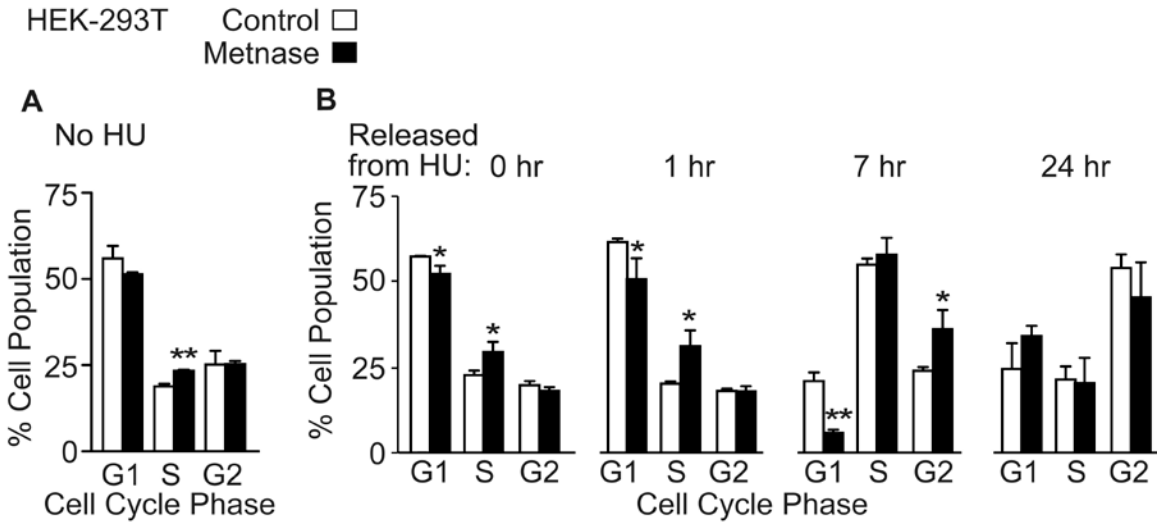

Figure 4-5. Metnase over expression promotes cell cycle progression after replication stress in HEK 293T cells.

A) Cell cycle distributions of log phase cultures of HEK-293T cells stably transfected with empty or Metnase overexpression vectors. B) Cell cycle distributions of HEK-293T cells, with or without Metnase overexpression, after 18 h treatment with 5 mM HU and release into normal growth medium for indicated times. Values are averages (±SD) of three experiments; * indicates $p < 0.05$, ** indicates $p < 0.01$.

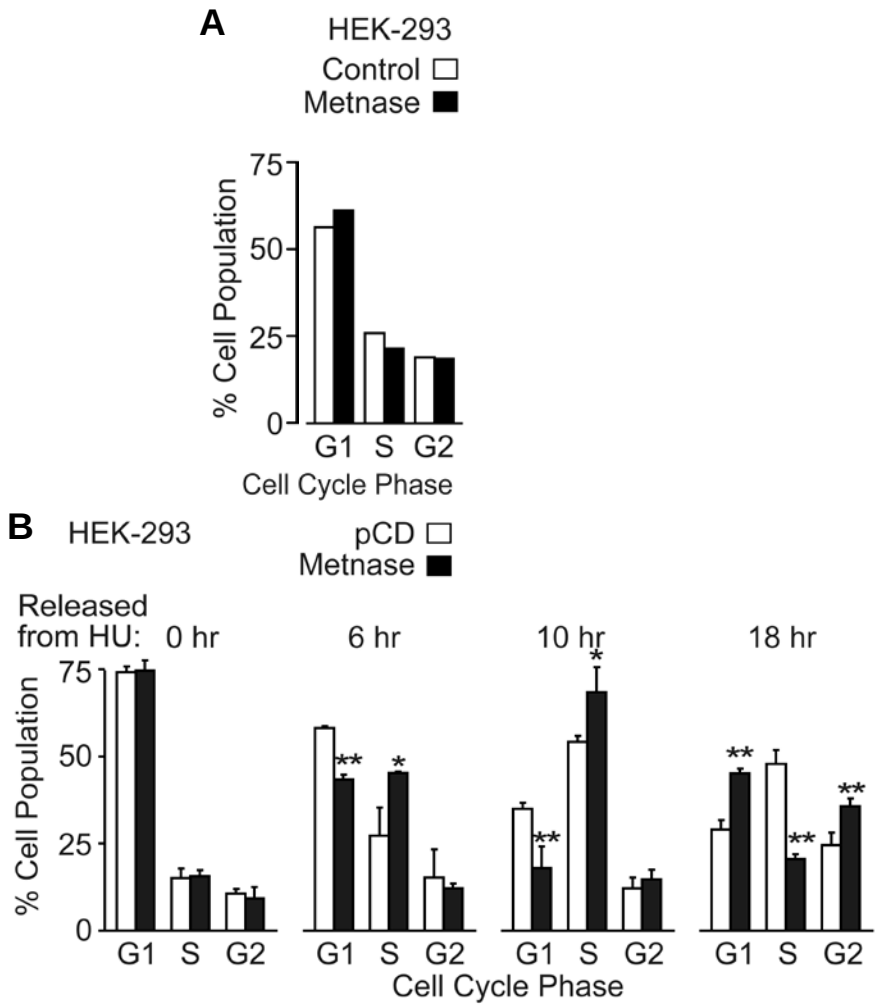

Figure 4-6. Metnase overexpression promotes cell cycle progression after replication stress in HEK293 cells.

A) Cell cycle distributions of log phase cultures of HEK-293 cells stably transfected with empty or Metnase overexpression vectors. Values are from one experiment. B) Cell cycle distributions of HEK-293 cells, with or without Metnase overexpression, after 18 h treatment with 5 mM HU and release into normal growth medium for indicated times. Values are averages (±SD) of three independent experiments; * indicates $p < 0.05$, ** indicates $p < 0.01$.

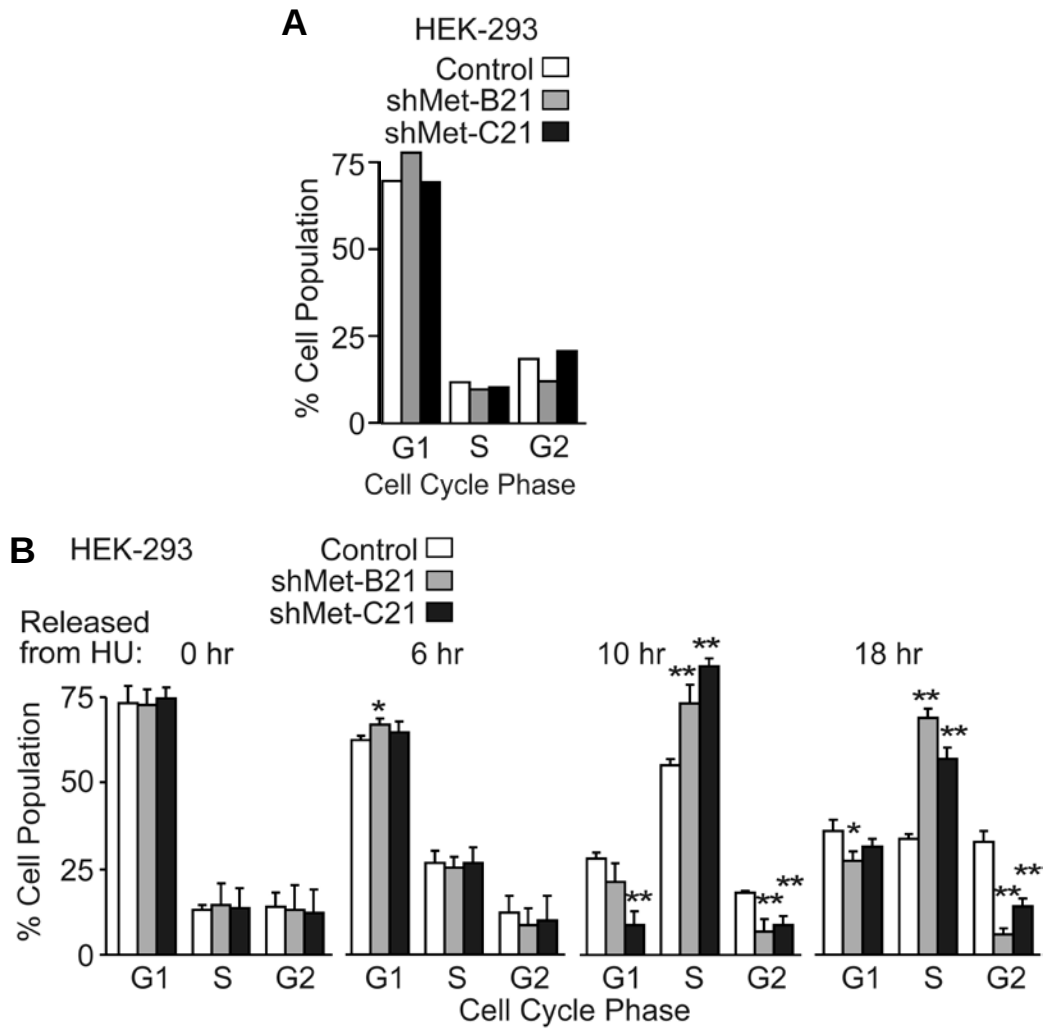

Figure 4-7. Metnase promotes cell cycle progression after replication stress in HEK293 cells.

A) Cell cycle distributions of log phase cultures of HEK-293 cells stably transfected with shRNA control or shRNA Metnase vectors. Values are from one experiment. B) Cell cycle distributions of HEK-293 cells transfected with shRNA control or shRNA Metnase vectors, after 18 h treatment with 5 mM HU and release into normal growth medium for indicated times. Values are averages (±SD) of three experiments; * indicates $p < 0.05$, ** indicates $p < 0.01$.

4.3. Metnase Promotes Replication Fork Restart

To gain a better understanding of the role of Metnase in replication and the replication stress response, we analyzed replication fork restart, new origin firing, and replication speed by using DNA fiber analysis. Log phase HEK-293 cells stably transfected with vectors expressing shRNA targeting Metnase, or GFP as control, were labeled with IdU for 10 min, then incubated with or without 5 mM HU for one h, briefly washed with thymidine and then incubated with CldU for 20 min. Cells were lysed on glass slides and DNA fibers were stretched by gravity, fixed, IdU was stained red and CldU was stained green, and DNA fibers were quantified using confocal-microscopy (Figures. 4-8 and 4-9A). In untreated control cells, ~90% of fibers showed adjacent red-green signals indicative of continuing forks, and ~10% had only green signals indicating forks that initiated after IdU was removed ("new forks"). When control cells were treated with HU, continuing forks (those that stalled and restarted) were moderately reduced to ~65% ($p = 0.0014$), new forks that initiated after HU treatment showed a slight but not statistically significant increase to ~20%, and ~15% of forks stopped and failed to restart. The pattern observed with untreated Metnase knockdown cells was similar to untreated wild-type cells, with predominantly continuing forks and a small percentage of new forks. Strikingly, when Metnase knockdown cells were treated with HU, the percentage of stopped forks greatly increased (to ~90%) and there was a corresponding large decrease in the percentage of continuing forks (both $P \leq 0.0008$). New forks were extremely rare in HU treated Metnase knockdown cells, however new forks are also rare in untreated

Metnase knocked-down cells, and the decrease with HU treatment was not statistically significant ($p = 0.3$). These results provide direct evidence that Metnase plays a critical role in restarting stalled replication forks, and further suggest that Metnase may regulate new origin firing when cells experience replication stress.

To determine whether Metnase regulates the speed of replication, we measured average fiber lengths. As expected, red fibers were shorter than green since cells were treated with IdU (red) for 10 min and CldU (green) for 20 min. Fibers were longer in unstressed cells than after HU treatment (Figure 4-9B). However, Metnase had no effect on fiber lengths in either HU treated or untreated cultures. We conclude that Metnase regulates the efficiency of replication fork restart, and possibly initiation after replication stress, but it has no effect on the speed of ongoing forks.

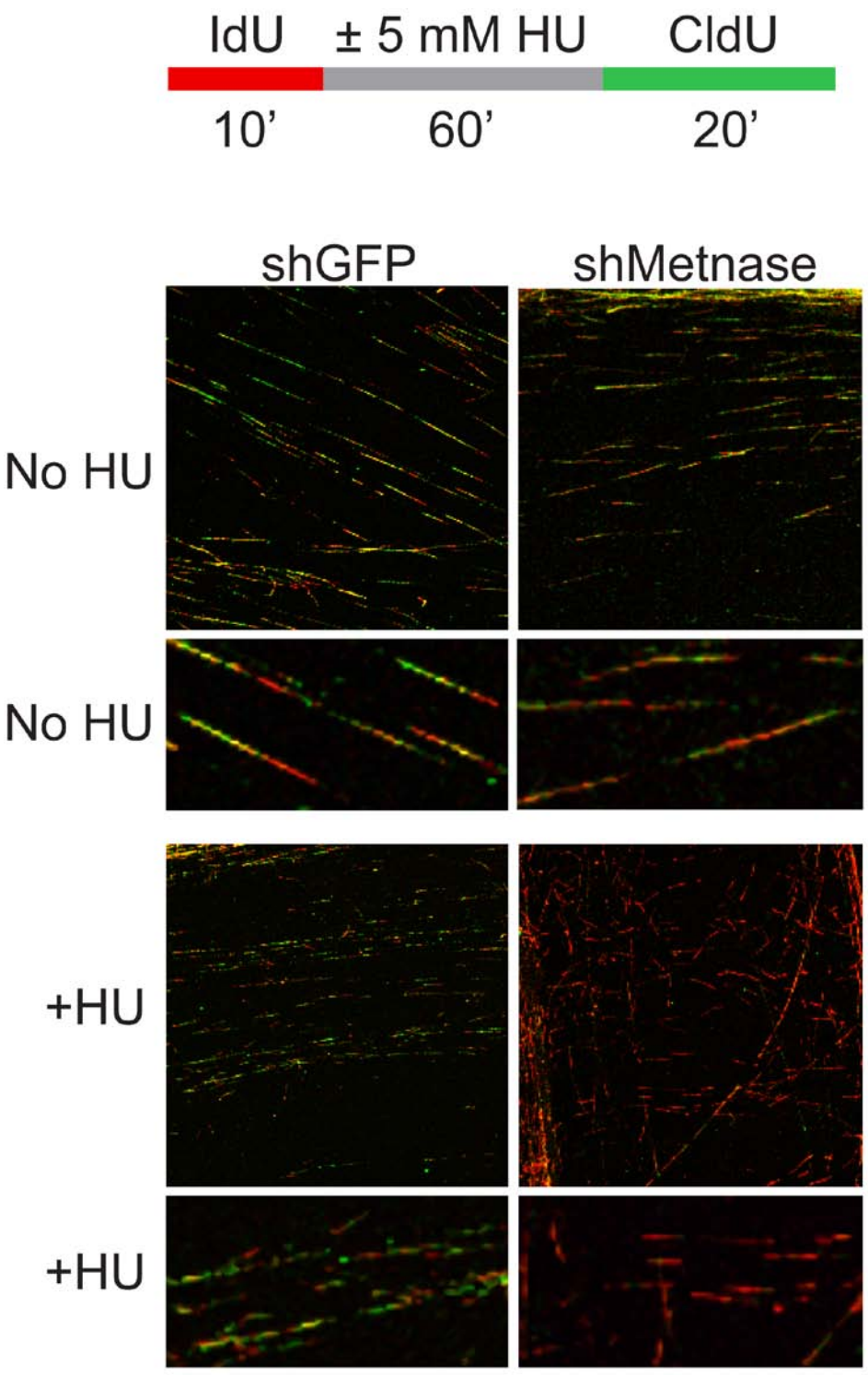
IdU
± 5 mM HU
CldU
10’
60’
20’
shGFP
shMetnase
No HU
No HU
+HU
+HU

Figure 4-8. Metnase promotes replication fork restart.

HEK-293 cells transfected with sh-GFP control or shMetnase were treated with HU. IdU and CldU labeling scheme is shown above representative confocal microscope images of DNA fibers, with IdU stained red and CldU stained green. Images were obtained using an LSM 510 confocal microscope and are representative of four independent experiments, each done in triplicate.

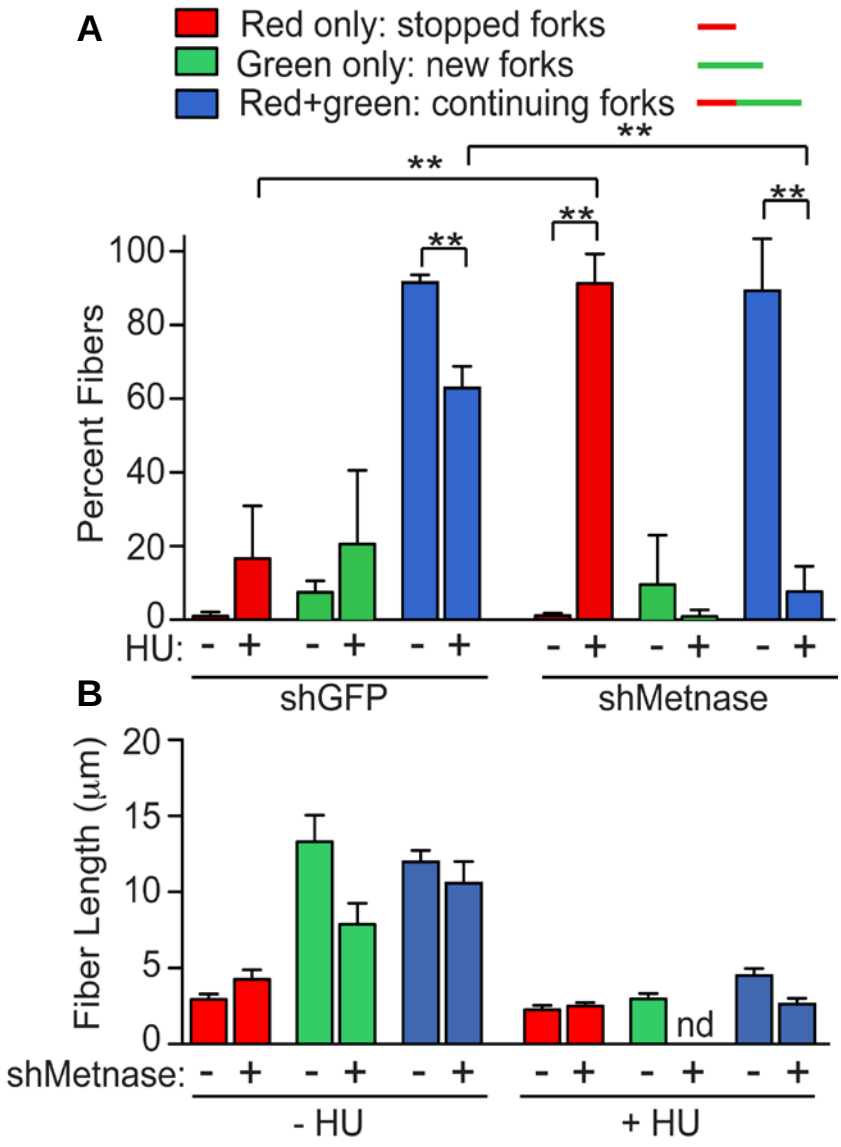

Figure 4-9. Metnase promotes replication fork restart.

A) Quantification of fiber images in Figure 3.8. At least 150 fibers were scored per treatment, per cell line in each of three experiments; ** indicates $p < 0.01$. B) Fiber lengths were measured by using LSM 510 Image Browser software. Plotted are averages (±SD) of triplicate experiments in which 150-500 fibers were scored per treatment, per experiment, nd=none detected.

4.4. Metnase Promotes Resolution of γ-H2AX Induced by Replication Stress

Replication stress causes fork collapse to DSEs marked by phosphorylation of histone H2AX to γ-H2AX. Elimination of the γ-H2AX signal over time reflects DSE/fork repair. Metnase and classical NHEJ proteins promote survival after replication stress and influence replication fork restart [99, 164-166] (this study), and Metnase promotes NHEJ and interacts with the key NHEJ protein DNA LigIV [139, 150]. We therefore tested whether Metnase influences resolution of HU-induced γ-H2AX by treating cells with 10 mM HU for 18 h, then releasing into normal growth medium and examining γ-H2AX by immunofluorescence microscopy. Since HEK-293 and HEK-293T cells used in these experiments adhere poorly, cells were cytospun prior to fixation and immunocytochemical staining. Consistent with the enhanced sensitivity of Metnase knock-down cells to HU, γ-H2AX persisted longer in the knock-down cells, with significant differences from controls at both 6 and 24 h after release from HU (Figure 4-10A, $p < 0.0001$). Similarly, overexpression of Metnase in HEK-293T cells accelerated the resolution of γ-H2AX signals (Figure 4-10B ($p \leq 0.0055$). Note that in all four cell lines, similar percentages of cells were γ-H2AX positive at the end of the 18 h HU treatment. These results indicate that Metnase promotes resolution of γ-H2AX after cells are released from replication stress, but Metnase does not prevent fork collapse to DSEs over the course of this relatively long HU treatment.

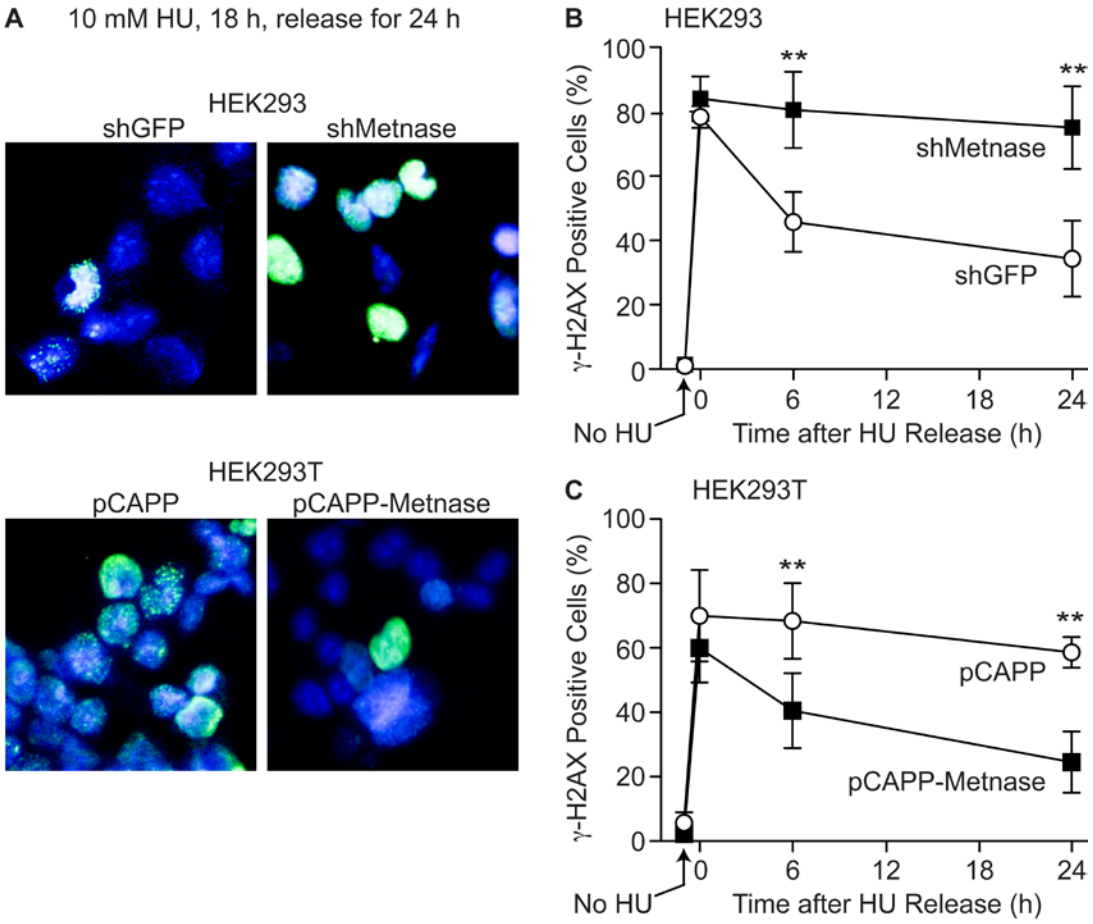

Figure 4-10. Metnase promotes resolution of replication stress-induced γ-H2AX.

(A) HEK-293 and HEK-293T cells over- or under-expressing Metnase were treated with 10 mM HU for 18 h and released into growth medium for 24 h. Aliquots of cells were removed at indicated times, cytospun, stained with DAPI (blue) and antibodies to γH2AX and imaged by confocal microscopy. (B) Percentage of γ-H2AX positive cells among total DAPI stained cells were. An average of >190 cells were counted per slide, 10 slides in each of three independent experiments. Values are plotted as average (±SD); ** indicates $p < 0.01$.

4.5. Metnase Co-immunoprecipitates with PCNA and RAD9

Since Metnase is involved in the replication stress response, we explored its interactions with proteins at the replication fork. PCNA is a key scaffold protein that mediates binding of numerous proteins in the replisome and promotes replication processivity . Metnase co-immunoprecipitated with PCNA, and vice versa, in unstressed cells and after treatment with HU (Figure 4-11A). PCNA interacts with many proteins that share a conserved binding motif, the PIP box, and Metnase has a PIP box (aa 121-128) with the same conserved amino acids found in PIP boxes in three PCNA interacting proteins, DMNT, DNA polymerase β, and RecQL5 . Interestingly, Metnase also co-immunoprecipitated with RAD9, a member of the 9-1-1 complex that is structurally and functionally related to PCNA, and that is recruited to stalled and/or collapsed replication forks (Figure 4-11B). Although this interaction appeared stronger when RAD9 was immunoprecipitated from HU treated cells, a similar enhancement was not seen with HU treatment when Metnase was immunoprecipitated. Metnase did not co-immunoprecipitate with the 32 kDa subunit of RPA (Figure 4-11C), indicating that Metnase is present within the replisome, but is not closely associated with ssDNA at stalled forks. These results indicate that Metnase is closely associated with replication stress factors that control TLS, fork processing via HR mechanisms, and checkpoint signaling.

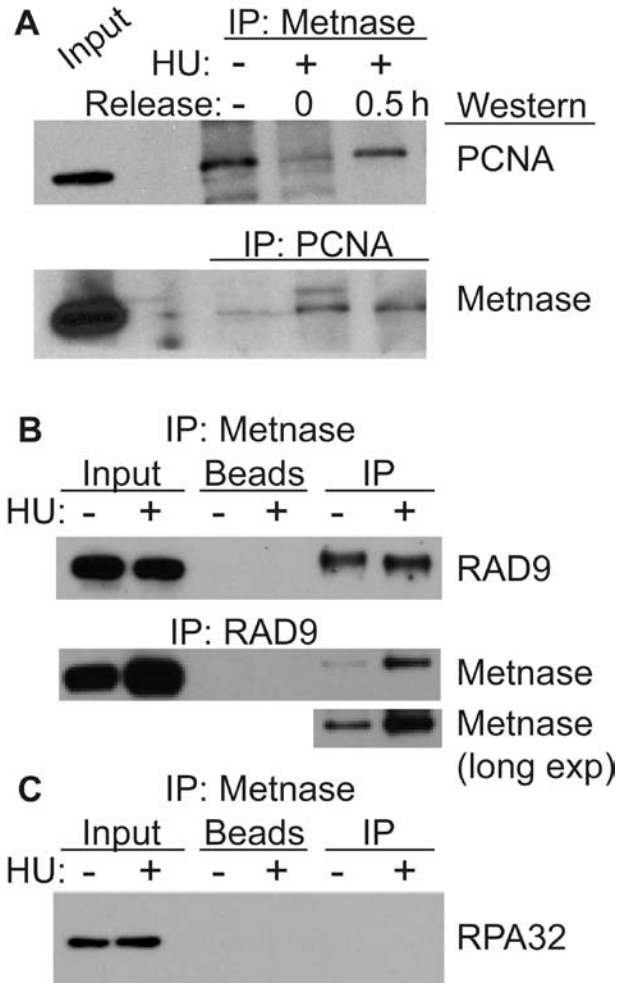

Figure 4-11. Metnase interacts with PCNA and RAD9, but not RPA32.

A) Reciprocal co-immunoprecipitation of V5-tagged Metnase and native PCNA from cells treated with 5 mM HU for 18 h, tested immediately or 30 min after release from HU, or untreated. Input represents 0.5% of immunoprecipitation. Results are representative of at least three independent experiments. B, C) Reciprocal co-immunoprecipitation of V5-tagged Metnase with native RAD9 and native RPA as in panel A, except HU treated cells were only tested immediately after treatment.

4.6. Metnase Interacts with TopoIIα and Promotes TopoIIα-Dependent Relaxation of Positively Supercoiled Plasmid DNA

Metnase interacts with TopoIIα and promotes TopoIIα-dependent chromosome decatenation [146]. TopoIIα is present in the replisome [122] and may function in DNA replication by relaxing of positive supercoils that accumulate ahead of replication forks [120]. We found that Metnase significantly enhanced TopoIIα-dependent relaxation of positive supercoils during a 5 min time course, but Metnase was not required to achieve full relaxation within an hour (Figure 4-12A, B). To gain insight into whether Metnase functions in the replication stress response through its interaction with TopoIIα, we tested whether the interaction between Metnase and TopoIIα was affected by replication stress. HEK-293 cells were treated with 5 mM HU for 3 h, and cell extracts were prepared and analyzed by co-immunoprecipitation of Metnase and TopoIIα. As shown in Figure 4-12C, Metnase and TopoIIα show a robust interaction regardless of which protein was immunoprecipitated, but this interaction was not affected by HU treatment. These results suggest that Metnase interaction with TopoIIα may promote TopoIIα processing of DNA structures in front of replication forks.

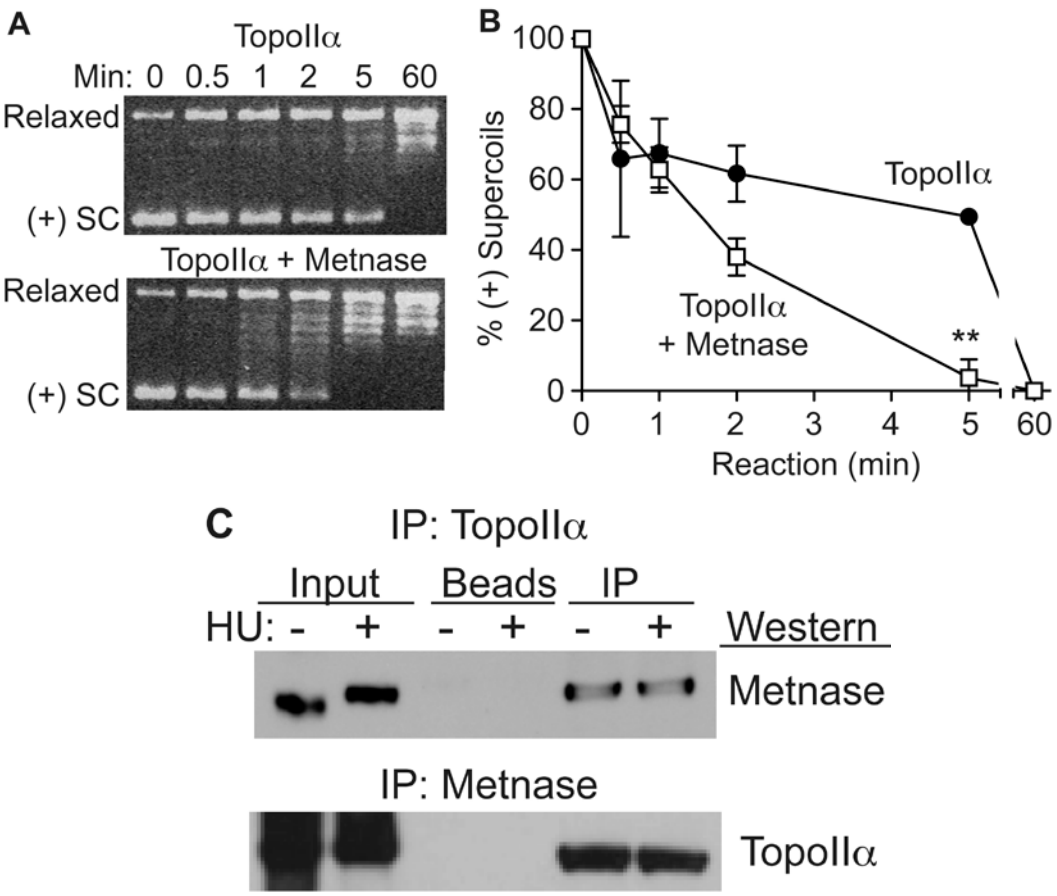

Figure 4-12. Metnase interacts with TopoIIα and stimulates relaxation of positive supercoils.

A) Predominantly positively-supercoiled plasmid DNA samples were treated with TopoIIα (2 U) with or without Metnase (180 ng) for indicated times, and topological forms were detected on ethidium bromide stained agarose gels. B) Gel images were scanned and the percentage of positively-supercoiled DNA remaining at each time point was quantitated. Values are averages (±SD) of two determinations per condition, normalized to 100% at t=0; ** indicates $p < 0.01$. C) Co-immunoprecipitation of V5-tagged Metnase and native TopoIIα; data presented as in Fig. 7B.

4.7. TopoIIα is not required for replication fork progression after DNA replication damage in cells expressing normal levels of Metnase

Based on our observations that Metnase interacts with TopoIIα and stimulates the relaxation of positive supercoils, we decided to investigate whether TopoIIα, perhaps through its interaction with Metnase, regulates replication fork re-start. We performed a DNA fiber assay using the TopoIIα inhibitor, ICRF-193, at two different concentrations [10 μM] and [25 μM] , and added it to cells treated with 5 mM HU for 1 h (Figure 4-14). The DNA fibers were quantified as described earlier (Methods section). The results shown in Figure 4-13A and B shown no significant difference in the fractions of new, stopped, or continuing forks, in normal HEK-293 cells or in Metnase knock-down cells upon treatment with ICRF-193. This suggests that the TopoIIα inhibition by ICRF-193 does not have an effect on replication fork re-start; therefore, TopoIIα does not appear to be directly involved in this process. We further investigated whether a second TopoIIα inhibitor, VP16 (which has been shown to affect cell growth in cancer cells lacking Metnase [147]), or a combination of VP16 and ICRF-193 would prevent timely replication fork restart in HEK-293 cells expressing normal levels of Metnase. The results shown in figure 4-14ABC indicate that there is no significant difference between treated cells and controls, as seen with ICRF-193 alone (Figure 4-13). It is important to note that the levels of stopped, new, and continuing forks are similar to the ones observed in the normal untreated controls (Figure 4-9A). Taken together these results indicate that TopoIIα is not directly involved in restarting stalled replication forks, and

therefore, the strong effect of Metnase on replication fork restart is likely to be independent of its interaction with TopoIIα.

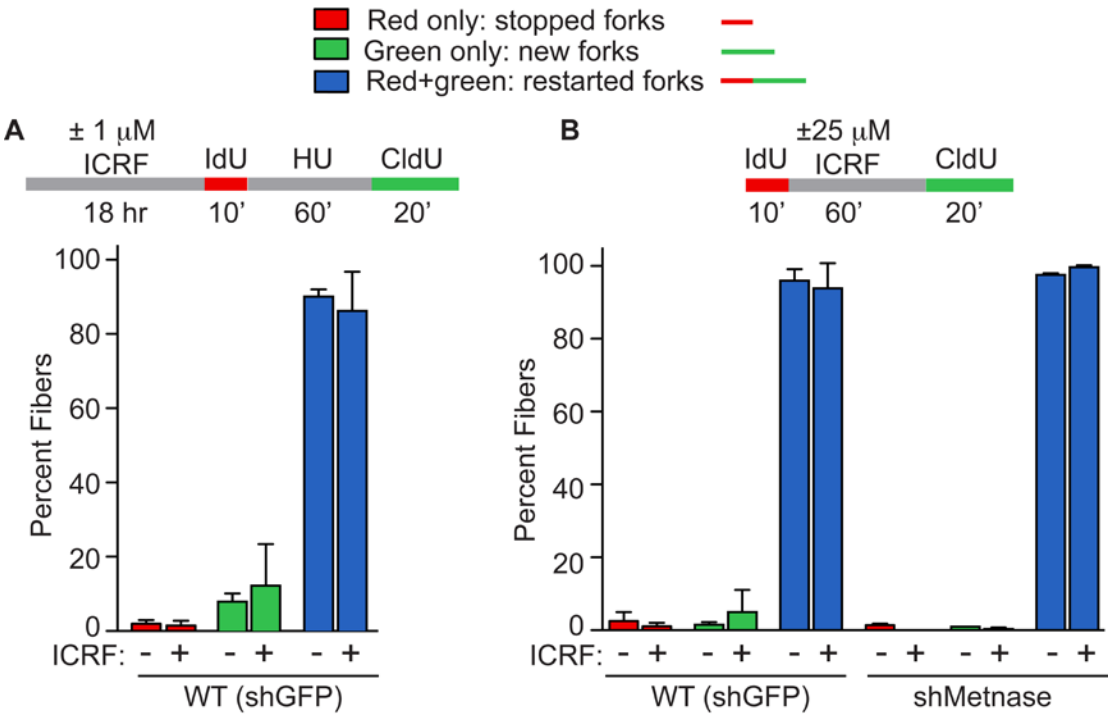

Figure 4-13. Topoisomerase II inhibitor ICRF-193 does not affect replication fork restart.

HEK-293 cells expressing normal levels of Metnase or shRNA Metnase were exposed to TopoII inhibitor A) ICRF-193 [1 μM] and subsequently labeled with IdU, treated with HU [5 mM] for 1 h, and labeled with CldU. B) Cells were treated with ICRF-193 [25 μM] only, in the absence of HU treatment. The quantification of stopped forks, new forks, and continuing forks, plotted are averages (±SD) of triplicate experiments in which 150-500 fibers were scored per treatment, per experiment. Values are averages (±SD) of three experiments; ** indicates $p < 0.01$.

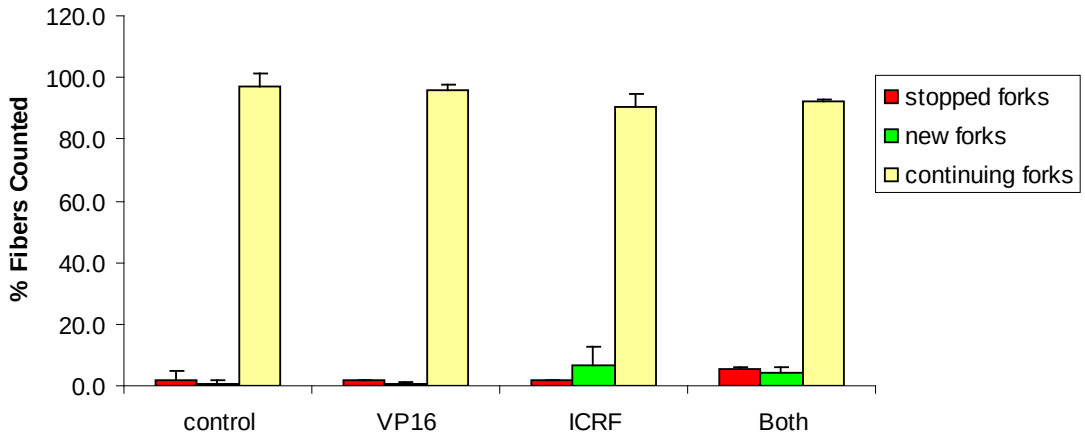

Figure 4-14. Topoisomerase II inhibitors ICRF-193 and VP16 do not affect replication fork restart after replication fork stress.

HEK 293 cells expressing normal levels of Metnase were exposed to TopoII inhibitors VP16 [25μM] and ICRF-193 [25μM] in the presence of HU [5 mM] for one hour. Quantification of stopped forks (red), new forks (green), and continuing forks (yellow) are plotted as averages (±SD) of triplicate experiments in which 150-500 fibers were scored per treatment, per experiment.

4.8. ATM plays a role in replication fork re-start independently of Metnase

ATR and ATM are signaling kinases involved in detection of different types DNA damage, including replication damage. By phosphorylating histones and other proteins, these kinases also promote recruitment of DNA repair proteins to DSBs. We investigated whether ATM functions with Metnase in replication fork restart by inhibiting ATM in normal and Metnase knock-down cells and assaying replication with the DNA fiber assay.

We addressed two questions: 1) Does ATM inhibition affect fork restart in wild type cells, and 2) is there genetic interactions between Metnase and ATM in fork restart (Metnase knocked-down). HEK-293 cells were treated with the ATM inhibitor KU55933 [10 μM], for 1 h under normal DNA replication conditions (log phase growing cells), and analyzed the DNA fibers as described earlier (Methods section). The control cells showed a significant increase in stopped forks (6.4 fold) in the presence of ATM inhibitor, $p< 0.01$ (Figure 4-15), reflecting a decrease (from 90.3% to 69.1%, $p< 0.01$) in continuing forks. These observations confirm that ATM plays an important role in replication fork repair. In Metnase knock-down cells, we also observed a significant increase in stopped forks (6 fold), $p< 0.05$, and a decrease in continuing forks (from 92.9% to 63.4%, $p< 0.01$). However, there were no differences in the percentages of stopped, new, and continuing forks between cells with normal and reduced Metnase in the presence of the ATM inhibitor, this suggests that Metnase may operate upstream of ATM or vice versa.

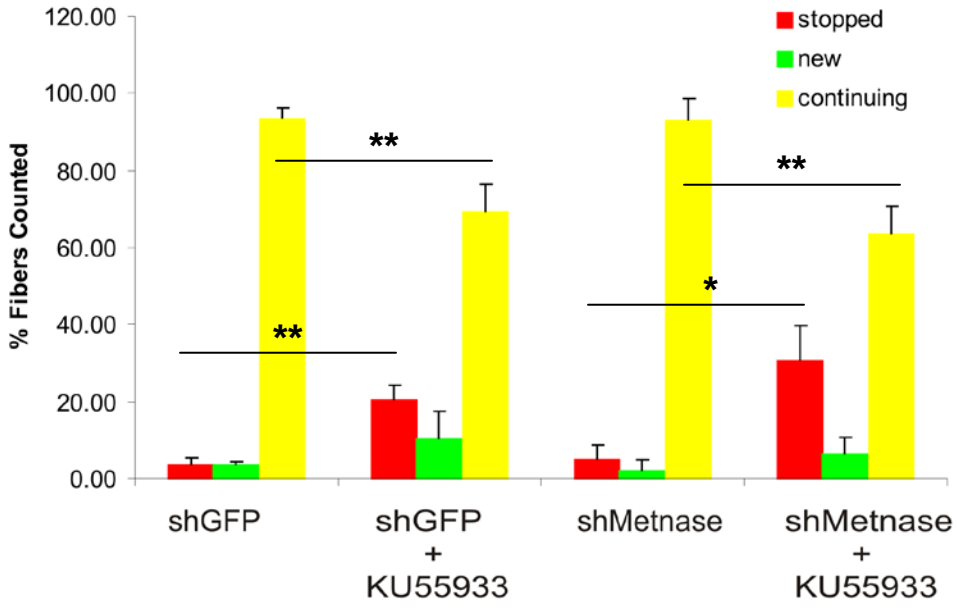

Figure 4-15. ATM is important for normal replication fork re-start, but functions independently of Metnase.

HEK293 cells containing normal or reduced levels of Metnase were treated with KU55933 [10 μM], an ATM inhibitor, for 1 hr under normal DNA replication conditions (i.e. log growing cells). At least 150 fibers were scored per treatment, per cell line for each of three experiments; * p≤ 0.05, ** p ≤ 0.01.

To further investigate the relationship between ATM and Metnase, we performed a colony survival assay using HEK-293 cells stably expressing shRNA control or shMetnase vectors, and KU55933 [70] at increasing doses for the entire period of the assay (~12 days). The results (Figure 4-16) showed no difference in colony formation ability of Metnase knock-down cells compared to controls. ATM inhibition kills in the presence or absence of Metnase, suggesting that Metnase and ATM function in the same pathway.

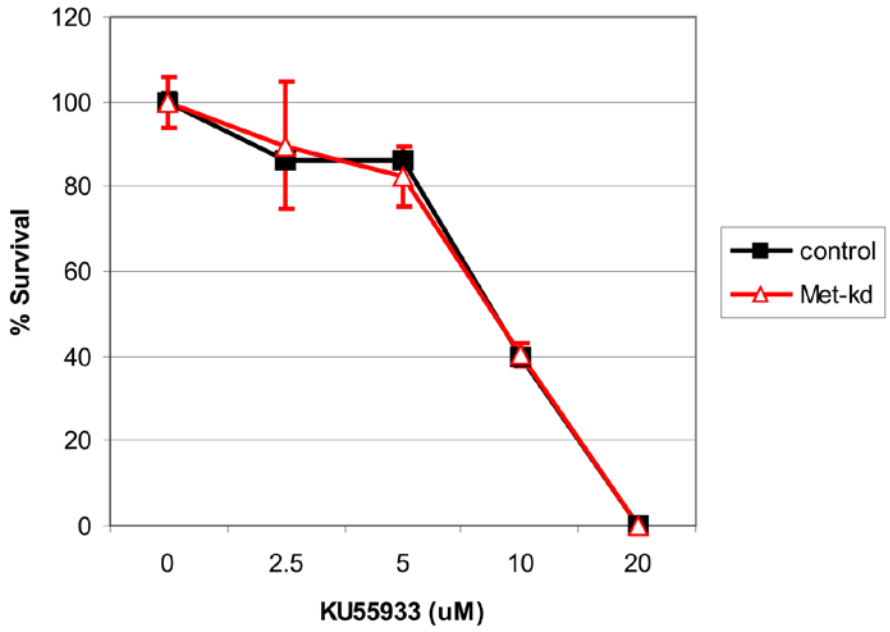

Figure 4-16. Metnase and ATM function in the same pathway.

Average percent cell survival (± SD) after KU55933, an ATM inhibitor. Treatments measured as relative plating efficiency for HEK-293 cells stably transfected with control or shRNA-Metnase vectors. Data are from 3 experiments per condition, values are averages (±SD).

4.9. Metnase Regulates Chk1 Phosphorylation During Replication Stress

Chk1 is a protein kinase that acts downstream of ATM/ATR kinase and is important in the DNA damage checkpoint control [167]. Chk1 becomes activated via phosphorylation of Ser 317 and Ser 345, which occurs in response to blocked DNA replication [168]. Ser 345 phosphorylation localizes Chk1 to the nucleus following checkpoint activation [169]. However, it has been shown recently that phosphorylation at Ser 317, in conjunction with phosphorylation of PTEN, is important for reentry into the cell cycle after replication fork stalling [170]. We examined Chk1 phosphorylation status of serine 317 in the presence and absence of Metnase after HU. We predicted that if Metnase operates upstream of Chk1, then when we inhibit Metnase we would see a change in Chk1 phosphorylation status after replication fork stalling. HEK-293 cells expressing normal or reduced levels of Metnase were treated with 5 mM HU for three hours and the phosphorylation status of Chk1 was then analyzed via Western blot. Figure 4-17A is a representative autoradiograph of two experiments showing Chk1 p-Ser 317, total Chk1, and actin as a loading control. The bands on both gels were quantified using ImageJ (Figure 4-17B) and protein amounts were normalized to untreated controls. The results show that cells lacking Metnase fail to activate Chk1 (p-Ser 317) in response to HU and they fail to increase total levels of Chk1. These observations suggest that Metnase may be a regulator of Chk1 function in response to replication fork damage.

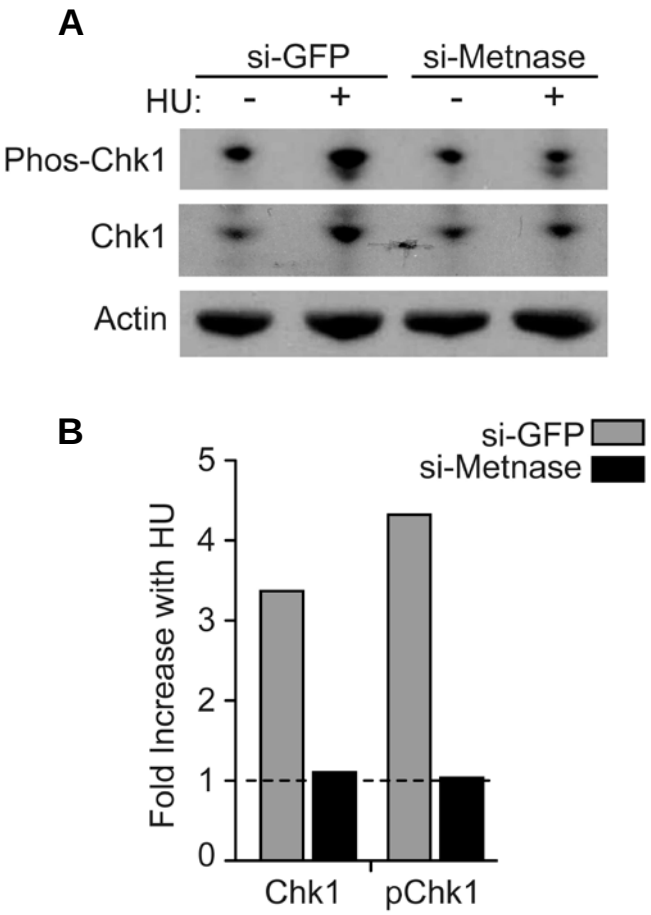

Figure 4-17. Metnase affects Chk1 phosphorylation after DNA replication stress.

A) HEK-293 cells under-expressing Metnase or expressing normal levels of Metnase were treated with 5 mM HU for 3 h, cells were subsequently lysed and protein extracted to check for Chk1 phosphorylation status using an antibody against Chk1 Serine 317 (which allows re-entry into the cell cycle after stalled DNA replication). Results are representative of two independent experiments. B) Quantification of A, done using ImageJ software. Chk1 and Chk1-P bands were normalized to actin controls, and compared to untreated controls that were assigned a value of 1 (dotted line).

4.10. Metnase Promotes Resolution of PARP-1 Foci After Replication Fork Damage

Recently proteins involved in NHEJ, such as PARP-1 and DNA-PK, have been implicated in the repair of stalled replication forks. Specifically, PARP-1 has been shown to be activated at stalled replication forks in an Mre11-dependent fashion (a member of the MRN complex) [132]. Furthermore, the Lee laboratory has shown that Metnase interacts with Nbs1, another member of the MRN complex [149]. Thus, we investigated whether PARP-1 and Metnase function in the same or different replication fork restart pathways. We used HEK293 cells expressing normal or reduced levels of Metnase for this analysis. Cells were treated simultaneously with 5 mM HU and NU1025 [10 μM] (a PARP-1 inhibitor) for 5 h. Subsequently cells were fixed, permeabilized, and stained to visualize PARP-1 foci. Figure 4-18A shows the quantification of the PARP-1 foci plotted as average foci per cell. The results show that cells lacking Metnase have significantly ($p < 0.01$) more foci per cell after damage by HU than control cells. Additionally, figure 4-18B shows a greater percentage of Metnase knock-down cells had more than five foci per cell compared to control cells. These results suggest that Metnase functions to resolve PARP-1 foci formed because of DNA replication fork damage; thus, possibly regulating the type of repair used at the fork. Alternatively, lack of Metnase could increase DSBs at stalled forks, which could lead to more PARP-1 foci independent of Metnase.

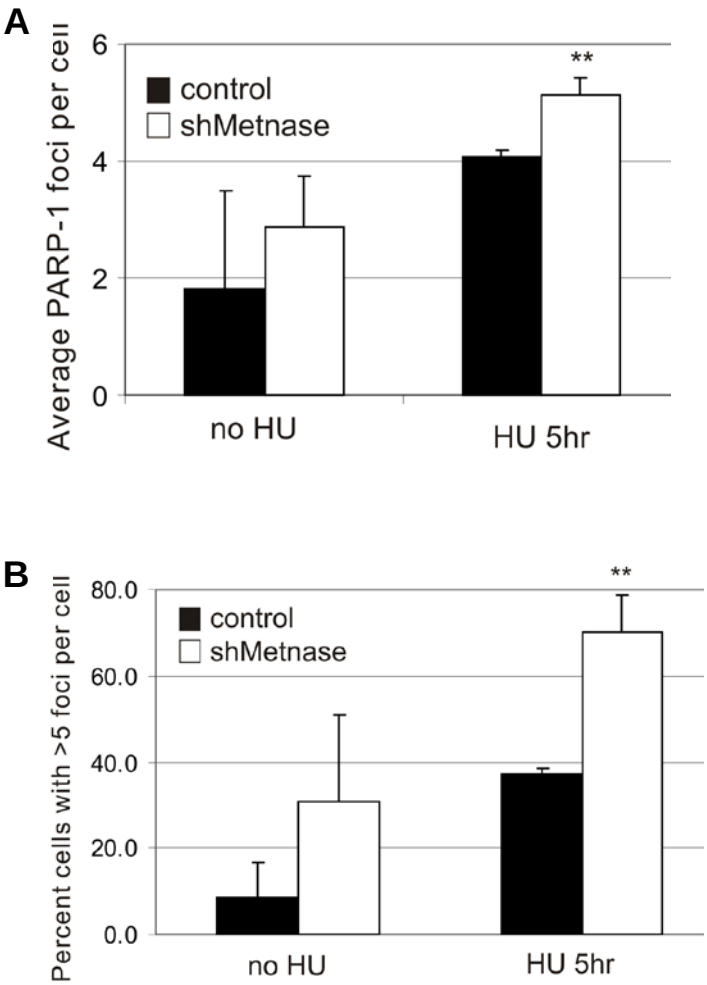

Figure 4-18. Metnase promotes resolution of replication stress-induced PARP-1 foci.

A) HEK-293 cells under-expressing Metnase were treated with 5 mM HU and KU55933 [10 μM] simultaneously for 5 h, cells were removed at indicated time, fixed, and permeabilized with paraformaldehyde, stained with DAPI (blue) and antibody to PARP-1 and imaged by confocal microscopy. On the supplement (next page) are representative microscopy images of cells stained with DAPI (blue), and PARP-1 (green). Average number of PARP-1 foci per cell were quantified and plotted, and percentage of all cell counted containing more

than 5 PARP-1 foci per cell was plotted as percentage. An average of >190 cells were counted per slide, 3 slides per treatment for three independent experiments. Values are plotted as average (±SD); ** indicates P ≤ 0.01.

Figure 4-18 supplement

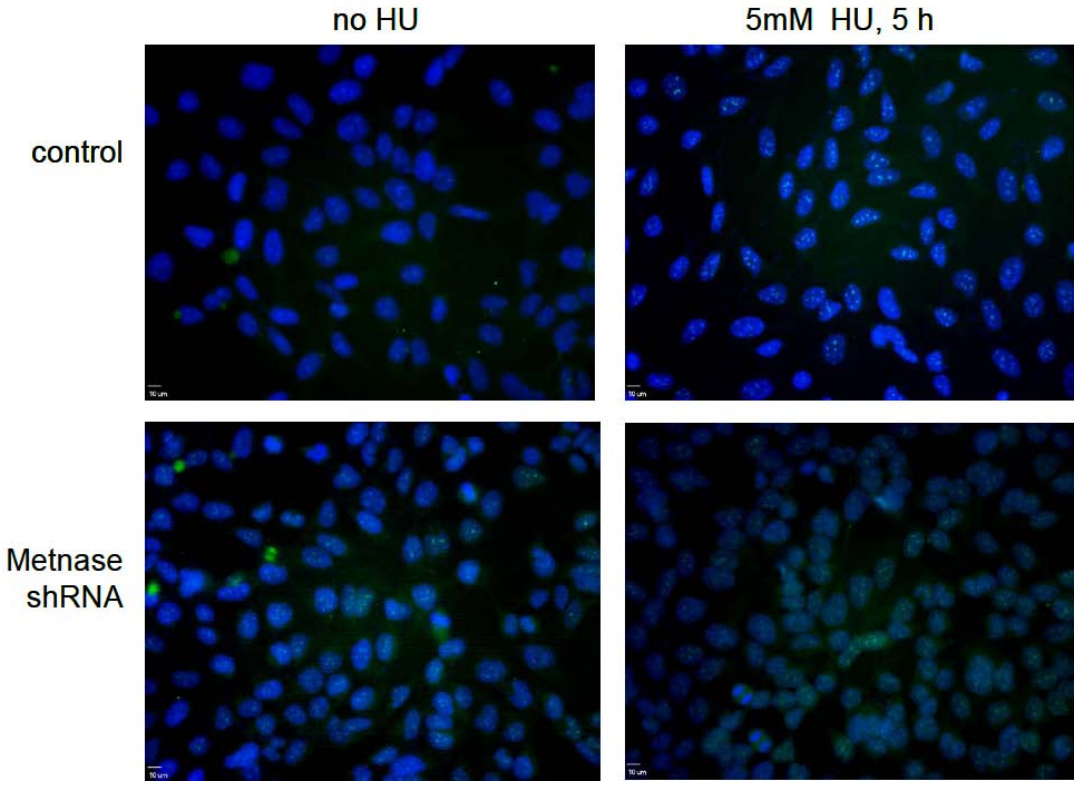

5. DISCUSSION

5.1. Metnase promotes cell proliferation

Early observations indicated that Metnase knock-down cells were mildly sensitive to ionizing radiation [139]. We also noticed that these cells grew slower than their normal Metnase expressing counterparts (Figure 4-1). This led us to hypothesize that the slow growth phenotype of the knock-down cells may be due to a replication defect. Therefore, we tested whether these cells would be susceptible to other DNA damaging agents. In colony formation assays, we discovered that Metnase knock-down cells were very sensitive to UV radiation (20 fold), HU (1000 fold), and CPT (10 fold) (Figure 4-2), all of which cause DNA replication fork stress (although UV also causes other types of stress, such as thymidine dimmers). These observations supported our hypothesis that Metnase may somehow play an important role in DNA replication fork stress and led us to investigate the role of Metnase in DNA replication in more detail.

5.2. Metnase promotes restart of stalled and collapsed replication forks

Metnase appeared very late in evolution, in anthropoid primates [134]. Yet, it is an important protein that influences several aspects of DNA metabolism including NHEJ, DNA integration, and chromosome decatenation [139, 146, 149, 150]. Through interaction with TopoIIα, it regulates cellular resistance to common chemotherapeutics [147, 148]. This research establishes another important role for Metnase in the replication stress response and provides possible mechanisms of action. Given its late appearance in evolution, it is not

surprising that Metnase does not influence normal replication fork progression. Instead, Metnase functions during replication stress. Replication fork damage and restart have historically been defined by using four assays: BrdU incorporation assay, propidium iodide (PI) staining for flow cytometric cell cycle analysis, replication fork bubble arc analysis, and more recently, DNA fiber analysis. In this work, we have used three of the four methodologies to define Metnase's role in the DNA replication stress response.

The role of Metnase in replication fork repair became clearer after we analyzed cells overexpressing and underexpressing this protein. Metnase levels affected BrdU incorporation, S phase progression by PI staining, and fork restart by DNA fiber analysis, but only when cells were subjected to replication stress (Figures 4-4 - 4-9). Metnase knockdown conferred a marked defect in BrdU incorporation after 3 h HU treatment compared to the control cells, and the opposite observation was made when cells overexpressed Metnase (Figure 4-4). Yet, under normal growth conditions, cells lacking Metnase incorporated BrdU at the same rate as the control cells. Since HU acts by causing nucleotide pools to be depleted, it can be concluded that Metnase plays a role in replication fork progression after stress, but not under normal replication conditions. The slower proliferation in Metnase knocked-down cells can be explained by sources of intrinsic replication fork stress causing the forks to stall. This suggests that Metnase's function is not essential for normal DNA replication, but rather is important to resolve stalled/collapsed replication forks.

Cell cycle analysis of cells lacking or overexpressing Metnase supported the hypothesis that it plays a role in replication fork stress recovery, but not in normal DNA replication. We used HEK-293T cells, which the Hromas laboratory discovered do not express Metnase (Figure 4-1), to analyze the effects of Metnase status in cell cycle progression. Metnase levels did not affect cell cycle progression in actively growing cells, with the exception of a slight increase in the number of cells in S-phase in HEK-293T overexpressing Metnase (Figure 4-5A). However, these cells had a delayed progression through S-phase when treated with HU and released, compared to cells overexpressing Metnase (Figure 4-5B). This delay was overcome by 24 h post treatment with HU. Thus, the S phase defect was not permanent and the cells were able to overcome the lack of Metnase. We observed similar results in HEK-293 cells overexpressing and under expressing Metnase (Figures 4-6 and 4-7). It is likely that Metnase helps to resolve stalled/collapsed replication forks. In the absence of Metnase, cells could follow alternate ways to resolve the fork, possibly through recruitment of other factors that may have similar functions as Metnase or that promote alternative repair mechanisms. Based on the two observations that lack of Metnase causes less BrdU incorporation and a delay in S-phase progression after release from HU-induced replication stress, we conclude that Metnase plays a role in replication fork restart after damage.

The most definitive assay revealing a role for Metnase in replication fork restart is DNA fiber analysis. This assay allowed us to determine in more detail whether Metnase functions in restart of stalled forks initiation, or initiation of new

forks after damage. The DNA fiber analysis also allowed us to ask whether Metnase affected replication fork rate. To our surprise, cells lacking Metnase and exposed to HU for 1 h were unable to start any new forks after damage by HU (Figures 4-8 and 4-9). Additionally, we observed a marked decrease in restarted forks as 90% of all forks observed failed to restart. These results indicate that Metnase plays a key role in restarting stalled forks, because the brief HU treatment mainly causes fork stalling. In addition, when forks collapse, restart is largely thought to be dependent on HR, an inherently slow process that involves RAD51 replacement of RPA on ssDNA, and strand invasion of sister chromatids by RAD51 coated DNA strands. When cells were subjected to longer periods of replication stress, Metnase promoted resolution of γ-H2AX (Figure 4-10), which marks collapsed forks. This indicates that Metnase also promotes restart of collapsed forks.

Metnase did not affect the rate of replication fork progression, even after stress. We measured the length of DNA fibers from cells lacking Metnase, treated with HU for 1 h, and compared them to cells containing normal levels of the protein (Figure 4-9). Cells lacking Metnase had the same average fiber length as the control cells under normal replication conditions, a result predicted by our hypothesis that Metnase does not play a role in normal replication fork progression. We did observe that fibers from cells treated with HU were shorter than those from untreated cells, as expected, but Metnase expression level did not affect fiber length. Thus, we conclude that Metnase does not play a role in

the rate of replication fork progression, even under replication fork stress conditions, once new forks are initiated or stalled forks are restarted.

5.3. Important role for Metnase in the DNA replication stress response

Metnase promotes NHEJ [139], and there are other NHEJ factors known to promote cell survival after replication stress, including PARP-1, Ku, Cernunos/XLF, and DNA-PK [126, 130-132, 165, 171]. NHEJ factors might promote rejoining of DSEs at different collapsed forks, but it seems that this type of repair would be highly inaccurate (and genome destabilizing) since each collapsed fork produces only a single broken end. It is possible that individual NHEJ factors promote fork restart through interactions with HR factors [172], or through recruitment by other proteins to the fork, as suggested for PARP-1 [132]. When replication forks stall, the initial cellular response is to stabilize the replisome to prevent fork collapse. We know from previous work from our laboratory and the Lee laboratory that Metnase interacts with the MRN component Nbs1 [149]. Thus, we hypothesized that Metnase could play a role in initial fork stabilization over a short period of replication stress, because altering Metnase levels had an effect on the percentage of stopped forks in the DNA fiber assay.

Metnase could stabilize or promote fork restart through its interactions with the replisome factors PCNA and RAD9. Although it is not yet known whether Metnase interacts directly with these proteins or if they are in a complex together, the fact that the Metnase SET domain has a conserved PCNA

interacting partner (PIP) box is highly suggestive that Metnase interacts directly with PCNA (Appendix 6.5). However, we did not observe any changes in level of protein interaction after replication fork damage, suggesting that the functions of these interacting proteins may be regulated through post-translational modifications such as phosphorylation or methylation. The Metnase SET domain encodes a protein methylase, and Metnase is known to methylate histone H3 and itself [139, 146]. Metnase could regulate PCNA and/or RAD9 function by methylating these proteins. PCNA regulates TLS through direct interactions with TLS polymerases [117]. Thus, Metnase may enhance fork restart after UV by enhancing TLS at UV lesions. Regardless of the specific mechanism, our results clearly place Metnase near stalled replication forks.

RAD9 has well-established roles in the intra-S checkpoint response [115]. It is possible that Metnase could promote fork restart by influencing checkpoint activation or downstream checkpoint-dependent processes such as inhibition of origin firing. We investigated the effects of Metnase on checkpoint factors downstream of RAD9, including Chk1 (discussed in more detail below). Metnase is not required for the p53/Chk2 arm of the DNA damage checkpoint response since replication stress-induced cell death in Metnase knockdown cells shows a robust apoptotic response (Figure 4-3). Metnase may have a more general role in fork restart through chromatin modification near stalled and collapsed forks. It is noteworthy that Metnase methylates histone H3 lysine 36, which is specifically associated with transcription [139]. Thus, Metnase could promote fork restart by enhancing access of repair factors to stalled and collapsed forks. We have

recently demonstrated that Metnase methylation of histone H3 promotes NHEJ repair factor recruitment to DSBs (Appendix 6.4). Thus, Metnase may act in similar ways at a stalled replication fork and modify histones in order to recruit repair factors to the fork.

Alternatively, Metnase could influence fork restart through its direct interaction with TopoIIα, another factor within the mammalian replisome [122]. TopoIIα is proposed to relax positive supercoils that form ahead of replication forks [120]. When replication forks stall, the MCM helicase complex can continue to unwind duplex DNA, uncoupled from the replicative polymerases, producing excess ssDNA that is bound by RPA and triggering the intra-S checkpoint [115, 173]. Continued DNA unwinding by MCM will also increase positive supercoiling that may drive unusual DNA structures at stalled forks [174]. By enhancing TopoIIα-dependent relaxation of positive supercoils, Metnase could promote a favorable topological state that results in timely fork restart, particularly when unusual structures form, such as replication fork regression (chicken feet), since the resolution of such structures is probably dependent on the topology of the stalled fork. Local topology could also influence restart of collapsed forks since HR-mediated invasion of broken ends into sister chromatids requires unwinding of the sister duplex. However, when we used TopoIIα inhibitors to test whether TopoIIα affected fork restart by DNA fiber analysis, fiber distributions were not affected (Figures 4-13 and 4-14). Thus, it is unlikely that the Metnase interaction with TopoIIα is important for restarting stalled forks. These results also suggest that the Metnase role in fork

restart is distinct from its role in promoting TopoIIα-mediated chromosome decatenation [146]. Note that the models described above are not mutually exclusive: Metnase may have different roles depending on the specific structures at stalled or collapsed replication forks, and may interact with different proteins depending on the type of function required.

5.4. Metnase may function independent of ATM

We hypothesized that Metnase may be regulated by the DNA repair PI3 kinase ATM since Metnase is involved in replication fork re-start and this kinase is known to be present at stalled replication forks, where it recruits and phosphorylates other repair factors. Treatment with the ATM inhibitor KU55933 showed that cells lacking Metnase were not affected in their colony formation abilities by the inhibition of ATM (Figure 4-16); which could suggest that Metnase and ATM do act in the same pathway and thus no difference in colony survival is observed when both proteins are functionally absent. Our observation that forks were not affected by the absence of Metnase when ATM was inhibited supports the idea that Metnase is not downstream of ATM signaling at a stalled replication fork. Alternatively, it is possible that Metnase functions upstream of ATM signaling and thus no differences would be observed in the DNA fiber assay. ATM has other downstream targets that are not only important for stalled replication fork stabilization, but also for the recruitment of replication fork repair factors. Those proteins could be interacting or regulating Metnase recruitment or function at a stalled replication fork. Chk1 is a protein kinase that acts

downstream of ATR and to a lesser extent ATM, and it plays an important role in DNA damage checkpoint control [167]. Chk1 becomes activated via phosphorylation of Ser 317 in response to blocked DNA replication [168] and it has been shown that phosphorylation at Ser 317, in conjunction with phosphorylation of PTEN, is important for cells to reenter the cycle following replication fork stalling [170]. We observed that phosphorylation of Chk1 at serine 317 was diminished in the absence of Metnase. These results support the hypothesis that Metnase regulates Chk1 as measured by Chk1 phosphorylation. Additionally, this may explain why cells lacking Metnase have a delayed S-phase progression: in cells lacking Metnase, Chk1 is not phosphorylated at serine-317 and cells are unable to re-enter the cell cycle after checkpoint arrest caused by HU damage. I hypothesize that the lack of Chk1 phosphorylation is not permanent since there are other factors, such as the MRN complex, that activate ATM/ATR at a stalled replication fork. Additionally, we observed that Metnase knock-down cells eventually recover from the S-phase delay, 24 h after treatment with HU (Figures 4-5 – 4-7). Nonetheless, this observation is very interesting and points to a potential mechanism by which Metnase may be regulating replication fork stabilization or repair.

5.5. PARP-1 and Metnase may function in the same pathway to repair stalled replication forks

PARP-1 is another example of a late-evolving protein, with functions in NHEJ and replication fork restart [132]. PARP-1 is not found in yeast, but is present in higher eukaryotes. It recruits the ancient DNA repair endonuclease MRE11 (a member of the MRN complex) to stalled forks, which is proposed to process structures at the forks, leading to RPA recruitment and eventual restart via HR. Additionally, we know that Metnase and Nbs1 (another member of the MRN complex) interact in response to IR damage [149]. Thus, Metnase and PARP-1 may functionally interact to promote fork restart at stalled replication forks. Metnase knock-down increases the number of PARP-1 foci in HU-treated cells (Figure 4-18); suggesting that Metnase helps resolve replication fork specific PARP-1 foci. A recent paper by the Helleday laboratory places PARP-1 at stalled replication forks by DNA fiber assays and BrdU foci co-localization [132]. Additionally, the same study demonstrated that PARP-1 mediates Mre11-dependent replication fork re-start. Thus, it is possible Metnase and PARP-1 collaborate to stabilize stalled replication forks through a common target, perhaps the MRN complex.

5.6. Limitations of this work

There are several limitations inherent in Metnase studies. The first limitation is that Metnase is only present in higher primates, thus it is difficult to study it in the context of animal models, such as mice or rats. This limits the

approach and the types of questions that can be addressed. For example, we have yet to ask whether Metnase plays any role in embryonic development, including bone marrow lineage determination, or cancer predisposition directly. However, the Hromas laboratory has been able to overexpress Metnase in mouse cells and make some interesting observations regarding chromosomal translocations, indicating that although Metnase is not present in mice, it is functional in mouse cells within the context of DNA DSB repair (Appendix 6.2 is a detailed review of mechanisms of leukemia translocations and the role of Metnase in these processes). This could open up avenues to investigate the role of Metnase in DNA repair pathways in a system where the protein is overexpressed. One can also imagine inducing tumors in animals and adding Metnase protein or Metnase inhibitors to study the function of Metnase in cancer progression and metastasis. A technical limitation of the present study is that it was done in only three cell lines. Thus, further testing of other cells, including primary cells, will be necessary to corroborate the observations made here. Additionally, due to the difficulties we encountered when growing Metnase knock-down cells and the lack of a high quality antibody against the native protein Metnase, most of the work presented here was done using overexpression of Metnase and in some cases using a V5-tagged version of the protein for protein isolation and Western blot analysis. These problems are likely to be overcome in the near future as the Hromas laboratory is producing a more specific monoclonal antibody against Metnase, and new technologies have

recently become available that will make the process of knocking down Metnase much easier.

5.7. Novel contributions to the field

The work presented here has contributed to the field of DNA repair in two ways: technical and knowledge based, both of which have advanced the field. There are two technical contributions. First, the optimization of the adenovirus expressing the restriction enzyme ISce-I for assays such as ChIP and HR, without causing extensive damage to cells, will facilitate future DNA repair studies. The Ad-ISce-I system creates a clean DSB in a consistent and reproducible manner, comparable to the HO endonuclease used to study yeast DSB repair. The power of this new tool is apparent in the work described in (Appendix 6.4). In addition, the optimization of the DNA fiber assay will facilitate studies that will lead to a better understanding of DNA. Secondly, this work adds to the understanding of the novel protein Metnase and its role in DNA replication. It adds a novel Metnase function in DNA replication fork repair to the growing list of Metnase functions and offers an explanation as to how this replication fork repair function may be regulated by identifying novel Metnase interacting factors. This is significant because Metnase could be used as a possible target for developing inhibitors that can be used as a cancer chemotherapy.

5.8. Future work

The work presented here has raised many important questions. One of the most basic question concerns the interactions between Metnase and other repair and replication stress response proteins. For example, does Metnase interact directly with PCNA and Rad9? If so, what are the specific interaction domains and how are these interactions regulated? Are there any post-translational modifications such as phosphorylation or methylation required for these interactions or for the “activation” or “deactivation” of these factors? It is known that Metnase automethylates, and automethylation regulates its functional interaction with TopoIIα-mediated chromosomal decatenation and that it methylates other factors such as histone H3 [148]. Therefore, it is important to study the methylase mutant produced by the Hromas laboratory to determine the significance of the methylase in each Metnase function. Once specific interaction domains have been identified, mutations in these domains should be analyzed in the assays used in the present study to determine how protein-protein interactions regulate Metnase function in the context of stalled replication forks.

Another question to address is whether Metnase acts in the same pathway as ATM at a stalled fork, and if so, how is this regulated? Some of the possible mutants already identified, such as the automethylation mutant, could be used to test whether Metnase methylation activity is upstream of ATM/ATR activation. Metnase has two potential PI3 kinase target sites that are under investigation. Additionally, one PI3 kinase has yet to be investigated in the context of Metnase in replication fork stabilization, DNA-PK. Although DNA-PK is

a well-characterized NHEJ specific kinase, there is new evidence that DNA-PK may also play a role in replication fork stabilization, and that this function may be related to PARP-1 [132]. The Helleday laboratory has already demonstrated that cells lacking DNA-PK show a similar, though less severe, replication fork restart defect to compared Metnase knock-down cells. It would be interesting to investigate whether a lack of Metnase would further prevent DNA-PK -/- cells from stabilizing a stalled replication fork (see Appendix 6.3 for details on DNA-PK and stalled replication forks, Fig 7). Another question to address is whether Metnase is directly phosphorylated by any of these kinases. ATM, ATR and/or DNA-PK may directly or indirectly regulate Metnase at stalled or collapsed replication forks.

Our preliminary results showed that cells lacking Metnase were unable to resolve PARP-1 foci after damage by HU. It will be interesting to determine whether this phenotype is HU specific or whether other DNA replication fork stressors, such as UV and CPT, would have a similar effect. Additionally, it would be interesting to determine if lack of Metnase augments the PARP-1 -/- phenotype observed by the Helleday laboratory as well. Does Metnase methylate PARP-1 as a way to regulate PARP-1 activity? If so, how is this modification regulated? Is there a direct interaction between PARP-1 and Metnase? Are the roles of Metnase and PARP-1 in replication fork stabilization related to their respective roles in NHEJ? This seems unlikely because Metnase and PARP-1 do not function in the same type of NHEJ pathway. Metnase functions in classical NHEJ while PARP-1 is thought to be part of the alternative

NHEJ pathway. However, during replication, it is possible that they work together in order to facilitate faster repair, perhaps by enhancing recruitment of other repair factors.

One very interesting issue, but technically demanding to address, is protein dynamics at a stalled replication fork: What factors are present, how quickly are they recruited, and how long are they retained? This would be best addressed by using Chromatin immunoprecipitation (ChIP) of various proteins at stalled replication forks. Dr. Sheema Mir in the Hromas lab, was able to detect NHEJ factor recruitment to a specific DSB site and characterize the kinetics of recruitment, and how this is regulated by Metnase's methylation of histone H3, using the Ad-ISce-I system I optimized (Appendix 6.4). It is possible that Metnase plays a similar role at stalled replication forks. Thus, Metnase may be recruited to stalled forks, and through methylation of histone H3 or other proteins, promote recruitment of proteins necessary for signaling and/or repair of the damage. I predict that this function of Metnase would be backed-up by another, slower mechanism since the replication phenotype, although severe in the short term, seems to be resolved within hours.

5.9. Concluding remarks

Prior studies have established that Metnase is highly expressed in actively proliferating tissues [139]. It has recently been shown that Metnase is frequently overexpressed in leukemia cell lines compared to normal counterparts. Importantly, downregulating Metnase greatly enhances tumor cell sensitivity to common chemotherapeutics including epididophylotoxins and anthracyclines [147, 148]. The current study establishes Metnase as a critical factor in the replication stress response. Metnase is therefore an excellent target for therapeutic strategies that block DNA synthesis, or that exploit defects of tumor cells in replication fork restart [175, 176], and it may prove to be an important target in the treatment of a wide variety of tumor types.

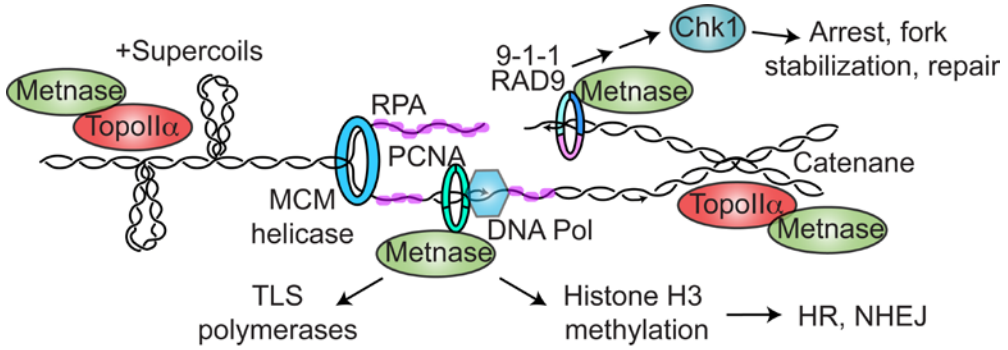

Figure 5-1. Potential roles of Metnase in the replication stress response.

We have shown here that Metnase interacts with PCNA and 9-1-1 component Rad9. Additionally, Metnase interacts with TopoIIα and stimulates relaxation of positively supercoiled DNA ahead of the replication fork. Previous work from our laboratory demonstrated that Metnase enhances chromosomal decatenation (behind the replication fork).

6. APPENDICES

6.1. Regulation of DNA double-strand break repair pathway choice

Authors: Meena Shrivastav, Leyma P De Haro, and Jac A Nickoloff

Cell Research (2008) 18:134-147.

Cell Research (2008) 18:134-147.

www.nature.com/cr

REVIEW

Regulation of DNA double-strand break repair pathway choice

Meena Shrivastav[1], Leyma P De Haro[1], Jac A Nickoloff[1]

[1]*Department of Molecular Genetics and Microbiology, University of New Mexico School of Medicine and Cancer Center, Albuquerque, NM 87131, USA*

DNA double-strand breaks (DSBs) are critical lesions that can result in cell death or a wide variety of genetic alterations including large- or small-scale deletions, loss of heterozygosity, translocations, and chromosome loss. DSBs are repaired by non-homologous end-joining (NHEJ) and homologous recombination (HR), and defects in these pathways cause genome instability and promote tumorigenesis. DSBs arise from endogenous sources including reactive oxygen species generated during cellular metabolism, collapsed replication forks, and nucleases, and from exogenous sources including ionizing radiation and chemicals that directly or indirectly damage DNA and are commonly used in cancer therapy. The DSB repair pathways appear to compete for DSBs, but the balance between them differs widely among species, between different cell types of a single species, and during different cell cycle phases of a single cell type. Here we review the regulatory factors that regulate DSB repair by NHEJ and HR in yeast and higher eukaryotes. These factors include regulated expression and phosphorylation of repair proteins, chromatin modulation of repair factor accessibility, and the availability of homologous repair templates. While most DSB repair proteins appear to function exclusively in NHEJ or HR, a number of proteins influence both pathways, including the MRE11/RAD50/NBS1(XRS2) complex, BRCA1, histone H2AX, PARP-1, RAD18, DNA-dependent protein kinase catalytic subunit (DNA-PKcs), and ATM. DNA-PKcs plays a role in mammalian NHEJ, but it also influences HR through a complex regulatory network that may involve crosstalk with ATM, and the regulation of at least 12 proteins involved in HR that are phosphorylated by DNA-PKcs and/or ATM.

Keywords: DNA repair, non-homologous end-joining, homologous recombination, DNA-PK, ATM, chromatin, genome stability

Cell Research (2008) **18**:134-147. doi: 10.1038/cr.2007.111; published online 24 December 2007

Introduction

DNA double-strand breaks (DSBs) pose a serious threat to cell viability and genome stability. DSBs are generated naturally when replication forks encounter blocking lesions such as those produced by metabolic byproducts of cellular respiration (reactive oxygen species (ROS)) leading to fork collapse [1]; during programmed genome rearrangements induced by nucleases, including yeast mating-type switching [2], V(D)J recombination [3], class-switch recombination [4], and meiosis [5]; and from physical stress when dicentric or catenated chromosomes are pulled to opposite poles during mitosis [6, 7]. DSBs are also produced when cells are exposed to DNA damaging agents including ionizing radiation (IR), which creates DSBs directly and indirectly via production of ROS [8]; chemical agents and UV light that create replication blocking lesions (alkyl adducts, pyrimidine dimers, and crosslinks) [9, 10]; and cancer chemotherapeutics that poison topoisomerase I, which produces replication-blocking lesions, or topoisomerase II, which traps the enzyme-DNA complex after DSB induction and can potentially produce DSBs during any phase of the cell cycle [11]. The failure to repair DSBs, or misrepair, can result in cell death or large-scale chromosome changes including deletions, translocations, and chromosome fusions that enhance genome instability and are hallmarks of cancer cells. Cells have evolved groups of proteins that function in signaling networks that sense DSBs or other DNA damage, arrest the cell cycle, and activate DNA repair pathways. These cellular responses

Correspondence: Jac A Nickoloff
Tel: +1 505 272 6960; Fax: +1 505 272 6029
E-mail: JNickoloff@salud.unm.edu

can occur at various stages of the cell cycle and are collectively called DNA damage checkpoints, but when cells suffer too much damage overlapping signaling pathways can trigger apoptosis to prevent propagation of cells with highly unstable genomes [12].

Eukaryotic cells repair DSBs primarily by two mechanisms: nonhomologous end-joining (NHEJ) and homologous recombination (HR). Frank DSBs, such as those produced by nucleases and IR, can be repaired by either pathway. DSBs produced by replication fork collapse are repaired primarily (or perhaps exclusively) by HR [1, 13]. Note that fork collapse produces a one-ended DSB, better described as a "double-strand end" (DSE). Because a DSE at a collapsed fork has no second end with which to rejoin, it is difficult to imagine how NHEJ can contribute to the repair of collapsed replication forks (Figure 1A). However, this does not rule out indirect roles for NHEJ proteins in replication fork restart (see below). Here we review factors that regulate DSB repair pathway choice, and therefore the discussion is focused primarily on the repair of frank DSBs (Figure 1B).

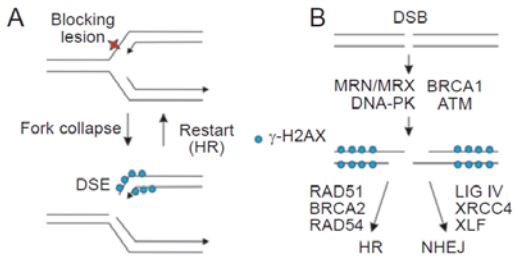

Figure 1 Differences between DSEs and DSBs. **(A)** Replication forks stall and may collapse when they encounter a blocking lesion or a nick, producing a DSE which induces H2AX phosphorylation adjacent to the break. Fork restart typically involves HR proteins. **(B)** A frank DSB may be repaired by NHEJ or HR. There is rapid phosphorylation of H2AX adjacent to DSBs, but in the immediate vicinity of the broken ends nucleosome eviction (and perhaps other processes such as histone exchange) results in reduced levels of γ-H2AX. Repair pathway choice may be controlled by the early acting proteins that influence both repair pathways. Once the commitment is made to a repair pathway, pathway-specific proteins drive the reaction toward HR or NHEJ products.

NHEJ and HR both contribute to genome stability and both pose risks of large- and small-scale genome rearrangement

NHEJ and HR pathways are often described as "error-prone" and "error-free" respectively, but this is an oversimplification. "Clean" DSBs with complementary overhangs, 5′ phosphates and 3′ hydroxyl groups, such as those produced by nucleases, can be precisely repaired by NHEJ. In yeast and mammalian cells, 25-50% of nuclease DSBs are repaired by precise NHEJ [14, 15]; note that these are minimum estimates because these measurements do not account for multiple cycles of cleavage and precise repair. When ends cannot be precisely rejoined, NHEJ typically involves alignment of one or a few complementary bases ("microhomology") to direct repair, leading to small deletions and sometimes small insertions. In mammalian cells NHEJ proceeds in a stepwise manner beginning with limited end-processing by the MRE11/RAD50/NBS1 (MRN) complex and perhaps other factors, end-binding by Ku comprising the Ku70 and Ku80 subunits, and recruitment of the DNA-dependent protein kinase catalytic subunit (DNA-PKcs), forming the trimeric DNA-PK holoenzyme. Once bound to broken ends, DNA-PK is activated and it phosphorylates itself and other targets including RPA, WRN, and Artemis; in cells lacking ATM, DNA-PK can also phosphorylate histone H2AX, termed γ-H2AX [16-24]. In the final step, DNA ligase IV, with its binding partners XRCC4 and XLF (also called Cernunnos), seals the break. The nuclease Artemis helps repair a subset of IR-induced DSBs by NHEJ, and is important for opening hairpins formed during V(D)J recombination [25, 26]. Terminal deoxynucleotidyl transferase (TdT) and two members of the polymerase X family (pol μ and pol λ) can modify NHEJ outcomes by non-templated addition of nucleotides to ends or by extending a 3′ single-stranded DNA (ssDNA) tail that can transiently pair via microhomology on the other broken end [27]. The breast cancer tumor suppressor protein BRCA1 has a role in NHEJ that may involve modulation of MRE11 [28], or chromatin remodeling via the Fanconi anemia ubiquitylation pathway [29]. An alternative Ligase III-mediated NHEJ pathway is promoted by PARP-1 and is more error-prone than classical NHEJ [30]. The yeast NHEJ machinery includes homologs of all of these proteins except DNA-PKcs, Artemis, and BRCA1. Further details about NHEJ protein biochemistry and repair mechanisms can be found in recent reviews [31-34] and in articles in this volume by Weterings and Chen, and Lieber *et al.*

HR is considered a more accurate mechanism for DSB repair because broken ends use homologous sequences elsewhere in the genome (sister chromatids, homologous chromosomes, or repeated regions on the same or different chromosomes) to prime repair synthesis. If the repair template is perfectly homologous, repair can be 100% accurate, although even in this case there is evidence from yeast that the repair polymerase is more error-prone than replicative polymerases, and point mutations arise at increased frequencies adjacent to DSB repair sites [35]. With the exception of sister chromatids, repair templates are often

not perfectly homologous, and in these cases HR results in loss of heterozygosity, with information transferred non-reciprocally from the unbroken (donor) locus to the broken (recipient) locus, a process termed gene conversion [36].

HR initiates with extensive 5′ to 3′ end-processing at broken ends, which in yeast is regulated by Mre11/Rad50/Xrs2 (MRX, the functional homolog of MRN), Exo1, and at least one other exonuclease [37]. The resulting 3′ ssDNA tails are bound by RPA, which is replaced with Rad51 in a reaction mediated by Rad52 and two Rad51 paralogs, Rad55 and Rad57. The resulting Rad51 nucleoprotein filament searches for and invades a homologous sequence, a process facilitated by Rad54. The Srs2 helicase is thought to dissociate Rad51 from ssDNA, allowing normal base-pairing of the invading and complementary donor strands and subsequent strand extension by DNA polymerase. The extended strand can dissociate and anneal with the processed end of the non-invading strand on the opposite side of the DSB in a process called synthesis-dependent strand annealing (SDSA), or both ends may invade producing a double-Holliday junction that is resolved to yield crossover or non-crossover recombinants. Once intermediates are resolved, the remaining ssDNA gaps and nicks are repaired by DNA polymerase and DNA ligase. As with NHEJ, most HR proteins are conserved through evolution, although mammals harbor a more elaborate set. For example, there are five Rad51 paralogs in mammals (Rad51B/C/D and XRCC2/3) but just two in yeast (Rad55/57). During meiotic HR, the Rad51 homolog Dmc1 participates in strand exchange with Rad51, an association conserved from yeast to human. Several mammalian HR proteins do not have homologs in yeast, including BRCA1 and BRCA2. As with NHEJ, the role of BRCA1 in HR is unclear, but it interacts with BRCA2 and functions within the Fanconi's anemia protein ubiquitylation pathway that may regulate protein-protein interactions and/or accessibility of repair factors to damage sites [29]. More detailed information about HR protein biochemistry and repair mechanisms is available in several recent reviews [2, 36-38] and in the article by Li and Heyer in this issue.

Crossovers are associated with a fraction of HR events and can have a stabilizing or destabilizing effect on the genome. In meiosis, crossovers are highly regulated such that at least one crossover occurs between each pair of homologous chromosomes to ensure proper chromosome segregation, yet excess crossovers are suppressed [39]. In mitosis, crossovers pose serious risks of large-scale genome alterations: half of the G2 phase crossovers between homologs result in loss of heterozygosity from the point of the crossover to the telomere, and crossovers between repeated regions on non-homologous chromosomes, the same chromosome, or sister chromatids can result in translocations, inversions, deletions, and gene duplications [36]. Defects in proteins that suppress mitotic crossovers, such as Sgs1 in yeast and its human homolog BLM, increase genome instability, and BLM defects also predispose to cancer [40, 41].

Yeast mutants lacking key HR proteins (i.e., Mre11, Rad51, Rad52, Rad54) are viable, but DSBs often go unrepaired and this results in cell death in haploids. Diploids usually survive the loss of a broken chromosome, or a full chromosome complement can be retained if a single end invades the homologous chromosome and primes repair synthesis to the end of the chromosome (> 100 Kb distant in some cases), a process called "break-induced replication" that results in large-scale loss of heterozygosity [42, 43]. In contrast, loss of key HR proteins in higher eukaryotes, including RAD51, BRCA1, and BRCA2, results in cell and/or embryonic lethality; viable mutants in these cases typically carry hypomorphic alleles or lethality is suppressed by p53 mutations. In other cases, as with mutations in higher eukaryotic HR proteins (e.g., RAD52 and RAD54), the HR defects are milder than those of the corresponding yeast mutant [44-46]. Although it has been argued that these differences may reflect changes in the functions of these proteins through evolution [47], we would argue that the greater requirement for RAD51 and BRCA1/2 in higher eukaryotes reflects the essential role of HR in restarting blocked or collapsed replication forks, which is probably required 100-fold more often in higher eukaryotes than in yeast because higher eukaryotic genomes are 100-fold larger than the yeast genome. The reduced requirement for certain HR proteins in higher eukaryotes may reflect diverged functions and/or functional redundancy with the elaboration of HR protein families and addition of new HR proteins, as proposed for RAD52 and BRCA2 [48].

Although NHEJ is responsible for the vast majority of tumorigenic chromosomal translocations [49], and even "correct" re-joining of broken ends by NHEJ often results in mutations at junctions, the NHEJ machinery plays a significant role in maintaining genome stability and suppressing tumorigenesis [50-54]. These results indicate that NHEJ is not indiscriminate, but instead mediates DSB repair with a fair degree of fidelity. The genome-stabilizing and tumor-suppressing functions of the HR machinery are similarly well established [36]. Thus, both DSB repair pathways play critical roles in maintaining genome stability and preventing cancer. In the following sections we discuss how cells modulate the relative levels of the two DSB repair pathways, and their respective fidelities, to maintain an appropriate level of genome stability. Several factors are important in this regulation, including the availability of repair templates, cell cycle phase, proliferation rate, and the functions of specific cell types.

DSB repair pathway choice in yeast and higher eukaryotes

Early studies of cell killing by IR gave rise to the notion that HR is the dominant mechanism of DSB repair in yeast. Yeast has very limited capacity for imprecise NHEJ, which is the main option for NHEJ repair of "dirty" ends produced by IR, as these ends require processing before rejoining in a process regulated by the MRX complex. Note that MRX also regulates the more extensive end-processing that resects broken ends to long 3′ tails early in HR; this resection is slowed but not eliminated in *mre11* mutants [55, 56], or in *mre11 exo1* double mutants, indicating that at least one other nuclease is involved [37]. MRX plays a critical role in processing IR-induced DSBs, and in removing Spo11 nuclease, which remains covalently bound to broken ends after it creates meiotic DSBs. Thus, both IR-induced HR and meiotic HR are markedly reduced in *mre11* mutants [57, 58]. In contrast, *mre11* mutants show relatively mild (< 2-fold) defects in HR stimulated by "clean" DSBs produced by HO nuclease [43, 55, 59], indicating that the low level of IR-induced HR in *mre11* mutants does not reflect an HR defect *per se*. By contrast, *mre11* mutation decreases (precise) NHEJ of HO-induced DSBs by ~100-fold [60, 61]. When HR is blocked and yeast cells are forced to repair a nuclease DSB by imprecise NHEJ, cell survival is a measure of such repair, which ranges from 0.01% to 0.2% [14, 61, 62]. In this assay, HO nuclease is expressed continuously; precise repair recreates the HO recognition site, which gets cleaved again; so cells are forced to repair DSBs by imprecise NHEJ to break the futile cycle. The low efficiency of imprecise NHEJ contrasts with the robust capacity of yeast to repair these DSBs by precise NHEJ, which we estimated at a minimum of 25% based on the increase in HR when NHEJ was blocked by *yku70*Δ mutation [14]; the remaining DSBs are repaired by the robust HR pathway.

It is not known why imprecise NHEJ is so inefficient in yeast compared to mammals, but the most likely reason is that mammals have at least three NHEJ proteins that are absent in yeast: DNA-PKcs, BRCA1, and Artemis. We propose that DNA-PKcs is the key missing protein because it facilitates alignment of non-complementary ends and regulates end-processing during NHEJ [63, 64]; BRCA1 has broader roles in DNA repair as well as roles in transcription and other cellular functions [65, 66], and Artemis has specialized roles in processing a small subset of broken ends [25].

Both precise and imprecise NHEJ are robust in higher eukaryotes. It can be difficult to distinguish precise NHEJ in a chromosomal context from the failure to induce a DSB, and precise NHEJ of transfected linear plasmids has often been used as a surrogate. The Waldman lab devised a clever assay with an integrated substrate carrying two I-*Sce*I nuclease recognition sites to show that the frequency of precise NHEJ is ~50% in mouse cells [15]. Naturally, imprecise NHEJ predominates for IR-induced DSBs, although this is strongly affected by cell cycle phase (see below). The imprecision of NHEJ during V(D)J recombination, initiated by RAG1/2 nuclease-induced DSBs, plays a major role in generating antibody diversity in mammals [67]. It is likely that robust imprecise NHEJ repair systems were a key driving force behind the evolution of adaptive immune systems.

The greater use of imprecise NHEJ in higher eukaryotes may also be related to their larger genome size. Although random small-scale deletions and insertions may have a lesser chance of affecting coding sequences in a mammalian genome (comprising only ~3% of the genome) than in a yeast genome (> 70% coding), it is now recognized that as much as 50% of mammalian genomes are transcribed into functional RNAs, including many microRNAs that regulate gene expression. The larger genomes of higher eukaryotes present a greater challenge of locating a homologous template for HR repair. However, it is remarkable that HR between ectopic loci, and between allelic loci on homologous chromosomes, is very efficient (albeit quite slow) even in the cells with the largest genomes. Nuclear architecture appears to confine chromosomes to well-defined territories, both in yeast and in mammalian cells [68, 69]. Although homologs are usually not in close proximity, chromosome territories could limit the "search space" and increase the efficiency of HR.

Differential DSB repair pathway choices in different cell types of a single species

A key factor that regulates HR efficiency is template availability; thus, it is not surprising that HR is more efficient in diploid than in haploid yeast. However, the relationship between ploidy and HR efficiency in yeast is not simple. It has been known for almost 50 years that tetraploids are more radiosensitive than diploids, and diploids that express both *MAT* alleles (*MAT***a** and *MAT*α – termed **a**/α) are more radioresistant than diploids that express only one copy of *MAT* (**a**/**a** or α/α diploids) [70]. These and other results indicate that HR efficiency is independently regulated by ploidy and the *MAT* loci [71-73]. Enhanced HR with greater availability of homologous templates indicates that template accessibility is rate limiting for HR. Of course, template availability increases in all cells when DNA is replicated in S phase; this factor is discussed in the section on cell cycle regulation below.

The mechanisms by which *MAT* heterozygosity enhances HR are still under investigation. One way to enhance

HR is to suppress or genetically inactivate NHEJ, as seen in yeast and mammalian cells [14, 74-76], and this strategy is used by wild-type yeast: the Nej1 protein interacts with Lif1 and enhances the ligase activity of the Dnl4/Lif1 complex, but Nej1 is expressed only in haploids because *NEJ1* is repressed by *MAT***a**1/α2, the transcriptional repressor expressed in (*MAT* heterozygous) diploids. *nej1*Δ mutants show an NHEJ defect as strong as NHEJ mutants *yku70/80*, *dnl4*, and *lif1* [77-79], and the suppression of Nej1 expression in diploids decreases NHEJ by ~10-fold. The expression of other NHEJ proteins does not appear to be regulated by *MAT*. Thus, an important mechanism by which haploids upregulate NHEJ and downregulate HR (and vice versa in diploids) is through *MAT*-dependent regulation of Nej1, and the variable contributions of NHEJ and HR in haploid and diploid yeast reflect independent changes in both DSB repair pathways.

A recent study showed that mutations in a number of genes regulated by the *MAT***a**1/α2 repressor (and other genes not regulated by *MAT*) suppressed the hypersensitivity of specific *rad51*, *rad52*, and *rad55* mutants to DNA damage induced by camptothecin and phelomycin. These suppressor mutations occurred in genes that encode NHEJ proteins like Nej1, the meiosis repressor Rme1 and its co-regulator Sin3, chromatin-associated proteins Pst2 and Rfs1, and an unknown protein Ygl193c [80]. Interestingly, these suppressor mutations acted differently for each of the HR protein defects, suggesting an extremely complex regulatory network. Note that some or perhaps most of these suppressor mutations do not act by directly regulating HR, particularly mutations in NHEJ genes. For example, the enhanced survival of *rad55*Δ *nej1*Δ relative to *rad55*Δ after treatment with camptothecin may reflect a reduction in lethal chromosome fusions mediated by NHEJ repair of the many DSBs that form when replication forks encounter DNA lesions [80].

HR plays a relatively minor role in DSB repair in many but not all types of higher eukaryotic cells. For example, chicken B lymphocytes generate antibody diversity via DSB repair by gene conversion rather than by imprecise NHEJ during V(D)J recombination as is common in mammals, so it is not surprising that HR is more robust in chicken B cells than in most types of mammalian cells. The high HR capacity of chicken B cells allows efficient HR-mediated gene targeting and gene replacement, and this has propelled chicken B cells, exemplified by the DT-40 system, to the forefront of vertebrate somatic cell genetics [81].

Mouse embryonic stem (ES) cells also display enhanced HR capacity that facilitates gene targeting and construction of novel mutant mice. A plausible explanation for the hyper-recombination phenotype of mouse ES cells is based on the observation that these rapidly dividing cells, while genotypically $p53^+$, are functionally $p53^-$ (or p53-suppressed) with respect to DNA damage responses [82]. Importantly, p53 is a well-known suppressor of HR [83-88]; thus, the functional inactivation of p53 in ES cells can explain their increased HR capacity. The p53 DNA damage response may be suppressed in ES cells to prevent cell cycle arrest during the early stages of development, which require rapid cell division. Note that ES cells retain a p53-independent apoptotic response pathway to rid the organism of cells with damaged genomes. It is equally plausible (and not mutually exclusive) that p53 is suppressed to enhance HR so that stalled or collapsed replication forks are restarted in a timely manner during the rapid cell divisions in early embryogenesis, and perhaps also to upregulate accurate DSB repair to help maintain genome integrity during this critical developmental stage.

Recent evidence indicates that NHEJ and HR are modulated during different stages of nervous system development in mice. This was inferred from genetic analysis showing that HR defects increased apoptosis in proliferating neural precursor cells and NHEJ defects increased apoptosis later in development, in differentiating cells [89]. The lack of effect of NHEJ defects during early development of the nervous system suggests not only that HR activity is enhanced, but also that HR is the predominant mode of DSB repair at this stage of development [89]. This suggests that there may be active suppression of NHEJ during early neural development. The stronger role for HR in proliferating nervous tissue early in development is reminiscent of the situation in ES cells noted above.

Cell-cycle regulation of DSB repair pathways

It has been known for some time that the balance between NHEJ and HR shifts during the cell cycle. Recent studies have begun to clarify the molecular mechanisms that regulate these cyclical shifts in the two repair pathways (summarized in Figure 2). Because template accessibility influences HR efficiency, it is not surprising that cells upregulate HR during S and G2 phases of the cell cycle when sister chromatids are available. In fact, sister chromatids are the preferred template for HR repair in yeast and mammalian cells [44, 90]. This preference probably reflects a proximity effect mediated by the close association of sister chromatids from the time they form in S phase until they segregate in anaphase. Sister chromatid cohesion is mediated by cohesins, and recent evidence indicates that cohesins migrate to DSB repair sites independently of the normal replication cycle [91]. Sister chromatid cohesion is a property of all eukaryotic cells. Yet, NHEJ remains active throughout S and G2 phases of the cell cycle [92]. This indicates that NHEJ competes for DSBs even when

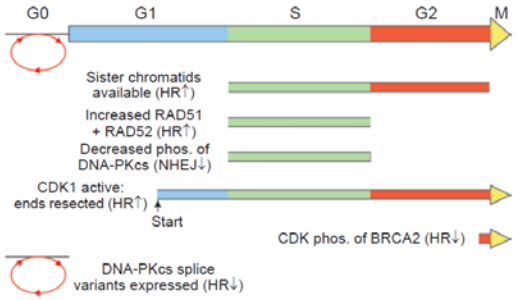

Figure 2 Cell cycle regulation of DSB repair pathway choice. The cell cycle is shown at the top and each line below indicates a specific mechanism that regulates NHEJ or HR in the indicated cell cycle phases. G0 indicates quiescent (non-cycling) cells.

homologous templates are in the immediate vicinity.

Increasing evidence indicates that the shift from NHEJ toward HR as cells progress from G1 to S/G2 is actively regulated in lower and higher eukaryotes. Early studies showed that RAD51 and RAD52 expression increases during S phase [93]. Cyclin-dependent kinases (CDKs) are key regulators of cell cycle progression. In *Saccharomyces cerevisiae*, the Cdc28 (CDK1) kinase is activated at a point in G1 phase called "Start" which commits to progress to S phase [94]. Ira *et al.* [95] analyzed resection of HO-induced DSBs at *MAT* and found that G1-arrested cells failed to initiate efficient end resection, which prevented loading of RPA and Rad51, and blocked Mec1 activation. Resection depends on CDK1 activity because suppression of CDK1 in G2 cells by overexpression of the CDK1 inhibitor Sic1, or by use of a mutant form of CDK1 blocked by the ATP analog 1-NMMPP1, also prevented end-resection and checkpoint activation. Interestingly, blocking CDK1 led to the persistence of Mre11 at the DSB site, suggesting that CDK1 activity is not required for MRX recruitment to broken ends, but is required for MRX regulation of end resection [95]. The Rad51 nucleoprotein filament is required for the homology search and strand invasion steps of HR. Thus, HR is blocked when ssDNA resection is prevented by inhibition of CDK1, and in early G1 when CDK1 is inactive.

Aylon *et al.* [96] reached similar conclusions using cells arrested in G1 with α-factor, a temperature-sensitive *cdc4* mutant that cannot initiate replication, and in cells treated with hydroxyurea, which blocks replication. In all cases HR was defective in the arrested cells. However, HR was observed in a significant fraction of a *cdc7* mutant population. The *cdc7* mutation prevents replication initiation, but not progression through later cell cycle phases in cells shifted to the restrictive temperature after replication has initiated. The fact that HR is blocked even in G1-arrested diploid cells argues that HR is tightly regulated by CDK-dependent cell cycle controls, and that the presence of a homologous template is not sufficient for HR competence. Given the suppression of HR in early G1, it is not surprising that G1-arrested budding yeast cells are capable of repairing DSBs by NHEJ [96], and similar results were obtained in fission yeast [97]. Caspari *et al.* [98] identified additional CDK-mediated HR regulatory mechanisms in fission yeast, showing that the Cdc2-cyclin B CDK is important in early HR when Rhp51 (Rad51 homolog) is assembled onto ssDNA, and at a late HR stage in which topoisomerase III helps resolve HR intermediates.

CDKs also regulate HR in mammalian cells. The West laboratory showed that CDK-mediated phosphorylation of serine 3291 of BRCA2 blocks the interaction of RAD51 with this C-terminal region of BRCA2 [99]. More recently, this group has shown that this phospho-regulated binding site for RAD51 recognizes RAD51 in its multimeric forms, including DNA-bound RAD51 nucleoprotein filaments and DNA-free multimers [100]. This particular phosphorylation is maximal in M phase and therefore represents one of the mechanisms by which HR is downregulated in M and early G1 phase. Interestingly, this cell cycle control of HR was bypassed when cells were irradiated, as this led to a rapid decrease in serine 3291 phosphorylation and increased association of BRCA2 with RAD51 to promote DSB repair by HR. Although not directly addressed experimentally, it seems likely that the decreased serine 3291 phosphorylation after IR is cell cycle independent, i.e., the DNA damage response network is able to bypass the normal cell cycle control of the BRCA2-RAD51 interaction.

A key requirement for mammalian NHEJ is the phosphorylation of clusters of serine and threonine residues in DNA-PKcs, targeted by DNA-PKcs itself and ATM. DNA-PKcs is *trans*-autophosphorylated at a cluster of six residues that includes T2609 (also called "ABCDE") [101, 102], at a separate cluster that includes S2056 (also called "PQR") [18, 103], and at T3950 [104]. T2609 is also phosphorylated by ATM – see below. DNA-PKcs kinase activity and phosphorylation of T2609 and T3950 are critical for NHEJ and cellular radioresistance [102, 105, 106]. Phosphorylation of the S2056 and T2609 clusters is reduced in irradiated S phase cells [103], and this may be part of a regulatory system that downregulates NHEJ in S phase. This model is consistent with biochemical assays showing decreased DNA-PK activity in S phase HeLa cells [107].

Proteins at the HR/NHEJ interface

The idea that the two DSB repair pathways compete for

DSBs was suggested by early experiments showing that plasmid DNA transfected into mammalian cells could be repaired by either pathway [108], and biochemical studies showing both NHEJ and HR proteins bind to broken ends [reviewed in refs. 109, 110]. The increase in HR seen in cells with NHEJ defects is consistent with passive shunting of DSBs from NHEJ to HR [14, 74-76]. However, it was recognized early that yeast Mre11 influenced both pathways [111], raising the possibility that the competition between the two pathways might be actively controlled, and several other proteins are now implicated in both pathways, including BRCA1, histone H2AX, PARP-1, RAD18, DNA-PKcs, and ATM. Although NHEJ factors are recruited to DSBs more rapidly than HR factors, and NHEJ and HR factors are independently recruited to DSBs, there is a significant period of time when both sets of factors are present at damage sites [112], consistent with the notion that pathway choice may be regulated by one or more proteins that act in both pathways.

As mentioned above, BRCA1 involvement in HR remains unclear but may reflect functional interactions with BRCA2, a critical mediator of the RAD51 strand transferase [66, 113-115], and its role in the Fanconi's anemia ubiquitylation pathway [29]. It is not clear how BRCA1 promotes NHEJ, although a study showing that BRCA1 negatively regulates end-processing by MRE11 endo- and exonucleases [116] suggests a plausible mechanism by which BRCA1 can influence both pathways. With respect to NHEJ, BRCA1 suppression of MRN-mediated end-processing may enhance NHEJ accuracy [reviewed in refs. 28, 115]. A recent report demonstrates that Chk2 phosphorylation of BRCA1 influences the fidelity of NHEJ [117]. Together, the results indicate that BRCA1 promotes genome stability by promoting error-free HR and by maximizing the fidelity of NHEJ. Because BRCA1 functions in both DSB repair pathways, it is possible that BRCA1 regulates pathway choice, but as yet there is no direct evidence to support this idea.

Histone H2AX is a subunit of the nucleosome that is rapidly phosphorylated over megabase domains at DSBs in mammalian chromatin, principally by ATM and ATR. The yeast H2AX homolog, H2A, is phosphorylated over kilobase domains at DSBs by the ATM and ATR homologs Tel1 and Mec1. H2AX phosphorylation plays a key role in DNA damage checkpoint activation, and its dephosphorylation is important for attenuating the checkpoint signal to allow the cell cycle to resume ([118], see also Huen and Chen in this volume). Mutation of the phosphorylated serine 129 residue in yeast H2A causes sensitivity to DNA-damaging agents and confers an NHEJ defect [119]. A recent study showed that deletions or amino acid substitutions in both C- and N-terminal H2A tails confer an NHEJ defect [120]. However, the nature of NHEJ defect is unclear because it was revealed in an assay involving rejoining of a transfected plasmid, which may not be chromatinized prior to repair. Mutation of the analogous residue in mouse H2AX (serine 139) confers a defect in conservative DSB repair by gene conversion [121]. Although direct measures of HR in yeast H2A mutants have not been reported, H2A phosphorylation is important for recruitment or retention of checkpoint and other repair factors to DSBs. For example, recruitment of the INO80 chromatin remodeling complex depends on H2A phosphorylation, and deletion of the INO80 subunit Arp8 results in ~4-fold reductions in HO-nuclease-induced *MAT* switching in haploids and allelic HR in diploids (Y-C Lo, T Tsukuda, R Sterk, S Krishna, MA Osley, JA Nickoloff, unpublished results). A recent study identified an interaction between the mouse Polycomb Group YY1 transcription factor and the INO80 chromatin remodeling complex, and showed that siRNA knockdown of either YY1 or the Ino80 subunit caused a specific defect in HR repair of DSBs [122]. It will be interesting to determine whether mammalian chromatin remodeling complexes like YY1-INO80 also regulate NHEJ. The roles of chromatin modification and remodeling in DNA repair were recently reviewed ([123, 124], see also the article by Huen and Chen in this issue).

PARP-1 functions with Ligase III in an alternative, lower fidelity NHEJ pathway, and PARP-1 competes with Ku for DSB ends [30]. Interestingly, PARP-1 defective DT-40 cells reportedly show reduced HR levels, inferred from camptothecin hypersensitivity, and normal resistance to camptothecin was restored in the PARP-1 defect cells by mutations that inactivate NHEJ [125]. Defects in RAD18 showed the same hypersensitivity and genetic interactions with NHEJ, and the double PARP-1/RAD18-defective mutant showed synergistic hypersensitivity to camptothecin, suggesting that RAD18 and PARP-1 independently promote HR and antagonize NHEJ [125]; however, a conflicting result was obtained in mouse ES cells [126]. Here, the PARP-1 mutant showed enhanced HR measured directly as enhanced HR-mediated gene targeting. While the reason for this discrepancy is not clear, these studies implicate PARP-1 (and RAD18) in regulating DSB repair pathway choice.

As mentioned above, increased HR in cells with NHEJ defects can be explained by a passive competition model. However, several lines of evidence suggest that DNA-PKcs is an active regulator of DSB repair pathway choice. The first evidence for this was the puzzling finding that inactivation of NHEJ by elimination of DNA-PKcs increased HR [74], but chemical inhibition of DNA-PKcs had the opposite effect [127]. Phosphorylation of DNA-PKcs is important for NHEJ [105], and biochemical experiments indicate that phosphorylation of the T2609 cluster causes

DNA-PKcs to dissociate from broken ends [106, 128-133]. Together, these results suggested a model in which chemically inhibited DNA-PKcs fails to dissociate from ends and thereby blocks access to other NHEJ repair factors and to HR repair factors. The inhibition of both DSB repair pathways by the specific inhibition of DNA-PKcs has important implications for tumor radiosensitization [127]. The importance of phosphorylation of DNA-PKcs for HR was underscored by a study showing that complementation of DNA-PKcs null CHO V3 cells with DNA-PKcs lacking the T2609 cluster sites gave the same phenotype as chemical inhibition of wild-type DNA-PKcs, i.e., HR was suppressed. Thus, blocking phosphorylation of the T2609 cluster converts DNA-PKcs into a dominant-negative regulator of HR [18].

The idea that DNA-PKcs regulates DSB repair pathway choice gained additional support when the Meek laboratory identified DNA-PKcs splice variants that lack the kinase domain [134]. Given the importance of DNA-PKcs kinase activity for NHEJ [105], it was not surprising that these kinase-inactive variants do not complement the radiosensitivity of DNA-PKcs null cells. However, the variants were particularly interesting because they had dominant negative effects on HR repair of DSBs, and therefore mimicked chemically inhibited full-length DNA-PKcs and the T2609 cluster mutant. The variants are expressed along with full-length DNA-PKcs only in quiescent cells, but they do not have a dominant negative effect on NHEJ. These results suggest that co-expression of full-length DNA-PKcs and kinase-inactive variants limits HR in quiescent cells, which lack preferred sister chromatid HR repair templates, while simultaneously maintaining a high capacity for DSB repair by NHEJ [134]. These results strongly support the notion that DNA-PKcs is a key regulator of DSB repair pathway choice in higher eukaryotes.

Co-regulation of HR by DNA-PKcs and ATM

HR is stimulated when DNA-PKcs is absent, but repressed when DNA-PKcs is chemically inhibited, harbors mutations in the T2609 autophosphorylation cluster, or is expressed as a kinase-inactive splice variant. We therefore reasoned that expression of a kinase-inactive mutant of DNA-PKcs (harboring a single lysine to arginine change near the kinase active site, K3752R) would similarly act as a dominant negative regulator of HR. Surprisingly, when CHO V3 cells were complemented with the K3752R mutant protein, HR was stimulated, with levels ~3-fold above the already elevated HR level seen in DNA-PKcs null cells (manuscript submitted). We used immunofluorescence microscopy to demonstrate that DNA-PKcs recruitment to foci after IR occurs independently of its kinase activity, suggesting that the kinase-inactive K3752R mutant somehow upregulates HR despite its association with broken ends and its inability to be autophosphorylated.

Several lines of evidence help explain the hyper-recombination phenotype of the K3752R mutant. First, ATM levels are reduced in cells lacking DNA-PKcs [135], but we found that ATM levels are restored in DNA-PKcs null cells upon expression of the DNA-PKcs K3752R mutant protein. Thus, DNA-PKcs regulates ATM levels independently of DNA-PKcs kinase activity. Second, two studies have shown that the DNA-PKcs T2609 cluster is also phosphorylated by ATM [102, 136]. DNA-PKcs has another cluster of phosphorylation sites that includes S2056, and phosphorylation of the T2609 and S2056 clusters regulates accessibility of repair factors to DSBs [18, 106, 128-133], but, unlike the T2609 cluster, the S2056 cluster is subject only to autophosphorylation [136]. Thus, in cells expressing DNA-PKcs K3752R, the S2056 cluster is not phosphorylated. Mutations in the S2056 cluster that block phosphorylation increase DSB-induced HR above the wild-type level, but not above the level seen in DNA-PKcs null cells [18]. Thus, the higher HR levels with DNA-PKcs K3752R cannot simply be due to failure to phosphorylate the S2056 cluster, but probably reflect the combined positive effects of preventing S2056 cluster phosphorylation, and the absence of competition by NHEJ. Presumably, the kinase-inactive DNA-PKcs K3752R mutant still needs to be released from broken ends by T2609 cluster phosphorylation, which is mediated by ATM [102, 136]. In this model, ATM-mediated phosphorylation of the T2609 cluster is one mechanism by which ATM promotes HR in cells expressing the DNA-PKcs K3752R mutant. Note that HR is strongly reduced by chemical inhibitors of DNA-PKcs and by kinase-inactive DNA-PKcs splice variants, but HR is strongly enhanced by kinase-inactive DNA-PKcs harboring the single amino acid K3752R mutation. One possibility is that DNA-PKcs adopts a conformation that blocks ATM phosphorylation of the T2609 cluster when inhibitors are bound to the DNA-PKcs active site, and when the protein lacks the entire kinase domain. The K3752R mutation, on the other hand, would be expected to have little or no effect on the gross structure of DNA-PKcs, and the mutant protein should therefore be recognized and phosphorylated by ATM in the same way as wild-type DNA-PKcs.

A second independent mechanism of HR promotion by ATM is through phosphorylation of other targets. ATM phosphorylates many targets, at least 12 of which have direct or indirect roles in HR (Figure 3A). Interestingly, 6 of these targets are also phosphorylated by DNA-PKcs. The role of ATM in HR has been puzzling. Spontaneous HR is enhanced in ATM-defective cells [137], but this may reflect a replication- or checkpoint-specific effect. For DSB-in-

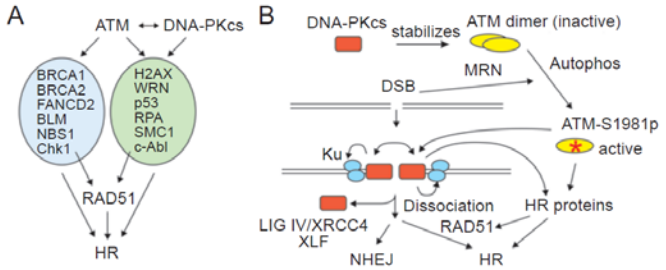

Figure 3 Model for co-regulation of NHEJ and HR by DNA-PKcs and ATM. **(A)** Lists of proteins involved in HR that are phosphorylated by ATM, and the subset that are phosphorylated by DNA-PKcs. ATM also phosphorylates DNA-PKcs. **(B)** DNA-PKcs stabilizes ATM, shown at the top as an inactive dimer. DSBs lead to MRN recruitment, ATM autophosphorylation on serine 1981, and dissociation into active monomers. The Ku heterodimer also arrives early at DSBs and recruits DNA-PKcs, which becomes activated upon DNA end-binding and phosphorylates itself, Ku, and other proteins. DNA-PKcs is phosphorylated by itself and ATM, causing DNA-PKcs to dissociate from ends and allowing access to NHEJ and HR proteins. In the absence of DNA-PKcs, ATM levels drop and HR is mildly enhanced because NHEJ no longer competes for DSBs. When DNA-PKcs is chemically inhibited, it remains bound to ends, blocking access to both HR and NHEJ factors. When DNA-PKcs harbors a point mutation in the kinase domain, it no longer supports NHEJ but does stabilize ATM, and ATM is able to phosphorylate its T2609 cluster (and all HR factors in panel **A**), greatly increasing HR.

duced HR, ATM appears to have a positive role [138, 139], perhaps through phosphorylation of H2AX [121]. However, direct measurements of DSB-induced HR showed no differences between wild-type and ATM-defective cells [140, 141], perhaps because DNA-PKcs fulfilled this role. Note that DNA-PKcs and ATM do not show simple redundancy with regard to H2AX phosphorylation. DNA-PKcs can phosphorylate H2AX in the absence of ATM, but not in its presence, or even in the presence of kinase-inactive ATM, suggesting that ATM physically blocks DNA-PKcs access to H2AX [reviewed in ref. 24]. Defects in mouse ATM and DMC1 confer similar meiotic HR defects [142]. Caffeine inhibits ATM (and other PI3 kinases) and markedly reduces DSB-induced HR [143], and we also found that the ATM-specific inhibitor KU55933 [144] blocks formation of IR-induced RAD51 foci (manuscript submitted). Together, these results support the idea that ATM promotes HR repair of DSBs. A positive role for ATM in HR can also explain the puzzling finding that DNA-PKcs null cells are hypersensitive to replication-blocking agents, which was taken as evidence of a limited role for NHEJ in restarting collapsed replication forks [145]. However, because DSEs at collapsed forks have no second end with which to rejoin (Figure 1A), we propose an alternative explanation, that in the absence of DNA-PKcs the reduced levels of ATM [135] inhibit HR-mediated replication fork restart.

In summary, HR is elevated in cells expressing DNA-PKcs K3752R and DNA-PKcs null cells because NHEJ competition is eliminated, and we propose that HR levels are highest in the DNA-PKcs K3752R mutant because the mutant protein restores ATM to its normal level and ATM is thus able to exert its full positive effect on HR, including phosphorylation of a large number of HR proteins, and the DNA-PKcs T2609 cluster to facilitate access of HR proteins to the broken ends (Figure 3B). ATM is also a positive regulator of NHEJ after IR [146], which reflects at least in part the phosphorylation of Artemis [25], and ATM has an important role in stabilizing broken ends during NHEJ-mediated V(D)J recombination [147], but these functions are unlikely to impact HR induced by nuclease DSBs.

Potential benefits of DSB repair pathway analysis

As we gain a better understanding of DSB repair mechanisms and the regulation of pathway choice, it is likely that basic mechanistic insights will translate into clinical benefits. The complex network of DSB repair proteins and the regulatory proteins including the PI3 kinases DNA-PKcs, ATM and ATR represent a rich set of potential targets to exploit in the development of more effective chemo- and radiotherapeutic strategies in cancer therapy. These targets may also be useful as biomarkers of genome instability to improve our ability to detect cancer in its earliest stages when treatments are most effective. Human gene therapy is currently hindered by risks associated with random integration of transgenes, with significant potential for insertional mutagenesis of tumor suppressors or inappropriate activation of oncogenes. Targeted gene therapy, including accurate gene replacement and transgene insertion into low-risk regions of the genome, depends on suppressing

NHEJ-mediated random integration and enhancing HR-mediated integration into desired loci. The proteins that regulate the choice between NHEJ and HR are excellent targets to manipulate to enhance gene targeting and unleash the full potential of targeted gene therapy with minimum risk of untoward side effects.

Acknowledgments

We thank D Chen and BPC Chen (University of Texas Southwestern Medical Center, USA), S Lees-Miller (University of Calgary, Canada), K Meek (Michigan State University, USA), MA Osley (University of New Mexico, USA), and members of the Nickoloff lab for helpful discussions and excellent collaborations. Our research on the NHEJ/HR interface is supported by National Cancer Institute Grant R01 CA100862 to JA Nickoloff.

References

1 Shen Z, Nickoloff JA. Mammalian homologous recombination repair and cancer intervention. In: Wei Q, Li L, Chen DJ, eds. DNA Repair, Genetic Instability, and Cancer. Singapore: World Scientific Publishing Co., 2007:119-156.
2 Paques F, Haber JE. Multiple pathways of recombination induced by double-strand breaks in *Saccharomyces cerevisiae*. *Microbiol Mol Biol Rev* 1999; **63**:349-404.
3 Franco S, Alt FW, Manis JP. Pathways that suppress programmed DNA breaks from progressing to chromosomal breaks and translocations. *DNA Repair (Amst)* 2006; **5**:1030-1041.
4 Chaudhuri J, Basu U, Zarrin A, *et al*. Evolution of the immunoglobulin heavy chain class switch recombination mechanism. *Adv Immunol* 2007; **94**:157-214.
5 Keeney S, Neale MJ. Initiation of meiotic recombination by formation of DNA double-strand breaks: mechanism and regulation. *Biochem Soc Trans* 2006; **34**:523-525.
6 Murnane JP. Telomeres and chromosome instability. *DNA Repair (Amst)* 2006; **5**:1082-1092.
7 Acilan C, Potter DM, Saunders WS. DNA repair pathways involved in anaphase bridge formation. *Genes Chromosomes Cancer* 2007; **46**:522-531.
8 Ward J. The nature of lesions formed by ionizing radiation. In: Nickoloff JA, Hoekstra MF, eds. DNA Damage and Repair: DNA Repair in Higher Eukaryotes. Totowa, NJ: Humana Press, 1998:65-84.
9 Limoli CL, Giedzinski E, Bonner WM, Cleaver JE. UV-induced replication arrest in the xeroderma pigmentosum variant leads to DNA double-strand breaks, γ-H2AX formation, and Mre11 relocalization. *Proc Natl Acad Sci USA* 2002; **99**:233-238.
10 Bosco EE, Mayhew CN, Hennigan RF, *et al*. RB signaling prevents replication-dependent DNA double-strand breaks following genotoxic insult. *Nucleic Acids Res* 2004; **32**:25-34.
11 Degrassi F, Fiore M, Palitti F. Chromosomal aberrations and genomic instability induced by topoisomerase-targeted antitumour drugs. *Curr Med Chem Anticancer Agents* 2004; **4**:317-325.
12 Su TT. Cellular responses to DNA damage: one signal, multiple choices. *Annu Rev Genet* 2006; **40**:187-208.
13 Rothstein R, Michel B, Gangloff S. Replication fork pausing and recombination or "gimme a break". *Genes Dev* 2000; **14**:1-10.
14 Clikeman JA, Khalsa GJ, Barton SL, Nickoloff JA. Homologous recombinational repair of double-strand breaks in yeast is enhanced by *MAT* heterozygosity through yKu-dependent and -independent mechanisms. *Genetics* 2001; **157**:579-589.
15 Lin Y, Lukacsovich T, Waldman AS. Multiple pathways for repair of double-strand breaks in mammalian chromosomes. *Mol Cell Biol* 1999; **19**:8353-8360.
16 Burma S, Chen BP, Murphy M, Kurimasa A, Chen DJ. ATM phosphorylates histone H2AX in response to DNA double-strand breaks. *J Biol Chem* 2001; **276**:42462-42467.
17 Collis SJ, DeWeese TL, Jeggo PA, Parker AR. The life and death of DNA-PK. *Oncogene* 2005; **24**:949-961.
18 Cui X, Yu Y, Gupta S, *et al*. Autophosphorylation of DNA-dependent protein kinase regulates DNA end processing and may also alter double-strand break repair pathway choice. *Mol Cell Biol* 2005; **25**:10842-10852.
19 Shao RG, Cao CX, Zhang H, *et al*. Replication-mediated DNA damage by camptothecin induces phosphorylation of RPA by DNA-dependent protein kinase and dissociates RPA:DNA-PK complexes. *EMBO J* 1999; **18**:1397-1406.
20 Burma S, Chen DJ. Role of DNA-PK in the cellular response to DNA double-strand breaks. *DNA Repair (Amst)* 2004; **3**:909-918.
21 Chan DW, Ye RQ, Veillette CJ, Lees-Miller SP. DNA-dependent protein kinase phosphorylation sites in Ku 70/80 heterodimer. *Biochemistry* 1999; **38**:1819-1828.
22 Karmakar P, Piotrowski J, Brosh RM, *et al*. Werner protein is a target of DNA-dependent protein kinase *in vivo* and *in vitro*, and its catalytic activities are regulated by phosphorylation. *J Biol Chem* 2002; **277**:18291-18302.
23 Yannone SM, Roy S, Chan DW, *et al*. Werner syndrome protein is regulated and phosphorylated by DNA-dependent protein kinase. *J Biol Chem* 2001; **276**:38242-38248.
24 Stucki M, Jackson SP. γH2AX and MDC1: anchoring the DNA-damage-response machinery to broken chromosomes. *DNA Repair (Amst)* 2006; **5**:534-543.
25 Riballo E, Kuhne M, Rief N, *et al*. A pathway of double-strand break rejoining dependent upon ATM, Artemis, and proteins locating to γ-H2AX foci. *Mol Cell* 2004; **16**:715-724.
26 Jeggo PA, O'Neill P. The Greek goddess, Artemis, reveals the secrets of her cleavage. *DNA Repair (Amst)* 2002; **1**:771-777.
27 Nick McElhinny SA, Havener JM, Garcia-Diaz M, *et al*. A gradient of template dependence defines distinct biological roles for family X polymerases in nonhomologous end joining. *Mol Cell* 2005; **19**:357-366.
28 Durant ST, Nickoloff JA. Good timing in the cell cycle for precise DNA repair by BRCA1. *Cell Cycle* 2005; **4**:1216-1222.
29 Huang TT, D'Andrea AD. Regulation of DNA repair by ubiquitylation. *Nat Rev Mol Cell Biol* 2006; **7**:323-334.
30 Wang M, Wu W, Wu W, *et al*. PARP-1 and Ku compete for repair of DNA double strand breaks by distinct NHEJ pathways. *Nucleic Acids Res* 2006; **34**:6170-6182.
31 Daley JM, Palmbos PL, Wu D, Wilson TE. Nonhomologous end joining in yeast. *Annu Rev Genet* 2005; **39**:431-451.
32 Lees-Miller SP, Meek K. Repair of DNA double strand breaks by non-homologous end joining. *Biochimie* 2003; **85**:1161-1173.

33 Burma S, Chen BP, Chen DJ. Role of non-homologous end joining (NHEJ) in maintaining genomic integrity. *DNA Repair (Amst)* 2006; **5**:1042-1048.
34 Rouse J, Jackson SP. Interfaces between the detection, signaling, and repair of DNA damage. *Science* 2002; **297**:547-551.
35 Strathern JN, Shafer BK, McGill CB. DNA synthesis errors associated with double-strand break repair. *Genetics* 1995; **140**:965-972.
36 Nickoloff JA. Recombination: mechanisms and roles in tumorigenesis. In: Bertino JR, ed. Encyclopedia of Cancer. 2nd Edition. San Diego, USA: Elsevier Science, 2002:49-59.
37 Krogh BO, Symington LS. Recombination proteins in yeast. *Annu Rev Genet* 2004; **38**:233-271.
38 West SC. Molecular views of recombination proteins and their control. *Nat Rev Mol Cell Biol* 2003; **4**:435-445.
39 Champion MD, Hawley RS. Playing for half the deck: the molecular biology of meiosis. *Nat Cell Biol* 2002; **4**(Suppl): s50-s56.
40 Myung K, Datta A, Chen C, Kolodner RD. SGS1, the *Saccharomyces cerevisiae* homologue of BLM and WRN, suppresses genome instability and homeologous recombination. *Nat Genet* 2001; **27**:113-116.
41 Cheok CF, Bachrati CZ, Chan KL, *et al*. Roles of the Bloom's syndrome helicase in the maintenance of genome stability. *Biochem Soc Trans* 2005; **33**:1456-1459.
42 Signon L, Malkova A, Naylor ML, Klein H, Haber JE. Genetic requirements for RAD51- and RAD54-independent break-induced replication repair of a chromosomal double-strand break. *Mol Cell Biol* 2001; **21**:2048-2056.
43 Krishna S, Wagener BM, Liu HP, *et al*. Mre11 and Ku regulation of double-strand break repair by gene conversion and break-induced replication. *DNA Repair (Amst)* 2007; **6**:797-808.
44 Dronkert MLG, Beverloo HB, Johnson RD, *et al*. Mouse *RAD54* affects DNA double-strand break repair and sister chromatid exchange. *Mol Cell Biol* 2000; **20**:3147-3156.
45 Essers J, Hendriks RW, Swagemakers SM, *et al*. Disruption of mouse RAD54 reduces ionizing radiation resistance and homologous recombination. *Cell* 1997; **89**:195-204.
46 Bezzubova O, Silbergleit A, Yamaguchi-Iwai Y, Takeda S, Buerstedde JM. Reduced X-ray resistance and homologous recombination frequencies in a RAD54$^{-/-}$ mutant of the chicken DT40 cell line. *Cell* 1997; **89**:185-193.
47 Sonoda E, Hochegger H, Saberi A, Taniguchi Y, Takeda S. Differential usage of non-homologous end-joining and homologous recombination in double strand break repair. *DNA Repair (Amst)* 2006; **5**:1021-1029.
48 Yang H, Jeffrey PD, Miller J, *et al*. BRCA2 function in DNA binding and recombination from a BRCA2-DSS1-ssDNA structure. *Science* 2002; **297**:1837-1848.
49 Zhang Y, Rowley JD. Chromatin structural elements and chromosomal translocations in leukemia. *DNA Repair (Amst)* 2006; **5**:1282-1297.
50 Karanjawala ZE, Grawunder U, Hsieh CL, Lieber MR. The nonhomologous DNA end joining pathway is important for chromosome stability in primary fibroblasts. *Curr Biol* 1999; **9**:1501-1504.
51 Ferguson DO, Sekiguchi JM, Chang S, *et al*. The nonhomologous end-joining pathway of DNA repair is required for genomic stability and the suppression of translocations. *Proc Natl Acad Sci USA* 2000; **97**:6630-6633.
52 Zha S, Alt FW, Cheng HL, Brush JW, Li G. Defective DNA repair and increased genomic instability in Cernunnos-XLF-deficient murine ES cells. *Proc Natl Acad Sci USA* 2007; **104**:4518-4523.
53 Sharpless NE, Ferguson DO, O'Hagan RC, *et al*. Impaired nonhomologous end-joining provokes soft tissue sarcomas harboring chromosomal translocations, amplifications, and deletions. *Mol Cell* 2001; **8**:1187-1196.
54 Tong WM, Cortes U, Hande MP, *et al*. Synergistic role of Ku80 and poly(ADP-ribose) polymerase in suppressing chromosomal aberrations and liver cancer formation. *Cancer Res* 2002; **62**:6990-6996.
55 Sugawara N, Haber JE. Characterization of double-strand break-induced recombination: homology requirements and single-stranded DNA formation. *Mol Cell Biol* 1992; **12**:563-575.
56 Lee SE, Moore JK, Holmes A, *et al*. *Saccharomyces* Ku70, Mre11/Rad50, and RPA proteins regulate adaptation to G2/M arrest after DNA damage. *Cell* 1998; **94**:399-409.
57 Bressan DA, Baxter BK, Petrini JHJ. The Mre11-Rad50-Xrs2 protein complex facilitates homologous recombination-based double-strand break repair in *Saccharomyces cerevisiae*. *Mol Cell Biol* 1999; **19**:7681-7687.
58 Moreau S, Ferguson JR, Symington LS. The nuclease activity of Mre11 is required for meiosis but not for mating type switching, end joining, or telomere maintenance. *Mol Cell Biol* 1999; **19**:556-566.
59 Ivanov EL, Sugawara N, White CI, Fabre F, Haber JE. Mutations in *XRS2* and *RAD50* delay but do not prevent mating-type switching in *Saccharomyces cerevisiae*. *Mol Cell Biol* 1994; **14**:3414-3425.
60 Milne GT, Jin S, Shannon KB, Weaver DT. Mutations in two Ku homologs define a DNA end-joining repair pathway in *Saccharomyces cerevisiae*. *Mol Cell Biol* 1996; **16**:4189-4198.
61 Moore JK, Haber JE. Cell-cycle and genetic requirements of two pathways of nonhomologous end-joining repair of double-strand breaks in *Saccharomyces cerevisiae*. *Mol Cell Biol* 1996; **16**:2164-2173.
62 Kramer KM, Brock JA, Bloom K, Moore JK, Haber JE. Two different types of double-strand breaks in *Saccharomyces cerevisiae* are repaired by similar *RAD52*-independent, nonhomologous recombination events. *Mol Cell Biol* 1994; **14**:1293-1301.
63 Hammarsten O, DeFazio LG, Chu G. Activation of DNA-dependent protein kinase by single-stranded DNA ends. *J Biol Chem* 2000; **275**:1541-1550.
64 Budman J, Chu G. Processing of DNA for nonhomologous end-joining by cell-free extract. *EMBO J* 2005; **24**:849-860.
65 Boulton SJ. Cellular functions of the BRCA tumour-suppressor proteins. *Biochem Soc Trans* 2006; **34**:633-645.
66 Brenneman MA. BRCA1 and BRCA2 in DNA repair and genome stability. In: Nickoloff JA, Hoekstra MF, eds. DNA Damage and Repair, Vol 3: Advances from Phage to Humans. Totowa, NJ: Humana Press, 2001:237-267.
67 Jung D, Giallourakis C, Mostoslavsky R, Alt FW. Mechanism and control of V(D)J recombination at the immunoglobulin heavy chain locus. *Annu Rev Immunol* 2006; **24**:541-570.
68 Cremer T, Cremer M, Dietzel S, *et al*. Chromosome territories – a functional nuclear landscape. *Curr Opin Cell Biol* 2006;

18:307-316.
69 Dekker J, Rippe K, Dekker M, Kleckner N. Capturing chromosome conformation. *Science* 2002; **295**:1306-1311.
70 Mortimer RK. Radiobiological and genetic studies on a polyploid series (haploid to hexaploid) of *Saccharomyces cerevisiae*. *Radiat Res* 1958; **9**:312-326.
71 Astrom SU, Okamura SM, Rine J. Yeast cell-type regulation of DNA repair. *Nature* 1999; **397**:310.
72 Lee SE, Paques F, Sylvan J, Haber JE. Role of yeast *SIR* genes and mating type in directing DNA double-strand breaks to homologous and non-homologous repair paths. *Curr Biol* 1999; **9**:767-770.
73 Nickoloff JA, Haber JE. Mating-type control of DNA repair and recombination in *Saccharomyces cerevisiae*. In: Nickoloff JA, Hoekstra MF, eds. DNA Damage and Repair, Vol 3: Advances from Phage to Humans. Totowa, NJ: Humana Press, 2001:107-124.
74 Allen C, Kurimasa A, Brennemann MA, Chen DJ, Nickoloff JA. DNA-dependent protein kinase suppresses double-strand break-induced and spontaneous homologous recombination. *Proc Natl Acad Sci USA* 2002; **99**:3758-3763.
75 Pierce AJ, Hu P, Han MG, Ellis N, Jasin M. Ku DNA end-binding protein modulates homologous repair of double-strand breaks in mammalian cells. *Genes Dev* 2001; **15**:3237-3242.
76 Delacote F, Han M, Stamato TD, Jasin M, Lopez BS. An *xrcc4* defect or Wortmannin stimulates homologous recombination specifically induced by double-strand breaks in mammalian cells. *Nucleic Acids Res* 2002; **30**:3454-3463.
77 Ooi SL, Shoemaker DD, Boeke JD. A DNA microarray-based genetic screen for nonhomologous end-joining mutants in *Saccharomyces cerevisiae*. *Science* 2001; **294**:2552-2556.
78 Valencia M, Bentele M, Vaze MB, *et al.* NEJ1 controls non-homologous end joining in *Saccharomyces cerevisiae*. *Nature* 2001; **414**:666-669.
79 Kegel A, Sjostrand JO, Astrom SU. Nej1p, a cell type-specific regulator of nonhomologous end joining in yeast. *Curr Biol* 2001; **11**:1611-1617.
80 Valencia-Burton M, Oki M, Johnson J, *et al.* Different mating-type-regulated genes affect the DNA repair defects of Saccharomyces RAD51, RAD52 and RAD55 mutants. *Genetics* 2006; **174**:41-55.
81 Yamazoe M, Sonoda E, Hochegger H, Takeda S. Reverse genetic studies of the DNA damage response in the chicken B lymphocyte line DT40. *DNA Repair (Amst)* 2004; **3**:1175-1185.
82 Aladjem MI, Itoh N, Utiyama H, Wahl GM. ES cells do not activate p53-dependent stress responses and undergo p53-independent apoptosis in response to DNA damage. *Curr Biol* 1998; **8**:145-155.
83 Mekeel KL, Tang W, Kachnic LA, *et al.* Inactivation of p53 results in high-rates of homologous recombination. *Oncogene* 1997; **14**:1847-1857.
84 Willers H, McCarthy EE, Wu B, *et al.* Dissociation of p53-mediated suppression of homologous recombination from G1/S cell cycle checkpoint control. *Oncogene* 2000; **19**:632-639.
85 Romanova LY, Willers H, Blagosklonny MV, Powell SN. The interaction of p53 with replication protein A mediates suppression of homologous recombination. *Oncogene* 2004; **23**:9025-9033.
86 Akyuz N, Boehden GS, Susse S, *et al.* DNA substrate dependence of p53-mediated regulation of double-strand break repair. *Mol Cell Biol* 2002; **22**:6306-6317.
87 Gatz SA, Wiesmuller L. p53 in recombination and repair. *Cell Death Differ* 2006; **13**:1003-1016.
88 Yoon D, Wang Y, Stapleford K, Wiesmuller L, Chen J. P53 inhibits strand exchange and replication fork regression promoted by human Rad51. *J Mol Biol* 2004; **336**:639-654.
89 Orii KE, Lee Y, Kondo N, McKinnon PJ. Selective utilization of nonhomologous end-joining and homologous recombination DNA repair pathways during nervous system development. *Proc Natl Acad Sci USA* 2006; **103**:10017-10022.
90 Kadyk LC, Hartwell LH. Sister chromatids are preferred over homologs as substrates for recombinational repair in *Saccharomyces cerevisiae*. *Genetics* 1992; **132**:387-402.
91 Watrin E, Peters JM. Cohesin and DNA damage repair. *Exp Cell Res* 2006; **312**:2687-2693.
92 Takata M, Sasaki MS, Sonoda E, *et al.* Homologous recombination and non-homologous end-joining pathways of DNA double-strand break repair have overlapping roles in the maintenance of chromosomal integrity in vertebrate cells. *EMBO J* 1998; **17**:5497-5508.
93 Chen FQ, Nastasi A, Shen ZY, *et al.* Cell cycle-dependent protein expression of mammalian homologs of yeast DNA double-strand break repair genes *RAD51* and *RAD52*. *Mutat Res* 1997; **384**:205-211.
94 Toone WM, Aerne BL, Morgan BA, Johnston LH. Getting started: regulating the initiation of DNA replication in yeast. *Annu Rev Microbiol* 1997; **51**:125-149.
95 Ira G, Pellicioli A, Balijja A, *et al.* DNA end resection, homologous recombination and DNA damage checkpoint activation require CDK1. *Nature* 2004; **431**:1011-1017.
96 Aylon Y, Liefshitz B, Kupiec M. The CDK regulates repair of double-strand breaks by homologous recombination during the cell cycle. *EMBO J* 2004; **23**:4868-4875.
97 Ferreira MG, Cooper JP. The fission yeast Taz1 protein protects chromosomes from Ku-dependent end-to-end fusions. *Mol Cell* 2001; **7**:55-63.
98 Caspari T, Murray JM, Carr AM. Cdc2-cyclin B kinase activity links Crb2 and Rqh1-topoisomerase III. *Genes Dev* 2002; **16**:1195-1208.
99 Esashi F, Christ N, Gannon J, *et al.* CDK-dependent phosphorylation of BRCA2 as a regulatory mechanism for recombinational repair. *Nature* 2005; **434**:598-604.
100 Esashi F, Galkin VE, Yu X, Egelman EH, West SC. Stabilization of RAD51 nucleoprotein filaments by the C-terminal region of BRCA2. *Nat Struct Mol Biol* 2007; **14**:468-474.
101 Douglas P, Sapkota GP, Morrice N, *et al.* Identification of *in vitro* and *in vivo* phosphorylation sites in the catalytic subunit of the DNA-dependent protein kinase. *Biochem J* 2002; **368**:243-251.
102 Chan DW, Chen BP-C, Prithivirasingh S, *et al.* Autophosphorylation of the DNA-dependent protein kinase catalytic subunit is required for rejoining of DNA double-strand breaks. *Genes Dev* 2002; **16**:2333-2338.
103 Chen BP, Chan DW, Kobayashi J, *et al.* Cell cycle dependence of DNA-dependent protein kinase phosphorylation in response to DNA double strand breaks. *J Biol Chem* 2005; **280**:14709-14715.
104 Douglas P, Cui X, Block WD, *et al.* The DNA-dependent protein

kinase catalytic subunit is phosphorylated *in vivo* on threonine 3950, a highly conserved amino acid in the protein kinase domain. *Mol Cell Biol* 2007; **27**:1581-1591.
105 Kurimasa A, Kumano S, Boubnov NV, *et al*. Requirement for the kinase activity of human DNA-dependent protein kinase catalytic subunit in DNA strand break rejoining. *Mol Cell Biol* 1999; **19**:3877-3884.
106 Ding Q, Reddy YV, Wang W, *et al*. Autophosphorylation of the catalytic subunit of the DNA-dependent protein kinase is required for efficient end processing during DNA double-strand break repair. *Mol Cell Biol* 2003; **23**:5836-5848.
107 Lee SE, Mitchell RA, Cheng A, Hendrickson EA. Evidence for DNA-PK-dependent and DNA-PK-independent DNA double-strand break repair pathways in mammalian cells as a function of the cell cycle. *Mol Cell Biol* 1997; **17**:1425-1433.
108 Roth D, Wilson JH. Relative rates of homologous and nonhomologous recombination in transfected DNA. *Proc Natl Acad Sci USA* 1985; **82**:3355-3359.
109 Haber JE. Partners and pathways: repairing a double-strand break. *Trends Biochem Sci* 2000; **16**:259-264.
110 Baumann P, West SC. Role of the human RAD51 protein in homologous recombination and double-stranded break repair. *Trends Biochem Sci* 1998; **23**:247-251.
111 Haber JE. The many interfaces of Mre11. *Cell* 1998; **95**:583-586.
112 Kim JS, Krasieva TB, Kurumizaka H, *et al*. Independent and sequential recruitment of NHEJ and HR factors to DNA damage sites in mammalian cells. *J Cell Biol* 2005; **170**:341-347.
113 Chen JJ, Silver D, Cantor S, Livingston DM, Scully R. BRCA1, BRCA2, and Rad51 operate in a common DNA damage response pathway. *Cancer Res* 1999; **59**:S1752-S1756.
114 Chen J, Silver DP, Walpita D, *et al*. Stable interaction between the products of the BRCA1 and BRCA2 tumor suppressor genes in mitotic and meiotic cells. *Mol Cell* 1998; **2**:317-328.
115 Gudmundsdottir K, Ashworth A. The roles of BRCA1 and BRCA2 and associated proteins in the maintenance of genomic stability. *Oncogene* 2006; **25**:5864-5874.
116 Paull TT, Cortez D, Bowers B, Elledge SJ, Gellert M. Direct DNA binding by Brca1. *Proc Natl Acad Sci USA* 2001; **98**:6086-6091.
117 Zhuang J, Zhang J, Willers H, *et al*. Checkpoint kinase 2-mediated phosphorylation of BRCA1 regulates the fidelity of nonhomologous end-joining. *Cancer Res* 2006; **66**:1401-1408.
118 Downey M, Durocher D. γH2AX as a checkpoint maintenance signal. *Cell Cycle* 2006; **5**:1376-1381.
119 Downs JA, Lowndes NF, Jackson SP. A role for *Saccharomyces cerevisiae* histone H2A in DNA repair. *Nature* 2000; **408**:1001-1004.
120 Moore JD, Yazgan O, Ataian Y, Krebs JE. Diverse roles for histone H2A modifications in DNA damage response pathways in yeast. *Genetics* 2007; **176**:15-25.
121 Xie A, Puget N, Shim I, *et al*. Control of sister chromatid recombination by histone H2AX. *Mol Cell* 2004; **16**:1017-1025.
122 Wu S, Shi Y, Mulligan P, *et al*. A YY1-INO80 complex regulates genomic stability through homologous recombination-based repair. *Nat Struct Mol Biol* 2007 Nov 18; doi:10.1038/nsmb1332.
123 Osley MA, Tsukuda T, Nickoloff JA. ATP-dependent chromatin remodeling factors and DNA damage repair. *Mutat Res* 2007; **618**:65-80.
124 Downs JA, Nussenzweig MC, Nussenzweig A. Chromatin dynamics and the preservation of genetic information. *Nature* 2007; **447**:951-958.
125 Saberi A, Hochegger H, Szuts D, *et al*. RAD18 and poly(ADP-ribose) polymerase independently suppress the access of nonhomologous end joining to double-strand breaks and facilitate homologous recombination-mediated repair. *Mol Cell Biol* 2007; **27**:2562-2571.
126 Dominguez-Bendala J, Masutani M, McWhir J. Down-regulation of PARP-1, but not of Ku80 or DNA-PKcs', results in higher gene targeting efficiency. *Cell Biol Int* 2006; **30**:389-393.
127 Allen C, Halbrook J, Nickoloff JA. Interactive competition between homologous recombination and non-homologous end joining. *Mol Cancer Res* 2003; **1**:913-920.
128 Chan DW, Lees-Miller SP. The DNA-dependent protein kinase is inactivated by autophosphorylation of the catalytic subunit. *J Biol Chem* 1996; **271**:8936-8941.
129 Calsou P, Frit P, Humbert O, *et al*. The DNA-dependent protein kinase catalytic activity regulates DNA end processing by means of Ku entry into DNA. *J Biol Chem* 1999; **274**:7848-7856.
130 Merkle D, Douglas P, Moorhead GBG, *et al*. The DNA-dependent protein kinase interacts with DNA to form a protein-DNA complex that is disrupted by phosphorylation. *Biochemistry* 2002; **41**:12706-12714.
131 Douglas P, Moorhead GBG, Ye RQ, Lees-Miller SP. Protein phosphatases regulate DNA-dependent protein kinase activity. *J Biol Chem* 2001; **276**:18992-18998.
132 Block WD, Yu Y, Merkle D, *et al*. Autophosphorylation-dependent remodeling of the DNA-dependent protein kinase catalytic subunit regulates ligation of DNA ends. *Nucleic Acids Res* 2004; **32**:4351-4357.
133 Reddy YV, Ding Q, Lees-Miller SP, Meek K, Ramsden DA. Non-homologous end joining requires that the DNA-PK complex undergo an autophosphorylation-dependent rearrangement at DNA ends. *J Biol Chem* 2004; **279**:39408-39413.
134 Convery E, Shin EK, Ding Q, *et al*. Inhibition of homologous recombination by variants of the catalytic subunit of the DNA-dependent protein kinase (DNA-PKcs). *Proc Natl Acad Sci USA* 2005; **102**:1345-1350.
135 Peng Y, Woods RG, Beamish H, *et al*. Deficiency in the catalytic subunit of DNA-dependent protein kinase causes down-regulation of ATM. *Cancer Res* 2005; **65**:1670-1677.
136 Chen BP, Uematsu N, Kobayashi J, *et al*. Ataxia telangiectasia mutated (ATM) is essential for DNA-PKcs phosphorylations at the Thr-2609 cluster upon DNA double strand break. *J Biol Chem* 2007; **282**:6582-6587.
137 Meyn MS. High spontaneous intrachromosomal recombination rates in ataxia-telangiectasia. *Science* 1993; **260**:1327-1330.
138 Morrison C, Sonoda E, Takao N, *et al*. The controlling role of ATM in homologous recombinational repair of DNA damage. *EMBO J* 2000; **19**:463-471.
139 Luo C-M, Tang W, Mekeel KL, *et al*. High frequency and error-prone DNA recombination in ataxia telangiectasia cell lines. *J Biol Chem* 1996; **271**:4497-4503.
140 Bolderson E, Scorah J, Helleday T, Smythe C, Meuth M. ATM is required for the cellular response to thymidine induced replication fork stress. *Hum Mol Genet* 2004; **13**:2937-2945.
141 Sakamoto S, Iijima K, Mochizuki D, *et al*. Homologous recom-

bination repair is regulated by domains at the N- and C-terminus of NBS1 and is dissociated with ATM functions. *Oncogene* 2007; **26**:6002-6009..

142 Barchi M, Mahadevaiah S, Di Giacomo M, *et al.* Surveillance of different recombination defects in mouse spermatocytes yields distinct responses despite elimination at an identical developmental stage. *Mol Cell Biol* 2005; **25**:7203-7215.

143 Wang H, Boecker W, Wang H, *et al.* Caffeine inhibits homology directed repair of I-SceI induced DNA double-strand breaks. *Oncogene* 2004; **23**:824-834.

144 Hickson I, Zhao Y, Richardson CJ, *et al.* Identification and characterization of a novel and specific inhibitor of the ataxia-telangiectasia mutated kinase ATM. *Cancer Res* 2004; **64**:9152-9159.

145 Lundin C, Erixon K, Arnaudeau C, *et al.* Different roles for nonhomologous end joining and homologous recombination following replication arrest in mammalian cells. *Mol Cell Biol* 2002; **22**:5869-5878.

146 Kuhne M, Riballo E, Rief N, *et al.* A double-strand break repair defect in ATM-deficient cells contributes to radiosensitivity. *Cancer Res* 2004; **64**:500-508.

147 Bredemeyer AL, Sharma GG, Huang CY, *et al.* ATM stabilizes DNA double-strand-break complexes during V(D)J recombination. *Nature* 2006; **442**:466-470.

6.2. Mechanisms of leukemia translocations

Authors: Jac A. Nickoloff, Leyma P. De Haro, Justin Wray and Robert Hromas

Current Opinion in Hematology (2008), 15:338–345.

Mechanisms of leukemia translocations

Jac A. Nickoloff, Leyma P. De Haro, Justin Wray and Robert Hromas

Departments of Molecular Genetics and Microbiology and Internal Medicine, the University of New Mexico Cancer Center, Albuquerque, New Mexico, USA

Correspondence to Robert Hromas, MD, Department of Internal Medicine, the University of New Mexico Cancer Center, Albuquerque, NM 87131, USA
Tel: +1 505 272 5837; fax: +1 505 272 5865;
e-mail: rhromas@salud.unm.edu

Current Opinion in Hematology 2008, 15:338–345

Purpose of review

This review highlights recent findings about the known DNA repair machinery, its impact on chromosomal translocation mechanisms and their relevance to leukemia in the clinic.

Recent findings

Chromosomal translocations regulate the behavior of leukemia. They not only predict outcome but they define therapy. There is a great deal of knowledge on the products of leukemic translocations, yet little is known about the mechanism by which those translocations occur. Given the large number of DNA double-strand breaks that occur during normal progression through the cell cycle, especially from V(D)J recombination, stalled replication forks or failed decatenation, it is surprising that leukemogenic translocations do not occur more frequently. Fortunately, hematopoietic cells have sophisticated repair mechanisms to suppress such translocations. When these defenses fail leukemia becomes far more common, as seen in inherited deficiencies of DNA repair. Analyzing translocation sequences in cellular and animal models, and in human leukemias, has yielded new insights into the mechanisms of leukemogenic translocations.

Summary

New data from animal models suggest a two hit origin of leukemic translocations, where there must be both a defect in DNA double-strand break repair and a subsequent failure of cell cycle arrest for leukemogenesis.

Keywords

chromosomal translocations, DNA double-strand break repair, nonhomologous end-joining, V(D)J recombination

Curr Opin Hematol 15:338–345

1065-6251

Introduction

The recognition that specific balanced chromosomal translocations not only were diagnostic of acute leukemia but also defined the future behavior of the disease was a seminal advance. Understanding how these translocations generated acute leukemias consumed much of the attention of those working in this area. The paradigm has been that acute leukemia required two genetic lesions, one which blocks differentiation of hematopoietic progenitors, usually a translocation that predates the formation of leukemia, and one that occurs later and stimulates proliferation, usually a point mutation [1]. However, the question of how such translocations are generated in the first place has received less attention. The mechanisms by which translocations originally occur are just beginning to be understood, as the pathways that repair DNA double-strand breaks (DSBs) are defined.

Requirements for chromosomal translocations

Chromosomal translocations require at least two simultaneous DSBs in separate chromosomes. A reciprocal translocation occurs when the free double-strand ends (DSEs) from one chromosome are ligated to the DSEs from the other. Thus, chromosomal translocations result from misrepair of DSBs. DSBs can be repaired through two major pathways, homologous recombination and nonhomologous end joining (NHEJ), both described below.

Chromosomal translocations reflect exchanges of chromosome arms and can theoretically occur between any loci on any two chromosomes. However, half of random exchanges produce unbalanced translocations that result in dicentric and acentric chromosomes (Fig. 1). Dicentric chromosomes typically cause lethal DSBs during mitosis, and acentric fragments are mitotically unstable and usually lost. Cells that manage to survive after forming a dicentric chromosome will usually show dramatic chromosomal instability as a result of breakage–bridge–fusion cycles, which are also a common outcome of telomere loss [2,3]. Translocations can also be reciprocal, with arms from different chromosomes switching places, or nonreciprocal if only one arm transfers to the broken end of another chromosome. Most

Figure 1 Types of chromosomal translocations

Nonhomologous chromosomes are diagrammed in gray or black, and circles indicate centromeres. Translocation junctions are often imperfect with small deletions or insertions created during NHEJ. Perfect junctions may be present in rare translocations that result from crossovers during homologous recombination. NHEJ, nonhomologous end joining.

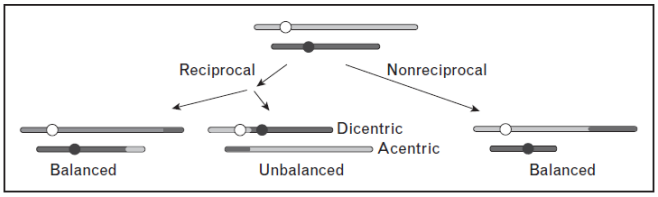

leukemia translocations are reciprocal translocations. Although reciprocal translocations can arise by crossing over during homologous recombination, most translocations appear to arise by NHEJ [4,5].

Because translocation involves joining fragments from different chromosomes, the basic requirements are two simultaneous DSBs, juxtaposition of the involved chromosomes, and abnormal DSB repair. There has been some debate about whether chromosomal translocations that are commonly seen in cancer reflect biases in DSB formation and chromosome juxtaposition or tumorigenic selection pressure. Even when it is clear that translocations result from defined DSBs, the requirement for rapid and uncontrolled growth imposes a strong selection for oncogene activation or tumor suppressor inactivation, and this selection pressure adequately explains translocation patterns in many cancers.

Translocations are greatly enhanced when DSBs occur simultaneously in two chromosomes [5]. For translocations to occur, the two broken ends at a DSB must first dissociate from each other and associate with broken ends from a different chromosome. Chromosomes occupy territories within the nucleus [6], suggesting another reason why DSBs at a certain locus may lead to a limited set of translocation products. For example, three-dimensional fluorescent in-situ hybridization (3D-FISH) analysis showed that mixed lineage leukemia (MLL) and its translocation partners, Eleven–nineteen leukaemia protein (ENL) and AML fused gene from chromosome 4 (AF4) are adjacently located in interphase nuclei [7]. Two factors that may regulate chromosome DSB end-coordination during NHEJ and homologous recombination are the Ku70/Ku80 heterodimer, which has end-binding, end-protection, and self-association activities, and the RAD50 subunit of the MRE11/RAD50/NBS1 (MRN) complex.

RAD50 is a member of the structural maintenance of chromosomes (SMC) protein family that may prevent translocations and other types of aberrant DSB repair by tethering broken ends [8]. Because translocations predominantly arise via NHEJ, it was surprising that the Ku70/Ku80 complex suppressed translocations. By monitoring broken ends cytologically, it was shown that in the presence of Ku70/Ku80, broken ends remain near each other for long periods of time, thus promoting their rejoining, whereas in cells lacking Ku70, ends migrate to different positions in the nuclease and repair is thus more likely to produce a translocation [9••,10••]. This result also indicates that these translocations are mediated by an alternative NHEJ pathway, independent of Ku70/Ku80.

Sources of endogenous double-strand breaks

DSBs arise spontaneously during normal DNA metabolism, including DNA replication and repair, and during programmed genome rearrangements, such as V(D)J recombination. Many DNA lesions block DNA polymerase, causing replication fork stalling. Stalled forks are stabilized by many factors including the checkpoint kinases ataxia telangiectasia mutated (ATM) and ataxia-telangiectasia and Rad3-related protein kinase (ATR), the DNA repair protein BLM, and the multifunctional single-strand DNA (ssDNA) binding protein replication protein A (RPA) [11]. However, if a stalled fork does not restart in timely manner, it may collapse, producing a DSE. Because a DSE has no second end with which to rejoin, conservative repair of collapsed replication forks is thought to involve homologous recombination-mediated strand invasion to reform the replication fork [12]. Alternatively, if multiple forks collapse, DSEs from different chromosomes may join and produce translocations.

In addition, topoisomerase IIα (TopoIIα) creates DSBs and passes double-stranded DNA through the break, decatenating tangled chromosomes before mitosis. If decatenation fails, DSBs may form when catenated chromosomes are pulled toward opposite spindle poles [13•].

Endogenous DSBs are also normally formed during lymphoid development. In B cells for example, V(D)J recombination is initiated by specific DSBs introduced into

recombination signal sequences by the RAG1/2 endonuclease. These DSBs are repaired by an error-prone, NHEJ-mediated deletion mechanism that creates novel V(D)J junctions in antibody coding sequences, a process that is instrumental in generating antibody diversity in mammals [14].

After B cells undergo the V(D)J maturation process, these antibody-producing cells can undergo a second round of genome rearrangement that switches a Cμ constant heavy chain region for a different region (Cα, Cγ, or Cε) that converts an immunoglobulin M (IgM) producing cell to one that produces immunoglobulin A (IgA), immunoglobulin G (IgG), or immunoglobulin E (IgE). This process is called class switch recombination (CSR), which is also stimulated by DSBs, but unlike V(D)J recombination, DSBs that catalyze CSR are not produced by direct nuclease cleavage. Rather, they arise indirectly following the deamination of cytidine residues in transcriptionally active, repetitive heavy chain switch regions by activation-induced cytidine deaminase. Deaminated cytidine residues are then processed by base excision repair enzymes to yield DSBs. These DSBs are repaired by a deletional NHEJ-mediated mechanism [15••].

During meiosis, endogenous DSBs are created at many loci by SPO11 endonuclease. Although SPO11 does not appear to recognize specific DNA sequences, most DSBs are created in gene promoter regions, although even within these hotspots, DSBs occur at varied locations. Meiotic DSBs are repaired by homologous recombination and typically involve interactions between homologous chromosomes [16]. As with other programmed DSBs, improper processing of meiotic DSBs can result in translocations [17].

Sources of exogenous DNA double-strand breaks

DSBs are produced by a wide variety of exogenous DNA damaging agents. Ionizing radiation, including X-rays, γ-rays, β-particles, and α-particles, can cause many types of DNA damage (Fig. 2). These include base damage (e.g. broken rings), single-strand breaks, DSBs, and inter and intra-strand crosslinks. Of these lesions, the vast majority of the cytotoxicity associated with ionizing radiation is due to DSBs. DSBs are also caused by radiomimetic drugs such as bleomycin, and by topoisomerase inhibitors.

Topoisomerase I (TopoI) is inhibited by the camptothecins, and TopoIIα is inhibited by the anthracyclines and etoposide, all of which are used in chemotherapy [18]. TopoI and TopoII inhibitors induce ATM Ser-1981 phosphorylation and phosphorylation of histone H2AX (γH2AX), both hallmarks of DSB damage [19]. Translocation breakpoints cluster in regions that are enriched in TopoIIα cleavage sites, matrix attachment regions, and nuclease hypersensitivity sites [20]. Importantly, TopoIIα inhibitors have been implicated in therapy-induced leukemias carrying translocations with breakpoints that map to TopoII cleavage sites, and display NHEJ-type junctions [20–22].

Finally, tobacco smoke is a known carcinogen that induces mutations and DSBs [23]. This DSB damage is mediated through free radicals and is dose dependent [24].

Figure 2 Genotoxic agents produce DNA lesions that are converted to double-strand breaks and processed by several repair pathways, most of which carry a risk of inducing chromosomal translocations.

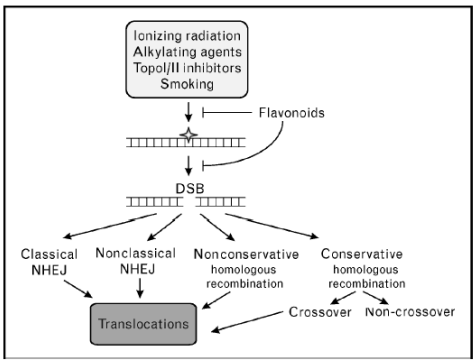

DSB, double-strand break; NHEJ, nonhomologous end joining.

Mechanisms of double-strand break repair

In mammalian cells, DSBs are repaired by NHEJ and homologous recombination. Homologous recombination can occur by conservative or nonconservative pathways. Conservative homologous recombination occurs in a stepwise manner that begins with 5′–3′ end resection regulated by the MRN complex, producing 3′ ssDNA tails of a kb or longer. ssDNA is coated with RPA, which is subsequently replaced by RAD51 in a reaction promoted by mediator proteins including five RAD51 paralogs (XRCC2, XRCC3, RAD51B, RAD51C, and RAD51D), RAD52, and breast cancer type 2 susceptibility protein (BRCA2). The RAD51–ssDNA filament searches for, and invades homologous sequences. The 3′-end of the invading strand is then extended by DNA polymerase past the original site of the DSB, and may then dissociate and anneal with the other resected end. Alternatively, the second can invade producing a double Holliday junction intermediate that can be resolved in two ways to produce crossover or noncrossover products.

One nonconservative form of homologous recombination is called single-strand annealing (SSA). SSA can repair a DSB present between or within linked repeats, or between repeats on different chromosomes if DSBs occur within or near each repeat. With linked repeats, end-resection uncovers complementary single strands in the two repeats that anneal to form a single repeat. This deletes one repeat and sequences between the repeats. Translocations result when SSA occurs between unlinked repeats, but this is rare because of the requirement for DSBs to occur essentially contemporaneously in or near both repeats [25]. In the absence of BRCA2, DSBs are repaired by nonconservative (SSA) homologous recombination subpathways that presumably lead to chromosomal instability [26].

There are two NHEJ pathways, including an efficient and well defined classical pathway and a less efficient alternative pathway (Fig. 3). Classical NHEJ is mediated by Ku complex (Ku70/Ku80), the catalytic subunit of DNA-dependent protein kinase (DNA-PKcs), XRCC4, and LigIV. The first step in NHEJ is the signaling of a DSB by the MRN complex, and then binding of Ku to broken ends, and recruitment of DNA-PKcs to form the active DNA-PK complex. DNA-PK is a member of the PI3 kinase family that is activated upon binding to DNA ends. In-vivo substrates of DNA-PK are unclear; however, there are several clusters of phosphorylation sites that are either autophosphorylated, or phosphorylated by ATM, or both. DNA-PK probably recruits the LigIV/XRCC4 complex to the break site, which catalyzes the rejoining step [27]. Depending on the particular type of DSB, other NHEJ accessory factors may be involved, including MRN (important for processing the dirty ends created by ionizing radiation) and the Artemis nuclease which is important for processing hairpins formed during V(D)J recombination [28]. Cernunos (also called XLF) is another accessory protein that interacts with the LigIV/XRCC4 complex, promotes classical NHEJ [29], and has been shown to be mutated in human immunodeficiency [30]. We recently described another accessory NHEJ component termed Metnase that methylates histones to open chromatin and processes DNA ends [31]. The suppressor of variegation-enhancer of zeste-trithorax (SET) domain protein Metnase promotes foreign DNA integration and links integration to NHEJ repair [31,32•].

Alternative NHEJ (also called backup or nonclassical NHEJ) is defined as NHEJ occurring in the absence of one or more classical NHEJ factors [14,15••,33]. Alternative NHEJ is less efficient than classical NHEJ, in part because of competition from the classical NHEJ factor DNA-PK [34]. At least in some contexts alternative NHEJ appears to be mediated by LigIII, and also involves poly(ADP)ribose polymerase-1 (PARP-1), a factor with roles in single-strand break repair [35]. In addition to its low efficiency, alternative NHEJ is characterized by a strong dependence on microhomology, and thus is more error prone than classical NHEJ. Both classical and nonclassical NHEJ are thought to mediate misrepair of DSBs leading to chromosomal translocations [15••,36].

Figure 3 Double-strand breaks can be repaired by two NHEJ pathways

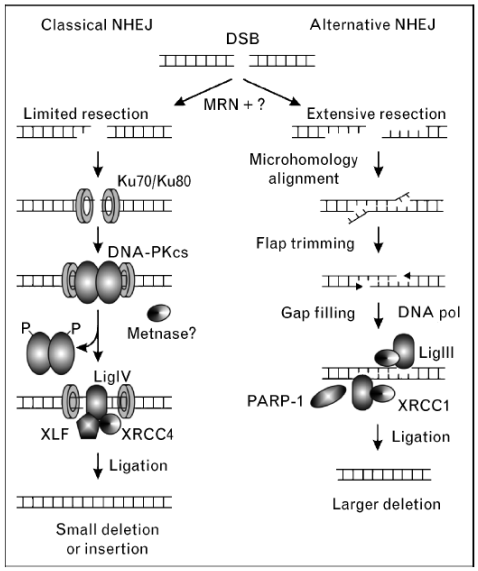

The classical pathway may be activated via the MRN complex, followed by end resection and binding of the Ku complex. DNA-PKcs is recruited next, along with other proteins. Finally, the ends are re-ligated by XRCC4/LigIV. In the nonclassical pathway, there is more extensive resection of the DNA ends and more frequent end alignment through microhomology. DNA flaps are trimmed and LigIII/XRCC1 ligate the ends. In the nonclassical pathway there is a greater chance of errors, such as large deletions, due to the extensive DNA end resection, microhomology alignment, and flap trimming. The second pathway is more likely to lead to translocations. DNA-PKcs, DNA-dependent protein kinase; DSB, double-strand break; MRN, MRE11/RAD50/NBS1; NHEJ, nonhomologous end joining; PARP-1, poly ADP ribose polymerase-1; XRCC1, X-ray repair complementing defective repair in Chinese hamster cells 1; XRCC4, X-ray repair complementing defective repair in Chinese hamster cells 4.

Inherited diseases related to double-strand break repair and associated malignancies

Inherited mutations in DSB repair components in humans generate a predisposition to leukemia and other cancers. These include Bloom's syndrome, Werner's syndrome, ataxia telangiectasia, Nijmegen breakage syndrome, and Fanconi's anemia (Table 1).

Table 1 Syndromes associated with DNA repair deficiencies, increased incidence of translocations, leukemia and other cancers

DNA repair disorder	Affected protein(s)	Clinical manifestations	Cellular function
Bloom's syndrome	BLM	Narrowing of the face, prominent nose, a butterfly shaped rash from sun exposure, a high-pitched voice, abnormal skin pigmentation, learning disabilities, mental retardation, immune deficiency, diabetes, anemia, male infertility, irregular female menstruation and cancer predisposition	Sensitive to replication fork challenges [hydroxyurea, ultraviolet (UV)], involved in S-phase checkpoint control, TopoIII interaction and Holliday junction resolvase activity
Werner's syndrome	WRN	Extreme early aging including a severe early onset cancer predisposition	3′–5′ Exonuclease activity, Holliday junction migration activity, telomere maintenance
Ataxia telangiectasia	ATM (AT-mutated)	Neurodegeneration, radiosensitivity, sterility, immunodeficiency and a predisposition to lymphomas and leukemias	Kinase involved in the G1/S, S, and G2/M checkpoints and DNA repair through both homologous recombination and NHEJ
Nijmegen break syndrome	NBS-1	Radiosensitivity, immunodeficiency, cancer predisposition, microcephaly and nuerodegeneration	Identification and signalling of DNA DSBs and the ensuing repair
Fanconi's anemia	FANCA, B, C, D1, D2, E, F, G, I, J, L, or M	Bone marrow failure, developmental abnormalities, and severe cancer predisposition	Replication fork re-start

ATM, ataxia telangiactasia mutated; DSBs, double-strand breaks; FANCA, Fanconi anemia-complementation group A; NHEJ, nonhomologous end joining.

Bloom's and Werner's syndromes result from mutations in genes that code for proteins related to the *E. coli* 3′–5′ RecQ helicase [37]. Bloom's syndrome cells in culture are markedly sensitive to hydroxyurea and ultraviolet light, but not ionizing radiation [38,39]. These studies firmly implicate the Bloom's syndrome protein BLM in replication-based DSB repair. BLM has recently been demonstrated to play a role in the processing of Holliday junctions resulting from stalled and collapsed replication forks. In this model, BLM associates with topoisomerase III (TopoIII) and functions as a Holliday junction resolvase [40,41••].

Mutations that cause Werner's syndrome affect the WRN protein, another RecQ family helicase that also possesses an ATP dependent 3′–5′ exonuclease motif [42–46]. Constantinou *et al.* [47] showed that WRN has the ability to branch migrate Holliday junctions during homologous recombination. WRN has also been shown to be important in telomere maintenance and cellular senescence [48•].

Ataxia telangiectasia has been shown to be the result of mutations in a specific gene named *ATM*. ATM is a serine/threonine kinase activated by DNA DSBs [49•]. It is a homodimer in undamaged cells and undergoes autophosphorylation in the presence of DNA DSBs [50]. Once phosphorylated on serine 1981, ATM is activated and it phosphorylates a number of important DNA repair factors including p53, CHK2, BRCA1, RPAp34, H2AX, SMC1, Fanconi anemia-complementation group D2 (FANCD2), RAD17, Artemis and NBS1 [49•]. ATM functions as an upstream regulator of both NHEJ and homologous recombination.

Nijmegen breakage syndrome is an autosomal recessive disorder shown to be the result of mutations in the NBS1 protein. It is part of the MRN complex that is conserved from yeast to mammals and functions in the identification and signaling of DNA DSBs [51]. The MRN complex is important in the activation of ATM and the initiation of a proper DNA damage response.

Fanconi's anemia is an inherited syndrome that presents as bone marrow failure, developmental abnormalities, and a severe cancer predisposition. Fanconi's anemia consists of 13 complementation groups [Fanconi anemia-complementation group A (FANCA), B, C, D1, D2, E, F, G, I, J, L, and M], each of which represent a specific gene that has been mutated or deleted [52•]. Fanconi's anemia can be autosomal recessive or sex-linked in inheritance, depending on the gene mutated. Fanconi's anemia cells are extremely sensitive to DNA crosslinking drugs such as mitomycin C and show phenotypes consisting of abnormal cell cycle regulation (extended G2), hypersensitivity to oxygen, increased apoptosis and accelerated telomere shortening [53].

All known Fanconi's anemia proteins function in a DNA repair pathway that is involved in the re-start of stalled replication forks. The majority of these protein products have been shown to form a complex that functions as the E3 specificity enzyme in monoubiquitination of FANCD2 after recognition of specific DNA structures. Ubiquitinated FANCD2 performs multiple tasks including the recruitment of BRCA2, enhancement of homologous recombination, and possibly the promotion of translesion DNA synthesis [52•].

Lessons learned from models of translocation

Franco *et al.* [54] have generated a number of animal models that examine the role of NHEJ components in translocations and oncogenesis, and the role of DNA

breaks in genomic instability and tumorigenesis [55,56]. Mice deficient for NHEJ components develop either embryonic lethality (seen in LigIV and XRCC4 deficiency) or severe combined immunodeficiency (seen with Ku70, Ku80, DNA-PK and Artemis deficiency). Occasionally these immunodeficient mice develop lymphoid neoplasia as they age. Interestingly, the embryonic lethality can be rescued by deleting p53, indicating that apoptosis after decreased repair of endogenous DSBs is the culprit for the lethality. When cells lacking both LigIV and p53 were exposed to radiation, large numbers of translocations were seen, and these mice developed lymphoma at a high rate. In contrast, wild-type or p53-deficient cells had few genomic abnormalities and a low incidence of lymphoma (LigIV-deficient but p53 +/+ cells arrested after radiation and could not be tested). These studies revealed several important concepts. First, the relative lack of translocations after the same radiation dose in wild-type cells compared with the LigIV−/− and p53 −/− cells indicates that the NHEJ pathway is less promiscuous than once thought. Second, translocations occur when a damaged cell with deficient NHEJ is forced to progress through the cell cycle, such as when p53 is deleted. This same phenomenon has been seen in p53 −/− mice also deficient in Ku80, DNA-PKcs, or XRCC4. These mice also develop lymphomas at a high rate.

Specific mechanisms of translocation in human leukemia

Etoposide has been associated with chromosomal translocations that result in acute leukemia, most commonly through translocations involving the *MLL* gene [57,58], or the runt-related transcription factor 1 (*RUNX1*) gene [59]. Balanced translocations involving chromosome bands 11q23 and 21q22 are highly characteristic of myelodysplasia and leukemia following therapy with etoposide [60–62]. The *MLL* translocations occur in a defined breakpoint cluster region (BCR) that spans 8.5 kbp between exons 5 and 11. This *MLL* BCR contains known nuclear matrix attachment regions, DNase hypersensitive sites, and TopoIIα cleavage sites. Treatment of cells with etoposide results in DSBs within this BCR [63–65].

Many breakpoints from both *MLL* and *RUNX1* translocations have been sequenced. Virtually none of these breakpoint junctions have any sequence homology between the partner genes, indicating that it is unlikely that homologus recombination played any role in the aberrant ligation of the translocation partners [20]. The junction sequences, however, do reveal classic signatures of NHEJ repair, such as microdeletions, duplications, microhomologies, and nontemplate insertions [20].

Leukemic rearrangements of *MLL* after DNA damage can also take the form of partial tandem duplications (PTDs) as opposed to reciprocal translocations. PTDs at the *MLL* locus are probably mediated by inter or intrachromosomal SSA between Alu sequences within the *MLL* locus [66]. In seven of nine *MLL* PTD junction sequences analyzed, recombination took place between Alu elements within the *MLL* gene locus [67]. This is consistent with SSA repair. Although most breakpoint junction sequences do not show evidence for such Alu-mediated recombination [20], as described above, when DSBs occur in Alu sequences, translocations can be generated by the SSA pathway [68].

In lymphoid cells endogenous DSBs are generated during V(D)J recombination or CSR. There are sequences elsewhere in the genome that resemble the heptamer and nonamer V(D)J recombination signal sequences [69]. These sites can become targets of RAG-mediated DSB generation and subsequent leukemogenic translocations [70] and can mediate *LMO2*, *Ttg1*, *SCL/TAL1*, and *SIL* translocations in acute T-cell leukemia [70].

Class switching from the μ heavy chain locus to the α, β, δ, or ε loci in the maturation of the immunoglobulin response can also generate DSBs that can be targets of translocations. For example, in the t(8;14) seen in Burkitt's lymphoma and some B-cell acute lymphoblastic leukemia (ALL), *c-myc* can be translocated to the switch region of the μ heavy chain gene [71].

Conclusion

It is clear that NHEJ DNA repair components are critical for preventing leukemogenic translocations. The finding that leukemia is a well described complication of inherited disorders of NHEJ repair as opposed to inherited disorders of homologus recombination such as BRCA1/2 deficiency is clinical evidence for this postulate. The role of subtle decreases in NHEJ activity in genomic instability in leukemia is not well explored. The most fascinating question is whether such subtle genomic instability predates the leukemogenic translocation, or whether it is a result of the leukemogenic transformation. There are several important clinical implications of defects in DNA repair predating the original translocation. First, such defects could be used to screen for patients at risk for leukemia. Second, reversing such defects would be an important therapeutic target. Such therapy could be used especially in environmental situations where exposure to DNA damaging agents could lead to leukemia, such as an accidental or purposeful radiation exposure.

There has been considerable discussion about leukemia being the result of two genetic lesions, one that stimulates proliferation, usually a point mutation, and one that

blocks differentiation, usually a translocation. However, these genetic lesions are probably the result of a preexisting genomic instability. This preexisting genomic instability may be the result of small defects in NHEJ repair and a coincidental defect in DNA damage cell cycle arrest. The coincidental existence of these two defects could underlie much of leukemia, and produce the translocations that have defined our efforts in this disease thus far. It is possible that these defects become obscured by the resultant transformation of the hematopoietic progenitor after translocation. Perhaps we should be focusing on the conditions that predate the translocation, as this may be an easier place to intervene. One could envision the time when our efforts in leukemia prevention exceed those in leukemia therapy.

References and recommended reading

Papers of particular interest, published within the annual period of review, have been highlighted as:

- • of special interest
- •• of outstanding interest

Additional references related to this topic can also be found in the Current World Literature section in this issue (pp. 425–426).

1 Kelly LM, Gilliland DG. Genetics of myeloid leukemias. Annu Rev Genomics Hum Genet 2002; 3:179–198.

2 Murnane JP. Telomeres and chromosome instability. DNA Repair 2006; 5:1082–1092.

3 Vukovic B, Beheshti B, Park P, *et al.* Correlating breakage–fusion–bridge events with the overall chromosomal instability and in vitro karyotype evolution in prostate cancer. Cytogenet Genome Res 2007; 116:1–11.

4 Richardson C, Moynahan ME, Jasin M. Double-strand break repair by interchromosomal recombination: suppression of chromosomal translocations. Genes Dev 1998; 12:3831–3842.

5 Richardson C, Jasin M. Frequent chromosomal translocations induced by DNA double-strand breaks. Nature 2000; 405:697–700.

6 Cremer T, Cremer M, Dietzel S, *et al.* Chromosome territories–a functional nuclear landscape. Curr Opin Cell Biol 2006; 18:307–316.

7 Gue M, Sun JS, Boudier T. Simultaneous localization of MLL, AF4 and ENL genes in interphase nuclei by 3D-FISH: MLL translocation revisited. BMC Cancer 2006; 6:20.

8 de Jager M, van Noort J, van Gent DC, *et al.* Human Rad50/Mre11 is a flexible complex that can tether DNA ends. Mol Cell 2001; 8:1129–1135.

9 •• Weinstock DM, Brunet E, Jasin M. Formation of NHEJ-derived reciprocal chromosomal translocations does not require Ku70. Nat Cell Biol 2007; 9:978–981.
The major repair pathway mediating translocations is NHEJ. However, the Ku complex, a major component of classical NHEJ, is not required indicating a significant role for nonclassical NHEJ in translocations.

10 •• Soutoglou E, Dorn JF, Sengupta K, *et al.* Positional stability of single double-strand breaks in mammalian cells. Nat Cell Biol 2007; 9:675–682.
Broken ends show spatial stability and do not migrate around the cell. This stability is a key factor in preventing translocations.

11 Andreassen PR, Ho GP, D'Andrea AD. DNA damage responses and their many interactions with the replication fork. Carcinogenesis 2006; 27:883–892.

12 Shen Z, Nickoloff JA. Mammalian homologous recombination repair and cancer intervention. In: Wei Q, Li L, Chen DJ, editors. DNA repair, genetic instability, and cancer. Singapore: World Scientific Publishing Co.; 2007. pp. 119–156.

13 • Damelin M, Bestor TH. The decatenation checkpoint. Br J Cancer 2007; 96:201–205.
A complete review of chromosome decatenation, highlighting the role it plays in chromosomal stability.

14 Lieber MR, Yu K, Raghavan SC. Roles of nonhomologous DNA end joining, V(D)J recombination, and class switch recombination in chromosomal translocations. DNA Repair 2006; 5:1234–1245.

15 •• Yan CT, Boboila C, Souza EK, *et al.* IgH class switching and translocations use a robust nonclassical end-joining pathway. Nature 2007; 449:478–482.
Shows that translocations associated with CSR are often mediated by nonclassical NHEJ.

16 Keeney S, Neale MJ. Initiation of meiotic recombination by formation of DNA double-strand breaks: mechanism and regulation. Biochem Soc Trans 2006; 34 (Pt 4):523–525.

17 Bandyopadhyay R, Heller A, Knox-DuBois C, *et al.* Parental origin and timing of de novo Robertsonian translocation formation. Am J Hum Genet 2002; 71:1456–1462.

18 Huang CH, Treat J. New advances in lung cancer chemotherapy: topotecan and the role of topoisomerase I inhibitors. Oncology 2001; 61 (Suppl 1): 14–24.

19 Kurose A, Tanaka T, Huang X, *et al.* Assessment of ATM phosphorylation on Ser-1981 induced by DNA topoisomerase I and II inhibitors in relation to Ser-139-histone H2AX phosphorylation, cell cycle phase, and apoptosis. Cytometry A 2005; 68:1–9.

20 Zhang Y, Rowley JD. Chromatin structural elements and chromosomal translocations in leukemia. DNA Repair 2006; 5:1282–1297.

21 Aplan PD. Causes of oncogenic chromosomal translocation. Trends Genet 2006; 22:46–55.

22 Felix CA, Kolaris CP, Osheroff N. Topoisomerase II and the etiology of chromosomal translocations. DNA Repair 2006; 5:1093–1108.

23 Kim H, Liu X, Kobayashi T, *et al.* Reversible cigarette smoke extract-induced DNA damage in human lung fibroblasts. Am J Respir Cell Mol Biol 2004; 31:483–490.

24 Collier AC, Dandge SD, Woodrow JE, Pritsos CA. Differences in DNA-damage in nonsmoking men and women exposed to environmental tobacco smoke (ETS). Toxicol Lett 2005; 158:10–19.

25 Weinstock DM, Richardson CA, Elliott B, Jasin M. Modeling oncogenic translocations: distinct roles for double-strand break repair pathways in translocation formation in mammalian cells. DNA Repair 2006; 5:1065–1074.

26 Tutt A, Bertwistle D, Valentine J, *et al.* Mutation in Brca2 stimulates error-prone homology-directed repair of DNA double-strand breaks occurring between repeated sequences. EMBO J 2001; 20:4704–4716.

27 Lobrich M, Jeggo PA. Harmonising the response to DSBs: a new string in the ATM bow. DNA Repair 2005; 4:749–759.

28 Jung D, Giallourakis C, Mostoslavsky R, Alt FW. Mechanism and control of V(D)J recombination at the immunoglobulin heavy chain locus. Annu Rev Immunol 2006; 24:541–570.

29 Ahnesorg P, Smith P, Jackson SP. XLF interacts with the XRCC4–DNA ligase IV complex to promote DNA nonhomologous end-joining. Cell 2006; 124:301–313.

30 Buck D, Malivert L, de Chasseval R, *et al.* Cernunnos, a novel nonhomologous end-joining factor, is mutated in human immunodeficiency with microcephaly. Cell 2006; 124:287–299.

31 Lee SH, Oshige M, Durant ST, *et al.* The SET domain protein Metnase mediates foreign DNA integration and links integration to nonhomologous end-joining repair. Proc Natl Acad Sci U S A 2005; 102:18075–18080.

32 • Roman Y, Oshige M, Lee YJ, *et al.* Biochemical characterization of a SET and transposase fusion protein. Metnase: its DNA binding and DNA cleavage activity. Biochemistry 2007; 46:11369–11376.
Emphasizes the importance of nuclease activities in NHEJ repair.

33 Wang H, Rosidi B, Perrault R, *et al.* DNA ligase III as a candidate component of backup pathways of nonhomologous end joining. Cancer Res 2005; 65:4020–4030.

34 Perrault R, Wang H, Wang M, *et al.* Backup pathways of NHEJ are suppressed by DNA-PK. J Cell Biochem 2004; 92:781–794.

35 Wang M, Wu W, Wu W, *et al.* PARP-1 and Ku compete for repair of DNA double strand breaks by distinct NHEJ pathways. Nucleic Acids Res 2006; 34:6170–6182.

36 Povirk LF. Biochemical mechanisms of chromosomal translocations resulting from DNA double-strand breaks. DNA Repair 2006; 5:1199–1212.

37 Umezu K, Nakayama K, Nakayama H. Escherichia coli RecQ protein is a DNA helicase. Proc Natl Acad Sci U S A 1990; 87:5363–5367.

38 Wang W, Seki M, Otsuki M, *et al.* The absence of a functional relationship between ATM and BLM, the components of BASC, in DT40 cells. Biochim Biophys Acta 2004; 1688:137–144.

39 Wang W, Seki M, Narita Y, *et al.* Possible association of BLM in decreasing DNA double strand breaks during DNA replication. EMBO J 2000; 19:3428–3435.

40 Bachrati CZ, Borts RH, Hickson ID. Mobile D-loops are a preferred substrate for the Bloom's syndrome helicase. Nucleic Acids Res 2006; 34:2269–2279.

41 •• Davies SL, North PS, Hickson ID. Role for BLM in replication-fork restart and suppression of origin firing after replicative stress. Nat Struct Mol Biol 2007; 14:677–679.
First report linking the Bloom's syndrome protein to repair of replication fork damage.

42 Shen JC, Gray MD, Oshima J, *et al.* Werner syndrome protein. I. DNA helicase and DNA exonuclease reside on the same polypeptide. J Biol Chem 1998; 273:34139–34144.

43 Huang S, Li B, Gray MD, *et al.* The premature ageing syndrome protein, WRN, is a 3′→5′ exonuclease. Nature Genet 1998; 20:114–116.

44 Huang S, Beresten S, Li B, *et al.* Characterization of the human and mouse WRN 3′→5′ exonuclease. Nucleic Acids Res 2000; 28:2396–2405.

45 Kamath-Loeb AS, Shen JC, Loeb LA, Fry M. Werner syndrome protein. II. Characterization of the integral 3′→5′ DNA exonuclease. J Biol Chem 1998; 273:34145–34150.

46 Suzuki N, Shimamoto A, Imamura O, *et al.* DNA helicase activity in Werner's syndrome gene product synthesized in a baculovirus system. Nucleic Acids Res 1997; 25:2973–2978.

47 Constantinou A, Tarsounas M, Karow JK, *et al.* Werner's syndrome protein (WRN) migrates Holliday junctions and co-localizes with RPA upon replication arrest. EMBO Rep 2000; 1:80–84.

48 • Hanada K, Hickson ID. Molecular genetics of RecQ helicase disorders. Cell Mol Life Sci 2007; 64:2306–2322.
Comprehensive review of the human DNA damage clinical syndromes, Bloom's and Werner's, that result from mutations of proteins related to RecQ.

49 • Lee JH, Paull TT. Activation and regulation of ATM kinase activity in response to DNA double-strand breaks. Oncogene 2007; 26:7741–7748.
Comprehensive review of ATM function.

50 Bakkenist CJ, Kastan MB. DNA damage activates ATM through intermolecular autophosphorylation and dimer dissociation. Nature 2003; 421:499–506.

51 Demuth I, Digweed M. The clinical manifestation of a defective response to DNA double-strand breaks as exemplified by Nijmegen breakage syndrome. Oncogene 2007; 26:7792–7798.

52 • Wang W. Emergence of a DNA-damage response network consisting of Fanconi anaemia and BRCA proteins. Nat Rev Genet 2007; 8:735–748.
Description of the role of the Fanconi's anemia complex in DNA repair.

53 Dokal I. Fanconi's anaemia and related bone marrow failure syndromes. Br Med Bull 2006; 77–78:37–53.

54 Franco S, Alt FW, Manis JP. Pathways that suppress programmed DNA breaks from progressing to chromosomal breaks and translocations. DNA Repair 2006; 5:1030–1041.

55 Ferguson DO, Alt FW. DNA double strand break repair and chromosomal translocation: lessons from animal models. Oncogene 2001; 20:5572–5579.

56 Mills KD, Ferguson DO, Alt FW. The role of DNA breaks in genomic instability and tumorigenesis. Immunol Rev 2003; 194:77–95.

57 Libura J, Slater DJ, Felix CA, Richardson C. Therapy-related acute myeloid leukemia-like MLL rearrangements are induced by etoposide in primary human CD34+ cells and remain stable after clonal expansion. Blood 2005; 105: 2124–2131.

58 Felix CA. Leukemias related to treatment with DNA topoisomerase II inhibitors. Medical and pediatric oncology 2001; 36:525–535.

59 Larson RA, Le Beau MM, Ratain MJ, Rowley JD. Balanced translocations involving chromosome bands 11q23 and 21q22 in therapy-related leukemia. Blood 1992; 79:1892–1893.

60 Pedersen-Bjergaard J, Philip P. Two different classes of therapy-related and de-novo acute myeloid leukemia? Cancer Genet Cytogenet 1991; 55:119–124.

61 Izumi T, Ohtsuki T, Ohya K, *et al.* Therapy-related leukemia with a novel 21q22 rearrangement. Cancer Genet Cytogenet 1996; 90:45–48.

62 Slovak ML, Bedell V, Popplewell L, *et al.* 21q22 balanced chromosome aberrations in therapy-related hematopoietic disorders: report from an international workshop. Genes Chromosomes Cancer 2002; 33:379–394.

63 Strissel PL, Strick R, Rowley JD, Zeleznik-Le NJ. An in vivo topoisomerase II cleavage site and a DNase I hypersensitive site colocalize near exon 9 in the MLL breakpoint cluster region. Blood 1998; 92:3793–3803.

64 Domer PH, Head DR, Renganathan N, *et al.* Molecular analysis of 13 cases of MLL/11q23 secondary acute leukemia and identification of topoisomerase II consensus-binding sequences near the chromosomal breakpoint of a secondary leukemia with the t(4;11). Leukemia 1995; 9:1305–1312.

65 Stanulla M, Schunemann HJ, Thandla S, *et al.* Pseudo-rearrangement of the MLL gene at chromosome 11q23: a cautionary note on genotype analysis of leukaemia patients. Mol Pathol 1998; 51:85–89.

66 Aplan PD. Chromosomal translocations involving the MLL gene: molecular mechanisms. DNA Repair 2006; 5:1265–1272.

67 Strout MP, Marcucci G, Bloomfield CD, Caligiuri MA. The partial tandem duplication of ALL1 (MLL) is consistently generated by Alu-mediated homologous recombination in acute myeloid leukemia. Proc Natl Acad Sci U S A 1998; 95:2390–2395.

68 Elliott B, Richardson C, Jasin M. Chromosomal translocation mechanisms at intronic alu elements in mammalian cells. Mol Cell 2005; 17:885–894.

69 Lewis SM, Agard E, Suh S, Czyzyk L. Cryptic signals and the fidelity of V(D)J joining. Mol Cell Biol 1997; 17:3125–3136.

70 Raghavan SC, Kirsch IR, Lieber MR. Analysis of the V(D)J recombination efficiency at lymphoid chromosomal translocation breakpoints. J Biol Chem 2001; 276:29126–29133.

71 Unniraman S, Schatz DG. AID and Igh switch region-Myc chromosomal translocations. DNA Repair 2006; 5:1259–1264.

6.3. DNA-PKcs and ATM co-regulate DNA double-strand break repair.

Authors: Meena Shrivastav, Cheryl A. Miller, Leyma P. De Haro, Stephen T. Durant, Benjamin P.C. Chen, David J. Chen, Jac A. Nickoloff

DNA Repair (2009) 8: 920–929.

DNA Repair 8 (2009) 920–929

Contents lists available at ScienceDirect

DNA Repair

journal homepage: www.elsevier.com/locate/dnarepair

DNA-PKcs and ATM co-regulate DNA double-strand break repair

Meena Shrivastav[a], Cheryl A. Miller[a], Leyma P. De Haro[a], Stephen T. Durant[a], Benjamin P.C. Chen[b], David J. Chen[b], Jac A. Nickoloff[a,*]

[a] Department of Molecular Genetics and Microbiology, University of New Mexico School of Medicine, Albuquerque, NM 87131, United States
[b] Division of Molecular Radiation Biology, University of Texas Southwestern Medical Center, Dallas, TX 75390, United States

ARTICLE INFO

Article history:
Received 11 November 2008
Received in revised form 9 May 2009
Accepted 14 May 2009
Available online 16 June 2009

Keywords:
DNA repair
Homologous recombination
Genome stability

ABSTRACT

DNA double-strand breaks (DSBs) are repaired by nonhomologous end-joining (NHEJ) and homologous recombination (HR). The NHEJ/HR decision is under complex regulation and involves DNA-dependent protein kinase (DNA-PKcs). HR is elevated in DNA-PKcs null cells, but suppressed by DNA-PKcs kinase inhibitors, suggesting that kinase-inactive DNA-PKcs (DNA-PKcs-KR) would suppress HR. Here we use a direct repeat assay to monitor HR repair of DSBs induced by I-*Sce*I nuclease. Surprisingly, DSB-induced HR in DNA-PKcs-KR cells was 2- to 3-fold above the elevated HR level of DNA-PKcs null cells, and ~4- to 7-fold above cells expressing wild-type DNA-PKcs. The hyperrecombination in DNA-PKcs-KR cells compared to DNA-PKcs null cells was also apparent as increased resistance to DNA crosslinks induced by mitomycin C. ATM phosphorylates many HR proteins, and ATM is expressed at a low level in cells lacking DNA-PKcs, but restored to wild-type level in cells expressing DNA-PKcs-KR. Several clusters of phosphorylation sites in DNA-PKcs, including the T2609 cluster, which is phosphorylated by DNA-PKcs and ATM, regulate access of repair factors to broken ends. Our results indicate that ATM-dependent phosphorylation of DNA-PKcs-KR contributes to the hyperrecombination phenotype. Interestingly, DNA-PKcs null cells showed more persistent ionizing radiation-induced RAD51 foci (but lower HR levels) compared to DNA-PKcs-KR cells, consistent with HR completion requiring RAD51 turnover. ATM may promote RAD51 turnover, suggesting a second (not mutually exclusive) mechanism by which restored ATM contributes to hyperrecombination in DNA-PKcs-KR cells. We propose a model in which DNA-PKcs and ATM coordinately regulate DSB repair by NHEJ and HR.

1. Introduction

Mammalian cells have integrated DNA damage response systems that sense DNA damage, activate signaling cascades, and effect repair. Defects in these systems lead to genome instability and predispose to cancer and other diseases. DNA double-strand breaks (DSBs) are a serious type of damage that can result in mutations, chromosome aberrations, and cell death. DSBs are produced by exogenous and endogenous factors such as ionizing radiation (IR) and nucleases, respectively, and are repaired by two major pathways, homologous recombination (HR) and nonhomologous end-joining (NHEJ). NHEJ is predominant in G0 and G1, and HR activity increases during S and G2 [1]. Proteins that mediate HR and NHEJ are largely distinct, but some have been implicated in both pathways. For example, defects in the yeast Mre11/Rad50/Xrs2 complex (MRE11/RAD50/NBS1—MRN in mammals) affect both HR and NHEJ, presumably reflecting Mre11 regulation of end processing and Rad50 end-tethering functions. DNA-dependent protein kinase (DNA-PK), comprising the catalytic subunit (DNA-PKcs), Ku70, and Ku80, is a key NHEJ factor, but it also influences HR [2–7]. However, the precise role of DNA-PKcs in HR regulation has been unclear.

DNA-PKcs is a phosphotidylinositol-3-kinase (PIK) family member recruited to DSBs by Ku and its kinase activity is stimulated ~10-fold upon binding to Ku-bound DNA ends [8]. DNA-PKcs promotes NHEJ and phosphorylates itself and other DNA damage response and repair proteins. DNA-PKcs kinase activity is critical for NHEJ [9]. Numerous in vitro phosphorylation targets of DNA-PKcs have been identified including Ku70, Ku80, XRCC4, Artemis, RPA, and p53. There is evidence that DNA-PKcs phosphorylates several targets in vivo, including itself, RPA, WRN, and Artemis [5,10–14], although the functional significance of these phosphorylated targets, other than DNA-PKcs itself, remains questionable [15].

ATM is another PIK family member with critical roles in DNA damage responses and cancer suppression. In undamaged cells,

Abbreviations: DSB, double-strand break; HR, homologous recombination; NHEJ, non-homologous end-joining; PIK, phosphotidylinositol-3-kinase; IR, ionizing radiation.

* Corresponding author. Present address: Department of Environmental and Radiological Health Sciences, Colorado State University, 1618 Campus Delivery, Ft. Collins, CO 80523, United States. Tel.: +1 970 491 6674; fax: +1 970 491 0623.
E-mail address: J.Nickoloff@colostate.edu (J.A. Nickoloff).

1568-7864/$ – see front matter © 2009 Elsevier B.V. All rights reserved.
doi:10.1016/j.dnarep.2009.05.006

ATM is an inactive dimer, but damage causes *trans*-autophosphorylation, TIP60-dependent acetylation, and dissociation into active monomers [16]. ATM phosphorylates DNA repair, checkpoint, and cell cycle control proteins, including p53, NBS1, MDM2, SMC1, CHK2, BRCA1, c-Abl, and H2AX [17–20]. ATM defective cells are sensitive to IR and show defects in DSB repair by NHEJ that are independent of the checkpoint defect [21–24]. Several lines of evidence suggest that ATM promotes DSB repair by HR [22,25–27]. Thus, both ATM and DNA-PKcs influence HR, and crosstalk between these kinases is suggested by their common H2AX target [28], the reduction in ATM levels upon RNAi down-regulation of DNA-PKcs [29], and by evidence that ATM phosphorylates DNA-PKcs after DNA damage [30].

DNA damage triggers phosphorylation of DNA-PKcs at several clusters of serine and threonine residues (including T2609, S2056, and T3950) that regulate DNA-PKcs function [15]. Phosphorylation of the T2609 cluster induces a conformational shift that promotes DNA-PKcs disassociation from broken ends, presumably increasing access of other repair factors to broken ends [31–37]. Other phosphorylation sites within DNA-PKcs may be even more important than the T2609 cluster for DNA-PKcs dissociation [15]. Nonetheless, mutations that prevent T2609 cluster phosphorylation markedly suppress HR stimulated by I-*Sce*I nuclease-induced DSBs (referred hereafter as "DSB-induced HR") [4]. There is some debate about whether the T2609 cluster is phosphorylated by ATM, DNA-PKcs or both kinases. T2609 phosphorylation was originally defined using in vitro assays [38]. Meek et al. [39] concluded that in vivo, both T2609 and S2056 clusters were primarily targets of autophosphorylation. However, in that study DNA-PKcs phosphorylation was analyzed in cell extracts, or with purified DNA-PKcs, after cells were treated with DNA damaging agents, raising the possibility that the observed autophosphorylation occurred in vitro. Another in vitro study showed that NHEJ required DNA-PKcs autophosphorylation, but was independent of ATM [40]. In contrast, a genetic analysis indicated that ATM plays an important role in T2609 cluster phosphorylation in vivo [30].

DSB-induced HR is increased in the absence of DNA-PKcs, Ku70, or XRCC4, which could reflect passive shunting of DSBs from NHEJ to HR [2,7]. However, chemical inhibition of DNA-PKcs, mutation of the T2609 cluster, and splice variants that lack the kinase domain, all reduce DSB-induced HR [3,4], indicating that DNA-PKcs actively regulates repair pathway choice. Because chemical inhibition of DNA-PKcs reduces DSB-induced HR, we hypothesized that HR would also be reduced in cells expressing catalytically inactive DNA-PKcs. We tested this in cells with integrated direct repeat HR substrates, which are reasonable models given that the human genome comprises ~50% repeated elements, and HR between repeated elements is linked to dozens of human diseases and is likely a key evolutionary driver [41,42]. We examined DSB-induced HR in cells expressing the catalytically inactive DNA-PKcs K3752R (KR) mutant. The K3752 residue lies in subdomain II outside the ATP binding pocket, but is nonetheless required for ATP binding and kinase activity [43], and DNA-PKcs-KR is NHEJ defective [9]. Surprisingly, we found that DSB-induced HR was ~2- to 3-fold higher in cells expressing DNA-PKcs-KR than in cells lacking DNA-PKcs, and ~4- to 7-fold higher than cells with wild-type DNA-PKcs. Because NHEJ is similarly defective in cells that lack DNA-PKcs or express DNA-PKcs-KR, the higher HR level in cells with DNA-PKcs-KR cannot be explained by passive shunting of DSBs from NHEJ toward HR, but rather that HR is directly or indirectly enhanced in cells expressing DNA-PKcs-KR. This enhanced HR was strongly suppressed by chemical inhibitors of ATM kinase whereas HR in cells lacking DNA-PKcs was unaffected by ATM inhibition. Based on these and other results we suggest a model in which ATM regulates HR by both DNA-PKcs-dependent and -independent mechanisms.

2. Materials and methods

2.1. Cell lines

CHO V3 derivatives with HR substrates and complemented with DNA-PKcs were described previously [2]. Complementation with DNA-PKcs-KR was performed using similar procedures, and cells were cultured as described [44]. VD-7 cells complemented with DNA-PKcs harboring alanine mutations of the T2609 cluster were described previously [4].

2.2. IR sensitivity and HR assays

All assays employed unsynchronized cells harvested from cultures that were ~65–75% confluent. Sensitivity to γ-rays was determined as described [2]. DSB-induced HR frequencies were determined as described [44]. Briefly, 4×10^5 cells were seeded into 35 mm dishes, incubated for 16 h, and lipofected with 2 μg of pCMV3xnls(I-*Sce*I) to induce DSBs, or 2 μg of negative control vector pCMV(I-*Sce*I$^-$). Twenty-four hours later, 2×10^4 cells were seeded to each of three 10 cm dishes, and after an additional 24 h, G418 (600 μg/ml, 100% active) was added. Cell viability was determined in parallel by seeding 500 cells per 10 cm dish in nonselective medium. Colonies were stained with 0.1% crystal violet in methanol and scored 10 days later. HR frequencies were calculated as the number of G418-resistant colonies per viable cell plated in selective medium. Recombinant products were analyzed by PCR, restriction mapping, and Southern hybridization to distinguish gene conversions from deletions, and to generate gene conversion tract spectra as described [44,45]. Transfection efficiency was assessed by flow cytometry with a GFP-I-SceI expression vector [46]. Global HR capacity was measured with a mitomycin C (MMC) sensitivity assay. Appropriate numbers of cells were seeded to 10 cm dishes, incubated for 4 h to allow attachment, exposed to 0–25 ng/ml MMC for 24 h, then growth media was replaced with fresh growth media, and colonies were stained and scored 10 days later.

2.3. Protein detection

Commercial antibodies included DNA-PKcs (NA57 and PC127, Calbiochem), ATM (AHP397, SeroTec and ab17995, Abcam), ATM phosphoserine 1981 (39529, Active Motif), RAD51 (PC130, Calbiochem), RPA (NA19, Calbiochem), and β-actin (CP01, Calbiochem). Antibodies to DNA-PKcs phospho-T2609 were described previously [38]. HRP-conjugated secondary anti-mouse IgG (NA931) and anti-rabbit IgG (NA934) were from Amersham Biosciences. FITC-conjugated secondary anti-rabbit IgG (Alexa Fluor-488; A11441) and anti-mouse IgG (Alexa Fluor-568; A11031,) were from Molecular Probes.

Whole cell extracts were prepared from ~1.5×10^7 cells using M-PER mammalian protein extraction reagent supplemented with Halt protease inhibitor cocktail mix and Halt phosphatase inhibitor cocktail mix (Thermo Scientific). Lysates were clarified by centrifugation and protein was quantified by Bradford assay (Bio-Rad). Protein (25–100 μg) was combined with 2× Laemmli loading buffer (150 mM Tris–HCl, pH 7.0, 10% β-mercaptoethanol, 20% glycerol, 3% SDS, and 0.01% bromphenol blue), boiled for 5 min, resolved on a 5–15% SDS-polyacrylamide gel, and transferred to PVDF membranes using 48 mM Tris–HCl, pH 7.4, 390 mM glycine, 0.1% SDS, and 5% methanol. For ATM Westerns, methanol and SDS were omitted from the transfer buffer. The membranes were incubated with primary antibody, stained with HRP-conjugated secondary antibodies, and signals were developed by chemiluminescence (SuperSignal Westpico Chemiluminescence reagent, Thermo Scientific).

For immunofluorescent detection, cells were grown on cover slips to ~45% confluency, exposed to γ-rays or mock-treated, fixed

at indicated times with 3% paraformaldehyde in PBS (pH 7.4) or 100% methanol, permeabilized with 0.1% Triton X-100 in PBS, and incubated with primary antibodies (prepared in 3% BSA in PBS). Primary antibodies were detected with Alexa-488 or Alexa 568 conjugated secondary antibodies (Molecular Probes), and cover slips were mounted in Vectashield mounting medium (Vector Laboratories, CA) and photographed with a Zeiss Axioscope fluorescence microscope equipped with a Zeiss Axiocam. Images were processed using Adobe Photoshop, or CorelDraw software. In all cases, identical software processing steps were performed on control and experimental images.

2.4. Statistical analysis

All statistical analyses were performed by using two-tailed Student's *t*-tests with Prism 5.0 software.

3. Results

3.1. Enhanced DSB-induced HR with kinase-inactive DNA-PKcs

To investigate DNA-PKcs roles in DSB-induced HR we expressed human DNA-PKcs in derivatives of CHO V3 (DNA-PKcs null) cells with single integrated copies of one of two related HR substrates with *neo* direct repeats, termed VD13 and V24 (Fig. 1A) [2]. I-*Sce*I-induced DSBs stimulate HR repair yielding *neo*$^+$ products that confer resistance to G418 by gene conversion with or without associated crossovers or by single-strand annealing [47]. I-*Sce*I DSBs are useful for identifying proteins that influence HR efficiency and/or outcome, but they do not fully mimic IR-induced DSBs which must be processed to produce ligatable/extendable ends, nor other damage produced by IR including single-strand breaks, base damage, and complex (multi-lesion) damage sites.

The VD13 and V24 cell lines were transfected with vectors for stable expression of wild-type human DNA-PKcs, or kinase-inactive DNA-PKcs-KR. Transfectants expressing similar levels of wild-type DNA-PKcs (designated "-C1") or DNA-PKcs-KR ("-KR3, -KR4, -KR6") were identified by Western blot (Fig. 1B). As shown previously [2,9],

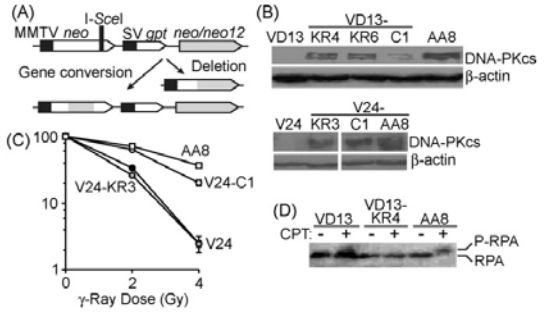

Fig. 1. Characterization of V3 derivatives expressing kinase-inactive DNA-PKcs. (A) HR substrates. The upstream *neo* is driven by the mouse mammary tumor virus promoter and is inactivated by insertion of an I-*Sce*I recognition site; the downstream *neo* has wild-type coding sequence but lacks a promoter. HR substrates in VD13 and V24 are identical except the substrate in V24 has 12 silent restriction fragment length polymorphisms at ~100 bp intervals (*neo12*) for mapping conversion tracts. (B) Expression of DNA-PKcs in V3 derivatives. Western blotting with anti-DNA-PKcs antibodies confirms expression of DNA-PKcs or DNA-PKcs-KR. CHO AA8 cells are wild-type controls and β-actin serves as loading control. (C) DNA-PKcs-KR does not confer radioresistance. Cell survival after IR treatment measured as relative plating efficiency (average ± SD) for V24 and its derivatives V24-C1 and V24-KR3 is shown. VD13 and its derivatives gave similar results (not shown). (D) DNA-PKcs-KR fails to phosphorylate RPA after camptothecin (CPT). Western blot of protein extracts from cells treated with 10 μM CPT or mock-treated for 1 h.

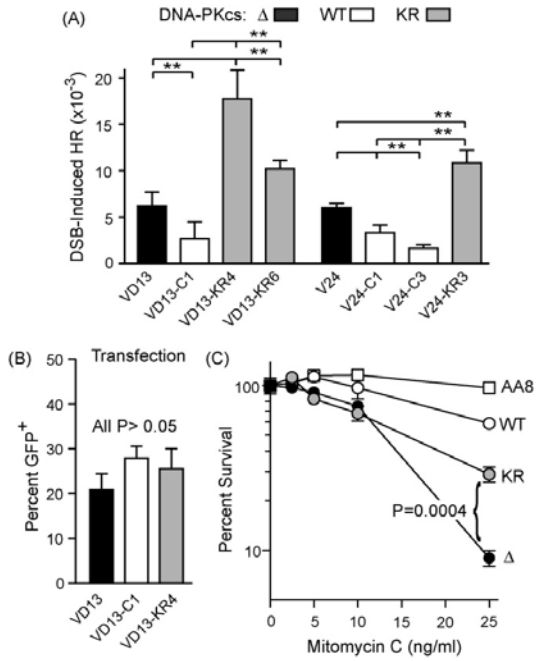

Fig. 2. DNA-PKcs-KR enhances HR. (A) DSB-induced HR frequencies are shown for cells expressing wild-type DNA-PKcs, DNA-PKcs-KR, or null (Δ). Values are averages (+SD) for 3–5 determinations. Double asterisks indicate significant differences at $P \leq 0.01$ (*t*-tests). (B) GFP transfection efficiencies measured by flow cytometry. (C) Percent survival as a function of MMC concentration in wild-type (AA8 and VD13-C1), DNA-PKcs-KR (VD13-KR4), and null (VD13) cells. Values are averages (±SD) for 3 determinations.

wild-type DNA-PKcs restored radioresistance to near wild-type levels (despite variation in DNA-PKcs expression levels), but DNA-PKcs-KR cells remained radiosensitive (Fig. 1C and data not shown). The topoisomerase inhibitor camptothecin (CPT) creates replication stress and replication-dependent phosphorylation of RPA by DNA-PKcs [10,48]. This response was seen in wild-type (AA8) and wild-type complemented VD13-C1 cells, but not in DNA-PKcs null (VD13) or DNA-PKcs-KR cells (Fig. 1D and data not shown). In the original demonstration of DNA-PKcs-dependent RPA phosphorylation after CPT, only ~50% of RPA was phosphorylated [10], whereas we observed essentially 100% phosphorylation in wild-type cells, reflecting the 10-fold higher CPT concentration in the present study. The radiosensitivity and defective RPA phosphorylation response confirm the kinase defect of DNA-PKcs-KR.

As seen previously [2], complementing VD13 and V24 cells with wild-type DNA-PKcs reduced DSB-induced HR by 2- to 3-fold (Fig. 2A). Surprisingly, VD13 derivatives with DNA-PKcs-KR had DSB-induced HR levels ~2- to 3-fold above DNA-PKcs null cells, and ~4- to 7-fold above wild-type (Fig. 2A). Similarly, DSB-induced HR was nearly 2-fold higher in V24 cells expressing DNA-PKcs-KR than null V24, and ~7-fold higher than wild-type (Fig. 2A). All cell lines showed equivalent transfection efficiencies with a GFP vector (Fig. 2B), indicating that the enhancement of DSB-induced HR by DNA-PKcs-KR is a general effect. To determine whether DNA-PKcs influences late HR stages, DSB-induced HR product spectra were generated. In wild-type cells, DSB-induced HR yields primarily continuous, short-tract, bidirectional gene conversions without crossovers (averaging 237 bp) [44]. Southern blot analysis of 19 and 24 DSB-induced HR products from VD13-KR4 and V24-KR3,

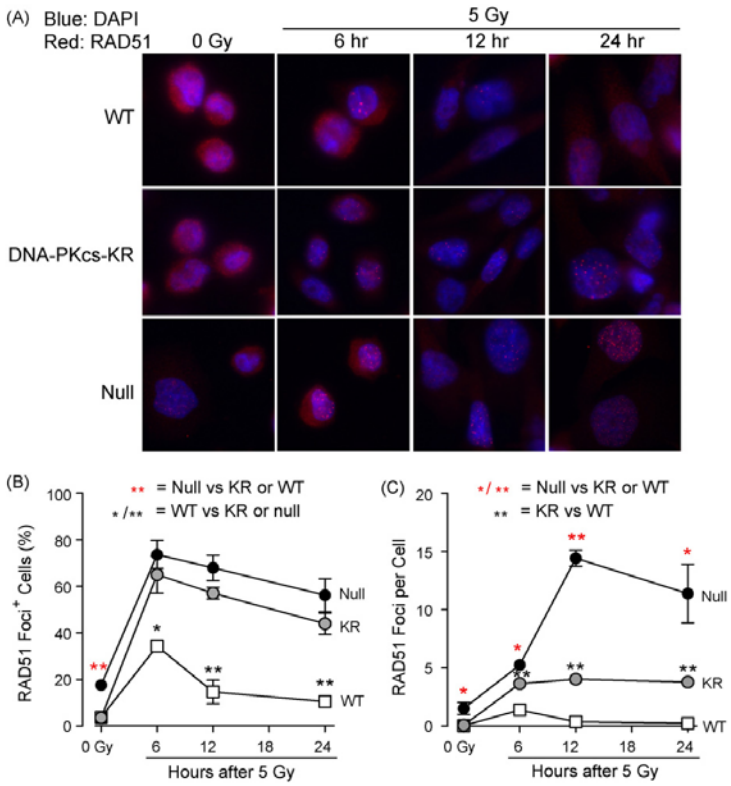

Fig. 3. IR-induced RAD51 foci resolve slowly in DNA-PKcs defective cells. (A) Representative immunofluorescent images of wild-type (AA8), DNA-PKcs null (VD13) and DNA-PKcs-KR (VD13-KR4) cells mock-treated or treated with 5 Gy IR. RAD51 was detected with anti-RAD51 antibodies (red) 6, 12, or 24 h after IR. Nuclei were stained blue (DAPI). Magnification = 40×. (B and C) Percentage of cells with 1 or more RAD51 foci, and number of RAD51 foci per cell. Values are averages ± SEM for three sets of images, with an average of 105 cells scored per data point. (*) indicates $P < 0.05$; (**) indicates $P < 0.01$.

respectively, showed that all 43 arose by gene conversion without crossovers. Conversion tracts from 30 V24-KR3 products were similar to wild-type: most were continuous and bidirectional, although average length was somewhat longer (354 bp). Thus, DNA-PKcs-KR affects HR efficiency, but not HR outcome, indicating that DNA-PKcs influences HR initiation, but not late HR stages.

Because NHEJ is the primary determinant of survival after IR [8,49], it is not surprising that the several-fold increase in HR in DNA-PKcs-KR does not increase IR resistance (Fig. 1A). Sensitivity to DNA crosslinking agents, such as MMC, is a highly sensitive measure of HR capacity because interstrand crosslink repair is strongly dependent on HR [50]. As shown in Fig. 2C, DNA-PKcs-KR cells were significantly more resistant to MMC than DNA-PKcs null cells. Together, these results indicate that DNA-PKcs-KR cells have a general hyperrecombination phenotype.

To further investigate the role of DNA-PKcs in HR regulation, we monitored RAD51 nuclear foci after IR [51]. These foci mark sites where RAD51 nucleoprotein filaments are formed, a necessary early HR step. RAD51 filaments search for and invade homologous sequences, and although filament formation and strand invasion are necessary early steps, studies with yeast and mammalian cells indicate that RAD51 turnover ("disassembly") is important to complete the HR process [52–55]. Thus, RAD51 foci mark sites of HR initiation, but not necessarily successful completion. RAD51 foci were scored in wild-type and DNA-PKcs mutant cells 6, 12, and 24 h after exposure to 5 Gy of γ-rays, and in untreated controls (Fig. 3). In untreated cells, there were slightly more RAD51 foci in DNA-PKcs null cells than wild-type or DNA-PKcs-KR cells, potentially reflecting defective NHEJ as well as other factors since DNA-PKcs-KR and null cells share a similar NHEJ defect. In this experiment, all three genetic backgrounds showed a peak in the percentage of cells with RAD51 foci 6 h after IR, and this declined over time. Wild-type cells had significantly fewer IR-induced RAD51 foci and foci resolved more quickly, reflecting fully functional NHEJ and HR systems. RAD51 persisted far longer in both DNA-PKcs null and DNA-PKcs-KR cells. Interestingly, although the two DNA-PKcs defective cell types had similar percentages of cells with IR-induced RAD51 foci (Fig. 3B), DNA-PKcs-KR cells had significantly fewer foci per cell than null cells (Fig. 3C). Because DNA-PKcs-KR and null cells have comparable NHEJ defects, this difference cannot be explained by differential NHEJ capacity. Instead, these results are consistent with DNA-PKcs-KR cells having a greater propensity to complete HR (i.e., resolve RAD51 foci), and are also consistent with their hyperrecombination phenotype (Fig. 2A and C).

3.2. *DNA-PKcs is recruited to DSBs independently of its kinase activity*

DNA-PKcs could regulate HR by direct action at DSBs, or indirectly through protein–protein interactions. However, any effect that requires a high level of kinase activity would likely require DNA ends since DNA-PKcs is fully activated by DNA end-binding

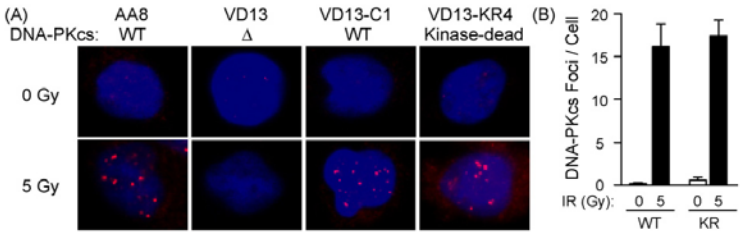

Fig. 4. DNA-PKcs is recruited to DSBs independently of its kinase activity. (A) Representative immunofluorescence images of DNA-PKcs foci 1 h after IR, detected with anti-DNA-PKcs antibodies. Nuclei are stained with DAPI (blue) and DNA-PKcs is stained red. Magnification = 100×. (B) Average number of DNA-PKcs foci per cell (±SEM); an average of 17 cells were scored per condition.

[8]. To further explore HR regulation by DNA-PKcs, we monitored DNA-PKcs focus formation after irradiation with 5 Gy γ-rays. DNA-PKcs foci were apparent in irradiated wild-type control (AA8) cells, in DNA-PKcs null cells complemented with wild-type DNA-PKcs or with DNA-PKcs-KR, but not in cells lacking DNA-PKcs (Fig. 4A). Irradiated cells expressing wild-type or DNA-PKcs-KR each had ~15 foci per cell whereas unirradiated and DNA-PKcs null cells had 0–1 foci (Fig. 4B). Fewer DNA-PKcs foci were detected than the >150 DSBs expected after 5 Gy IR, perhaps because DNA-PKcs may accumulate at detectable levels at a small fraction of DSBs. We conclude that

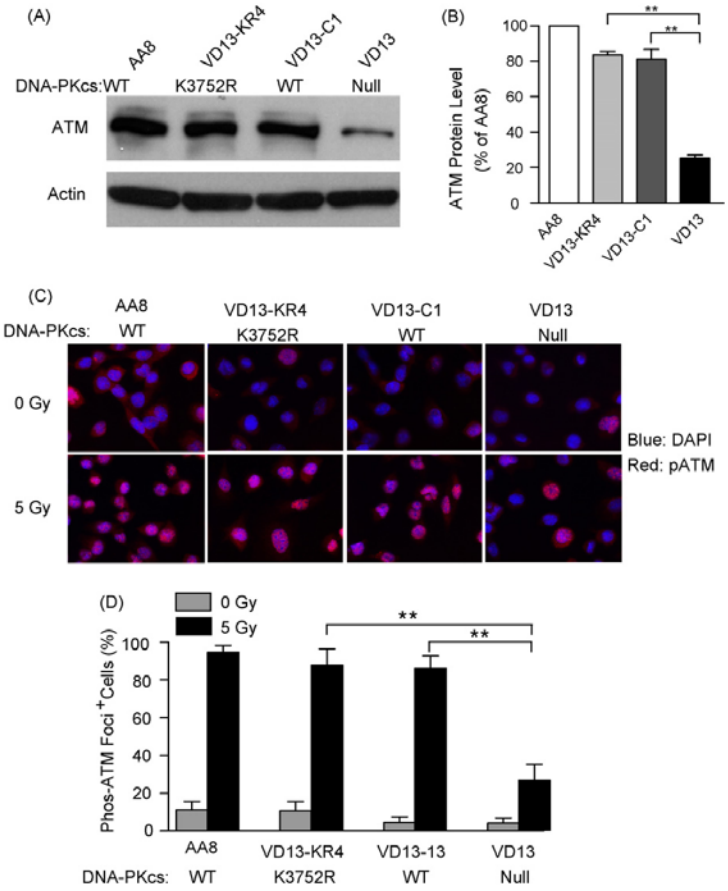

Fig. 5. Robust IR-induced ATM S1981 phosphorylation in wild-type and DNA-PKcs-KR mutant cells, but not in DNA-PKcs null cells. (A) Representative Western blot of ATM in cells expressing wild-type DNA-PKcs, DNA-PKcs-KR, or null; β-actin is the loading control. (B) Quantitation of ATM protein levels by scanning densitometry of three blots including the blot shown in panel A. For each blot, ATM levels were first normalized to actin levels, then the averages of normalized values (+SEM) for the three blots were plotted as a percentage of AA8 values. (**) indicates $P \leq 0.01$. (C) Representative images of activated ATM (pATM) detected with a phospho-S1981-specific antibody. Cells were fixed 1 h after IR. Magnification = 40×. (D) Percentage of cells with at least one phospho-S1981 focus. Values are averages (+SEM) for 3–6 images; an average of 40 cells were scored per condition. (**) indicates $P \leq 0.0011$.

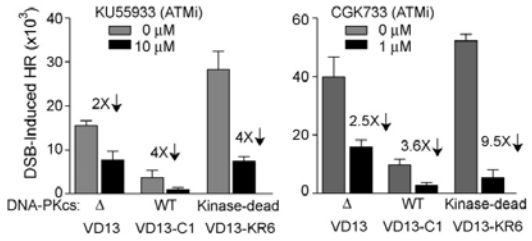

Fig. 6. Suppression of DSB-induced HR by ATM inhibitors is proportional to ATM protein levels. The ATM inhibitors KU55933 or CGK733 were present for 30 min before transfection with the I-*Sce*I expression vector, absent during transfection, and present for 12 h post-transfection, then medium was replaced with selective (G418) medium and cells were incubated for 10 days before staining with crystal violet. Plotted are average HR frequencies (+SD) for 2–3 determinations per strain.

DNA-PKcs recruitment to IR-induced DSBs occurs independently of its kinase activity, consistent with the results with laser-induced damage [56], raising the possibility that DNA-PKcs regulates HR at least in part through its presence at DNA ends.

3.3. DNA-PKcs regulates ATM levels independently of DNA-PKcs kinase activity

We next examined potential roles of ATM in the hyperrecombination phenotype of DNA-PKcs-KR cells because ATM is implicated in HR regulation, and ATM protein level decreases rapidly when DNA-PKcs is reduced by siRNA [29]. To test whether DNA-PKcs regulation of ATM levels depends on DNA-PKcs kinase activity, we measured total ATM levels and ATM activation by IR (S1981 phosphorylation) [16] in wild-type, DNA-PKcs null, and DNA-PKcs-KR cells (Fig. 5). Consistent with Peng et al. [29], ATM was reduced 3-fold in DNA-PKcs null cells, but ATM was largely restored by complementation with either wild-type DNA-PKcs or DNA-PKcs-KR (Fig. 5A and B). Cells expressing wild-type DNA-PKcs or DNA-PKcs-KR showed robust ATM S1981 phosphorylation after IR, but this response was attenuated by 3-fold in DNA-PKcs null cells (Fig. 5C and D), correlating well with ATM protein levels. Thus, ATM protein level depends on DNA-PKcs, but this regulation is independent of DNA-PKcs kinase activity.

3.4. Chemical inhibition of ATM reduces DSB-induced HR, phosphorylation of the DNA-PKcs T2609 cluster, and IR-induced RAD51 foci

Low concentrations of caffeine inhibit the kinase activity of ATM kinase, and higher concentrations also inhibit ATR and DNA-PKcs [57]. Caffeine sensitizes cells to the lethal effects of IR by inactivating the ATM-dependent G2/M DNA damage checkpoint [58]. Caffeine also suppresses both DSB-induced HR, and IR-induced RAD51 focus formation, but these effects are independent of the checkpoint defect [59]. However, no prior evidence directly linked caffeine-suppression of DSB-induced HR with ATM inhibition. To explore this possibility, we measured DSB-induced HR in cells treated with the highly specific ATM inhibitor KU55933 [60]. DSB-induced HR was reduced 4-fold by KU55933 in cells expressing wild-type DNA-PKcs or DNA-PKcs-KR, both of which express normal ATM levels, but only 2-fold in DNA-PKcs null cells with reduced ATM expression (Fig. 6). Similar results were obtained with CGK733 (Fig. 6), another ATM inhibitor [61]. The marked reduction in DSB-induced HR in DNA-PKcs-KR cells is clear evidence that these inhibitors suppress HR independently of DNA-PKcs kinase inhibition. Note that absolute HR levels varied by ~2-fold in the KU55933 and CGK733 experiments reflecting different transfection efficiencies on different days. Similar trends were observed with caffeine, a relatively non-specific ATM inhibitor (supplementary Fig. S1). At the doses used, none of the ATM inhibitors had a significant effect on cell viability in these genetic backgrounds (data not shown). The lesser effects of the ATM inhibitors in DNA-PKcs null cells are consistent with the lower ATM protein level in these cells (Fig. 5A and B).

The DNA-PKcs T2609 cluster can be phosphorylated by DNA-PKcs itself and by ATM [30,38,62,63]. Phosphorylation of the T2609 cluster (and other sites) can increase access of repair factors to DNA ends by causing conformation shifts and/or DNA-PKcs dissociation from broken ends [3,4,15]. Because autophosphorylation of the T2609 cluster is not possible in DNA-PKcs-KR cells, we investigated ATM-dependent phosphorylation of the T2609 cluster as a potential contributor to the DNA-PKcs-KR hyperrecombination phenotype. We measured T2609 phosphorylation (pT2609) and RAD51 foci in irradiated wild-type and DNA-PKcs-KR mutant cells in the presence or absence of the ATM inhibitor KU55933. The pT2609 antibody detects pT2609 on Western blots [30], but also detects another protein phosphorylated after IR, revealed as a low level signal (and generally smaller foci) in cells expressing mutant DNA-PKcs in which the T2609 cluster residues are changed to alanine (ABCDE; Fig. 7A) or lacking DNA-PKcs (data not shown). To quantitate pT2609 foci, the average number of foci in the ABCDE mutant was subtracted from values obtained with cells expressing wild-type DNA-PKcs or DNA-PKcs-KR. In wild-type cells, pT2609 foci were strongly induced 1 h after IR (Fig. 7A), with >20% of cells showing >10 foci (Fig. 7B). This signal decreased to background levels by 6 h after IR (data not shown). IR also strongly induced pT2609 in DNA-PKcs-KR cells; this is an ATM-dependent event as it was completely eliminated by the ATM inhibitor KU55933 (Fig. 7A, B). KU55933 did not completely eliminate pT2609 foci in wild-type cells, consistent with residual DNA-PKcs autophosphorylation (Fig. 7A, B). Similar results were obtained with caffeine (data not shown).

Interestingly, KU55933 had identical effects on RAD51 foci, reducing RAD51 foci in wild-type cells and eliminating them in DNA-PKcs-KR cells (Fig. 7C and D). Again, similar results were seen with CGK733 (data not shown), as reported with caffeine [59]. The differential effects of ATM inhibition in wild-type vs. DNA-PKcs-KR cells can be explained by residual DNA-PKcs autophosphorylation of T2609 in wild-type, a pathway that is blocked in the DNA-PKcs-KR mutant. Note also that RAD51 foci were unaffected by KU55933 in cells lacking DNA-PKcs, consistent with the low level of ATM in these cells. The results in Figs. 6 and 7 demonstrate a strong correlation among IR-induced pT2609, IR-induced RAD51 foci, and DSB-induced HR.

4. Discussion

DNA-PKcs has emerged as a key regulator of both NHEJ and HR. DNA-PKcs plays critical roles in NHEJ which repairs 70–85% of nuclease-induced DSBs in log-phase mammalian cells [3,64]. Thus, the 2- to 5-fold increase in DSB-induced HR in cells lacking DNA-PKcs, Ku, or XRCC4 is consistent with passive shunting of DSBs toward HR [2,6,7]. However, chemical inhibition of DNA-PKcs, and DNA-PKcs isoforms lacking the kinase domain, suppress DSB-induced HR [3,4], indicating that DNA-PKcs regulation of HR is not solely due to passive shunting. The current data demonstrating that a DNA-PKcs kinase-inactive point mutant increases DSB-induced HR and MMC resistance above levels observed in DNA-PKcs null cells further supports the idea that DNA-PKcs actively regulates NHEJ and HR, and reveals additional complexity in this regulation. NHEJ factors are recruited to laser-induced DSBs more rapidly than HR factors but there is a significant period of time when both sets of factors are present at damage sites [65], providing an opportunity for crosstalk. Our study suggests two general ways that DNA-PKcs regulates DSB-induced HR: through modulation of ATM levels (and ATM activity), and through end accessibility to repair factors.

4.1. Indirect regulation of HR by DNA-PKcs through ATM

In addition to its well-characterized checkpoint signaling functions, ATM has been implicated in several aspects of HR. ATM inhibitors reduce DSB-induced HR and block IR-induced RAD51 foci (Figs. 6, 7, S1) [3,59]. Note that ATM inhibitors reduce HR in cells expressing wild-type DNA-PKcs and DNA-PKcs-KR, but not in DNA-PKcs null cells (Fig. 6), which have low ATM levels (Fig. 5). The fact that ATM can phosphorylate the DNA-PKcs T2609 cluster [30], and that this modification, along with other phosphorylated residues in DNA-PKcs, regulates end accessibility (see below), suggests a mechanism by which ATM regulates HR through DNA-PKcs modification, contributing to the hyperrecombination phenotype of DNA-PKcs-KR cells. Genetic and molecular analyses indicate that ATM promotes HR repair of DSBs that arise independently of replication (i.e., from IR or I-*Sce*I) [25,26]. Part of this ATM role is phosphorylation of H2AX because DSB-induced HR is reduced several-fold in H2AX$^{-/-}$ cells [27]. Although two reports suggested that ATM does not promote DSB-induced HR [66,67], this may reflect redundancy with DNA-PKcs since DNA-PKcs can phosphorylate both itself, including the T2609 cluster [15], and H2AX [68]. Also, defects in mouse ATM and DMC1, a meiosis-specific RAD51 homolog, cause very similar meiotic repair defects [69].

Among known or suspected ATM targets, at least 12 are implicated in HR [70]. Importantly, six of these targets are also phosphorylated by DNA-PKcs (Fig. 8A). Moreover, ATM levels are controlled by DNA-PKcs in many cell types [29] (this study) and DNA-PKcs and ATM each phosphorylate the DNA-PKcs T2609 cluster that is important for NHEJ [30,38,62] and for HR [4], indicating that these proteins coordinately regulate DSB repair. We show here that DNA-PKcs controls ATM levels independently of DNA-PKcs kinase activity, indicating that ATM stabilization does not depend on DNA-PKcs-mediated phosphorylation of ATM or other targets. Also, the level of activated ATM after IR is normal in cells expressing DNA-PKcs-KR, but not in DNA-PKcs null cells (Fig. 5C and D). The restoration of ATM protein by DNA-PKcs-KR is likely a major contributor to the hyperrecombination phenotype of DNA-PKcs-KR cells. A key ATM target is the c-Abl kinase, which regulates RAD51 activity. Defects in c-Abl or ATM delay IR-induced RAD51 focus formation [71], suggesting that these proteins act early during RAD51 filament formation. Importantly, c-Abl phosphorylation of RAD51

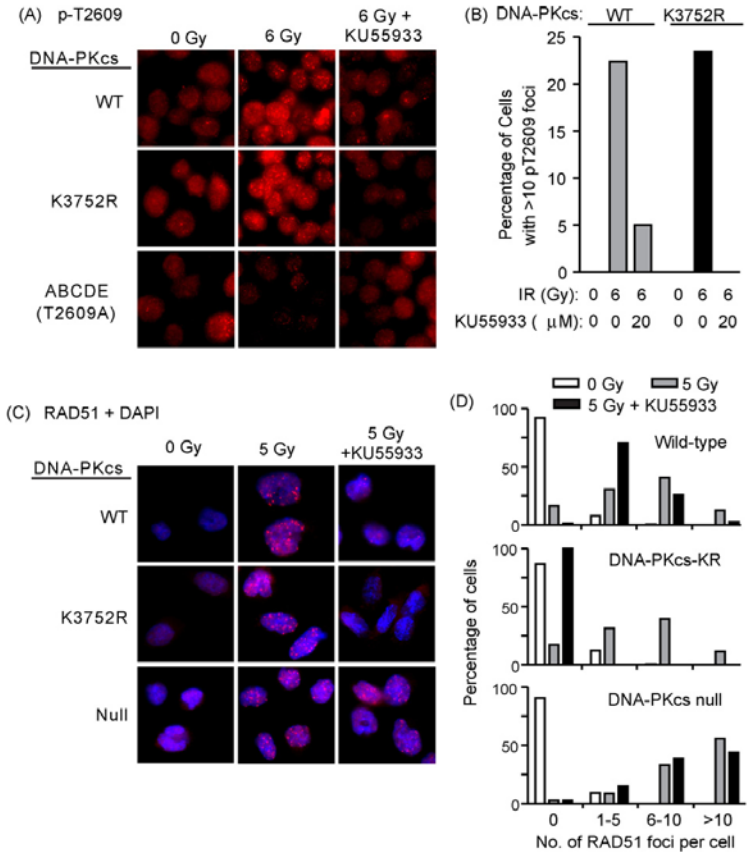

Fig. 7. IR-induced phosphorylation of the DNA-PKcs T2609 cluster correlates with RAD51 focus formation. (A) Representative images of cells probed with antibodies against pT2609. Cells expressing wild-type DNA-PKcs, DNA-PKcs-KR, or the ABCDE mutant were untreated or treated with 20 μM KU55933 for 30 min prior to IR or mock exposure, fixed 1 h later, and probed for pT2609. Magnification = 40×. (B) Quantitative analysis of pT2609 foci in wild-type and DNA-PKcs-KR cells. The average number of foci in the ABCDE mutant was subtracted from wild-type or DNA-PKcs-KR values with equivalent treatment to correct for non-specific foci. Foci were scored in an average of 112 nuclei per treatment. (C) Representative images of IR-induced RAD51 foci in DNA-PKcs null or derivatives expressing wild-type DNA-PKcs or DNA-PKcs-KR. Cells were treated with 20 μM KU55933 for 30 min prior to IR or mock exposure, and fixed 6 h later and probed with anti-RAD51 antibodies (red). Nuclei were stained with DAPI (blue). Magnification = 40×. (D) Frequency distributions of IR-induced RAD51 foci based on scoring an average of 208 cells per condition.

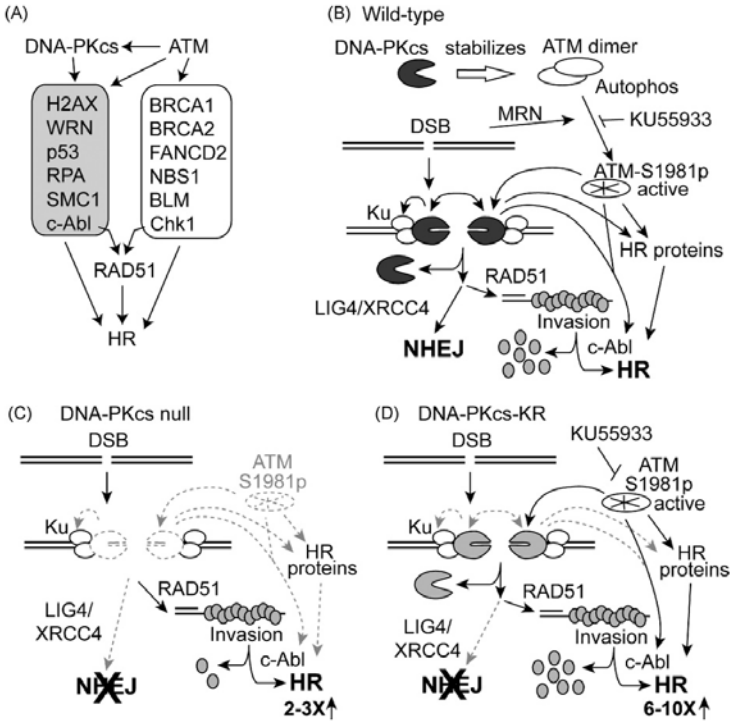

Fig. 8. Model for DNA-PKcs and ATM regulation of NHEJ and HR. See text for details.

reduces RAD51 affinity for single-stranded DNA, so this modification may drive RAD51 filament disassembly, a key late-stage process in the maturation of HR intermediates to HR products [52–55]. In DNA-PKcs null cells, ATM levels are reduced but not eliminated, and IR-induced RAD51 foci are readily detected (Fig. 3). In the DNA-PKcs-KR mutant, with normal ATM levels, IR also induces RAD51 foci but they are not as persistent as those in DNA-PKcs null cells (Fig. 3C). One interpretation of these results is that longer lived RAD51 foci in DNA-PKcs null cells represent sites where HR intermediates fail to mature into products, whereas more quickly resolved RAD51 foci in DNA-PKcs-KR cells reflect successful completion of HR. Interestingly, ATM defective cells show increased IR-induced RAD51 foci [72], which indicates that RAD51 foci form independently of ATM, and consistent with the idea that ATM promotes RAD51 turnover. Given that many HR proteins are targeted by ATM (Fig. 8A), this is but one example of how restoration of ATM in DNA-PKcs-KR cells might contribute to the hyperrecombination phenotype of DNA-PKcs-KR cells.

4.2. HR regulation by DNA-PKcs through end accessibility

Phosphorylation of the DNA-PKcs T2609 and S2056 clusters regulates accessibility of broken ends to repair factors [5,31–37]. In DNA-PKcs-KR, the S2056 cluster is not phosphorylated because this cluster is subject only to autophosphorylation [30]. Mutations in the S2056 cluster that block phosphorylation increase DSB-induced HR above the wild-type level, but not above the level seen in DNA-PKcs null cells [5], unlike DNA-PKcs-KR which does increase HR above that in null cells (Fig. 2). Thus, the higher HR levels with DNA-PKcs-KR cannot be fully explained by the absence of S2056 cluster phosphorylation, but probably also reflects the absence of NHEJ competition since NHEJ strongly depends on DNA-PKcs kinase activity [9] but only weakly depends on S2056 cluster phosphorylation [5]. Because the T2609 cluster is phosphorylated in vivo by ATM [30], ATM may play an important role in this (and perhaps other) DNA-PKcs modifications that regulate end accessibility by releasing DNA-PKcs or effecting conformational changes, particularly when DNA-PKcs autophosphorylation is blocked in DNA-PKcs-KR cells. This view is supported by the marked reduction in T2609 phosphorylation in DNA-PKcs-KR cells treated with ATM inhibitors (Fig. 7A and B). Although ATM-mediated modifications of DNA-PKcs-KR may be sufficient to allow HR to proceed, ATM cannot replace DNA-PKcs kinase activity during NHEJ [9].

DNA-PKcs-KR was shown to dissociate more slowly from laser-induced DSBs than wild-type DNA-PKcs, perhaps reflecting slower kinetics of ATM-dependent phosphorylation vs. autophosphorylation, and this was proposed to inhibit NHEJ [56]. However, slow dissociation of DNA-PKcs-KR may not reduce DSB-induced HR since HR occurs more slowly than NHEJ, and minor delays may not be detected in DSB-induced HR assays since HR products are selected two days after DSB induction. It is also possible that DNA-PKcs dynamics differ at I-*Sce*I vs. laser-induced DSBs.

HR levels increase when cells progress from G1 to S/G2 when sister chromatids become available as HR repair templates. If T2609 phosphorylation is required for DNA-PKcs dissociation from ends before end processing for HR, it is curious that IR-induced T2609 phosphorylation is lower in S phase than G1 phase [63]. DNA-PKcs recruitment to DSBs may be attenuated in S phase. This would reduce T2609 phosphorylation because DNA-PKcs is likely to be phosphorylated only when bound to DSBs. Alternatively, T2609 may be phosphorylated in S phase at undetectable, but sufficient levels to increase end accessibility, or accessibility may increase

at later times. The reduction in T2609 phosphorylation in S phase was observed 30 min after IR [63] whereas HR occurs over several hours. As above, T2609 phosphorylation may also differ between IR- and I-*Sce*I-induced DSBs. In any case, our data indicate that T2609 is phosphorylated in DNA-PKcs-KR cells, this is blocked by ATM inhibitors, and blocking T2609 phosphorylation correlates with reduced RAD51 foci and reduced HR (Figs. 6 and 7).

4.3. Co-regulation of DSB repair by DNA-PKcs and ATM

The regulation of ATM levels by DNA-PKcs and phosphorylation of DNA-PKcs by ATM suggest that these proteins function in an integrated manner to regulate DSB repair by NHEJ and HR. In Fig. 8 we propose a model for co-regulation of NHEJ and HR by DNA-PKcs and ATM. In wild-type cells, DNA-PKcs promotes NHEJ which suppresses HR; this involves auto- and/or ATM-dependent phosphorylation of DNA-PKcs increasing end accessibility (shown as DNA-PKcs release in Fig. 8B). Because ATM targets many HR proteins (Fig. 8A), the low ATM level in DNA-PKcs null cells, and its restoration by DNA-PKcs-KR, can account for the higher DSB-induced HR levels in DNA-PKcs-KR cells. In both cases, the competing NHEJ pathway is inactive, but in the absence of DNA-PKcs only a moderate increase in HR is seen because the ATM level is low (Fig. 8C). In cells expressing DNA-PKcs-KR, NHEJ is also inactive but ATM is expressed at a normal level and activated normally by damage, thus ATM can exert its full positive effect(s) on DSB-induced HR (Fig. 8D). ATM inhibitors like KU55933 block HR in wild-type and DNA-PKcs-KR cells (Fig. 8B and D), but not DNA-PKcs null cells (Fig. 8C). Included in this model are DNA-PKcs- and ATM-dependent phosphorylation of c-Abl, which is proposed to disassemble RAD51 filaments (light grey ovals) during a late HR stage. This is but one example of how ATM might enhance HR in DNA-PKcs-KR cells compared to DNA-PKcs null cells. Also, note that c-Abl phosphorylates DNA-PKcs (not shown in Fig. 8), and probably DNA-PKcs-KR as well, providing a feedback loop [73].

In conclusion, our results indicate that DSB repair pathway choice and efficiency are regulated by DNA-PKcs and ATM, and that ATM promotes HR repair of DSBs arising independently of replication by phosphorylating DNA-PKcs and HR factors. DSB repair by NHEJ and HR contribute to genome stability, both pathways are likely to play significant roles in tumor resistance to chemo- and radio-therapy, and targeting these pathways may improve the efficacy of cancer therapy. The manipulation of HR and NHEJ pathways also holds promise for improving gene-targeting efficiency in laboratory and gene therapy settings.

Conflict of interest statement

None.

Acknowledgements

We thank K. Meek, S. Lees-Miller, P. Jeggo, and members of the Nickoloff lab for helpful discussions. We acknowledge support from the UNM Cancer Center Fluorescence Microscopy and Flow Cytometry Facilities which receive support from NCRR S10 RR14668, NSF MCB9982161, NCRR P20 RR11830, NCI R24 CA88339, NCRR S10 RR19287, NCRR S10 RR016918 and NCI P30 CA118100 awards. This work was supported by NCI grants R01 CA100862 (JAN), R01 CA50519 (DJC) and P01 CA92584 (DJC).

Appendix A. Supplementary data

Supplementary data associated with this article can be found, in the online version, at doi:10.1016/j.dnarep.2009.05.006.

References

[1] M. Shrivastav, L.P. De Haro, J.A. Nickoloff, Regulation of DNA double-strand break repair pathway choice, Cell Res. 18 (2008) 134–147.
[2] C. Allen, A. Kurimasa, M.A. Brennemann, D.J. Chen, J.A. Nickoloff, DNA-dependent protein kinase suppresses double-strand break-induced and spontaneous homologous recombination, Proc. Natl. Acad. Sci. U.S.A. 99 (2002) 3758–3763.
[3] C. Allen, J. Halbrook, J.A. Nickoloff, Interactive competition between homologous recombination and non-homologous end joining, Mol. Cancer Res. 1 (2003) 913–920.
[4] E. Convery, E.K. Shin, Q. Ding, W. Wang, P. Douglas, J.A. Nickoloff, S. Lees-Miller, K. Meek, Inhibition of homologous recombination by variants of the catalytic subunit of the DNA-dependent protein kinase (DNA-PKcs), Proc. Natl. Acad. Sci. U.S.A. 102 (2005) 1345–1350.
[5] X. Cui, Y. Yu, S. Gupta, Y.M. Cho, S.P. Lees-Miller, K. Meek, Autophosphorylation of DNA-dependent protein kinase regulates DNA end processing and may also alter double-strand break repair pathway choice, Mol. Cell. Biol. 25 (2005) 10842–10852.
[6] F. Delacote, M. Han, T.D. Stamato, M. Jasin, B.S. Lopez, An *xrcc4* defect or Wortmannin stimulates homologous recombination specifically induced by double-strand breaks in mammalian cells, Nucleic Acids Res. 30 (2002) 3454–3463.
[7] A.J. Pierce, P. Hu, M.G. Han, N. Ellis, M. Jasin, Ku DNA end-binding protein modulates homologous repair of double-strand breaks in mammalian cells, Genes Dev. 15 (2001) 3237–3242.
[8] S.P. Lees-Miller, K. Meek, Repair of DNA double strand breaks by non-homologous end joining, Biochimie 85 (2003) 1161–1173.
[9] A. Kurimasa, S. Kumano, N.V. Boubnov, M.D. Story, C.S. Tung, S.R. Peterson, D.J. Chen, Requirement for the kinase activity of human DNA-dependent protein kinase catalytic subunit in DNA strand break rejoining, Mol. Cell. Biol. 19 (1999) 3877–3884.
[10] R.G. Shao, C.X. Cao, H. Zhang, K.W. Kohn, M.S. Wold, Y. Pommier, Replication-mediated DNA damage by camptothecin induces phosphorylation of RPA by DNA-dependent protein kinase and dissociates RPA:DNA-PK complexes, EMBO J. 18 (1999) 1397–1406.
[11] S. Burma, D.J. Chen, Role of DNA-PK in the cellular response to DNA double-strand breaks, DNA Repair 3 (2004) 909–918.
[12] D.W. Chan, R.Q. Ye, C.J. Veillette, S.P. Lees-Miller, DNA-Dependent protein kinase phosphorylation sites in Ku 70/80 heterodimer, Biochemistry 38 (1999) 1819–1828.
[13] P. Karmakar, J. Piotrowski, R.M. Brosh, J.A. Sommers, S.P.L. Miller, W.H. Cheng, C.M. Snowden, D.A. Ramsden, V.A. Bohr, Werner protein is a target of DNA-dependent protein kinase in vivo and in vitro, and its catalytic activities are regulated by phosphorylation, J. Biol. Chem. 277 (2002) 18291–18302.
[14] S.M. Yannone, S. Roy, D.W. Chan, M.B. Murphy, S.R. Huang, J. Campisi, D.J. Chen, Werner syndrome protein is regulated and phosphorylated by DNA-dependent protein kinase, J. Biol. Chem. 276 (2001) 38242–38248.
[15] K. Meek, V. Dang, S.P. Lees-Miller, DNA-PK: the means to justify the ends? Adv. Immunol. 99 (2008) 33–58.
[16] C.J. Bakkenist, M.B. Kastan, DNA damage activates ATM through intermolecular autophosphorylation and dimer dissociation, Nature 421 (2003) 499–506.
[17] M.B. Kastan, D.S. Lim, S.T. Kim, D. Yang, ATM—a key determinant of multiple cellular responses to irradiation, Acta Oncol. 40 (2001) 686–688.
[18] R. Kitagawa, C.J. Bakkenist, P.J. McKinnon, M.B. Kastan, Phosphorylation of SMC1 is a critical downstream event in the ATM-NBS1-BRCA1 pathway, Genes Dev. 18 (2004) 1423–1438.
[19] R. Baskaran, L.D. Wood, L.L. Whitaker, C.E. Canman, S.E. Morgan, Y. Xu, C. Barlow, D. Baltimore, A. Wynshaw-Boris, M.B. Kastan, J.Y. Wang, Ataxia telangiectasia mutant protein activates c-Abl tyrosine kinase in response to ionizing radiation, Nature 387 (1997) 516–519.
[20] S. Burma, B.P. Chen, M. Murphy, A. Kurimasa, D.J. Chen, ATM phosphorylates histone H2AX in response to DNA double-strand breaks, J. Biol. Chem. 276 (2001) 42462–42467.
[21] M.E. Dar, T.A. Winters, T.J. Jorgensen, Identification of defective illegitimate recombinational repair of oxidatively-induced dna double-strand breaks in ataxia telangiectasia cells, Mutat. Res. 384 (1997) 169–179.
[22] M. Kuhne, E. Riballo, N. Rief, K. Rothkamm, P.A. Jeggo, M. Lobrich, A double-strand break repair defect in ATM-deficient cells contributes to radiosensitivity, Cancer Res. 64 (2004) 500–508.
[23] E. Riballo, M. Kuhne, N. Rief, A. Doherty, G.C. Smith, M.J. Recio, C. Reis, K. Dahm, A. Fricke, A. Krempler, A.R. Parker, S.P. Jackson, A. Gennery, P.A. Jeggo, M. Lobrich, A pathway of double-strand break rejoining dependent upon ATM, Artemis, and proteins locating to γ-H2AX foci, Mol. Cell 16 (2004) 715–724.
[24] A.L. Bredemeyer, G.G. Sharma, C.Y. Huang, B.A. Helmink, L.M. Walker, K.C. Khor, B. Nuskey, K.E. Sullivan, T.K. Pandita, C.H. Bassing, B.P. Sleckman, ATM stabilizes DNA double-strand-break complexes during V(D)J recombination, Nature 442 (2006) 466–470.
[25] C. Morrison, E. Sonoda, N. Takao, A. Shinohara, K. Yamamoto, S. Takeda, The controlling role of ATM in homologous recombinational repair of DNA damage, EMBO J. 19 (2000) 463–471.
[26] C.-M. Luo, W. Tang, K.L. Mekeel, J.S. DeFrank, P.R. Anne, S.N. Powell, High frequency and error-prone DNA recombination in ataxia telangiectasia cell lines, J. Biol. Chem. 271 (1996) 4497–4503.

[27] A. Xie, N. Puget, I. Shim, S. Odate, I. Jarzyna, C.H. Bassing, F.W. Alt, R. Scully, Control of sister chromatid recombination by histone H2AX, Mol. Cell 16 (2004) 1017–1025.
[28] T. Stiff, M. O'Driscoll, N. Rief, K. Iwabuchi, M. Lobrich, P.A. Jeggo, ATM and DNA-PK function redundantly to phosphorylate H2AX after exposure to ionizing radiation, Cancer Res. 64 (2004) 2390–2396.
[29] Y. Peng, R.G. Woods, H. Beamish, R. Ye, S.P. Lees-Miller, M.F. Lavin, J.S. Bedford, Deficiency in the catalytic subunit of DNA-dependent protein kinase causes down-regulation of ATM, Cancer Res. 65 (2005) 1670–1677.
[30] B.P. Chen, N. Uematsu, J. Kobayashi, Y. Lerenthal, A. Krempler, H. Yajima, M. Lobrich, Y. Shiloh, D.J. Chen, Ataxia telangiectasia mutated (ATM) is essential for DNA-PKcs phosphorylations at the Thr-2609 cluster upon DNA double strand break, J. Biol. Chem. 282 (2007) 6582–6587.
[31] D.W. Chan, S.P. Lees-Miller, The DNA-dependent protein kinase is inactivated by autophosphorylation of the catalytic subunit, J. Biol. Chem. 271 (1996) 8936–8941.
[32] P. Calsou, P. Frit, O. Humbert, C. Muller, D.J. Chen, B. Salles, The DNA-dependent protein kinase catalytic activity regulates DNA end processing by means of Ku entry into DNA, J. Biol. Chem. 274 (1999) 7848–7856.
[33] D. Merkle, P. Douglas, G.B.G. Moorhead, Z. Leonenko, Y. Yu, D. Cramb, D.P. Bazett-Jones, S.P. Lees-Miller, The DNA-dependent protein kinase interacts with DNA to form a protein-DNA complex that is disrupted by phosphorylation, Biochemistry 41 (2002) 12706–12714.
[34] P. Douglas, G.B.G. Moorhead, R.Q. Ye, S.P. Lees-Miller, Protein phosphatases regulate DNA-dependent protein kinase activity, J. Biol. Chem. 276 (2001) 18992–18998.
[35] Q. Ding, Y.V. Reddy, W. Wang, T. Woods, P. Douglas, D.A. Ramsden, S.P. Lees-Miller, K. Meek, Autophosphorylation of the catalytic subunit of the DNA-dependent protein kinase is required for efficient end processing during DNA double-strand break repair, Mol. Cell. Biol. 23 (2003) 5836–5848.
[36] W.D. Block, Y. Yu, D. Merkle, J.L. Gifford, Q. Ding, K. Meek, S.P. Lees-Miller, Autophosphorylation-dependent remodeling of the DNA-dependent protein kinase catalytic subunit regulates ligation of DNA ends, Nucleic Acids Res. 32 (2004) 4351–4357.
[37] Y.V. Reddy, Q. Ding, S.P. Lees-Miller, K. Meek, D.A. Ramsden, Non-homologous end joining requires that the DNA-PK complex undergo an autophosphorylation-dependent rearrangement at DNA ends, J. Biol. Chem. 279 (2004) 39408–39413.
[38] D.W. Chan, B.P.-C. Chen, S. Prithivirasingh, A. Kurimasa, M.D. Story, J. Qin, D.J. Chen, Autophosphorylation of the DNA-dependent protein kinase catalytic subunit is required for rejoining of DNA double-strand breaks, Genes Dev. 16 (2002) 2333–2338.
[39] K. Meek, P. Douglas, X. Cui, Q. Ding, S.P. Lees-Miller, trans Autophosphorylation at DNA-dependent protein kinase's two major autophosphorylation site clusters facilitates end processing but not end joining, Mol. Cell. Biol. 27 (2007) 3881–3890.
[40] L.F. Povirk, R.Z. Zhou, D.A. Ramsden, S.P. Lees-Miller, K. Valerie, Phosphorylation in the serine/threonine 2609-2647 cluster promotes but is not essential for DNA-dependent protein kinase-mediated nonhomologous end joining in human whole-cell extracts, Nucleic Acids Res. 35 (2007) 3869–3878.
[41] P.L. Deininger, M.A. Batzer, Mammalian retroelements, Genome Res. 12 (2002) 1455–1465.
[42] P. Stankiewicz, J.R. Lupski, Genome architecture, rearrangements and genomic disorders, Trends Genet. 18 (2002) 74–82.
[43] L.N. Johnson, M.E. Noble, D.J. Owen, Active and inactive protein kinases: structural basis for regulation, Cell 85 (1996) 149–158.
[44] D.G. Taghian, J.A. Nickoloff, Chromosomal double-strand breaks induce gene conversion at high frequency in mammalian cells, Mol. Cell. Biol. 17 (1997) 6386–6393.
[45] H. Lu, X. Guo, X. Meng, J. Liu, J. Wray, C. Allen, J.A. Nickoloff, Z. Shen, The BRCA2-interacting protein BCCIP functions in RAD51 and BRCA2 focus formation and homologous recombinational repair, Mol. Cell. Biol. 25 (2005) 1949–1957.
[46] C. Allen, C.A. Miller, J.A. Nickoloff, The mutagenic potential of a single DNA double-strand break is not influenced by transcription, DNA Repair 2 (2003) 1147–1156.
[47] J.A. Nickoloff, Recombination: mechanisms and roles in tumorigenesis, in: J.R. Bertino (Ed.), Encyclopedia of Cancer, Second ed., Elsevier Science (USA), San Diego, 2002, pp. 49–59.
[48] W.D. Block, Y. Yu, S.P. Lees-Miller, Phosphatidyl inositol 3-kinase-like serine/threonine protein kinases (PIKKs) are required for DNA damage-induced phosphorylation of the 32 kDa subunit of replication protein A at threonine 21, Nucleic Acids Res. 32 (2004) 997–1005.
[49] L.H. Thompson, D. Schild, The contribution of homologous recombination in preserving genome integrity in mammalian cells, Biochimie 81 (1999) 87–105.
[50] D.T. Bergstralh, J. Sekelsky, Interstrand crosslink repair: can XPF-ERCC1 be let off the hook? Trends Genet. 24 (2008) 70–76.
[51] E. Raderschall, K. Stout, S. Freier, V. Suckow, S. Schweiger, T. Haaf, Elevated levels of Rad51 recombination protein in tumor cells, Cancer Res. 62 (2002) 219–225.
[52] C.W. Fung, G.S. Fortin, S.E. Peterson, L.S. Symington, The *rad51-K191R* ATPase-defective mutant is impaired for presynaptic filament formation, Mol. Cell. Biol. 26 (2006) 9544–9554.
[53] A.A. Davies, J.Y. Masson, M.J. McLlwraith, A.Z. Stasiak, A. Stasiak, A.R. Venkitaraman, S.C. West, Role of BRCA2 in control of the RAD51 recombination and DNA repair protein, Mol. Cell 7 (2001) 273–282.
[54] J.A. Solinger, K. Kiianitsa, W.D. Heyer, Rad54, a Swi2/Snf2-like recombinational repair protein, disassembles Rad51:dsDNA filaments, Mol. Cell 10 (2002) 1175–1188.
[55] M. Shinohara, S.L. Gasior, D.K. Bishop, A. Shinohara, Tid1/Rdh54 promotes colocalization of Rad51 and Dmc1 during meiotic recombination, Proc. Natl. Acad. Sci. U.S.A. 97 (2000) 10814–10819.
[56] N. Uematsu, E. Weterings, K. Yano, K. Morotomi-Yano, B. Jakob, G. Taucher-Scholz, P.O. Mari, D.C. van Gent, B.P. Chen, D.J. Chen, Autophosphorylation of DNA-PKCS regulates its dynamics at DNA double-strand breaks, J. Cell Biol. 177 (2007) 219–229.
[57] J.N. Sarkaria, E.C. Busby, R.S. Tibbetts, P. Roos, Y. Taya, L.M. Karnitz, R.T. Abraham, Inhibition of ATM and ATR kinase activities by the radiosensitizing agent, caffeine, Cancer Res. 59 (1999) 4375–4382.
[58] B.B. Zhou, P. Chaturvedi, K. Spring, S.P. Scott, R.A. Johanson, R. Mishra, M.R. Mattern, J.D. Winkler, K.K. Khanna, Caffeine abolishes the mammalian G(2)/M DNA damage checkpoint by inhibiting ataxia-telangiectasia-mutated kinase activity, J. Biol. Chem. 275 (2000) 10342–10348.
[59] H. Wang, W. Boecker, H. Wang, X. Wang, J. Guan, L.H. Thompson, J.A. Nickoloff, G. Iliakis, Caffeine inhibits homology directed repair of I-SceI induced DNA double-strand breaks, Oncogene 23 (2004) 824–834.
[60] I. Hickson, Y. Zhao, C.J. Richardson, S.J. Green, N.M. Martin, A.I. Orr, P.M. Reaper, S.P. Jackson, N.J. Curtin, G.C. Smith, Identification and characterization of a novel and specific inhibitor of the ataxia-telangiectasia mutated kinase ATM, Cancer Res. 64 (2004) 9152–9159.
[61] J. Won, M. Kim, N. Kim, J.H. Ahn, W.G. Lee, S.S. Kim, K.Y. Chang, Y.W. Yi, T.K. Kim, Small molecule-based reversible reprogramming of cellular lifespan, Nat. Chem. Biol. 2 (2006) 369–374.
[62] P. Douglas, G.P. Sapkota, N. Morrice, Y.P. Yu, A.A. Goodarzi, D. Merkle, K. Meek, D.R. Alessi, S.P. Lees-Miller, Identification of in vitro and in vivo phosphorylation sites in the catalytic subunit of the DNA-dependent protein kinase, Biochem. J. 368 (2002) 243–251.
[63] B.P. Chen, D.W. Chan, J. Kobayashi, S. Burma, A. Asaithamby, K. Morotomi-Yano, E. Botvinick, J. Qin, D.J. Chen, Cell cycle dependence of DNA-dependent protein kinase phosphorylation in response to DNA double strand breaks, J. Biol. Chem. 280 (2005) 14709–14715.
[64] F. Liang, M.G. Han, P.J. Romanienko, M. Jasin, Homology-directed repair is a major double-strand break repair pathway in mammalian cells, Proc. Natl. Acad. Sci. U.S.A. 95 (1998) 5172–5177.
[65] J.S. Kim, T.B. Krasieva, H. Kurumizaka, D.J. Chen, A.M. Taylor, K. Yokomori, Independent and sequential recruitment of NHEJ and HR factors to DNA damage sites in mammalian cells, J. Cell Biol. 170 (2005) 341–347.
[66] E. Bolderson, J. Scorah, T. Helleday, C. Smythe, M. Meuth, ATM is required for the cellular response to thymidine induced replication fork stress, Hum. Mol. Genet. 13 (2004) 2937–2945.
[67] S. Sakamoto, K. Iijima, D. Mochizuki, K. Nakamura, K. Teshigawara, J. Kobayashi, S. Matsuura, H. Tauchi, K. Komatsu, Homologous recombination repair is regulated by domains at the N- and C-terminus of NBS1 and is dissociated with ATM functions, Oncogene 26 (2007) 6002–6009.
[68] M. Stucki, S.P. Jackson, γH2AX and MDC1: anchoring the DNA-damage-response machinery to broken chromosomes, DNA Repair 5 (2006) 534–543.
[69] M. Barchi, S. Mahadevaiah, M. Di Giacomo, F. Baudat, D.G. de Rooij, P.S. Burgoyne, M. Jasin, S. Keeney, Surveillance of different recombination defects in mouse spermatocytes yields distinct responses despite elimination at an identical developmental stage, Mol. Cell. Biol. 25 (2005) 7203–7215.
[70] A. Traven, J. Heierhorst, SQ/TQ cluster domains: concentrated ATM/ATR kinase phosphorylation site regions in DNA-damage-response proteins, Bioessays 27 (2005) 397–407.
[71] S.S. Yuan, H.L. Chang, E.Y. Lee, Ionizing radiation-induced Rad51 nuclear focus formation is cell cycle-regulated and defective in both ATM(−/−) and c-Abl(−/−) cells, Mutat. Res. 525 (2003) 85–92.
[72] R.S. Maser, K.J. Monsen, B.E. Nelms, J.H.J. Petrini, hMre11 and hRad50 nuclear foci are induced during the normal cellular response to DNA double-strand breaks, Mol. Cell. Biol. 17 (1997) 6087–6096.
[73] S. Kharbanda, P. Pandey, S. Jin, S. Inoue, A. Bharti, Z.M. Yuan, R. Weichselbaum, D. Weaver, D. Kufe, Functional interaction between DNA-PK and c-Abl in response to DNA damage, Nature 386 (1997) 732–735.

6.4. A Histone Code for DNA Repair by Non-Homologous End Joining

Authors: Sheema Fnu, Elizabeth A. Williamson, **Leyma P. De Haro**, Justin Wray, Mark Brenneman, Suk-Hee Lee, Jac A. Nickoloff, and Robert Hromas

(Submitted for publication to Nature)

Letter

A Histone Code for DNA Repair by Non-Homologous End Joining

Sheema Fnu[1], Elizabeth A. Williamson[1], Leyma P. De Haro[1], Justin Wray[1], Mark Brenneman[2], Suk-Hee Lee[3], Jac A. Nickoloff[4], and Robert Hromas[1,5]

1- **University of New Mexico Cancer Center and Department of Internal Medicine, University of New Mexico School of Medicine, Albuquerque, NM, 87131.**
2- **Department of Genetics, Rutgers University, Piscataway, NJ 08854.**
3- **Department of Biochemistry and Molecular Biology, Indiana University Medical Center, Indianapolis, IN 46202.**
4- **Department of Environmental and Radiological Health Sciences, Colorado State University, Fort Collins, CO 80523.**
5- **To whom correspondence should be addressed: rhromas@salud.unm.edu, T: 1-505-272-5837, F: 1-505-272-2841.**

Histone methylation can alter chromatin configuration, and thereby regulate many essential cellular functions, including transcription, replication, genome stability, and apoptosis, epigenetically coding for cell behavior[1]. Such methylation regulated by histone methylases, usually sharing a SET motif, and demethylases, usually sharing a Jumonji domain[2,3]. Histone methylation has been hypothesized to play an important role in DNA double-strand break (DSB) repair, the most genotoxic type of DNA damage[4-6]. Previously described histone methylation events related to DNA repair are not induced by DNA damage[7-9], and therefore other histone modifications that might code for DNA damage have been sought. We surveyed histone 3 dimethylation events for induction by radiation, which produces DNA DSBs, and found that histone 3 lysine 36 dimethylation (H3K36me2) was the only such event induced. Non-homologous end-joining (NHEJ) is the major mammalian DSB repair pathway[10,11]. The NHEJ DNA repair factor Metnase has a SET domain that dimethylates H3K36[12]. Using a human cell system that rapidly generates a single defined DSB in the vast majority of cells, we found that Metnase rapidly localized to DSBs, and directly mediated the local formation of H3K36me2. H3K36me2 was found to interact with the early NHEJ repair components NBS1, MRE11, and Ku70, after DSB formation, and its presence at the induced DSB was correlated with the concentration of these early repair components at DSBs. An H3K36 demethylase has recently been described, the Jumonji (JmjC) domain protein JHDM1a (also FBXL11), and this was found to reduce the presence of H3K36me2 at a single DSB, and repress DSB repair, by inhibiting Metnase's ability to induce H3K36me2. Thus, these experiments reveal a cognate histone methylase/demethylase pair that defines a histone code for NHEJ repair.

Given that histone methylation can regulate genomic stability, its role in DNA repair has been widely pursued. There is some evidence that histone methylation may indeed play a role in DNA repair. The DSB repair component 53BP1 is recruited to sites of damage by methylated histone 3 lysine 79 (H3K79) and histone 4 lysine 20 (H4K20)[7-9]. However, neither H3K79 nor H4K20 methylation is induced by DNA damage[9] (also supplementary Fig. 1), so another histone methylation event coding for DNA damage has been sought.

We used western blot analysis to survey H3 dimethylation changes formed after induction of DSBs by γ-rays. This analysis revealed that the major immediate H3 dimethylation event was H3K36me2, which was induced up to 14-fold within 15 min after radiation-induced DSB formation (Fig. 1A, Supplementary Figs. S1, S2). This led us to hypothesize that a specific SET domain protein mediated this methylation event. We focused on the NHEJ DNA repair factor Metnase, which has a SET domain that dimethylates H3K36, improves survival after γ-ray exposure[12], and is recruited to sites of DNA damage[13,14]. To test whether H3K36me2 was associated with DSB formation and repair, and whether Metnase could mediate this methylation event, we generated a model human cell system that allowed rapid induction of a single DSB within a defined, unique sequence that would preferentially be repaired by NHEJ. We engineered a human sarcoma cell line, termed HT1904, to contain a unique I-SceI site in a single puromycin acetyltransferase (puro) gene sequence, which does not share homology with any other sequence in the genome (Supplementary Fig. S3). Using adenoviral-mediated transduction of the gene encoding I-SceI endonuclease, 90% of cells generated a single DSB within 60 min (Supplemental Fig. S4A)[15-17]. If DSBs were induced in the puro sequence after DNA replication, homologous recombination repair could occur between sister chromatids, but this is unlikely because DSBs would usually occur in both sister chromatids.

Thus, repair of the DSB induced by I-SceI will be predominantly by the NHEJ pathway, and the kinetics of DSB repair can measured using quantitative real-

time PCR (q-RT PCR). Consistent with its known ability to enhance NHEJ repair[12,13], over-expression of Metnase increased by up to 4-fold the amount of re-ligated DNA analyzed with PCR primers spanning the I-SceI site (Supplementary Fig. S4B, see also Fig. 4B). The recruitment of proteins such as H3K36me2 and Metnase to this DSB can be detected by chromatin immunoprecipitation (ChIP) analysis and quantified by q-RT PCR. Functional ChIP primer targets were identified within one nucleosome (152 nt) of the I-SceI site to monitor events immediately adjacent to the DSB (Supplementary Table 1).

Using the HT1904 system, we used ChIP to determine whether H3K36 was dimethylated at the induced DSB (Fig. 1B, Supplementary Fig. S5). H3K36me2 was not present at the region adjacent to the I-SceI site before DSB induction, but it was markedly induced within 1 h of DSB induction and was maintained for at least 8 h, and then declined over a 24-42 h period of repair. Other H3 methylation events were detected at the DSB by ChIP analysis to a far lesser extent than H3K326me2 (Fig. 1B). H3K36me2 was only detected adjacent to the DSB; it was barely detected at a site 650 bp from the DSB (not shown). Next, we tested whether the H3K36 methylase Metnase was also present adjacent to the induced DSB by ChIP analysis in the HT1904 system. We found that Metnase was recruited to the DSB with very similar kinetics to the induction of H3K36me2, and that Metnase recruitment to the DSB was increased in HT1904 cells overexpressing Metnase, and decreased when Metnase levels were decreased by siRNA (Fig. 1C, Supplementary Fig. S5). Since H3K36me2 and Metnase were indeed both present at the induced DSB, we tested whether altering Metnase levels could affect the formation of H3K36me2 at the DSB site. Increasing Metnase levels indeed enhanced the formation of H3K36me2 at the DSB region while repressing Metnase had the opposite effect (Fig. 1D), suggesting that Metnase is responsible for H3K36 dimethylation at DSBs.

However, it was possible that H3K36 dimethylation only correlated with the presence of Metnase, but was not caused by it, so we next analyzed whether the D248S SET domain mutant of Metnase, which fails to promote NHEJ[12] (also Fig. 4c), was also deficient in H3K36 dimethylation at DSBs. Unlike wild-type Metnase, the D248S Metnase mutant did not induce H3K36me2 at the DSB (Fig. 1E), indicating that H3K36 dimethylation at DSBs is directly caused by Metnase . H3K36me2 correlates with the maintenance of intra-genic transcription[18,19], but the mechanism by which it promotes NHEJ was unclear.

Since there is evidence that 53BP1 is recruited to DNA DSBs by methylated histones[7-9], we postulated that H3K36me2 might similarly recruit repair components to DSBs. We again induced the formation of H3K36me2 with γ-rays, immunoprecipitated H2K36me2, and then analyzed the immunoprecipitate for the presence of early NHEJ factors (Fig. 2). We found that components of the MRE11-RAD50-NBS1 DSB sensor complex, and Ku70, an NHEJ factor that binds to DNA ends at DSBs[10,11], were all present in the H3K36me2 immunoprecipitate, and the association of these early NHEJ factors with H3K36me2 appeared to be induced by radiation. However, the late NHEJ factor DNA Ligase IV[10,11], was not detected in the H3K36me2 immunoprecipitate. In addition, 53BP1 was not detected in the H3K36me2 immunoprecipitate, consistent with its recruitment by other methylated histones[7-9]. Based on these findings, we examined whether Metnase levels regulated the recruitment of MRE11, phosphorylated NBS1 (a product of ATM kinase activity), and Ku70 to the region adjacent to an induced DSB by ChIP in HT1904 cells. We found that increasing Metnase enhanced the recruitment of each of these repair components to the DSB , and repressing Metnase levels decreased their recruitment (Fig. 3).

JHDM1a has been identified as a H3K36 demethylase[20,21]. Conserved across species, JHDM1a specifically demethylates H3K36me2 in vitro and in vivo.

Thus, JHDM1a was an intriguing candidate as a regulatory partner to Metnase during the DSB-induced histone modifications described here. We examined whether over-expression of JHDM1a could alter the presence of H3K36me2 at the induced DSB in HT1904 cells. Increasing the expression of JHDM1a in HT1904 cells dramatically reduced the formation of H3K36me2 at the induced DSB site (Fig. 4A, Supplementary Fig. S8). Moreover, JHDM1a over-expression also blocked the ability of Metnase to induce H3K36me2 at the DSB site. These changes in H3K36 dimethylation have significant functional consequences as over-expression of JHDM1a prevented Metnase from enhancing DSB repair in the HT1904 system (Fig. 4B, D), similar to the D248S Metnase mutant (Fig. 4C), implying that Metnase promotes NHEJ capability through methylation of H3K36. Thus, JHDM1a opposes the effect of Metnase on DSB induced H3K36 methylation and DSB repair by NHEJ. It is possible that JHDM1a could serve to negatively regulate NHEJ repair during the cell cycle, however it is more likely that it restores chromatin to its native state after DSB repair.

In this study we have identified: 1) a histone code for DNA DSB damage, H3K36me2; 2) the cognate histone 3 methylase/demethylase regulatory pair that mediates the formation and removal of this code; and 3) a role for H3K36me2 in recruiting early NHEJ components to DNA adjacent to DSBs Thus, H3K36me2 has a place alongside phosphorylated H2Ax and ubiquitylated H2A as DNA damage-induced histone modifications that recruit repair components and enhance repair[22-26]. Given that H3K36me2 is detected near DSBs soon after DSB induction, and that H3K36me2 co-immunoprecipitates with early NHEJ components, it is possible that H3K36me2 dimethylation catalyzes an early cascade of repair events at DSBs. Alternatively,, H3K36me2 may stabilize early NHEJ repair factors at the DSB, after their recruitment by free DNA ends. While JHDM1a may initially inhibit H3K36me2 formation, it may ultimately complete repair by removing this dimethyl tag at the DSB site, and perhaps enhance release of repair components from that site. With its early role in chromatin

regulation of DSB repair, and evidence that high Metnase levels may mediate clinical resistance to radiation or chemotherapy, Metnase is an attractive target for enhancing tumor response to these modalities[27,28].

Methods

Full Methods accompany this paper in supplementary information on-line.

REFERENCES

1. Trievel, R.C. Structure and function of histone methyltransferases. Crit Rev Eukaryot Gene Expr. 14,147-69 (2004).
2. Agger, K., Christensen, J., Cloos, P.A., & Helin, K. The emerging functions of histone demethylases. Curr Opin Genet Dev. 18, 159-68 (2008).
3. Lan, F., Nottke, A.C., & Shi, Y. Mechanisms involved in the regulation of histone lysine demethylases. Curr Opin Cell Biol. 20, 316-25 (2008).
4. Peng, J.C., Karpen, G.H. Heterochromatic genome stability requires regulators of histone H3 K9 methylation. PLoS Genet. 5, e1000435 (2009).
5. Muñoz, I.M., & Rouse, J. Control of histone methylation and genome stability by PTIP. EMBO Rep. 10, 239-45 (2009).
6. Oda, H., *et al*. Monomethylation of histone H4-lysine 20 is involved in chromosome structure and stability and is essential for mouse development. Mol Cell Biol. 29, 2278-95 (2009).
7. Botuyan, M.V., *et al.* Structural basis for the methylation state-specific recognition of histone H4-K20 by 53BP1 and Crb2 in DNA repair. Cell 127, 1361-73 (2006).
8. Sanders, S.L., *et al*. Methylation of histone H4 lysine 20 controls recruitment of Crb2 to sites of DNA damage. Cell. 119, 603-14 (2004).
9. Huyen, Y., *et al.* Methylated lysine 79 of histone H3 targets 53BP1 to DNA double-strand breaks. Nature 432, 406-11 (2004).

10. Hartlerode, A.J., & Scully, R. Mechanisms of double-strand break repair in somatic mammalian cells. Biochem J. 423, 157-68 (2009).

11. Pardo, B., Gómez-González, B., & Aguilera, A. DNA repair in mammalian cells: DNA double-strand break repair: how to fix a broken relationship. Cell Mol Life Sci. 66, 1039-56 (2009).

12. Lee, S.H., *et al*. The SET domain protein Metnase mediates foreign DNA integration and links integration to nonhomologous end-joining repair. Proc Natl Acad Sci U S A 102, 18075-80 (2005).

13. Roman, Y., *et al.* Biochemical characterization of a SET and transposase fusion protein, Metnase: its DNA binding and DNA cleavage activity. Biochemistry 46, 11369-76 (2007).

14. Beck, B.D., Park, S.J., Lee, Y.J., Roman, Y., Hromas, R.A., & Lee, S.H. Human Pso4 is a Metnase (SETMAR)-binding partner that regulates Metnase function in DNA repair. J Biol Chem. 283, 9023-30 (2008).

15. Golding, S., *et al.* Double strand break repair by homologous recombination is regulated by cell cycle-independent signaling via ATM in human glioma cells. J. Biol. Chem. 279, 15402–15410 (2004).

16. Anglana, M. & Bacchetti, S. Construction of a recombinant adenovirus for efficient delivery of the I-SceI yeast endonuclease to human cells and its application in the in vivo cleavage of chromosomes to expose new potential telomeres. Nucleic Acids Res. 27, 4276-4281 (1999).

17. Valerie, K., *et al.* Improved radiosensitization of rat glioma cells with adenovirus-expressed mutant herpes simplex virus thymidine kinase in combination with acyclovir. Cancer Gene Therapy 7, 879–884 (2000).

18. Rao, B., Shibata, Y., Strahl, B.D., & Lieb, J.D. Dimethylation of histone H3 at lysine 36 demarcates regulatory and nonregulatory chromatin genome-wide. Mol Cell Biol. 25, 9447-59 (2005).

19. Morris, S.A., *et al.* H3 K36 methylation is associated with transcription elongation in Schizosaccharomyces pombe. Eukaryot Cell 4, 1446-54 (2005).

20. Anand, R., & Marmorstein, R. Structure and mechanism of lysine-specific demethylase enzymes. J Biol Chem. 282, 35425-9 (2007).

21. Tsukada, Y., *et al.* Histone demethylation by a family of JmjC domain-containing proteins. Nature 439, 811-6 (2006).

22. Escargueil, A.E., Soares, D.G., Salvador, M., Larsen, A.K., & Henriques, J.A. What histone code for DNA repair? Mutat Res. 658, 259-70 (2008).

23. Sedelnikova, O.A., Pilch, D.R., Redon, C., & Bonner W.M. Histone H2AX in DNA damage and repair. Cancer Biol Ther. 2, 233-5 (2003).

24. Huen, M.S., *et al.* RNF8 transduces the DNA-damage signal via histone ubiquitylation and checkpoint protein assembly. Cell 131, 901-14 (2007).

25. Sobhian, B., *et al*. P80 targets BRCA1 to specific ubiquitin structures at DNA damage sites. Science 316, 1198-202 (2007).

26. Kim, H., Chen, J., & Yu, X. Ubiquitin-binding protein RAP80 mediates BRCA1-dependent DNA damage response. Science 316, 1202-5 (2007).

27. Wray, J., et al. Metnase mediates chromosome decatenation in acute leukemia cells. Blood 114, 1852-8 (2009).

28. Wray, J., et al. Metnase mediates resistance to topoisomerase II inhibitors in breast cancer cells. PLoS One 4, e5323 (2009)

Acknowledgements: The authors gratefully acknowledge the support of NIH R01 GM084020 (J.A.N.), R01 CA100862 (J.A.N.), an APRC supplement to CA100862 (J.A.N. and R.H.), NIH R01 CA102283 (R.H.), NIH R01 HL075783 (R.H.), NIH RO1 CA139429 (R.H.), and the Leukemia and Lymphoma Society SCOR 7388-06 (R.H.).

Author Contributions: S.F., E.W., and J.W. designed and performed experiments, L. D. H. and M. B. generated essential reagents, S.-H. L. analyzed data and wrote the manuscript, J.A.N. designed experiments, analyzed data and

wrote the manuscript, and R.H. conceived of the project, designed experiments, analyzed data and wrote the manuscript.

FIGURE LEGENDS

Figure 1. Dimethylation of H3K36 by Metnase at DSBs. A, Western analysis demonstrating that H3K36me2 is induced rapidly after exposure to γ-rays (8 Gy). **B,** Time course ChIP analysis of methylated H3 species quantified by real time PCR adjacent to a single induced DSB. There was no detectable methylated H3 prior to DSB induction. For all ChIP experiments, each time point is the average of three measurements repeated at least twice, normalized to GAPDH. C**,** ChIP analysis of Metnase adjacent to a single induced DSB. There was no detectable Metnase prior to DSB induction. **D,** ChIP analysis demonstrating that Metnase levels alter H3K36me2 formation adjacent to a DSB. There was no detectable H3K36me2 at the DSB region prior to DSB induction. **E,** Overexpression of the Metnase D248S SET domain mutant does not induce H3K36me2 formation at a DSB.

Figure 2. Co-Immunoprecipitation of DNA repair factors with H3K36me2. Immunoprecipitation of H3K36me2 was performed in HT1904 cells mock treated (C), or 15 and 60 min after 10 Gy γ-ray exposure.

Figure 3. ChIP analysis of early DNA repair factors at a single induced DSB. Increasing Metnase levels enhances recruitment of Ku70 (A), phosphorylated NBS1 (B), and MRE11 (C) to a DSB, while repressing Metnase reduced recruitment of these factors. These proteins were not detectable adjacent to the DSB site prior to DSB induction.

Figure 4. The JHDM1a histone demethylase counteracts Metnase histone methylase and DSB repair activities. A, ChIP analysis in cells

overexpreressing JHDM1a show reduced H3K36me2 near a DSB, and JHDM1a overexpression blocks the effect of overexpressed Metnase on H3K36me2 formation (compare with Fig. 1D and 1E). B**,** Over-expression of Metnase enhances DSB repair, as measured by reduced amount of unligated I-SceI PCR product (see also Supplementary Fig. S4B). Repressing Metnase slows DSB repair. C**,** Over-expression of the Metnase D248S SET domain mutant decreased repair . **D,** Over-expression of JHDM1a blocked the ability of overexpressed Metnase to promote DSB repair (compare with panel B).

Figure 1

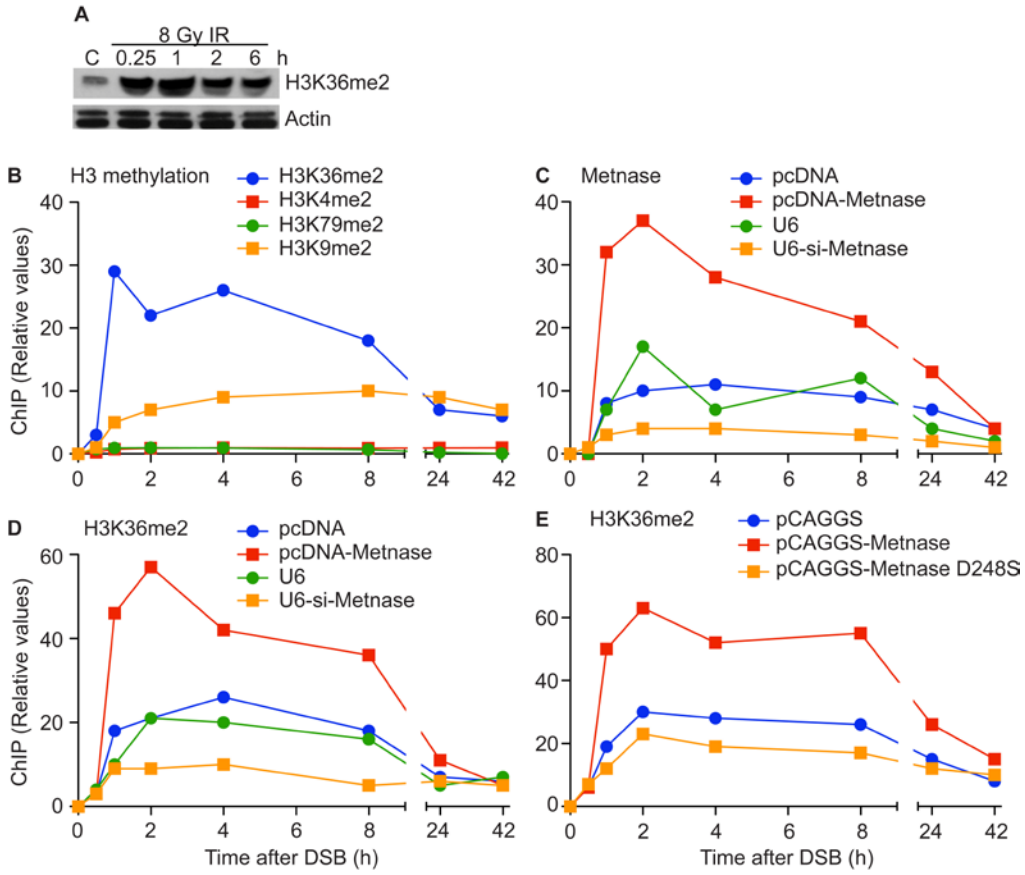

Figure 2

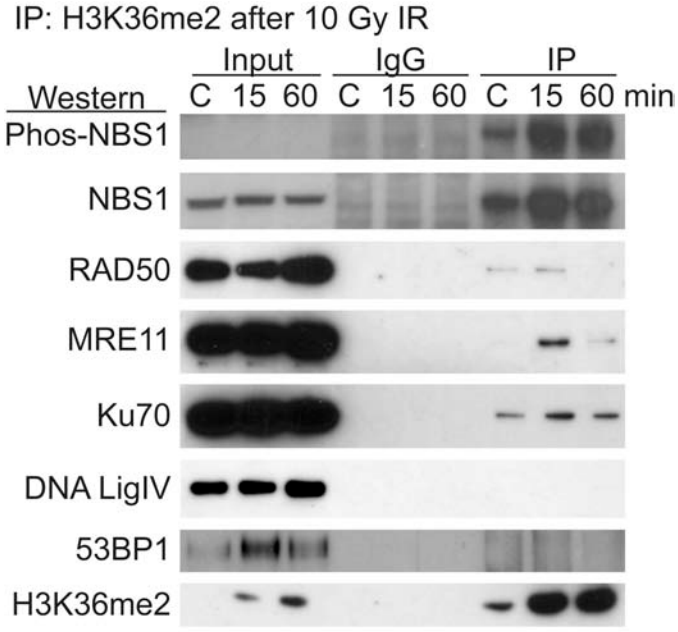

Figure 3

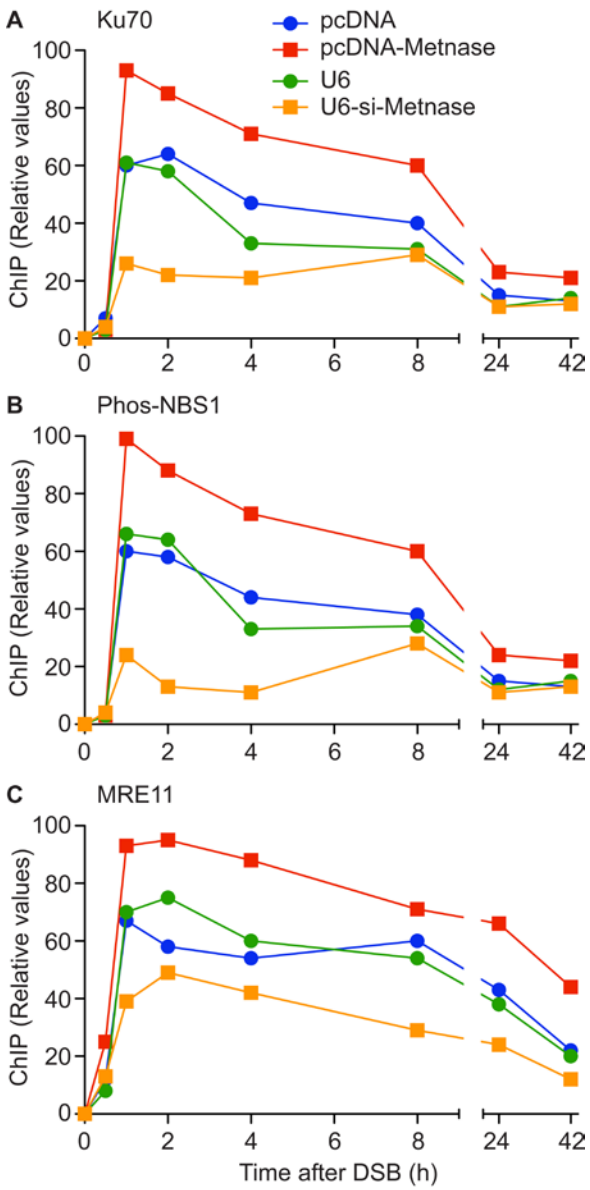
A
Ku70
pcDNA
pcDNA-Metnase
U6
U6-si-Metnase
ChIP (Relative values)
B
Phos-NBS1
C
MRE11
Time after DSB (h)

Figure 4

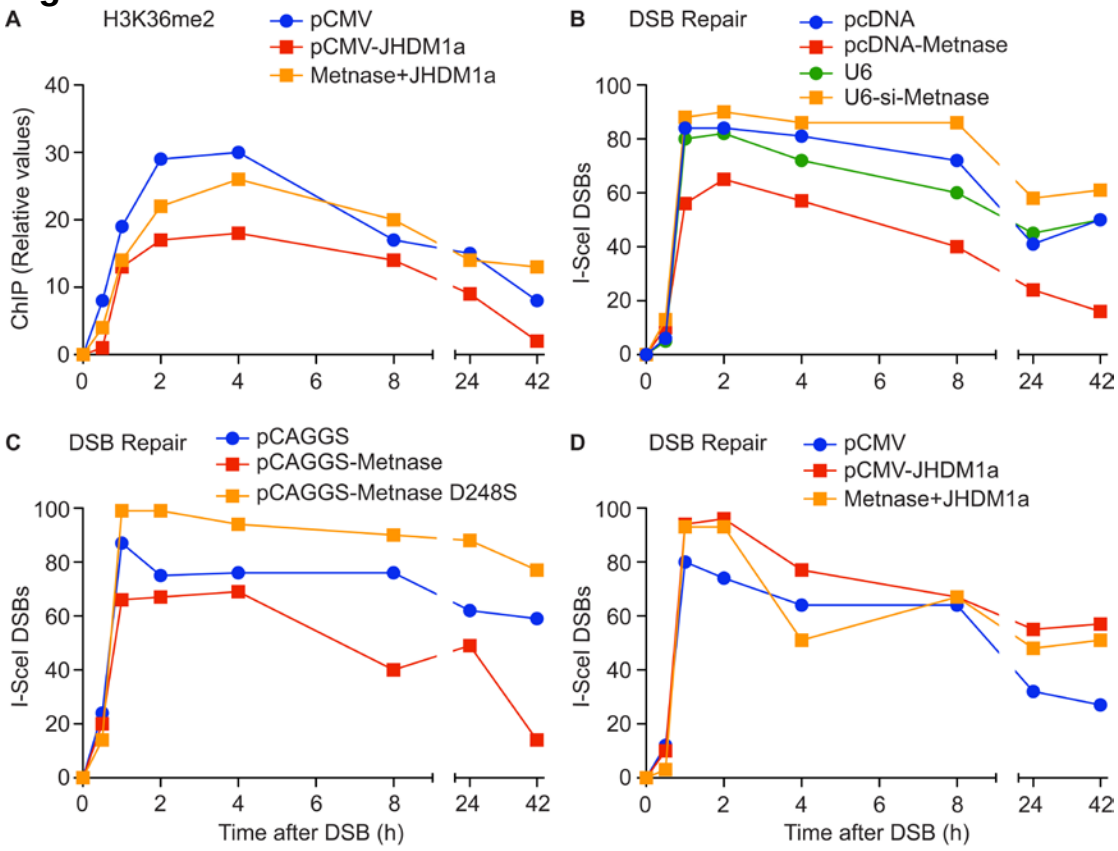
A
H3K36me2
pCMV
pCMV-JHDM1a
Metnase+JHDM1a
ChIP (Relative values)
B
DSB Repair
pcDNA
pcDNA-Metnase
U6
U6-si-Metnase
I-SceI DSBs
C
DSB Repair
pCAGGS
pCAGGS-Metnase
pCAGGS-Metnase D248S
I-SceI DSBs
Time after DSB (h)
D
DSB Repair
pCMV
pCMV-JHDM1a
Metnase+JHDM1a
I-SceI DSBs
Time after DSB (h)

Supplementary Methods

Cell lines- HT1904 cells were derived from the human sarcoma cell line HT1080 by stably transfecting a linearized vector containing the puro gene with the phosphogylcerol kinase promoter, and containing an I-Sce-I site (TGGTTCCTGG***ATTACCCTGTTATCCCTA***CGCGCCGGGG, with the I-SceI site in bold italics flanked by puro sequence). This vector also contained a blasticidin resistance cassette for selection. HT1904 cells were cloned from a single blasticidin resistant colony, and Southern analysis was used to determine that there was a single integrated puro sequence (Supplemental Fig. S3). HT1904 cells and its derivatives with altered Metnase or JHDM1a expression levels were cultured in DMEM with 10% heat-inactivated fetal calf serum supplemented with antibiotics and anti-fungal agents. HT1904 express Metnase at moderate levels, making them amenable to both over- and underexpression. HEK-293T cells, which do not express Metnase, were transfected with a pcDNA-Metnase to overexpress Metnase, or with empty pcDNA vector as control.

I-SceI adenovirus generation, quantification and transduction- Adenovirus expressing I-sceI was a kind gift from K. Valerie[17]**.** The virus was propagated using AD293 cells as previously described[16-18]. Briefly, cells were washed with PBS, and then 5mL of OptiMEM (Invitrogen, Carlsbad, CA) containing 10 viral particles per cell was added, and cells were incubated at 37^0C for 2 h, then 10 mL of DMEM containing 10% serum (Thermoscientific, Waltham, MA) and 1% penicillin/streptomycin (Invitrogen) was added. Cells were incubated for 4 days, collected and centrifuged at 8000 rpm for 10 min at 4^0C, and supernatant was removed. The cell pellet was subjected to 5 snap-freeze cycles using methanol/dry ice, then centrifuged at 3000 rpm for 30 min at 4^0C. The supernatant was purified using cesium chloride density gradient centrifugation at 32000 rpm at 10^0C for 22 hours. The virus was stored in virus storage buffer (20 mM Tris-HCl pH 8, 4mM MgCl, 10% sucrose) at -80^0C. Quantification was done using the protocol outlined in the adEasy manual (Qbiogene, Carlsbad, CA).

We routinely obtained viral titers of 3 x 10^9 viral particles/μL. HT1904 cells were exposed to the I-SceI adenovirus at an MOI of 1000 (Supplementary Fig. S4) for 3 h, and then washed three times in media to remove the adenovirus. For all experiments using adenoviral I-SceI transduction, time 0 was before infection with adenovirus and subsequent time points were measured after adenovirus removal. At the time of viral media removal, no cells had the ISce-I site cleaved, but within 60 minutes after adenovirus removal, ~90% of the cells had the puro sequence cleaved as analyzed by real time PCR with primers spanning the I-SceI site (Supplementary Fig. S4B).

Manipulation of Metnase and JHDM1a expression- Cells over-expressing V5-tagged Metnase were generated by electroporation with pCDNA-Metnase (neomycin selectable), and cells under-expressing Metnase were generated by electroporation with U6-siRNA Metnase (hygromycin selectable) as previously described[12,27,28]. Controls were transfected with empty pcDNA or a U6 vector that expresses an siRNA targeted to GFP siRNA. JHDM1a was overexpressed by transfection of a pCMV-JHDM1a vector (Open Biosystems, ThermoFisher Scientific, Pittsburgh, PA), with empty vector as control. Metnase and JHDM1a protein levels were assessed by Western analysis with anti-Metnase or anti-JHDM1a antiserum normalized to actin as described[12] for each experiment (Supplementary Fig. S7). To prepare cell extracts for Western analysis, cells were briefly washed with phosphate-buffered saline and lysed in a buffer containing 25 mm HEPES (pH 7.5), 0.3 M NaCl, 1.5 mM $MgCl_2$, 0.2 mM EDTA, 0.5% Triton X-100, 20 mM β-glycerolphosphate, 1 mM sodium vanadate, 1 mM dithiothreitol, and protease inhibitor cocktails (Sigma). Cell lysates (50 μg) were separated by SDS-PAGE, and the proteins were transferred to a PVDF membrane (Millipore, Billerica, MA) and immunoblotted with primary antibody followed by peroxidase-coupled secondary antibody (GE Healthcare, UK) and detected by enhanced chemiluminescence (West Pico Supersignal reagent; Thermo Fisher Scientific, Pittsburgh, PA) and visualized on Kodak X-Omat film.

RNA Extraction and Amplification

Total RNA was extracted using an RNA-Easy kit (Qiagen, Germany). One microgram of total RNA was reverse transcribed using SuperScript III and random hexamers (Invitrogen). PCR reactions were performed with primers listed in Supplementary Table 1.

Co-Immunoprecipitation

HT1904 cells were treated with 10 Gy of γ-rays and allowed to recover for 15 min or 60 min. Total protein lysates were prepared as above at each time point as well as from untreated HT1904 cells. Protein lysates were immunoprecipitated with H3K36me2 antibody (Cell Signaling, Danvers, MA) and protein A/G (1:1) agarose beads (Calbiochem) overnight at 4^{o}C. The agarose beads were gently pelleted and washed three times with lysis buffer and three times with cold PBS. The beads were resuspended in lysis buffer and the proteins were analyzed by Western blotting using the following primary antibodies: anti-H3K36me2, anti-phospho-Nbs1(Ser343), anti-Nbs1 (from Cell Signaling, Danvers, MA); anti-Mre11, anti-Ku70 (from BD Biosciences, San Jose, CA); anti-53BP1 (Abcam, Cambridge, MA); anti-Rad50 (Genetex, Irvine, CA); or anti-DNA Ligase IV (Genway, San Diego, CA).

ChIP analysis

ChIP was performed was using primer pairs 152 bp and 650 bp from the I-SceI site. ChIP was performed before I-SceI adenovirus infection and at 0.5, 1, 2, 4, 8, 24, 42 hours after removal of the I-SceI adenovirus. Triplicate plates of 10^{7} exponentially growing HT1904 cells per experimental condition per time point were washed with PBS and incubated for 10 min with 1% formaldehyde; after quenching the reaction with 0.125 M glycine, cells were harvested and pelleted. Pellets were resuspended in 2 ml lysis buffer (0.1 M PIPES pH 8, 1 M KCl, 10% NP-40), incubated on ice for 30 min, and dounced 10 times. Nuclei were pelleted for 10 min at 4°C, resuspended in 1 ml of nuclear lysis buffer without EDTA (50 mM Tris–HCl, pH 8, 0.5% deoxycholic acid). Digestion was performed

with 40 U of micrococcal nuclease (MNase I, New England Biolabs) at room temperature for 15 min, and then stopped by placing the reaction at 4°C, and adding EDTA to a final concentration of 20 mM. ChIP assays were performed with 3 µg of the following antibodies: anti-Metnase[12], anti-histone H3K36me2 (Cell Signaling), anti-XRCC4 (Abcam), anti-Mre11 (Abcam), anti-Ligase IV (Sigma, St Louis, MO), anti-histone 3 (Cell Signaling), anti-KU 80 (Cell Signaling), anti-phospho NBS1 (ser343, Cell Signaling), anti-NBS1 (Cell Signaling), anti-phospho H2Ax (Millipore, Billerica, MA), anti-H3K79me2 (Millipore), anti-H3K9me2 (Cell Signaling), anti-H3K4me2 (Cell Signaling), and anti-H3K27me2 (Cell Signaling). Chromatin crosslinks were reversed by adding NaCl to a final concentration of 0.3 M followed by incubation at 65°C overnight with RNase A (10 µg/µl), then at 50°C for 3 hours with Proteinase K. Finally, the DNA was purified using Qiagen purification kit and visualized on a 2% agarose gel. DNA associated with immunoprecipitated protein was then quantified using real time PCR.

Real-time PCR

Quantitative real-time PCR was performed using SYBR green reagent (Applied Biosystems, USA) with an ABI PRISM 7000 Sequence Detection System. Primers were designed to amplify genomic regions of 120–180 bp in size (Supplementary Table 1). All experimental values were normalized to the input DNA using amplification of GAPDH (Supplementary Table 1).

Supplementary Figure legends

Figure S1- Survey of H3 dimethylation after ionizing radiation. Western analysis of 5 different H3 dimethylation sites in samples isolated before (C) or indicated times after 10 Gy γ-ray exposure.

Figure S2- Metnase overexpression enhances H3K36me2 formation after ionizing radiation. Western blot analysis of HEK-293T cells transfected with pcDNA or pcDNA-Metnase and irradiated with 10 Gy γ-rays. Proteins extracts were prepared * h after irradiation and analyzed by Western blot.

Fig. S3. Schematic of the vector stably transduced into HT1080 human sarcoma cells to generate a cell line with a single I-SceI site in a unique sequence. The locations of the I-SceI site and the ChIP primer sets 152 and 604 bp from the I-SceI site are shown.

Figure S4- Analysis of DSB induction. (A) q-RT PCR analysis of the PCR product product using primers spanning the I-SceI site. Plotted are relative values calculated as the inverse of the total amount of amplified puro DNA compared to input GAPDH DNA for I-SceI adenovirus MOIs of 100 and 1000. (B) Schematic of PCR primers spanning the I-SceI site and agarose gel analysis of PCR products from samples isolated 1-24 h after I-SceI adenovirus transduction.

Figure S5- ChIP analysis with primers 152 bp from the I-SceI site of H3K36me2 (left) or Metnase (right) from samples collected before (C), and 2 or 4 h after I-SceI adenovirus transduction in cells expressing normal (pcDNA and U6), high (pcDNA-Metnase) or low levels of Metnase.

Figure S6- Time course of I-SceI expression. Cells were collected before (C) or at indicated times after I-SceI adenovirus transduction, total RNA was isolated

and subjected to RT-PCR analysis by amplifying I-SceI mRNA or 18S rRNA as loading control.

Figure S7- Metnase expression levels are stable throughout the 42 h time course. Western blot analyses of Metnase, with actin as loading control, were performed in HT1904 derivatives expressing Metnase at normal (pcDNA and U6), high (pcDNA-Metnase) or low (U6-siRNA-Metnase) levels. Control lanes (C) show normal expression, and remaining lanes are from samples isolated at indicated times after I-SceI adenovirus transduction.

Fig. S8. Western analysis of JHDM1a expression. HT1904 cells transfected with pCMV-JHDM1a vector or empty pCMV vector were analyzed by Western blot using anti-JHDM1a antibodies with actin as loading control.

Figure S1

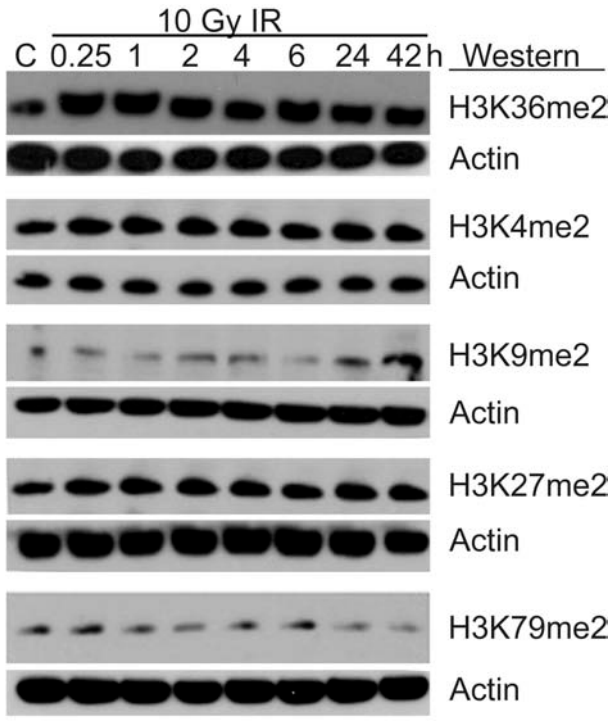

Figure S2

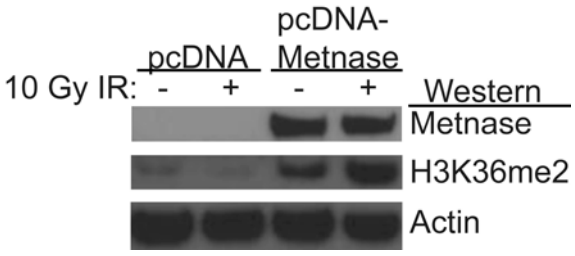

Figure S3

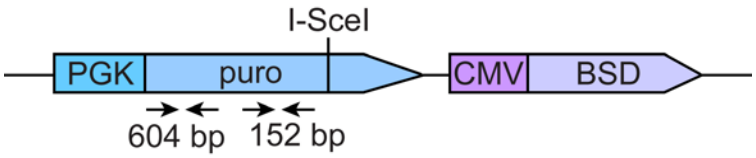

Figure S4

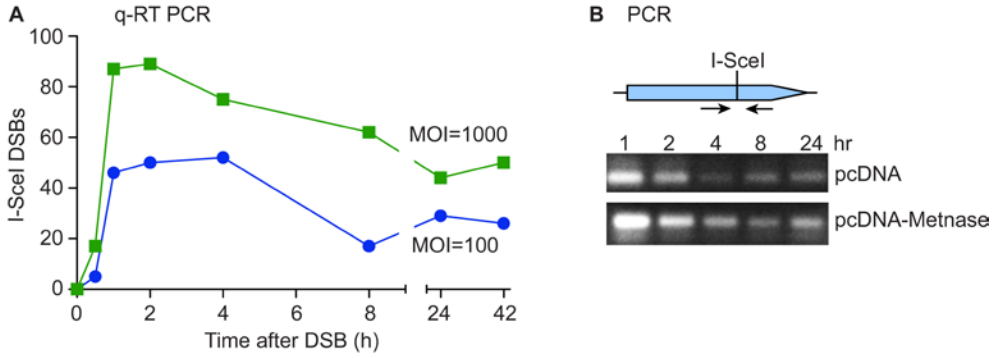

‘

Figure S5

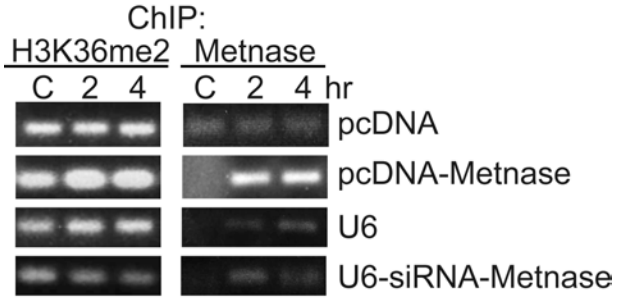

Figure S6

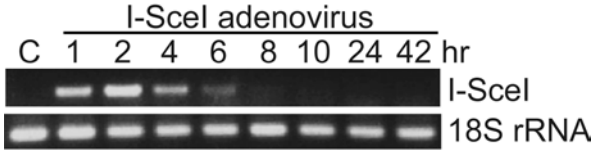

Figure S7

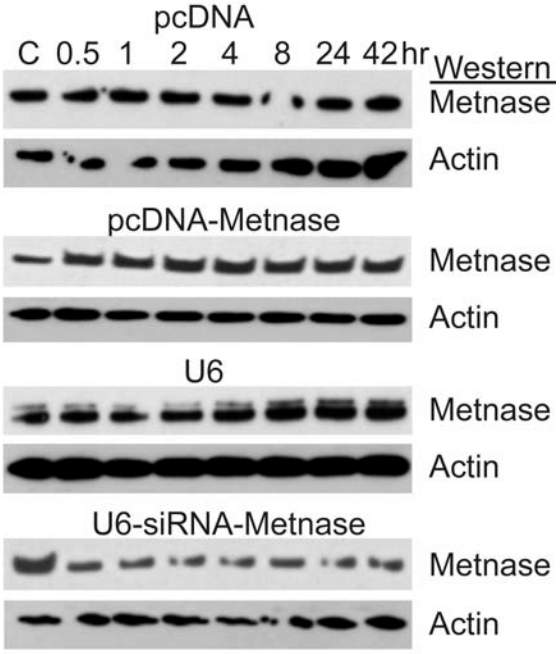

Fig. S8

Table 1

Primer Name	Sequence (5’ – 3’)
I-SceI Forward	CCCGGCTGCCCGCGCAGCAAC
I-SceI Reverse	TTGCGGGGCGCGGAGGTCTCCA
152 Forward	TACGCACCCTCGCCGCCGCGTTCG
152 Reverse	TGCGCGGGCCGATCTCGGCGA
650 Forward	AGCAGCCCCGCTGGCACTTGGCGC
650 Reverse	CTCAGCGGTGCTGTCCATCTGCAC
GAPDH Forward	TCGGTTCTTGCCTCTTGTC
GAPDH Reverse	CTTCCATTCTGTCTTCCACTC

6.5. Summary of PIP containing proteins and their functions.

Table 6-1. Conserved PIP boxes in Metnase and other human DNA repair/metabolism proteins.

Protein	Function(s)	PIP box*	Reference
Metnase	NHEJ, decatenation, fork restart	(119) VVQKGLQ-FH	[139]
PARP-1	DNA repair, fork restart	(668) PVQDLIKMIF	[177]
DNMT1	DNA methyltransferase	(162) TRQTTITSHF	[178]
DNA Polβ	DNA repair polymerase	(215) VEQLQKV-HF	[179]
p66	DNA polδ subunit	(454) NRQVSITGFF	[180]
MYH	BER glycosylase	(521) MGQQVLDNFF	[181]
UNG2	BER glycosylase	(2) IGQKTLYSFF	[182]
XPB	NER endonuclease	(988) QTQLRIDSFF	[183]
BLM	DNA repair helicase	(81) TNQQRVKDFF	[184]
RECQL5β	DNA repair helicase	(962) EAQN-LIRHF	[184]
p15 PAF	Cell growth promotion	(60) KWQKGIGEFF	[185]
ING1b	Apoptosis	(7) GEQLHLVNY	[186]
MDM2	E3 ubiquitin ligase	(481) PIQMIVLTYF	[187]
WSTF	Chromatin remodeling	(662) LLQDEIAEDY (1024)RYQDIIHSIH (1099)ALQASVIKKF (1432)TEQCLVALLH	[188]
	Consensus PIP box:	[K-A]Qxx-I/L/Vxx(F/Y/H/W)$_2$	[117]

*All proteins have the core PIP Q-I/L/V motif, and nearly all (including Metnase) have the C-terminal pair of F/Y/H residues (shown in red). Many PIP boxes have upstream K and/or A residues; Metnase, and PARP-1 have conservative substitutions (V for A) at this position, indicated in green.

6.6. Metnase Promotes Restart of Stalled and Collapsed Replication Forks

Authors: **Leyma P. De Haro***, Justin Wray*, Elizabeth A. Williamson, Stephen T. Durant, Lori Corwin, Amanda C. Gentry, Neil Osheroff, Suk-Hee Lee, Robert Hromas, and Jac A. Nickoloff

(in revision for publication to Nucleic Acids Research)

Metnase Promotes Restart of Stalled and Collapsed Replication Forks

Leyma P. De Haro[1]*, Justin Wray[2]*, Elizabeth A. Williamson[2], Stephen T. Durant[1], Lori Corwin[2], Amanda C. Gentry[3], Neil Osheroff[3], Suk-Hee Lee[4], Robert Hromas[2], and Jac A. Nickoloff[1†]

[1]Department of Molecular Genetics and Microbiology, Cancer Research and Treatment Center, University of New Mexico School of Medicine, Albuquerque, NM, 87131, USA

[2]Division of Hematology-Oncology, Cancer Research and Treatment Center, University of New Mexico School of Medicine, Albuquerque, NM 87131, USA

[3]Departments of Biochemistry and Medicine, Vanderbilt University School of Medicine, Nashville, TN 37232-0146, USA

[4]Department of Biochemistry and Molecular Biology, Indiana University School of Medicine, Indianapolis, IN 46202- 5122, USA

*These authors contributed equally to the work.

Keywords: DNA damage, hydroxyurea, DNA fiber analysis, genome stability
Running Title: Metnase Promotes Replication Fork Restart

[†]Address correspondence to (present address): Jac A. Nickoloff, Department of Environmental and Radiological Health Sciences, Colorado State University, Ft. Collins, CO 80523, USA Tel. 970-491-6674; Fax 970-491-0623; Email J.Nickoloff@colostate.edu

ABSTRACT

Metnase is a recently evolved human protein with methylase (SET) and nuclease domains that is widely expressed, especially in proliferating tissues. Metnase interacts with DNA ligase IV, promotes non-homologous end-joining (NHEJ), and knockdown causes mild hypersensitivity to ionizing radiation. Metnase also promotes plasmid and viral DNA integration, and topoisomerase IIα (TopoIIα)-dependent chromosome decatenation. NHEJ factors have been implicated in replication stress response, and TopoIIα has been proposed to relax positive supercoils in front of replication forks. Here we show that Metnase promotes cell proliferation, but it does not alter cell cycle distributions, or the speed of replication fork progression. However, Metnase knockdown greatly sensitized cells to replication stress induced by hydroxyurea, UV light, and the topoisomerase I poison camptothecin, and conferred a marked defect in restart of stalled replication forks. Metnase also promotes resolution of phosphorylated histone H2AX, a marker of DNA double-strand breaks at collapsed forks, and it co-immunoprecipitates with PCNA, and RAD9, a member of the PCNA-like RAD9-HUS1-RAD1 complex that has key roles in the intra-S checkpoint. Metnase also promotes TopoIIα-mediated relaxation of positively supercoiled DNA. Together these results establish Metnase as a key factor that promotes restart of both stalled and collapsed replication forks.

INTRODUCTION

Cellular systems that maintain genome stability are critical for cancer suppression. The failure to accurately repair DNA damage, including single-strand damage and double-strand breaks, is strongly linked to cancer initiation and progression. DNA damage is caused by intrinsic factors associated with cellular metabolism, such as reactive oxygen species and hydrogen peroxide, and extrinsic factors, such as ionizing radiation, UV radiation, and chemotherapeutic agents including reactive chemicals, topoisomerase poisons, and hydroxyurea (HU) which depletes nucleotide pools (1,2). Cells are particularly vulnerable to DNA damage during DNA replication because many DNA lesions cause replication forks to stall. Cellular responses to replication stress are extremely important in cancer therapy, as a number of chemotherapeutic drugs target DNA metabolism and cause replication stress, including topoisomerase poisons and HU. Cells respond to stalled forks in several ways. Single-stranded DNA (ssDNA) bound by RPA accumulates at stalled forks and is a major signal for downstream events including fork repair and checkpoint activation. The replisome at stalled forks is stabilized by proteins that function in DNA repair and the DNA damage checkpoint response, including RPA, ATR-ATRIP, ATM, BLM, and INO80 (3-6); the action of these proteins may preserve the fork structure while the damage is repaired, allowing replication to resume. Alternatively, error-prone translesion synthesis (TLS)

polymerases may be recruited to monoubiquitinated proliferating cell nuclear antigen (PCNA), allowing lesion bypass in a damage tolerance pathway (7,8). Type I and type II topoisomerases play key roles in normal DNA replication. Topoisomerase I (type I) is thought to play a major role in relaxing positive supercoils produced in front of replication forks during duplex DNA unwinding by the replicative helicase . Topoisomerase IIα (TopoIIα), a type II enzyme, has roles in chromosome condensation and decatenation, is also present in the replisome, and is proposed to relax positive supercoils ahead of replication forks (9-11). Although it is known that topoisomerase poisons cause replication stress, specific roles for topoisomerases in response to replication stress have not been defined.

If stalled forks are not restarted in a timely manner, they may be converted to unusual DNA structures and collapse creating a one-ended double-strand break or "double-strand end" (DSE). Certain types of damage, such as single-strand breaks, may cause direct fork collapse to DSEs. As with double-strand breaks, the checkpoint kinases ATM and ATR are recruited to DSEs and activated, leading to histone H2AX phosphorylation (γ-H2AX) in the vicinity of DSEs (12). This chromatin modification is important for fork repair and checkpoint activation, and once collapsed forks are repaired, γ-H2AX is replaced by unmodified H2AX (13-15). Homologous recombination (HR), involving RAD51-mediated strand invasion, plays a major role in restarting stalled and collapsed forks (5). NHEJ factors also play a role in cell survival after replication stress (16).

Replication stress activates the intra-S checkpoint (5). ssDNA-RPA at stalled forks is bound by ATRIP leading to activation of its obligate binding partner ATR. ATR activation depends on RAD17 (plus Rfc2-5) loading of the RAD9-HUS1-RAD1 complex (9-1-1; a scaffold and processivity factor structurally related to PCNA) through a RAD9-RPA interaction. RAD9 recruits TopBP1, an essential factor for ATR activation. ATR phosphorylates RAD17, which recruits Claspin to be phosphorylated by ATR, and phosphorylated RAD17-Claspin promotes ATR phosphorylation/activation of Chk1 kinase, which phosphorylates proteins that stabilize the stalled fork and prevent late origin firing.

Metnase is a human protein that interacts with DNA ligase IV, topoisomerase IIα (TopoIIα), Pso4, and NBS1, and promotes NHEJ, DNA integration, and TopoIIα-dependent chromosome decatenation (17-20). Metnase has SET (protein methylase) and nuclease domains. It methylates histone H3 at lysines 4 and 36, which are associated with "open" chromatin and may increase accessibility of repair factors to damaged DNA. Metnase knockdown confers mild sensitivity to ionizing radiation (17). Because Metnase functions in NHEJ and regulates TopoIIα activity, we investigated whether it plays a role in replication or replication fork restart after stress. We show here that Metnase promotes cell proliferation, and cell survival after replication stress caused by HU, the topoisomerase I poison camptothecin (CPT), and UV-B. Metnase does not influence replication fork progression, but it strongly influences restart of stalled forks. Additionally, it co-immunoprecipates with

PCNA and RAD9. We further show that Metnase promotes resolution of HU-induced γ-H2AX foci, enhances TopoIIα-dependent relaxation of positively supercoiled DNA, and co-immunoprecipitates with PCNA and RAD9. These results establish Metnase as a key regulatory factor in the human replication stress response.

MATERIALS AND METHODS

Cell lines, RNAi-suppression of Metnase, and expression of V5-tagged Metnase

Cell lines were cultured in D-MEM with 10% (v/v) fetal bovine serum supplemented with 100 U/ml penicillin and 100 μg/ml streptomycin, or 1× antimycotic/antibiotic (Invitrogen, Carlsbad, CA), respectively. Metnase was overexpressed in HEK-293 and HEK-293T cells as described (19). V5-tagged Metnase expression was confirmed by Western blot with a monoclonal antibody against the V5 tag (Invitrogen). Metnase was downregulated by transfecting cells with a pRNA/U6-Metnase RNAi vector and selecting in growth medium with 150-200 μg/ml hygromycin B (Sigma-Aldrich, St. Louis, MO), or with an Metnase shRNA vector (pRS-shMetnase). Control cells were transfected with empty pRNA/U6 or pRS-shGFP vectors. Metnase expression was measured by RT-PCR and by Western blots using antibodies to native Metnase as described (17).

Cell proliferation and replication stress sensitivity assays

Cell proliferation was analyzed in triplicate in treated or mock-treated populations incubated in fully supplemented media at 37°C, 5% CO_2, and at indicated times cells were harvested and counted with a Coulter counter. Cell sensitivity to CPT and HU was determined by seeding 1000 cells per 10 cm (diameter) dish in drug-free medium (to determine plating efficiency, PE), and 100,000 cells per dish in medium with CPT or HU, incubating for indicated times, then cells were rinsed with PBS, fresh growth medium was added, and cells were incubated for 12-14 days before colonies were stained with 0.1% crystal violet in methanol and counted. For UV sensitivity, cells were seeded and incubated for 24 h as above, rinsed with PBS, exposed to UVB in a biological safety cabinet equipped with a Phillips UVB fluorescent bulb, then fresh growth medium was added and cells were incubated and colonies scored. UV doses were determined by using a UVX dosimeter (UVP, Upland, CA). PE was calculated as the number of colonies divided by the number of cells plated without drug or UVB treatment. Percent survival was calculated as the number of colonies formed with drug or UVB treatment divided by the number of cells plated times the PE.

Cell cycle distributions and cell death

Cell cycle distributions were measured by fixing cells with 70% ethanol and staining with 0.2 mg/ml propidium iodide in a fresh solution containing 1% (v/v) Triton X-100 and 2 U of DNAse-free RNAse (all from Sigma-Aldrich) for 15 min

at 37°C or 30 min at room temperature. Samples were analyzed using a FACScan or a FACScalibur flow cytometer (Becton Dickinson, Franklin Lakes, NJ). The percentages of cells in G1, S, or G2/M phases were calculated by dividing the number of cells in each cell cycle stage by the total number of PI positive cells after normalizing to controls that were not stained with PI and converting values to percentages. Apoptosis and cell death were analyzed by flow-cytometric measurement of annexin-V expression and propidium iodide incorporation by using the Annexin V-FITC Apoptosis Detection Kit I (BD Pharmingen, San Diego, CA). All flow cytometry data were analyzed with FlowJo software (Ashland, OR, http://www.flowjo.com/).

DNA replication by BrdU incorporation and DNA fiber analysis

Log phase cells, or cells treated with 5 mM HU for 18 h were washed with PBS and released into fully supplemented D-MEM containing 10 μM BrdU. Aliquots were removed at indicated times, cells were fixed, permeabilized, and stained using the FITC BrdU Flow Kit (BD Pharmingen), and analyzed by flow cytometry as above. DNA fibers were analyzed as described (21). Briefly, cells were grown in six-well tissue culture dishes, 20 μM IdU was added to growth medium, mixed and incubated for 10 min at 37°C. Media was removed and cells were washed with PBS, followed by a 100 μM thymidine wash. Then, cells were either treated with HU or mock treated, medium was replaced with fresh medium containing 20 μM CldU and cells were incubated for 20 min at 37°C. Cells were harvested, resuspended in PBS, 2500 cells were transferred to a positively charged microscope slide (Superfrost/Plus, Daigger, Vernon Hills, IL), lysed with 6 μl of 0.5% SDS, 200 mM Tri-HCl, pH 7.4, 50 mM EDTA, and incubated at room temperature for ~5 min. Slides were tilted to allow DNA to spread via gravity, covered with aluminum foil, air-dried for 8 min, fixed for 5 min with 3:1 methanol:acetic acid (prepared fresh), air dried for 8 min, and stored in 70% ethanol at 4°C overnight. Slides were deproteinized in 2.5 N HCl at 37°C for 1 h, blocked with 5% BSA and labeled sequentially for 1 h each with mouse anti-BrdU antibody (BD Biosciences, San Jose, CA), secondary goat anti-mouse Alexa-568 (Invitrogen), rat anti-BrdU (Accurate Chemical, Westbury, NY), and secondary donkey anti-rat Alexa-488 (Invitrogen). Slides were mounted in PermaFluor aqueous, self-sealing mounting medium (Thermoscientific, Waltham, MA). DNA fibers were visualized using an LSM 510 confocal microscope (Zeiss, Thornwood, NY) optimized for each Alexa dye. Images were analyzed using Zeiss LSM Image Browser software.

Analysis of γ-H2AX positive cells

Cells were treated with 10 mM HU for 18 h in fully supplemented D-MEM, released into fully supplemented D-MEM for indicated times, harvested, cytospun, and fixed as described previously (22). Cells were re-hydrated in PBS for 5 min at room temperature and blocked with 2% BSA in PBS for 30 min. Primary staining was done with γ-H2AX monoclonal mouse antibody (Merck, Nottingham, UK) incubated at 4˚C overnight. Cells were washed 3 times in TBS-

T for 5 min at room temperature. Secondary staining was accomplished with an Alexa488-tagged goat anti-mouse antibody (Invitrogen) for 1 h at room temperature. The cells were washed 3 times in TBS-T for 5 min at room temperature, then covered in Vectashield mounting media with DAPI (Vector Laboratories, Burlingame, CA) and sealed. Images were obtained with a Radiance 2100 inverted confocal microscope **(**BioRad, Hercules, CA) fitted with filter sets specific for DAPI and FITC/Alexa488. Images were optimized consistently with the ImageJ program (http://rsb.info.nih.gov/ij/).

Protein immunoprecipitation

Protein samples were pre-treated with 4 U of DNaseI, incubated at 37°C for 10 min, immunoprecipitated using 0.5-5 mg of protein and antibodies to V5, PCNA (Abcam, Cambridge, MA), RAD9 (Abcam), or TopoIIα (TopoGEN, Port Orange, FL), samples were incubated overnight at 4°C, then 25 µl of A/G (1:1) agarose beads (Invitrogen) were added and incubated for 1 h at 4°C, centrifuged at 300 $\times$ g for 2 min at 4°C. Supernatants were removed and beads were washed four times with M-PER buffer (Thermoscientific). Beads were centrifuged at 300 $\times$ g for 2 min at 4°C, boiled for 10 min, and centrifuged at 300 $\times$ g for 2 min at 4°C. The supernatants were transferred to new tubes, samples were boiled for 10 min, separated by SDS-PAGE, and analyzed by Western blotting.

Relaxation of positive supercoiled DNA

Positively supercoiled DNA was prepared as described (9). Positive supercoil relaxation reactions were performed in a total volume of 20 µl in 10 mM Tris-HCl, pH 7.9, 175 mM KCl, 0.1 mM EDTA, 5 mM $MgCl_2$, 2.5% glycerol, 0.5 mM ATP (USB Co., Cleveland, OH), 2 U TopoIIα, 180 ng Metnase (when noted), and 0.3 µg DNA. Aliquots were removed at indicated times and reactions were stopped with 4 µl of 0.77% SDS, 77 mM EDTA. Products were separated on 1% agarose gels and densitometry was performed using Image J software. Background values were subtracted from signals, resulting values were normalized to signals at initial time points, and plotted as function of time in two independent experiments.

RESULTS

Metnase promotes cell proliferation

Metnase is expressed in a wide variety of human tissues (17) and in all human cell lines tested, except those transformed by T-antigen such as HEK-293T cells (unpublished results). Overexpression of Metnase in HEK-293T increases cell proliferation (19). HEK-293 cells express Metnase, but not T-antigen, and stable shRNA knockdown of Metnase in HEK-293 cells significantly reduced cell proliferation rate compared to control cells (Figure 1A). We have shown previously and confirmed in this study that Metnase overexpression in HEK-293T increases cell proliferation (Figure 1B). Moreover, cells stably transfected with Metnase shRNA vectors either cease to proliferate after 2-3 months or

revert to normal. These results indicate that Metnase promotes proliferation of human cells, and suggest that Metnase is very important for growth of human cells that do not express T antigen.

Metnase promotes cell survival and DNA replication after replication stress

The effect of Metnase on cell proliferation, coupled with its DNA repair properties and functional interaction with TopoIIα (17,19), suggested that Metnase may have a role in replication and/or rescuing cells from replication stress at sites of spontaneous DNA damage. We therefore tested whether Metnase regulates sensitivity to replication stress induced by HU, CPT, and UV-B (Figure 2A). Metnase knockdown sensitized HT1080 cells to 1 mM HU by more than 1000-fold ($P = 0.01$), and to 0.2-0.5 μM CPT by nearly 10-fold ($P \leq 0.011$) (all statistical analyses in this study were performed by using t tests). Metnase knockdown sensitized HEK-293 cells to a UV-B dose of 11.2 J/m^2 by nearly 20-fold ($P = 0.007$). When cultured in a low concentration of HU (0.1 mM), HEK-293 cells proliferated at a slow rate, but Metnase knockdown cells showed almost no proliferative capacity; this effect specifically reflects the Metnase defect since Metnase overexpression in HEK-293T significantly enhanced proliferation under these conditions (Figure 2B). The hypersensitivity of Metnase knockdown cells to replication stress reflects, at least in part, enhanced cell death via apoptosis, as shown by the nearly 30-fold increase in the apoptosis marker annexin V, and >6-fold increase in inviable cells (unable to exclude propidium iodide) (both $P < 0.005$). The marked sensitivity of Metnase knockdown cells to replication stress contrasts with their mild sensitivity to ionizing radiation (17).

To investigate the mechanism by which Metnase promotes cell proliferation and resistance to replication stress, we tested whether Metnase expression level influenced DNA replication by measuring BrdU incorporation and cell cycle distributions by flow cytometry, in unstressed cells and after release from replication stress. In log phase (untreated) HEK-293 cells, Metnase knockdown had no effect on BrdU incorporation during a 30 min incubation (Figure 3A). However, when cells were pretreated with 5 mM HU for 18 h and then released into BrdU, Metnase knockdown in HEK-293 significantly reduced BrdU incorporation (~2-fold), and Metnase overexpression in HEK-293T significantly increased BrdU incorporation (Figure 3B, C). Although neither over- nor underexpression of Metnase significantly affected cell cycle distributions of unstressed cells (Supplemental Figure S1A), when treated with 5 mM HU for 18 h and released, HEK-293T cells overexpressing Metnase entered S-phase more rapidly than control cells (seen 1 h after release from HU), and entered G2 phase more rapidly (seen 7 h after release from HU (Supplemental Figure S1B). Somewhat stronger effects were seen when Metnase was overexpressed in HEK-293 cells (Supplemental Figure S1C); this may reflect the fact that HEK-293T cells show robust proliferation even though they do not express Metnase. When HEK-293 Metnase knockdown cells were treated with 5 mM HU for 18 h and released, the opposite effect was seen. In two independent

knockdown cell lines, there were marked accumulations of S phase cells 10 and 18 h after release from HU (Supplemental Figure S1D), indicating that Metnase knockdown prolongs S phase after replication stress. These results support the idea that Metnase promotes DNA replication in cells recovering from replication stress.

Metnase promotes replication fork restart

To gain a better understanding of the role of Metnase in replication and the replication stress response, we analyzed replication fork restart, new origin firing, and replication speed by using DNA fiber analysis. Log phase HEK-293 cells stably transfected with vectors expressing shRNA targeting Metnase, or GFP as control, were labeled with IdU for 10 min, then incubated with or without 5 mM HU for one h, briefly washed with thymidine and then incubated with CldU for 20 min. Cells were lysed on glass slides and DNA fibers were stretched by gravity, fixed, IdU was stained red and CldU was stained green, and DNA fibers were quantified using confocal-microscopy (Figure 4A, B). In untreated control cells, ~90% of fibers showed adjacent red-green signals indicative of continuing forks, and ~10% had only green signals indicating forks that initiated after IdU was removed ("new forks"). When control cells were treated with HU, continuing forks (those that stalled and restarted) were moderately reduced to ~65% ($P = 0.0014$), new forks that initiated after HU treatment showed a slight but not statistically significant increase to ~20%, and ~15% of forks stopped and failed to restart. The pattern observed with untreated Metnase knockdown cells was similar to untreated wild-type cells, with predominantly continuing forks and a small percentage of new forks. Strikingly, when Metnase knockdown cells were treated with HU, the percentage of stopped forks greatly increased (to ~90%) and there was a corresponding large decrease in the percentage of continuing forks (both $P \leq 0.0008$). New forks were extremely rare in HU treated Metnase knockdown cells, however new forks are also rare in untreated cells, and the decrease with HU treatment was not statistically significant ($P = 0.3$). These results provide direct evidence that Metnase plays a critical role in restarting stalled replication forks, and further suggest that Metnase may regulate new origin firing when cells experience replication stress.

To determine whether Metnase regulates the speed of replication, we measured average fiber lengths. As expected, red fibers were shorter than green since cells were treated with IdU (red) for 10 min and CldU (green) for 20 min. Fibers were longer in unstressed cells than after HU treatment (Figure 4C). However, Metnase had no effect on fiber lengths in either HU treated or untreated cultures. We conclude that Metnase regulates the efficiency of replication fork restart, and possibly initiation after replication stress, but it has no effect on the speed of ongoing forks.

Metnase promotes resolution of γ-H2AX induced by replication stress

Replication stress causes fork collapse to DSEs marked by phosphorylation of histone H2AX to γ-H2AX. Elimination of the γ-H2AX signal over time reflects

DSE/fork repair. Metnase and classical NHEJ proteins promote survival after replication stress and influence replication fork restart (21,23-25) (this study), and Metnase promotes NHEJ and interacts with the key NHEJ protein DNA LigIV (17,18). We therefore tested whether Metnase influences resolution of HU-induced γ-H2AX by treating cells with 10 mM HU for 18 h, then releasing into normal growth medium and examining γ-H2AX by immunofluorescence microscopy. Because HEK-293 and HEK-293T cells used in these experiments adhere poorly, cells were cytospun prior to fixation and immunocytochemical staining. For this reason, individual γ-H2AX foci are not always detectable. Instead γ-H2AX signals typically appears as diffuse nuclear staining and cells were scored as either γ-H2AX positive or negative (representative images are shown in Figure 5A). Consistent with the enhanced sensitivity of Metnase knockdown cells to HU, γ-H2AX persisted longer in the knockdown cells, with significant differences from controls at both 6 and 24 h after release from HU (Figure 5B, $P < 0.0001$). Similarly, overexpression of Metnase in HEK-293T cells accelerated the resolution of γ-H2AX signals (Figure 5C ($P \leq 0.0055$). Note that in all four cell lines, similar percentages of cells were γ-H2AX positive at the end of the 18 h HU treatment. These results indicate that Metnase promotes resolution of γ-H2AX after cells are released from replication stress, but Metnase does not prevent fork collapse to DSEs over the course of this relatively long HU treatment.

Metnase co-immunoprecipitates with PCNA and RAD9

Because Metnase is involved in the replication stress response, we explored its interactions with proteins at the replication fork. PCNA is a key scaffold protein that mediates binding of numerous proteins in the replisome and promotes replication processivity (7). Metnase co-immunoprecipitated with PCNA, and vice versa, in unstressed cells and after treatment with HU (Figure 6A). PCNA-interacting proteins share a conserved binding motif, the PIP box. Metnase has a highly conserved PIP box (Supplemental Table S1) suggesting it directly interacts with PCNA. Interestingly, Metnase also co-immunoprecipitated with RAD9, a member of the 9-1-1 complex that is structurally and functionally related to PCNA, and that is recruited to stalled and/or collapsed replication forks (Figure 6B). Although this interaction appeared stronger when RAD9 was immunoprecipitated from HU treated cells, a similar enhancement was not seen with HU treatment when Metnase was immunoprecipitated. Metnase did not co-immunoprecipitate with the 32 kDa subunit of RPA (Figure 6C), indicating that Metnase is present within the replisome, but is not closely associated with ssDNA at stalled forks. These results indicate that Metnase is closely associated with replication stress factors that control TLS, fork processing via HR mechanisms, and checkpoint signaling.

Metnase interacts with TopoIIα and promotes TopoIIα-dependent relaxation of positively supercoiled plasmid DNA

Metnase interacts with TopoIIα and promotes TopoIIα-dependent chromosome decatenation (19). TopoIIα is present in the replisome (11) and has been implicated in DNA replication through relaxation of positive supercoils that accumulate ahead of replication forks (9). We found that Metnase significantly enhanced TopoIIα-dependent relaxation of positive supercoils during a 5 min time course, but Metnase was not required to achieve full relaxation within an hour (Figure 7A, B). To gain insight into whether Metnase functions in the replication stress response through its interaction with TopoIIα, we tested whether the interaction between Metnase and TopoIIα was affected by replication stress. HEK-293 cells were treated with 5 mM HU for 3 h, and cell extracts were prepared and analyzed by co-immunoprecipitation of Metnase and TopoIIα. As shown in Figure 7C, Metnase and TopoIIα show a robust interaction regardless of which protein was immunoprecipitated, but this interaction was not affected by HU treatment. These results suggest that Metnase interaction with TopoIIα may promote TopoIIα processing of DNA structures in front of replication forks.

DISCUSSION

Although Metnase appeared very late in evolution, in anthropoid primates (26), it influences several important aspects of DNA metabolism including NHEJ, DNA integration, and chromosome decatenation (17-20). Through interaction with TopoIIα, it regulates cellular resistance to common chemotherapeutics (22,27). The present study establishes another important role for Metnase in the replication stress response. Given how late Metnase appeared in evolution, it is not surprising that it does not influence replication fork progression. Instead, Metnase functions during replication stress since Metnase affected BrdU incorporation, S phase progression, and fork restart by DNA fiber analysis only when cells were subjected to replication stress (Figures 3, 4, S1). Metnase knockdown conferred a marked defect in fork restart during a 20 min period after a brief (1 h) HU treatment (Figure 4). This result indicates that Metnase plays a key role in restarting stalled forks, because the brief HU treatment will cause mainly fork stalling. Also, when forks collapse, restart is largely dependent on HR, an inherently slow process that involves RAD51 replacement of RPA on ssDNA, and strand invasion of sister chromatids by RAD51 filaments (5). However, when cells were subjected to longer periods of replication stress, Metnase promoted resolution of γ-H2AX (Figure 5), which marks collapsed forks. This indicates that Metnase also promotes restart of collapsed forks. Another late-evolving protein that functions in replication fork restart is PARP-1. PARP-1 is not found in yeast, but is present in higher eukaryotes. PARP-1 recruits the ancient DNA repair endonuclease MRE11 to stalled forks, which is proposed to process structures at stalled forks, leading to RPA recruitment and eventual restart via HR (28).

Metnase might promote replication fork restart in a variety of ways, as illustrated in Figure 8. Metnase promotes NHEJ (17) and other factors involved in NHEJ are known to promote cell survival after replication stress (16,24).

NHEJ factors might promote rejoining of DSEs at collapsed forks, but it seems that this type of repair would be highly inaccurate (and genome destabilizing) since each collapsed fork produces only a single broken end. It is possible that NHEJ factors promote fork restart indirectly through interactions with HR factors (29). When replication forks stall, the initial cellular response is to stabilize the replisome to prevent fork collapse. Metnase does not appear to play a role in fork stabilization over an extended period of replication stress, because altering Metnase levels had no effect on the percentage of cells with collapsed forks (γ-H2AX positive) after an 18 h HU treatment (Figure 5). Although it is clear that Metnase promotes resolution of γ-H2AX signals, further studies are required to determine whether this reflects enhanced repair of collapsed forks via NHEJ or other mechanisms.

Metnase could promote fork restart through its interactions with the replisome factors PCNA and RAD9. Although it is not yet known whether Metnase interacts directly with these proteins, the fact that the Metnase SET domain has a conserved PIP box is highly suggestive that Metnase interacts directly with these proteins. Regardless, our results clearly place Metnase in the vicinity of stalled replication forks. The Metnase SET domain encodes a protein methylase, and Metnase is known to methylate histone H3 and itself (17,19). Metnase could regulate PCNA and/or RAD9 function by methylating these proteins. PCNA regulates TLS through direct interactions with TLS polymerases (7), thus Metnase may enhance fork restart after UV by enhancing TLS at UV lesions.

RAD9 has well-established roles in the intra-S checkpoint response (5). Metnase could promote fork restart by influencing checkpoint activation or downstream checkpoint-dependent processes such as inhibition of origin firing. We are currently investigating the effects of Metnase on checkpoint factors downstream of RAD9, including Chk1. Metnase is not required for the p53/Chk2 arm of the DNA damage checkpoint response since replication stress-induced cell death in Metnase knockdown cells shows a robust apoptotic response (Figure 2C). Metnase may have a more general role in fork restart through chromatin modification in the vicinity of stalled and collapsed forks. It is noteworthy that Metnase methylates histone H3 lysines 4 and 36, which are specifically associated with “open” chromatin (17). Thus, Metnase could promote fork restart by enhancing access of repair factors to stalled and collapsed forks.

Finally, Metnase could influence fork restart through its direct interaction with TopoIIα, another factor within the mammalian replisome (11). TopoIIα is proposed to relax positive supercoils that form ahead of replication forks (9). When replication forks stall, the MCM helicase complex can continue to unwind duplex DNA, uncoupled from the replicative polymerases, producing excess ssDNA that is bound by RPA and triggering the intra-S checkpoint (5,30). Continued DNA unwinding by MCM will also increase positive supercoiling that may drive unusual DNA structures at stalled forks (30). By enhancing TopoIIα-dependent relaxation of positive supercoils, Metnase could promote a favorable

topological state that results in timely fork restart, particularly when unusual structures form, such as “chicken feet,” since the resolution of such structures is probably dependent on the topology of the stalled fork. Local topology could also influence restart of collapsed forks since HR-mediated invasion of broken ends into sister chromatids requires unwinding of the sister duplex. Note that the models described above are not mutually exclusive: Metnase may have different roles depending on the specific structures at stalled or collapsed replication forks.

Prior studies have established that Metnase is highly expressed in actively proliferating tissues (17). We have recently shown that Metnase is frequently overexpressed in leukemia and breast cancer cell lines, and importantly, downregulating Metnase greatly enhances tumor cell sensitivity to common chemotherapeutics including epididophylotoxins and anthracyclines (22,27). The current study establishes Metnase as a critical factor in the replication stress response. Metnase is therefore an excellent target for therapeutic strategies that block DNA synthesis, or that exploit defects of tumor cells in replication fork restart (31,32), and it may prove to be an important target in the treatment of a wide variety of tumor types.

FUNDING

This work was supported by the National Institute of Health [R01 CA100862 and R01 GM084020 to J.A.N., R01 HL093606 to R.H., R01 GM033944 to N.O., F31 CA132628 to L.P.D.H., and A.C.G. was supported by T32 CA09582]. Images in this paper were generated in the University of New Mexico Cancer Center Fluorescence Microscopy Facility which received support from the National Institutes of Health [P30 CA118100]; the National Science Foundation [MCB9982161]; and the National Center for Research Resources [S10 RR14668, P20 RR11830, S10 RR19287, S10 RR016918], the University of New Mexico Health Sciences Center, and the University of New Mexico Cancer Center. Flow cytometry data was generated in the Flow Cytometry Shared Resource Center supported by the University of New Mexico Health Sciences Center and the University of New Mexico Cancer Center**.**

ACKNOWLEDGEMENTS

We thank Miret Aladjem and Amanda Wraith Quijas for assistance in establishing the DNA fiber assay.

REFERENCES

1. Hanks, S., Coleman, K., Reid, S., Plaja, A., Firth, H., FitzPatrick, D., Kidd, A., Méhes, K., Nash, R., Robin, N. *et al.* (2004) Constitutional aneuploidy and cancer predisposition caused by biallelic mutations in BUB1B. *Nat. Genet.*, **36**, 1159-1161.
2. Burma, S., Chen, B.P. and Chen, D.J. (2006) Role of non-homologous end joining (NHEJ) in maintaining genomic integrity. *DNA Repair*, **5**, 1042-1048.
3. Zou, Y., Liu, Y., Wu, X. and Shell, S.M. (2006) Functions of human replication protein A (RPA): from DNA replication to DNA damage and stress responses. *J. Cell. Physiol.*, **208**, 267-273.
4. Shimada, K., Oma, Y., Schleker, T., Kugou, K., Ohta, K., Harata, M. and Gasser, S.M. (2008) Ino80 chromatin remodeling complex promotes recovery of stalled replication forks. *Curr. Biol.*, **18**, 566-575.
5. Budzowska, M. and Kanaar, R. (2009) Mechanisms of dealing with DNA damage-induced replication problems. *Cell Biochem. Biophys.*, **53**, 17-31.
6. Davies, S.L., North, P.S. and Hickson, I.D. (2007) Role for BLM in replication-fork restart and suppression of origin firing after replicative stress. *Nat. Struct. Mol. Biol.*, **14**, 677-679.
7. Moldovan, G.L., Pfander, B. and Jentsch, S. (2007) PCNA, the maestro of the replication fork. *Cell*, **129**, 665-679.
8. Niimi, A., Brown, S., Sabbioneda, S., Kannouche, P.L., Scott, A., Yasui, A., Green, C.M. and Lehmann, A.R. (2008) Regulation of proliferating cell nuclear antigen ubiquitination in mammalian cells. *Proc. Natl. Acad. Sci. USA*, **105**, 16125-16130.
9. McClendon, A.K., Rodriguez, A.C. and Osheroff, N. (2005) Human topoisomerase IIalpha rapidly relaxes positively supercoiled DNA: implications for enzyme action ahead of replication forks. *J. Biol. Chem.*, **280**, 39337-39345.
10. Wang, J.C. (2002) Cellular roles of DNA topoisomerases: a molecular perspective. *Nat. Rev. Mol. Cell Biol.*, **3**, 430-440.
11. Jiang, H.Y., Hickey, R.J., Abdel-Aziz, W., Tom, T.D., Wills, P.W., Liu, J. and Malkas, L.H. (2002) Human cell DNA replication is mediated by a discrete multiprotein complex. *J. Cell. Biochem.*, **85**, 762-774.
12. Ward, I.M. and Chen, J. (2001) Histone H2AX is phosphorylated in an ATR-dependent manner in response to replicational stress. *J. Biol. Chem.*, **276**, 47759-47762.
13. Chanoux, R.A., Yin, B., Urtishak, K.A., Asare, A., Bassing, C.H. and Brown, E.J. (2008) ATR and H2AX cooperate in maintaining genome stability under replication stress. *J. Biol. Chem.*, **284**, 5994-6003.
14. Downey, M. and Durocher, D. (2006) γH2AX as a checkpoint maintenance signal. *Cell Cycle*, **5**, 1376-1381.
15. Keogh, M.C., Kim, J.A., Downey, M., Fillingham, J., Chowdhury, D., Harrison, J.C., Onishi, M., Datta, N., Galicia, S., Emili, A. *et al.* (2006) A

phosphatase complex that dephosphorylates γH2AX regulates DNA damage checkpoint recovery. *Nature*, **439**, 497-501.
16. Lundin, C., Erixon, K., Arnaudeau, C., Schultz, N., Jenssen, D., Meuth, M. and Helleday, T. (2002) Different roles for nonhomologous end joining and homologous recombination following replication arrest in mammalian cells. *Mol. Cell. Biol.*, **22**, 5869-5878.
17. Lee, S.H., Oshige, M., Durant, S.T., Rasila, K.K., Williamson, E.A., Ramsey, H., Kwan, L., Nickoloff, J.A. and Hromas, R. (2005) The SET domain protein Metnase mediates foreign DNA integration and links integration to nonhomologous end-joining repair. *Proc. Natl. Acad. Sci. USA*, **102**, 18075-18080.
18. Hromas, R., Wray, J., Lee, S.H., Martinez, L., Farrington, J., Corwin, L.K., Ramsey, H., Nickoloff, J.A. and Williamson, E.A. (2008) The human set and transposase domain protein Metnase interacts with DNA Ligase IV and enhances the efficiency and accuracy of non-homologous end-joining. *DNA Repair*, **7**, 1927-1937.
19. Williamson, E.A., Rasila, K.K., Corwin, L.K., Wray, J., Beck, B.D., Severns, V., Mobarak, C., Lee, S.H., Nickoloff, J.A. and Hromas, R. (2008) The SET and transposase domain protein Metnase enhances chromosome decatenation: regulation by automethylation. *Nucleic Acids Res.*, **36**, 5822-5831.
20. Beck, B.D., Park, S.J., Lee, Y.J., Roman, Y., Hromas, R.A. and Lee, S.H. (2008) Human PSO4 is a Metnase (SETMAR) binding partner that regulates Metnase function in DNA repair. *J. Biol. Chem.*, **283(14):9023-30**, 9023-9030.
21. Shimura, T., Torres, M.J., Martin, M.M., Rao, V.A., Pommier, Y., Katsura, M., Miyagawa, K. and Aladjem, M.I. (2008) Bloom's syndrome helicase and Mus81 are required to induce transient double-strand DNA breaks in response to DNA replication stress. *J. Mol. Biol.*, **375**, 1152-1164.
22. Wray, J., Williamson, E.A., Fnu, S., Lee, S.-H., Libby, E., Willman, C.L., Nickoloff, J.A. and Hromas, R. (2009) Metnase mediates chromosome decatenation in acute leukemia cells. *Blood*, **114**, 1852-1858.
23. Arnaudeau, C., Tenorio Miranda, E., Jenssen, D. and Helleday, T. (2000) Inhibition of DNA synthesis is a potent mechanism by which cytostatic drugs induce homologous recombination in mammalian cells. *Mutat. Res.*, **461**, 221-228.
24. Arnaudeau, C., Lundin, C. and Helleday, T. (2001) DNA double-strand breaks associated with replication forks are predominantly repaired by homologous recombination involving an exchange mechanism in mammalian cells. *J. Mol. Biol.*, **307**, 1235-1245.
25. Shao, R.G., Cao, C.X., Zhang, H., Kohn, K.W., Wold, M.S. and Pommier, Y. (1999) Replication-mediated DNA damage by camptothecin induces phosphorylation of RPA by DNA-dependent protein kinase and dissociates RPA:DNA-PK complexes. *EMBO J.*, **18**, 1397-1406.

26. Cordaux, R., Udit, S., Batzer, M.A. and Feschotte, C. (2006) Birth of a chimeric primate gene by capture of the transposase gene from a mobile element. *Proc. Natl. Acad. Sci. USA*, **103**, 8101-8106.
27. Wray, J., Williamson, E.A., Royce, M., Shaheen, M., Beck, B.D., Lee, S.H., Nickoloff, J.A. and Hromas, R. (2009) Metnase mediates resistance to topoisomerase II inhibitors in breast cancer cells. *PLoS ONE*, **4**, e5323.
28. Bryant, H.E., Petermann, E., Schultz, N., Jemth, A.S., Loseva, O., Issaeva, N., Johansson, F., Fernandez, S., McGlynn, P. and Helleday, T. (2009) PARP is activated at stalled forks to mediate Mre11-dependent replication restart and recombination. *EMBO J.*, **28**, 2601-2615.
29. Shrivastav, M., Miller, C.A., De Haro, L.P., Durant, S.T., Chen, B.P., Chen, D.J. and Nickoloff, J.A. (2009) DNA-PKcs and ATM co-regulate DNA double-strand break repair. *DNA Repair*, **8**, 920-929.
30. Forsburg, S.L. (2008) The MCM helicase: linking checkpoints to the replication fork. *Biochem. Soc. Trans.*, **36**, 114-119.
31. Bryant, H.E., Schultz, N., Thomas, H.D., Parker, K.M., Flower, D., Lopez, E., Kyle, S., Meuth, M., Curtin, N.J. and Helleday, T. (2005) Specific killing of BRCA2-deficient tumours with inhibitors of poly(ADP-ribose) polymerase. *Nature*, **434**, 913-917.
32. Farmer, H., McCabe, N., Lord, C.J., Tutt, A.N., Johnson, D.A., Richardson, T.B., Santarosa, M., Dillon, K.J., Hickson, I., Knights, C. *et al.* (2005) Targeting the DNA repair defect in BRCA mutant cells as a therapeutic strategy. *Nature*, **434**, 917-921.

Figure Legends

Figure 1. Metnase promotes cell proliferation. A) Cell growth was monitored in HEK-293 cells transfected with shGFP (control) or shMetnase vectors. B) Cell growth was monitored in HEK-293-T cells, which do not normally express Metnase, transfected with the pCAPP-Metnase expression vector or empty pCAPP. Plotted are averages (±SD) of 2-3 determinations per time-point. * indicates $P<0.05$, ** indicates $P<0.01$. Metnase expression is shown in representative Western blots with β-actin loading control (insets).

Figure 2. Metnase promotes cell survival after DNA replication stress. A) Average percent cell survival (± SD) after HU, CPT, or UV-B treatments measured as relative plating efficiency for HT1080 or HEK-293 cells stably transfected with control or shRNA-Metnase vectors. Data are from 2-3 independent experiments per condition; * indicates $P = 0.0127$, ** indicates $P \leq 0.01$. B) Average growth rates (±SD) of control HEK-293 and sh-Metnase knockdown cells, and control HEK-293T or Metnase overexpression cells in medium containing 0.1 mM HU; data are from 2-3 independent experiments per cell line. C) HEK-293 control or Metnase knockdown cells were treated with 5 mM HU for 6 h and the percentages of cells expressing annexin V or incorporating propidium iodide were determined by flow cytometry. Values are averages (±SD) from 3 independent experiments.

Figure 3. Metnase promotes DNA replication after release from replication stress. A) Log phase HEK-293 cells expressing normal or low levels of Metnase were incubated with 10 μM BrdU for 30 min and average percentages (±SD) of $BrdU^+$ cells are shown for two determinations per strain. B) HEK-293 control and Metnase knockdown cells were treated with 5 mM HU for 3 h and released into medium with 10 μM BrdU. Average fold increases (±SD) in the percentage of $BrdU^+$ cells relative to untreated cells (no HU, no BrdU) are plotted for 3 independent experiments per cell line. * indicates $P = 0.042$, ** indicates $P = 0.0047$. C) BrdU incorporation after HU release from HEK-293T control and Metnase overexpression cells as in panel B, except cells were treated with HU for 18 h; * indicates $P \leq 0.03$.

Figure 4. Metnase promotes replication fork restart. A) IdU and CldU labeling scheme is shown above representative confocal microscope images of DNA fibers, with IdU stained red and CldU stained green. B) Quantification of fiber types. At least 150 fibers were scored per treatment, per cell line for each of three experiments; ** indicates $P \leq 0.0014$. C) Fiber lengths were measured by using LSM 510 Image Browser software. Plotted are averages (±SD) of triplicate experiments in which 150-500 fibers were scored per treatment, per experiment. nd, none detected.

Figure 5. Metnase promotes resolution of replication stress-induced γ-H2AX. A) Representative confocal microscope images of HEK-293 and HEK-293T cells over- or under-expressing Metnase were treated with 10 mM HU for 18 h and released into growth medium for 24 h. Aliquots of cells were removed at indicated times, cytospun, stained with DAPI (blue) and antibodies to γH2AX (green) and imaged by confocal microscopy. B) Percentage of γ-H2AX positive cells among total DAPI stained cells. An average of >190 cells were counted per slide, 10 slides per experiment. Values are averages (±SD); ** indicates $P \leq 0.0055$.

Figure 6. Metnase interacts with PCNA and RAD9, but not RPA32. A) Reciprocal co-immunoprecipitation of V5-tagged Metnase and native PCNA from cells treated with 5 mM HU for 18 h, tested immediately or 30 min after release from HU, or untreated. Input represents 0.5% of immunoprecipitation. Results are representative of at least three independent experiments. B, C) Reciprocal co-immunoprecipitation of V5-tagged Metnase with native RAD9 and native RPA as in panel A, except HU treated cells were only tested immediately after treatment.

Figure 7. Metnase interacts with TopoIIα and stimulates relaxation of positive supercoils. A) Predominantly positively-supercoiled plasmid DNA samples were treated with TopoIIα (2 U) with or without Metnase (180 ng) for indicated times, and topological forms were detected on ethidium bromide stained agarose gels. B) Gel images were scanned and the percentage of positively-supercoiled DNA remaining at each time point was quantitated. Values are averages (±SD) of two determinations per condition, normalized to 100% at t=0; ** indicates $P = 0.007$. C) Co-immunoprecipitation of V5-tagged Metnase and native TopoIIα; data presented as in Figure 6B.

Figure 8. Potential roles of Metnase in the replication stress response. See text for details.

Figure 1

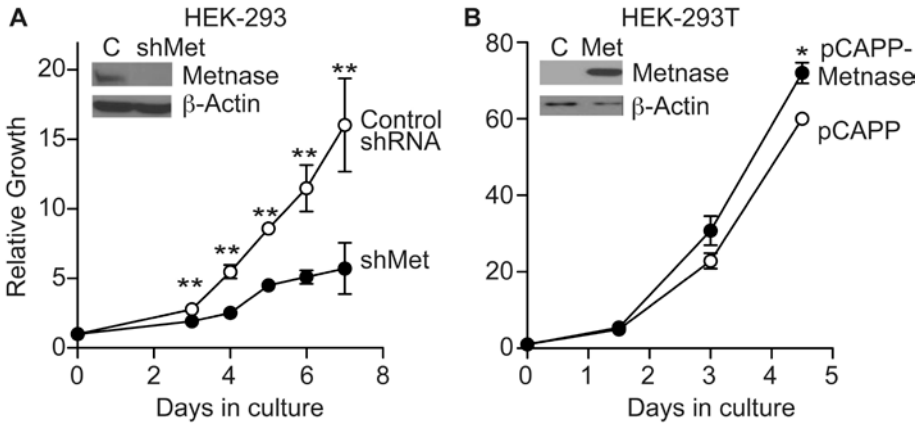

Figure 2

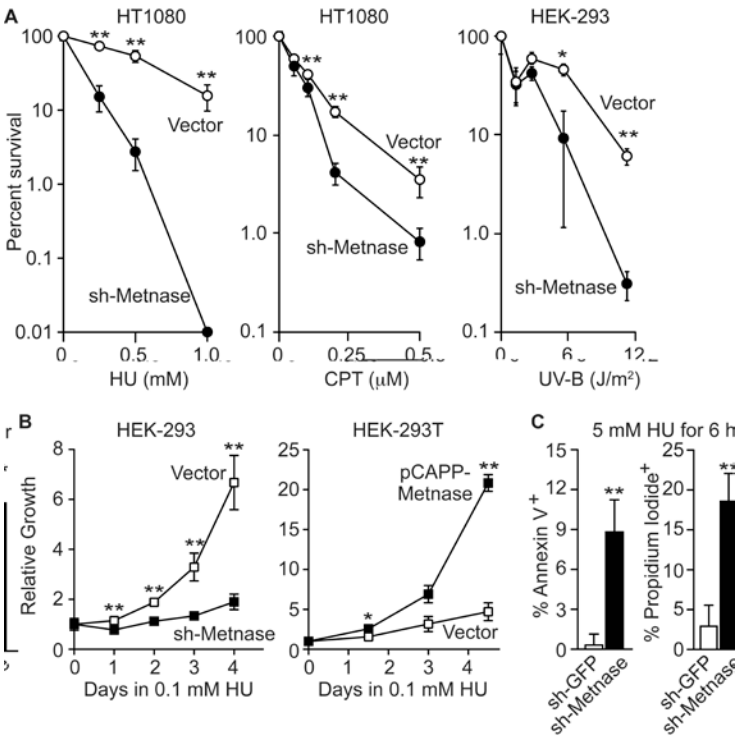

Figure 3

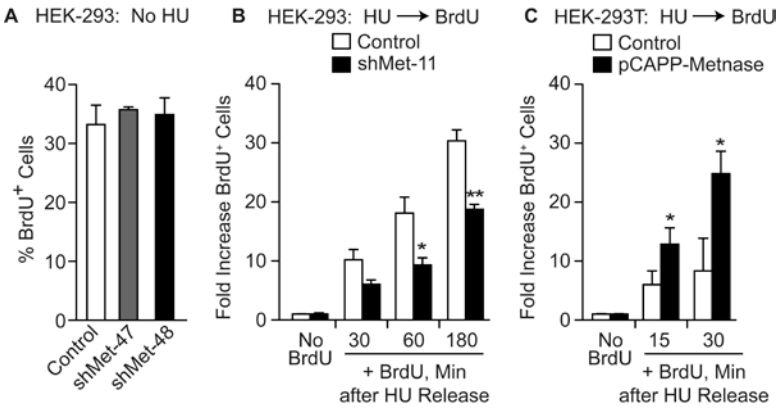

Figure 4

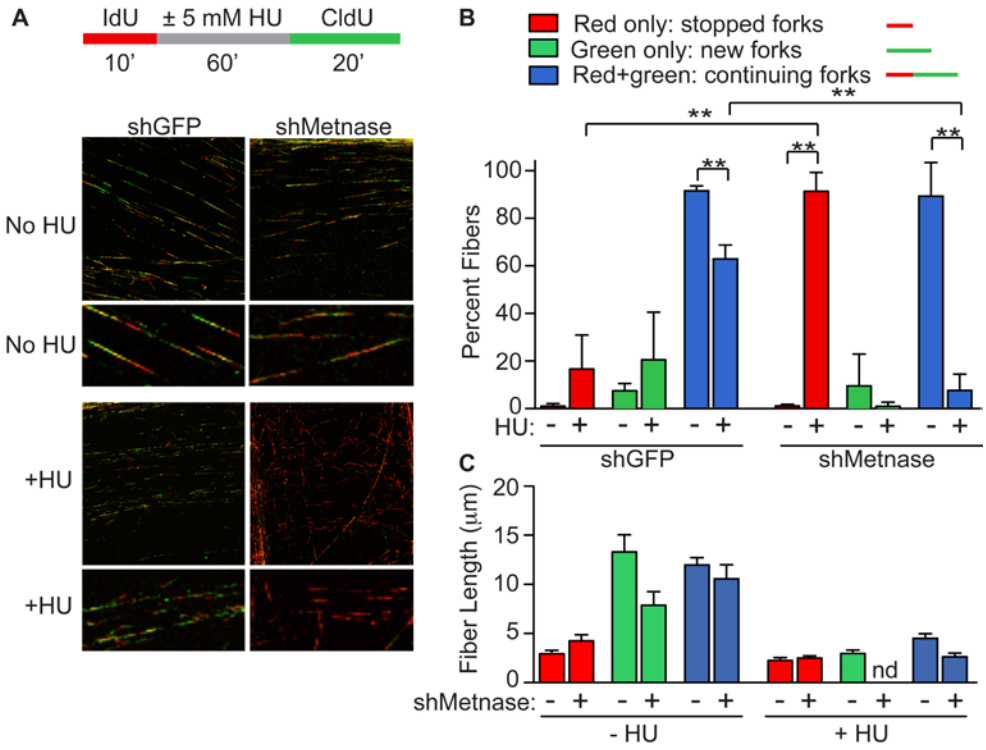

Figure 5

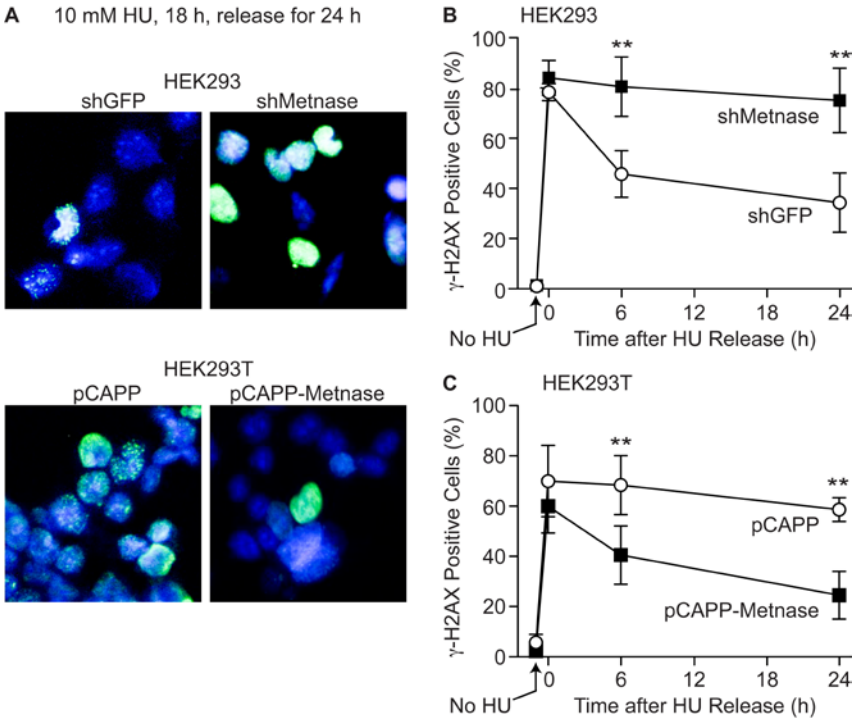
A
10 mM HU, 18 h, release for 24 h
HEK293
shGFP
shMetnase
HEK293T
pCAPP
pCAPP-Metnase
B
HEK293
γ-H2AX Positive Cells (%)
shMetnase
shGFP
No HU
Time after HU Release (h)
C
HEK293T
pCAPP
pCAPP-Metnase

Figure 6

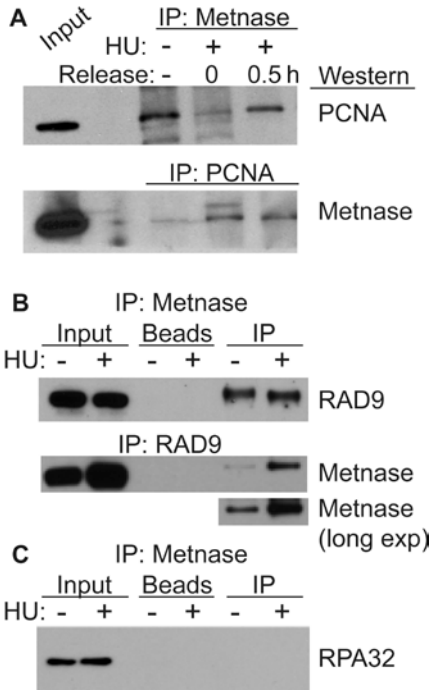

Figure 7

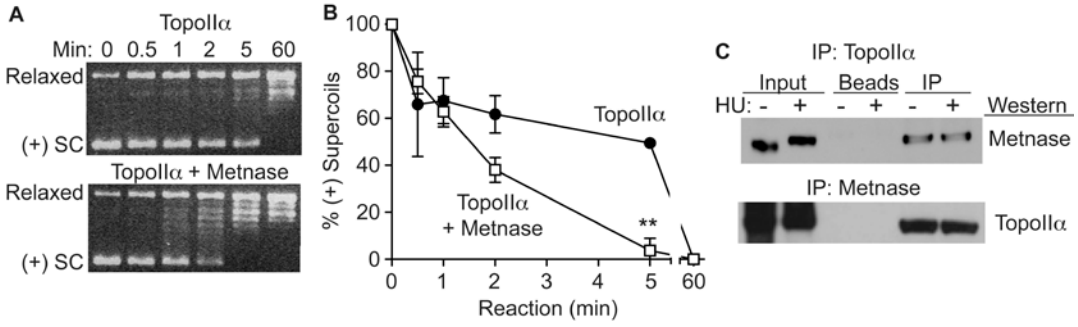

Figure 8.

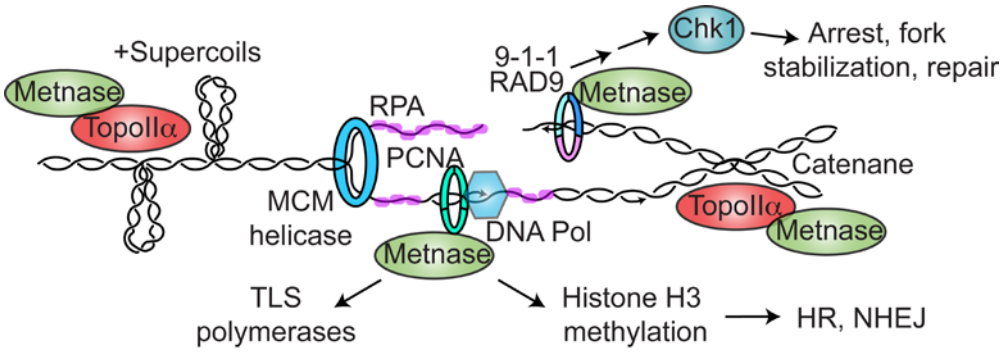
+Supercoils
Metnase
TopoIIα
RPA
PCNA
MCM
helicase
DNA Pol
Metnase
9-1-1
RAD9
Chk1
Arrest, fork
stabilization, repair
Metnase
Catenane
TopoIIα
Metnase
TLS
polymerases
Histone H3
methylation
HR, NHEJ

Supplemental information

Figure S1

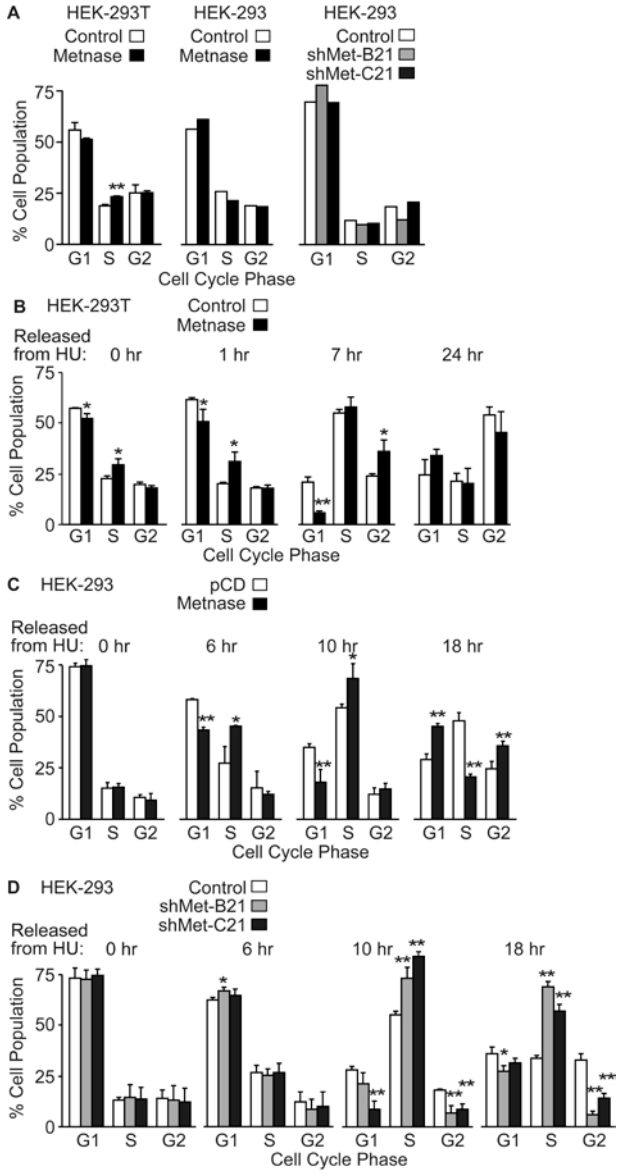

Figure S1. Metnase promotes cell cycle progression after replication stress. A) Cell cycle distributions of log phase cultures of HEK-293T, HEK-293 cells stably transfected with empty or Metnase overexpression vectors, and HEK-293 cells stably transfected with empty or Metnase knockdown vectors. Values in left graph are averages (±SD) from three experiments; other graphs show data from single experiments. B, C) Cell cycle distributions of HEK-293T or HEK-293 cells, with or with Metnase overexpression, after 18 h treatment with 5 mM HU and release into normal growth medium for indicated times. Values are averages (±SD) of three experiments; * indicates $P < 0.05$, ** indicates $P < 0.01$. D) Cell cycle distributions of HEK-293 cells, with or without Metnase knockdown following HU release. Data presented as in panels B and C.

Table S1. Conserved PIP boxes in Metnase and other human DNA repair/metabolism proteins.

Protein	Function(s)	PIP box*	Reference
Metnase	NHEJ, decatenation, fork restart	(119) VVQKGLQ-FH	(1)
PARP-1	DNA repair, fork restart	(668) PVQDLIKMIF	(2)
DNMT1	DNA methyltransferase	(162) TRQTTITSHF	(3)
DNA Polβ	DNA repair polymerase	(215) VEQLQKV-HF	(4)
p66	DNA polδ subunit	(454) NRQVSITGFF	(5)
MYH	BER glycosylase	(521) MGQQVLDNFF	(6)
UNG2	BER glycosylase	(2) IGQKTLYSFF	(7)
APE2	BER endonuclease	(288) RGQKNLKSYF	(8)
XPB	NER endonuclease	(988) QTQLRIDSFF	(9)
BLM	DNA repair helicase	(81) TNQQRVKDFF	(10)
RECQL5β	DNA repair helicase	(962) EAQN-LIRHF	(10)
p15 PAF	Cell growth promotion	(60) KWQKGIGEFF	(11)
ING1b	Apoptosis	(7) GEQLHLVNY	(12)
MDM2	E3 ubiquitin ligase	(481) PIQMIVLTYF	(13)
WSTF	Chromatin remodeling	(662) LLQDEIAEDY (1024)RYQDIIHSIH (1099)ALQASVIKKF (1432)TEQCLVALLH	(14)
	Consensus PIP box:	[K-A]Qxx-I/L/Vxx(F/Y/H/W)$_2$	(15)

*All proteins have the core PIP Q-I/L/V motif, and nearly all (including Metnase) have the C-terminal pair of F/Y/H residues (shown in red). Many PIP boxes have upstream K and/or A residues; Metnase, and PARP-1 have conservative substitutions (V for A) at this position, indicated in green.

Supplemental References

1. Lee, S.H., Oshige, M., Durant, S.T., Rasila, K.K., Williamson, E.A., Ramsey, H., Kwan, L., Nickoloff, J.A. and Hromas, R. (2005) The SET domain protein Metnase mediates foreign DNA integration and links integration to nonhomologous end-joining repair. *Proc. Natl. Acad. Sci. USA*, **102**, 18075-18080.
2. Frouin, I., Maga, G., Denegri, M., Riva, F., Savio, M., Spadari, S., Prosperi, E. and Scovassi, A.I. (2003) Human proliferating cell nuclear antigen, poly(ADP-ribose) polymerase-1, and p21waf1/cip1. A dynamic exchange of partners. *J. Biol. Chem.*, **278**, 39265-39268.
3. Chuang, L.S., Ian, H.I., Koh, T.W., Ng, H.H., Xu, G. and Li, B.F. (1997) Human DNA-(cytosine-5) methyltransferase-PCNA complex as a target for p21WAF1. *Science*, **277**, 1996-2000.
4. Kedar, P.S., Kim, S.J., Robertson, A., Hou, E., Prasad, R., Horton, J.K. and Wilson, S.H. (2002) Direct interaction between mammalian DNA polymerase beta and proliferating cell nuclear antigen. *J. Biol. Chem.*, **277**, 31115-31123.
5. Ducoux, M., Urbach, S., Baldacci, G., Hubscher, U., Koundrioukoff, S., Christensen, J. and Hughes, P. (2001) Mediation of proliferating cell nuclear antigen (PCNA)-dependent DNA replication through a conserved p21(Cip1)-like PCNA-binding motif present in the third subunit of human DNA polymerase delta. *J. Biol. Chem.*, **276**, 49258-49266.
6. Parker, A., Gu, Y., Mahoney, W., Lee, S.H., Singh, K.K. and Lu, A.L. (2001) Human homolog of the MutY repair protein (hMYH) physically interacts with proteins involved in long patch DNA base excision repair. *J. Biol. Chem.*, **276**, 5547-5555.
7. Otterlei, M., Warbrick, E., Nagelhus, T.A., Haug, T., Slupphaug, G., Akbari, M., Aas, P.A., Steinsbekk, K., Bakke, O. and Krokan, H.E. (1999) Post-replicative base excision repair in replication foci. *EMBO J.*, **18**, 3834-3844.
8. Tsuchimoto, D., Sakai, Y., Sakumi, K., Nishioka, K., Sasaki, M., Fujiwara, T. and Nakabeppu, Y. (2001) Human APE2 protein is mostly localized in the nuclei and to some extent in the mitochondria, while nuclear APE2 is partly associated with proliferating cell nuclear antigen. *Nucleic Acids Res.*, **29**, 2349-2360.
9. Gary, R., Ludwig, D.L., Cornelius, H.L., MacInnes, M.A. and Park, M.S. (1997) The DNA repair endonuclease XPG binds to proliferating cell nuclear antigen (PCNA) and shares sequence elements with the PCNA-binding regions of FEN-1 and cyclin-dependent kinase inhibitor p21. *J. Biol. Chem.*, **272**, 24522-24529.
10. Kanagaraj, R., Saydam, N., Garcia, P.L., Zheng, L. and Janscak, P. (2006) Human RECQ5β helicase promotes strand exchange on synthetic DNA structures resembling a stalled replication fork. *Nucleic Acids Res.*, **34**, 5217-5231.

11. Yu, P., Huang, B., Shen, M., Lau, C., Chan, E., Michel, J., Xiong, Y., Payan, D.G. and Luo, Y. (2001) p15(PAF), a novel PCNA associated factor with increased expression in tumor tissues. *Oncogene*, **20**, 484-489.
12. Scott, M., Bonnefin, P., Vieyra, D., Boisvert, F.M., Young, D., Bazett-Jones, D.P. and Riabowol, K. (2001) UV-induced binding of ING1 to PCNA regulates the induction of apoptosis. *J. Cell Sci.*, **114**, 3455-3462.
13. Banks, D., Wu, M., Higa, L.A., Gavrilova, N., Quan, J., Ye, T., Kobayashi, R., Sun, H. and Zhang, H. (2006) L2DTL/CDT2 and PCNA interact with p53 and regulate p53 polyubiquitination and protein stability through MDM2 and CUL4A/DDB1 complexes. *Cell Cycle*, **5**, 1719-1729.
14. Poot, R.A., Bozhenok, L., van den Berg, D.L., Steffensen, S., Ferreira, F., Grimaldi, M., Gilbert, N., Ferreira, J. and Varga-Weisz, P.D. (2004) The Williams syndrome transcription factor interacts with PCNA to target chromatin remodelling by ISWI to replication foci. *Nat. Cell Biol.*, **6**, 1236-1244.
15. Moldovan, G.L., Pfander, B. and Jentsch, S. (2007) PCNA, the maestro of the replication fork. *Cell*, **129**, 665-679.

6.7. New Techniques Developed for the Laboratory

Adenovirus expressing ISce-I used for HR assays and Chromatin Immunoprecipitation

The adenovirus expressing ISce-I was a kind gift from Kristoffer Valerie [152]**.** The virus was propagated in AD293 cells (Stratagene, La Jolla, CA) using a method adapted from previously described protocols [152-154].

Note: All media used when handling the virus should is warmed to room temperature.

Reagents:

Virus Storage Buffer (2x):

20 mM Tris-HCl pH 8.0

4 mM $MgCl_2$ (FW 203.3)

10% Sucrose

Dilute in PBS

2x Adenovirus Storage buffer:

20 mM Tris-HCl pH 8.0

4 mM $MgCl_2$

Lysis Buffer:

0.1% SDS

10 mM Tris-HCl pH 7.4

1 mM EDTA

Adenovirus Propagation

1. Grow Ad293 cells to ~50% confluence in 20 cm tissue culture dishes (according to manufacturer's instructions). Wash cells with PBS once.

2. Add 5 mL of OptiMEM to cells.

3. Mix virus in 1 mL OptiMEM per plate (10 viruses per cell).

4. Add the virus mixture to the cells and swirl to mix.

5. Incubate at 37°C for 2 h.

6. Add 10 mL of 10% DMEM (do not use antimycotic as this will cause cell death, do not remove virus from the media).

7. Incubate for 3-5 days (usually after 4 days cells will start floating, when >80% of cells are floating virus can be harvested).

Note: It is very important that the space between cells and virus be reduced to a minimum to ensure efficient contact (through diffusion) between virus particles and cells, so adjust the volume of growth medium according to the dimensions of the dish you are using.

Harvesting Viral Particles

1. Harvest cells (remove cells that are attached by flushing with media).
2. Collect cells in a 250 mL bottle (sterilized).
3. Spin at 8000 rpm (7169 x g) for 10 min at 4°C and remove supernatant.
4. Resuspend cell pellet in 8 mL PBS and transfer to a 50 mL conical tube.

5. Freeze at -80°C.

6. Thaw at 37°C and immediately vortex for 30 sec.

7. Freeze in methanol/dry ice bath.

8. Repeat steps 5-6 **four** times.

9. Centrifuge at 3000 rpm (1000 x g) for 30 min at 4°C.

10. Transfer 8 mL of supernatant to a new tube and add 4.4 g of CsCl.

11. Weigh 1 mL of CsCl mixture (it should be ~1.35 g/mL)

12. Adjust density to be 1.35 g/mL by adding CsCl.

13. Centrifuge at 32,000 rpm (22937 x g) at 10°C for 22 h.

14. Remove the viral particle band with 18G needle.

15. Add equal volume of 2x viral storage buffer.

16. Aliquot in a small volume (10 µL) and store at -80°C.

Determination of virus concentration by OD_{260} reading:

Conversion factor: 1.1×10^{12} viral particles/OD_{260}. Quantification was done using the protocol outlined in AdEasy vector system manual by Quantum Biotechnologies (Qbiogene, Carlsbad, CA). This protocol routinely produces virus titers of 3×10^{9} viral particles/µL.

Adenovirus Infection for Creating an ISce-I DSB

In order to use the Ad-ISce-I to create a DSB, one must use cells that have an engineered ISce-I site already, for example HT256 cells, or HT1080-1904 (see Appendix for more details and references).

1. Wash cells with PBS once.
2. Add 5 mL of OptiMEM to cells. It is very important that the space between cells and floating virus be reduced to a minimum to ensure efficient contact (through diffusion) between virus particles and cells. Therefore, adjust the volume of media according to the dimensions of the dish you are using (i.e., use 1 ml of OptiMEM for a 10 cm dish and 5 mL for a 20 cm dish).
3. Mix virus in an appropriate volume of virus dilution buffer to achieve a multiplicity of infection (MOI) of 100-1000 virus particles per cell.
4. Add the virus mixture to the cells and swirl to mix.
5. Incubate at 37°C for 3 h when infecting CHO or HT1080 cells (incubation times may need to be adjusted to suit specific cell lines).
6. Remove media and add fresh growth medium to cells. Incubate overnight to allow cells to recuperate.
7. Cells are ready for manipulation (i.e. electroporation, drug treatment, homologous recombination assay, chromatin immunoprecipitation, etc.)

Note: Allow only 1-2 freeze-thaw cycles of the virus stocks. DO NOT store virus in OptiMEM, store in virus storage buffer.

Results

Ad ISce-I does not affect plating efficiency of human cells and is a useful tool for homologous recombination assays

HT1080-1885 cells contain a single ISce-I site within the neomycin gene and have been engineered to measure HR (described in more detail in [155]). HT1080-1885 cells were infected with the ISce-I containing adenovirus at 100 and 1000 multiplicity of infection (MOI) for 3 h. After the infection period cells were counted, plated (500 cells), and allowed to form colonies for 7 days. The plating efficiency was calculated by dividing the number of colonies formed by the number of cells plated, and converting it to percentage values. Results in figure 3-1A show that the plating efficiency did not vary between the no virus control and the control virus (beta-galactosidase containing adenovirus), demonstrating that the adenovirus alone does not affect colony formation ability. The plating efficiency of cells infected with Ad-ISce-I was slightly lower than the two controls; however, this difference was not statistically significant. Nonetheless, this difference could indicate that the Ad-ISce-I affects colony formation ability of cells; however, neither the virus nor single DSB have an effect on colony formation. We tested whether Ad-ISce-I could be effectively used for the HR assay, and Figure 3-1B represents an example of results obtained. Results showed that indeed Ad-ISce-I gives comparable results to using plasmid ISce-I as compared to HR frequency values obtained using ISce-I from a plasmid [155-158]. Furthermore, the HR frequency increased as the MOI

is increased. This is a valuable new tool to use in the HR assay since there is minimal cell killing compared to other methods such as electroporation or lipofectamine infection, and it yields similar results in the HR assay. Chinese Hamster Ovary (CHO 33) cells, engineered to contain the ISce-I site, had similar results to the 1885 cells (Figure 3-2), and the HR frequency was comparable to previously obtained values [159]. There were two important differences between the 1885 cells and the CHO33 cells; however, in the CHO33 cells the plating efficiency significantly decreased as the viral MOI is increased, and the DSB-induced HR frequency was only detected at an MOI of 1000. The requirement for a higher MOI with CHO cells is consistent with the fact that CHO cells express fewer adenovirus receptors than human cells [160].

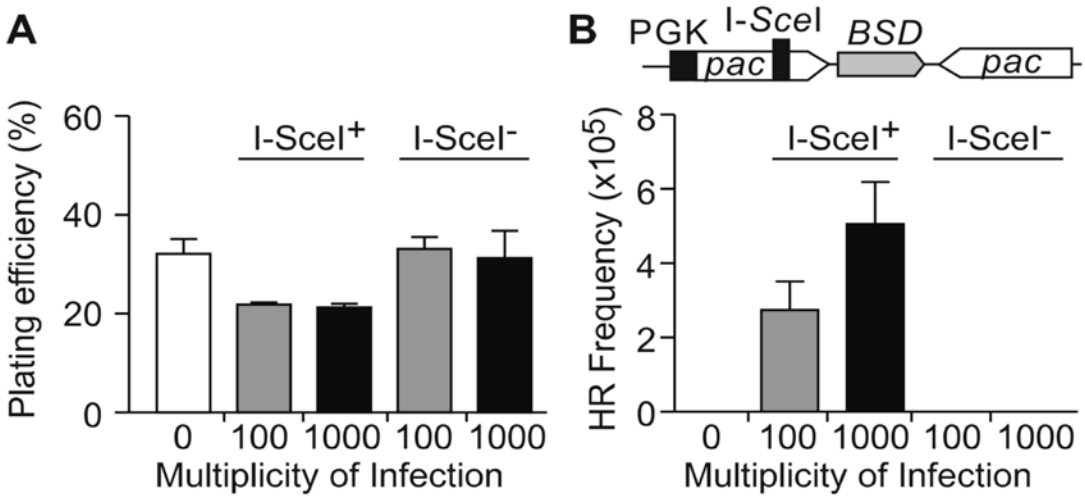

Figure 6.7-1. Ad-ISce-I does not affect plating efficiency in human cells and is a useful tool in HR assays.

(A) Plating efficiency of HT1080-1885. PE was calculated as the number of colonies formed divided by the number of cells plated, times 100. (B) HR assay done in HT1080-1885 cells. HR frequencies were determined by dividing the number of puromycin resistant colonies (reflects HR), divided by the number of cells plated times the PE. Cells were treated with no virus, Ad-ISce-I (I+), or Ad-βgal (I-). 100 and 1000 MOI Ad-ISce-I were used. Values represent averages (±SD) for three independent experiments.

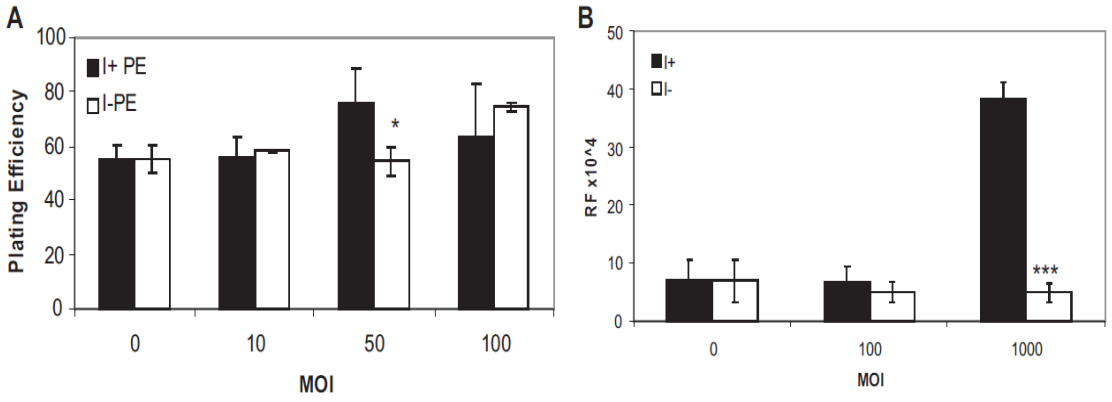

Figure 6.7-2. Ad-ISce-I does not affect plating efficiency in Chinese hamster ovary (CHO) cells.

(A) Plating efficiency of CHO-33 cells. PE was calculated as the number of colonies formed divided by the number of cells plated, times 100. (B) Homologous recombination assay done in CHO-33 cells. HR frequency was determined by taking the number of colonies selected, divided by the number of cells plated times the PE. Cells were treated with no virus, Ad-ISce-I (I+), or Ad-βgal (I-), 100 and 1000 MOI Ad-ISce-I were used, represent three independent experiments, *p<0.05,***p<0.001 (t-test).

Ad-ISce-I rapidly induces DSBs into the ISce-I site

In order to test whether the Ad-ISce-I would be an effective tool to use to detect recruitment of proteins to a DSB site, we first tested its ability to form a cut at the ISce-I site. We used quantitative PCR (qPCR) to amplify a 200 bp product using primers homologous to sequences on either side of the ISce-I site. In the presence of an intact ISce-I site, a qPCR product can be amplified. However, when the site has been cut, there is no amplification. Therefore, we measured the disappearance of the qPCR product and interpreted it as “cutting” at the ISce-I site. For more details on the specific primers used and the qPCRF conditions please consult Appendix 6.4. We measured the disappearance of the 200 bp product that amplifies across the ISce-I break site in CHO33 and HT1080 cell lines (Figure 2.3). At six hours post infection, we observed more than 60% ISce-I cutting in CHO33 cells and HT1080-1885 cells. Additionally, the human HT1080-1885 cell line required a higher MOI for cutting as compared to the CHO cells. These results have been repeated in other cell lines such as HT1080-1904 (a HT1080 derivative containing an ISce-I substrate with puromycin selection marker), with similar results (Appendix 6.4). Thus, these results demonstrate that the Ad-ISce-I virus can be used as a tool to create efficient DSB formation at a defined recognition site using qPCR. Rapid, efficient, and reproducible cutting, with minimal side effects to cells is necessary to study recruitment of proteins to DSB sites in response to a break. Ad-ISce-I allows us to measure recruitment of repair proteins, via ChIP, within minutes of a break occurring. Using this system we have detected early protein recruitment,

studied the kinetics of recruitment, determined how close (how many bases or kb) away from the break site the proteins have localized, and have asked whether post-translational modifications affect protein recruitment to a break site. Specifically, we have used this tool to study how Metnase affects recruitment of proteins in the NHEJ pathway to a DSB site (Appendix 6.4).

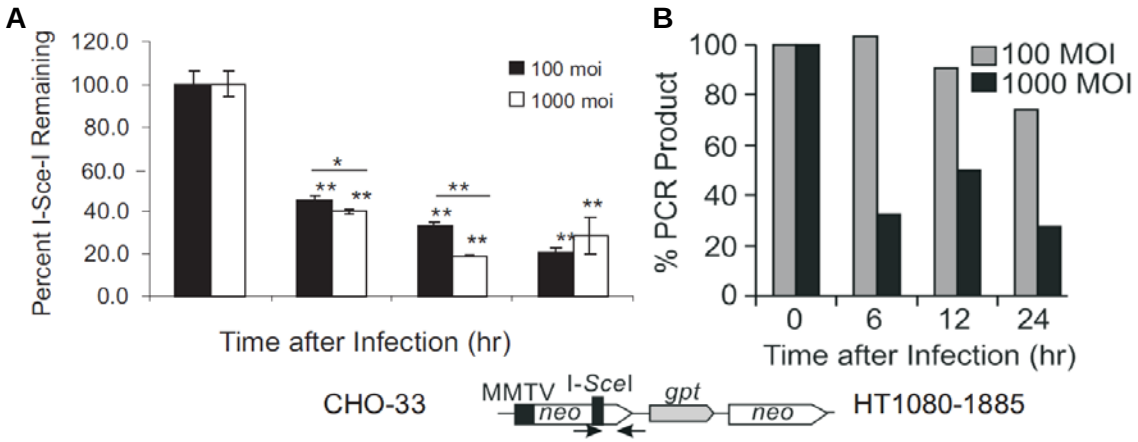

Figure 6.7-3. Ad-ISce-I cuts ISce-I site rapidly and effectively.

(A) CHO-33 cells and (B) HT1080-1885 cells. Percent PCR product remaining after infection by Ad-ISce-I at 100 or 1000 MOI, results normalized to GAPDH (internal control). Representative of three independent experiments, each done in triplicate, *p<0.05, **p<0.0001 (t-test).

Next, we tested whether Ad-ISce-I infection would have an effect on cell cycle progression, since many DNA damage response pathways are regulated during the cell cycle. To test whether Ad-ISce-I affects the cell cycle we conducted two experiments. The first was a Ad-ISce-I dose response experiment to test if higher MOI would affect cell cycle. The second experiment was a time course after adenovirus infection, to test whether the virus would have an effect on cell cycle progression over time. We infected CHO33 and HT1080-1885 cells with Ad-ISce-I or Ad-βgal (an adenovirus containing the same DNA as Ad-ISce-I, but carrying a β-gal gene instead of the ISce-I) control for a period of up to 96 hours and stained cells for flow cytometry analysis as described in section 3.1. The results, shown in Figure 3-4, revealed that Ad-ISce-I infection did not have a significant effect on cell cycle progression even at the highest viral titer of 1000 MOI in both cell lines tested. Therefore Ad-ISce-I is a useful tool for studying DNA repair pathways since the infection by the virus alone does not alter the cell cycle. However, these observations are limited to the cell lines currently tested. When using this system in other cell lines, it will be important to repeat these experiments and determine the optimal MOI to use for each cell line.

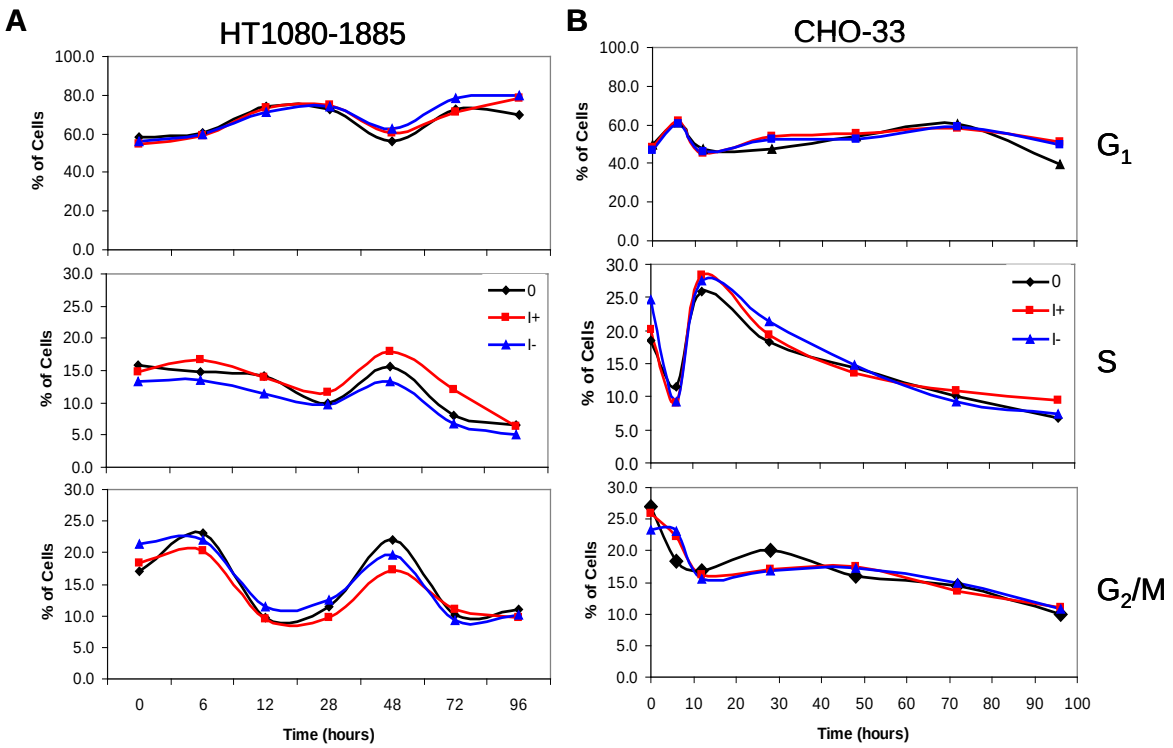

Figure 6.7-4. Ad-ISce-I does not affect cell cycle progression in human and hamster cells.

Cell cycle profiles of human cell line HT1080-1885 (A) and Chinese hamster ovary (CHO-33) (B) in response to 100 MOI Ad-ISce-I over time. Results are representative of two different experiments, 0= control without virus, I+ = Ad-ISce-I virus, I- = Ad-βgal (control).

DNA Fiber Analysis

The DNA fiber analysis was developed originally by Parra and Windle [161]. Merrick and colleagues [162] used this method to label ongoing replication forks *in vivo*. I developed it further by adapting the procedure used by the Aladjem lab [130] and Pommier laboratories [163]. DNA fiber analysis was used to monitor DNA synthesis, by analyzing the incorporation of two 5-bromo-2-deoxyuridine (BrdU) analogs, 5-iodo-2-deoxyuridine (IdU) and 5-chloro-2-deoxyuridine (CldU), both of which are nucleoside analogs of thymidine. The analogs are given sequentially, one is added, then a treatment that causes replication fork stress or damage is given (typically 5 mM HU, which causes nucleotide pools to be depleted), and then the other analog is added. Then the DNA fibers are stretched as described in methods and the DNA is labeled with primary and secondary-fluorescent antibodies against the analogs, and finally visualized using a confocal microscope. The images obtained can be analyzed in several ways. For example, one can measure the percentage of a type of fiber, and determine whether forks were started, stopped, or continued after a certain treatment that stresses replication forks (HU in this study). Fiber length can also be measured using image analysis software (such as ImageJ), and the nucleotide incorporation rate can be determined (see Fig 2.5). However, this method has its limitations. Technically, the background fluorescence needs to be eliminated by a series of optimization experiments. One should always include in the experiments a control where each of the labeling dyes is given alone, in order to assess background binding of the antibodies, tested by using IdU but

only adding CldU antibodies and vice versa. Control experiments leaving out primary or secondary antibodies should be done every time a new cell line is being optimized and every time a new antibody batch is started. Additionally, one should never incubate the antibodies together, especially the primary antibodies, since they are both BrdU specific and can recognize both labeling dyes (IdU and CldU). Technically, this method has the limitation that the labeling is time dependent, thus a short fiber could indicate a slow incorporation rate or a stalled fork. Additionally, this method does not allow for distinctions between a stalled and a collapsed fork although in combination with other types of experiments, such as H2AX foci formation, this information can be discerned.

Reagents
10 mM IdU
10 mM CIdU
PBS
70 % ethanol
100 % methanol
2.5 N HCl
5 % BSA in PBS
PBS-T (Triton 0.1 %)
DAPI (optional)
100 µM Thymidine
Mounting medium: PermaFluor™ aqueous mounting medium, self-sealing (Thermoscientific cat #: TA-030-FM)
Positively charged slides (Daigger supperfrost/plus microslides, frosted cat# G15978Z)
Microscope cover slides (VWR micro cover glass 24 x 50 mm cat# 48393 241)

SDS-Lysis Buffer:
0.5% SDS
200 mM Tri-HCl (pH 7.4)
50mM EDTA

Antibodies:
Mouse anti-BrdU (1:50) for IdU (BD Biosciences cat # 347580)
Rat anti-BrdU (1:100) for CldU (Accuratechemical cat # OBT0030)

Day 1: (Perform the following steps in the dark or under low light)

1. Grow cells in 10 mm culture dishes (or 6 well plates).
2. Add 20 μM IdU (final concentration) to growth media, mix and incubate for 10 min at 37°C.
3. Remove growth media and wash cells with PBS two times.
4. Add 100 μM thymidine for 1 min to wash out the IdU before incubation with the CldU nucleotide analog.
5. Wash cells with PBS.
6. Add complete growth medium.
7. Add the treatment drug (i.e., 5 mM HU for 1-6 h or mock treat controls).
8. Remove media and wash cells twice with PBS.
9. Add 20 μM CldU and incubate cells for 20 min at 37°C.
10. Remove media and wash once with PBS.
11. Harvest cells by trypsinization, spin cells at 1000 rpm (112 x g) for 5 min at 4°C, wash once with PBS. Resuspend cells in 1.5 mL of PBS and determine cell concentration using a hemocytometer.
12. Transfer cells to a new eppendorf tube, spin down cells for 5 min at 5,000 rpm (2800 x g) at 4°C.
13. Add PBS to make a final concentration of 1-2 $x10^6$ cell/mL. Cells may be stored at 4°C overnight (do not store more than 2 days as the cells will lyse and the DNA will not spread properly or at all).

14. Add 2 µL of cell sample to the top of the slide lying horizontally (not more than 2,500 cells).
15. Add 6 µL of SDS lysis buffer and immediately pipette mixture up, down 5-6 times, and stir to spread gently with the same tip (avoid creating bubbles).
16. Incubate for 5-8 min (3 min in low humidity climates).
17. Tilt the slide at an angle such that the droplet reaches the bottom of the slide in at least 30 sec. (figure 3-5).
18. Cover slides with aluminum foil and air dry for 8 min at room temperature
19. Fix with 3:1 methanol: acetic acid (prepared fresh) for 5 min.
20. Dry the slides for 8 min and store in 70% EtOH at 4°C overnight

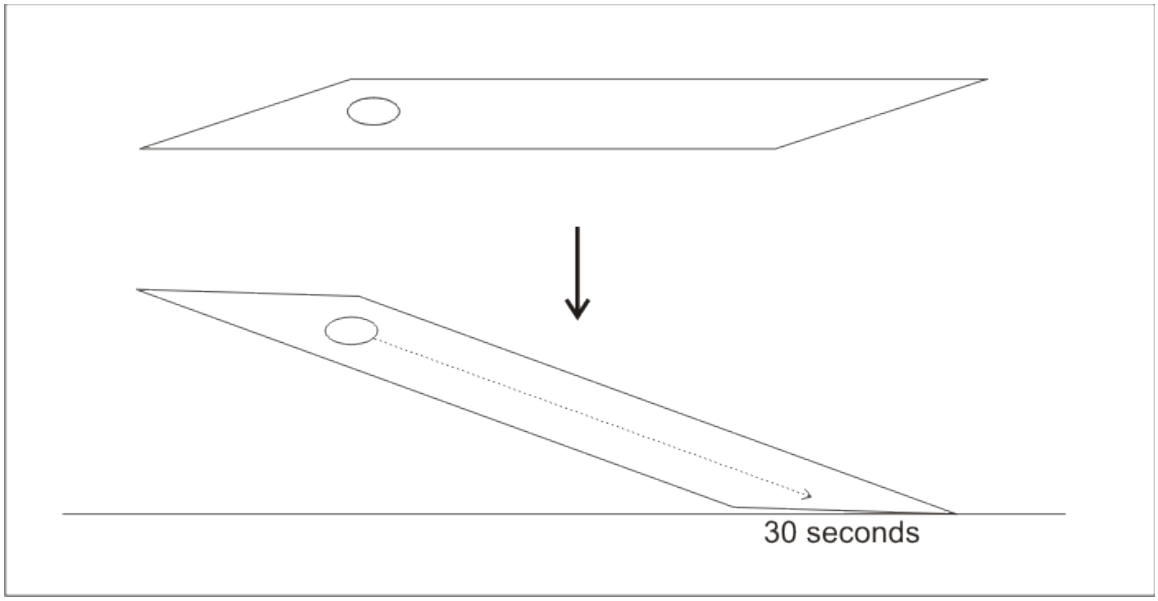

Figure 6.7-5. Diagram of "dropping" DNA on a slide for Fiber Assay.

The DNA should be put on a slide toward one of the short edges. Raise one end of the slide so that the DNA droplet can slide down and reach the bottom in not less than 30 sec. The DNA should be spread down the middle of the slide as much as possible as this will facilitate microscopy.

Day 2: (Perform the following steps under low, indirect light)

1. Incubate slides in 100% MeOH at room temperature for 5 min.
2. Wash twice with PBS for 5 min each.
3. Add 150 µL of 2.5 N HCl to each slide, cover with parafilm and incubate at 37°C in a wet box for 1 h (a wet box can be constructed from an empty plastic pipette tip box with the bottom covered with a wet paper towel, this prevents the slides from drying).
4. Wash twice with PBS for 5 min each.
5. Add 150 µL of 5% BSA to each slide, cover slides and incubate at 37°C in a wet box for 15 min.
6. Wash with PBS once.
7. Add 150 µL mouse anti-BrdU (1:50 dil. in 0.5 % BSA in PBS) to detect IdU, incubate at 37°C for 1 h.
8. Wash slide three times with PBS-0.1 % Triton for 3-5 min, then rinse with PBS.
9. Add 150 µL goat anti-mouse Alexa 568 (1:100 in 0.5 % BSA in PBS); incubate at 37°C for 1 h.
10. Wash slide three times with PBS-0.1% Triton for 3-5 min each, then rinse with PBS.
11. Add 150 µL rat anti-BrdU (1:100, 0.5 % BSA in PBS) to detect CIdU; incubate at 37°C for 1 h.
12. Wash slide three times with PBS-0.1% Triton for 3-5 min, then rinse with PBS.

13. Add 150 µL donkey anti-rat Alexa 488 (1:100 in 0.5 % BSA in PBS) to detect CIdU; incubate at 37°C for 1 h.
14. Wash slide three times with PBS-0.1% Triton for 3-5 min, then rinse with PBS.
15. Stain slides with DAPI (125 µg/mL in PBS), incubate at R.T. for 1h (this is optional because DAPI staining is not always visible in the microscope).
16. Wash twice with PBS for 5 min each.
17. Add 25 µL of mounting medium (without DAPI) and cover with a cover slip.
18. Allow the slides to dry overnight in the dark and store at 4°C overnight or until ready to visualize with a microscope (slides can be stored for ~6 months without significant degradation of the fluorescent signals).
19. Image DNA fibers with a confocal microscope at 63x magnification (oil immersion).

Notes:

1. It is very important that the protocol be followed mostly under dark or low indirect light conditions because the labeling dyes are light sensitive.
2. Do not alter the order of antibody or incubation times because both antibodies used are BrdU specific and can recognize both dyes. The order specified in this protocols gives optimal results.

3. Do not spread more than 2,500 cells per slide because more cells means more DNA and that will result in fibers grouping and spreading together and will not be quantifiable.
4. At step 13 of Day 1, cells can only be stored overnight, not for several days as the cell will lyse and no fibers can be obtained.
5. DNA fibers are best visualized with a confocal microscope with 40x or 63x magnification, 100x magnification is not required or necessary.
6. Optimize microscope settings to minimize bleed-through and to maximize resolution of the fibers. Consult microscope manuals to learn how to do optimization.

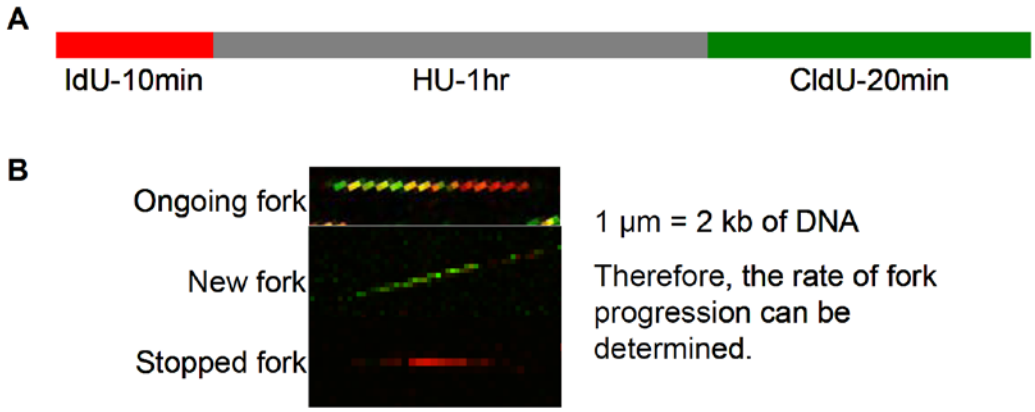

Figure 6.7-6. Diagram of DNA fiber technique and example of a result.

(A) Diagram of the time course of nucleotide analog labeling. (B) Confocal microscopy image examples of DNA fibers. An ongoing fork is a fork that started incorporating analogs during the first step of the process (IdU) and can be seen as a fiber with a combination of red, green, and yellow (overlap of both analogs). A new fork is seen as only green fibers because it only incorporated the second analog (CldU). A stopped fork is seen as only red, as it incorporated the first analog (IdU), but failed to incorporate the second (CldU). One µm in fiber length is the equivalent of 2 kb of DNA; therefore, the DNA replication fork rate can be calculated by converting the length of a fiber to kilobases and dividing that number by the number of minutes the DNA was exposed to the labeling analog, providing a rate in kb/min.

7. REFERENCES

1. Jemal, A., et al., *Cancer Statistics, 2009.* CA a Cancer Journal for Clinitians, 2009. **59**(4): p. 225-249.
2. Jemal, A., et al., *Cancer occurrence.* Methods Mol Biol, 2009. **471**: p. 3-29.
3. Jemal, A., et al., *Cancer statistics, 2008.* CA Cancer J Clin, 2008. **58**(2): p. 71-96.
4. Jemal, A., et al., *Cancer statistics, 2007.* CA Cancer J Clin, 2007. **57**(1): p. 43-66.
5. Hao, Y., et al., *U.S. congressional district cancer death rates.* Int J Health Geogr, 2006. **5**: p. 28.
6. *US Census Bureau*. 2000.
7. Marte, B., *Lack of Principles.* Nature Milestones Cancer, 2006. **1**(1): p. S8-S9.
8. Schimke, R.T., et al., *Gene amplification and drug resistance in cultured murine cells.* Science, 1978. **202**(4372): p. 1051-5.
9. Eggleston, A.E., *Indirect but just as effective.* Nature Milestones Cancer, 2006. **1**(1): p. S21-S22.
10. Knudson, A.G., Jr., *Mutation and cancer: statistical study of retinoblastoma.* Proc Natl Acad Sci U S A, 1971. **68**(4): p. 820-3.
11. Nordling, C.O., *A new theory on cancer-inducing mechanism.* Br J Cancer, 1953. **7**(1): p. 68-72.
12. Pulverer, B., *Cell cycle and DNA damage checkpoints.* Nature Milestones Cancer, 2006. **1**(1): p. S20.
13. Buchkovich, K., L.A. Duffy, and E. Harlow, *The retinoblastoma protein is phosphorylated during specific phases of the cell cycle.* Cell, 1989. **58**(6): p. 1097-105.
14. Kuerbitz, S.J., et al., *Wild-type p53 is a cell cycle checkpoint determinant following irradiation.* Proc Natl Acad Sci U S A, 1992. **89**(16): p. 7491-5.
15. Kastan, M.B., et al., *A mammalian cell cycle checkpoint pathway utilizing p53 and GADD45 is defective in ataxia-telangiectasia.* Cell, 1992. **71**(4): p. 587-97.
16. Kastan, M.B., et al., *Participation of p53 protein in the cellular response to DNA damage.* Cancer Res, 1991. **51**(23 Pt 1): p. 6304-11.
17. Juang, S.H., et al., *D-501036, a novel selenophene-based triheterocycle derivative, exhibits potent in vitro and in vivo antitumoral activity which involves DNA damage and ataxia telangiectasia-mutated nuclear protein kinase activation.* Mol Cancer Ther, 2007. **6**(1): p. 193-202.
18. Paques, F. and J.E. Haber, *Multiple pathways of recombination induced by double-strand breaks in Saccharomyces cerevisiae.* Microbiol. Mol. Biol. Rev., 1999. **63**: p. 349-404.

19. Franco, S., F.W. Alt, and J.P. Manis, *Pathways that suppress programmed DNA breaks from progressing to chromosomal breaks and translocations.* DNA Repair (Amst), 2006. **5**(9-10): p. 1030-41.
20. Chaudhuri, J., et al., *Evolution of the immunoglobulin heavy chain class switch recombination mechanism.* Adv Immunol, 2007. **94**: p. 157-214.
21. Neale, M.J. and S. Keeney, *Clarifying the mechanics of DNA strand exchange in meiotic recombination.* Nature, 2006. **442**(7099): p. 153-8.
22. Deming, P.B., et al., *The human decatenation checkpoint.* Proc Natl Acad Sci U S A, 2001. **98**(21): p. 12044-9.
23. Ward, J., *The nature of lesions formed by ionizing radiation*, in *DNA Damage and Repair: DNA Repair in Higher Eukaryotes*, J.A. Nickoloff and M.F. Hoekstra, Editors. 1998, Humana Press: Totowa, NJ. p. 65-84.
24. Limoli, C.L., et al., *UV-induced replication arrest in the xeroderma pigmentosum variant leads to DNA double-strand breaks, γ-H2AX formation, and Mre11 relocalization.* Proc. Natl. Acad. Sci. USA, 2002. **99**(1): p. 233-8.
25. Bosco, E.E., et al., *RB signaling prevents replication-dependent DNA double-strand breaks following genotoxic insult.* Nucleic Acids Res, 2004. **32**(1): p. 25-34.
26. Degrassi, F., M. Fiore, and F. Palitti, *Chromosomal aberrations and genomic instability induced by topoisomerase-targeted antitumour drugs.* Curr Med Chem Anticancer Agents, 2004. **4**(4): p. 317-25.
27. Ahnesorg, P., P. Smith, and S.P. Jackson, *XLF interacts with the XRCC4-DNA ligase IV complex to promote DNA nonhomologous end-joining.* Cell, 2006. **124**(2): p. 301-13.
28. Andreassen, P.R., G.P. Ho, and A.D. D'Andrea, *DNA damage responses and their many interactions with the replication fork.* Carcinogenesis, 2006. **27**(5): p. 883-92.
29. Damelin, M. and T.H. Bestor, *The decatenation checkpoint.* Br J Cancer, 2007. **96**(2): p. 201-5.
30. Keogh, M.C., et al., *A phosphatase complex that dephosphorylates γH2AX regulates DNA damage checkpoint recovery.* Nature, 2006. **439**(7075): p. 497-501.
31. Huang, C.H. and J. Treat, *New advances in lung cancer chemotherapy: topotecan and the role of topoisomerase I inhibitors.* Oncology, 2001. **61 Suppl 1**: p. 14-24.
32. Kurose, A., et al., *Assessment of ATM phosphorylation on Ser-1981 induced by DNA topoisomerase I and II inhibitors in relation to Ser-139-histone H2AX phosphorylation, cell cycle phase, and apoptosis.* Cytometry A, 2005. **68**(1): p. 1-9.
33. Kim, H., et al., *Reversible cigarette smoke extract-induced DNA damage in human lung fibroblasts.* Am J Respir Cell Mol Biol, 2004. **31**(5): p. 483-90.

34. Collier, A.C., et al., *Differences in DNA-damage in non-smoking men and women exposed to environmental tobacco smoke (ETS).* Toxicol Lett, 2005. **158**(1): p. 10-9.
35. Lee, C.P., et al., *Epstein-Barr virus BGLF4 kinase induces premature chromosome condensation through activation of condensin and topoisomerase II.* J Virol, 2007. **81**(10): p. 5166-80.
36. Bakkenist, C.J. and M.B. Kastan, *DNA damage activates ATM through intermolecular autophosphorylation and dimer dissociation.* Nature, 2003. **421**(6922): p. 499-506.
37. Shrivastav, M., L.P. De Haro, and J.A. Nickoloff, *Regulation of DNA double-strand break repair pathway choice.* Cell Res, 2008. **18**(1): p. 134-47.
38. Enomoto, T., *Functions of RecQ family helicases: Possible involvement of Bloom's and Werner's syndrome gene products in guarding genome integrity during DNA replication.* J. Biochem., 2001. **29**: p. 501-507.
39. Bloom, D., *Congenital telangiectatic erythema resembling lupus erythematosus in dwarfs; probably a syndrome entity.* AMA Am J Dis Child, 1954. **88**(6): p. 754-8.
40. Wang, D. and S.J. Lippard, *Cisplatin-induced post-translational modification of histones H3 and H4.* J. Biol. Chem., 2004. **279**(20): p. 20622-5.
41. Wang, S., et al., *The catalytic subunit of DNA-dependent protein kinase selectively regulates p53-dependent apoptosis but not cell-cycle arrest.* Proc. Natl. Acad. Sci. USA, 2000. **97**: p. 1584-1588.
42. Wu, L., et al., *The Bloom's syndrome gene product interacts with topoisomerase III.* J. Biol. Chem., 2000. **275**(13): p. 9636-9644.
43. Karow, J.K., et al., *The Bloom's syndrome gene product promotes branch migration of Holliday junctions.* Proc. Natl. Acad. Sci. USA, 2000. **97**: p. 6504-6508.
44. Shen, J.C., et al., *Werner syndrome protein I. DNA helicase and DNA exonuclease reside on the same polypeptide.* J. Biol. Chem., 1998. **273**: p. 34139-34144.
45. Huang, P., *Excision of mismatched nucleotides from DNA: a potential mechanism for enhancing DNA replication fidelity by the wild-type p53 protein.* Oncogene, 1998. **17**(#3): p. 261-270.
46. Huang, S.R., et al., *Characterization of the human and mouse WRN 3'*arrow5' exonuclease.* Nucleic Acids Res., 2000. **28**(12): p. 2396-2405.
47. Suzuki, K., *Multistep nature of x-ray-induced neoplastic transformation in mammalian cells: genetic alterations and instability.* J. Radiat. Res., 1997. **38**(#1): p. 55-63.
48. Constantinou, A., et al., *Werner's syndrome protein (WRN) migrates Holliday junctions and co-localizes with RPA upon replication arrest.* EMBO Reports, 2000. **1**: p. 80-84.

49. Girard, P.M., et al., *Radiosensitivity in Nijmegen Breakage syndrome cells is attributable to a repair defect and not cell cycle checkpoint defects.* Cancer Res., 2000. **60**(#17): p. 4881-4888.
50. Wang, L., R. Wang, and K. Herrup, *E2F1 works as a cell cycle suppressor in mature neurons.* J Neurosci, 2007. **27**(46): p. 12555-64.
51. Dokal, I., *Fanconi's anaemia and related bone marrow failure syndromes.* Br Med Bull, 2006. **77-78**: p. 37-53.
52. Wang, L., S.K. Roy, and D.A. Eastmond, *Differential cell cycle-specificity for chromosomal damage induced by merbarone and etoposide in V79 cells.* Mutat Res, 2007. **616**(1-2): p. 70-82.
53. Moynahan, M.E., T.Y. Cui, and M. Jasin, *Homology-directed DNA repair, mitomycin-C resistance, and chromosome stability is restored with correction of a Brca1 mutation*

Cancer Res., 2001. **61**: p. 4842-4850.
54. Zhong, Q., et al., *Deficient nonhomologous end-joining activity in cell-free extracts from Brca1-null fibroblasts.* Cancer Res., 2002. **62**: p. 3966-3970.
55. Zhong, Q., et al., *BRCA1 facilitates microhomology-mediated end joining of DNA double strand breaks.* J. Biol. Chem., 2002. **277**: p. 28641-28647.
56. Yuan, S.S.F., et al., *BRCA2 is required for ionizing radiation-induced assembly of RAD51 complex in vivo.* Cancer Res., 1999. **59**: p. 3547-3551.
57. Moynahan, M.E., A.J. Pierce, and M. Jasin, *BRCA2 is required for homology-directed repair of chromosomal breaks.* Mol. Cell, 2001. **7**(#2): p. 263-272.
58. Xia, F., et al., *Deficiency of human BRCA2 leads to impaired homologous recombination but maintains normal nonhomologous end joining.* Proc. Natl. Acad. Sci. USA, 2001. **98**: p. 8644-8649.
59. Larminat, F., et al., *Deficiency in BRCA2 leads to increase in non-conservative homologous recombination.* Oncogene, 2002. **21**(33): p. 5188-92.
60. Powell, S.N., H. Willers, and F. Xia, *BRCA2 keeps Rad51 in line: high-fidelity homologous recombination prevents breast and ovarian cancer?* Mol. Cell, 2002. **10**: p. 1262-1263.
61. Yang, H., et al., *BRCA2 function in DNA binding and recombination from a BRCA2-DSS1-ssDNA structure.* Science, 2002. **297**: p. 1837-1848.
62. Bork, P., et al., *A superfamily of conserved domains in DNA damage responsive cell cycle checkpoint proteins.* FASEB Journal, 1997. **11**: p. 68-76.
63. Teer, J.K., et al., *Proliferating human cells hypomorphic for origin recognition complex 2 and pre-replicative complex formation have a defect in p53 activation and Cdk2 kinase activation.* J Biol Chem, 2006. **281**(10): p. 6253-60.
64. Yu, Q., et al., *Antisense inhibition of Chk2/hCds1 expression attenuates DNA damage-induced S and G2 checkpoints and enhances apoptotic activity in HEK-293 cells.* FEBS Lett., 2001. **505**: p. 7-12.

65. Ahn, J.Y., et al., *Phosphorylation of threonine 68 promotes oligomerization and autophosphorylation of the Chk2 protein kinase via the forkhead-associated (FHA) domain.* J. Biol. Chem., 2002. **277**: p. 19389-19395.
66. Xu, X., L.M. Tsvetkov, and D.F. Stern, *Chk2 activation and phosphorylation-dependent oligomerization.* Mol. Cell. Biol., 2002. **22**: p. 4419-4432.
67. Chen, Y. and R.Y. Poon, *The multiple checkpoint functions of CHK1 and CHK2 in maintenance of genome stability.* Front Biosci, 2008. **13**: p. 5016-29.
68. Blasina, A., et al., *Caffeine inhibits the checkpoint kinase ATM.* Curr. Biol., 1999. **9**(19): p. 1135-8.
69. Bolderson, E., et al., *ATM is required for the cellular response to thymidine induced replication fork stress.* Hum. Mol. Genet., 2004. **13**(23): p. 2937-45.
70. Hickson, I., et al., *Identification and characterization of a novel and specific inhibitor of the ataxia-telangiectasia mutated kinase ATM.* Cancer Res., 2004. **64**(24): p. 9152-9.
71. Rodriguez, R. and M. Meuth, *Chk1 and p21 cooperate to prevent apoptosis during DNA replication fork stress.* Mol Biol Cell, 2006. **17**(1): p. 402-12.
72. Stiff, T., et al., *ATR-dependent phosphorylation and activation of ATM in response to UV treatment or replication fork stalling.* Embo J, 2006. **25**(24): p. 5775-82.
73. Girard, P.M., et al., *Nbs1 promotes ATM dependent phosphorylation events including those required for G1/S arrest.* Oncogene, 2002. **21**: p. 4191-4199.
74. Zhang, Y., et al., *NBS1 knockdown by small interfering RNA increases ionizing radiation mutagenesis and telomere association in human cells.* Cancer Res., 2005. **65**(13): p. 5544-53.
75. Lebel, M., et al., *The Werner syndrome gene product co-purifies with the DNA replication complex and interacts with PCNA and topoisomerase I.* J Biol Chem, 1999. **274**(53): p. 37795-9.
76. Cooper, M.P., et al., *Ku complex interacts with and stimulates the Werner protein.* Genes Dev., 2000. **14**(#8): p. 907-912.
77. Kamath-Loeb, A.S., et al., *Functional interaction between the Werner Syndrome protein and DNA polymerase delta.* Proc Natl Acad Sci U S A, 2000. **97**(9): p. 4603-8.
78. Li, B.M. and L. Comai, *Functional interaction between Ku and the Werner syndrome protein in DNA end processing.* J. Biol. Chem., 2000. **275**(#37): p. 28349-28352.
79. Pichierri, P., et al., *Werner's syndrome cell lines are hypersensitive to camptothecin-induced chromosomal damage.* Mutat Res, 2000. **456**(1-2): p. 45-57.

80. Brosh, R.M., et al., *Werner syndrome protein interacts with human flap endonuclease 1 and stimulates its cleavage activity.* EMBO J., 2001. **20**(20): p. 5791-5801.
81. Prince, P.R., M.J. Emond, and R.J. Monnat, *Loss of Werner syndrome protein function promotes aberrant mitotic recombination.* Genes Dev., 2001. **15**: p. 933-938.
82. Yannone, S.M., et al., *Werner syndrome protein is regulated and phosphorylated by DNA-dependent protein kinase.* J. Biol. Chem., 2001. **276**(41): p. 38242-38248.
83. Karmakar, P., et al., *Werner protein is a target of DNA-dependent protein kinase in vivo and in vitro, and its catalytic activities are regulated by phosphorylation.* J. Biol. Chem., 2002. **277**(21): p. 18291-18302.
84. Oshima, J., et al., *Lack of WRN results in extensive deletion at nonhomologous joining ends.* Cancer Res., 2002. **62**(2): p. 547-551.
85. Rodriguez-Lopez, A.M., et al., *Asymmetry of DNA replication fork progression in Werner's syndrome.* Aging Cell, 2002. **1**(1): p. 30-9.
86. Saintigny, Y., et al., *Homologous recombination resolution defect in Werner syndrome.* Mol. Cell. Biol., 2002. **22**: p. 6971-6978.
87. Baynton, K., et al., *WRN interacts physically and functionally with the recombination mediator protein RAD52.* J Biol Chem, 2003. **278**(38): p. 36476-86.
88. Franchitto, A., J. Oshima, and P. Pichierri, *The G2-phase decatenation checkpoint is defective in Werner syndrome cells.* Cancer Res, 2003. **63**(12): p. 3289-95.
89. Pichierri, P., F. Rosselli, and A. Franchitto, *Werner's syndrome protein is phosphorylated in an ATR/ATM-dependent manner following replication arrest and DNA damage induced during the S phase of the cell cycle.* Oncogene, 2003. **22**(10): p. 1491-500.
90. Romanova, L.Y., et al., *The interaction of p53 with replication protein A mediates suppression of homologous recombination.* Oncogene, 2004. ***in press**.
91. Mohaghegh, P., et al., *The Bloom's and Werner's syndrome proteins are DNA structure-specific helicases.* Nucleic Acids Res., 2001. **29**(13): p. 2843-2849.
92. Franchitto, A. and P. Pichierri, *Bloom's syndrome protein is required for correct relocalization of RAD50/MRE11/NBS1 complex after replication fork arrest.* J. Cell Biol., 2002. **157**(1): p. 19-30.
93. Imamura, O., et al., *Werner and Bloom helicases are involved in DNA repair in a complementary fashion.* Oncogene, 2002. **21**(6): p. 954-963.
94. Wu, L. and I.D. Hickson, *The Bloom's syndrome helicase stimulates the activity of human topoisomerase IIIalpha.* Nucleic Acids Res, 2002. **30**(22): p. 4823-9.
95. Sengupta, S., et al., *BLM helicase-dependent transport of p53 to sites of stalled DNA replication forks modulates homologous recombination.* EMBO J., 2003. **22**: p. 1210-1222.

96. Wu, L. and I.D. Hickson, *The Bloom's syndrome helicase suppresses crossing over during homologous recombination.* Nature, 2003. **426**(6968): p. 870-874.
97. Cheok, C.F., et al., *The Bloom's syndrome helicase promotes the annealing of complementary single-stranded DNA.* Nucleic Acids Res., 2005. **33**(12): p. 3932-3941.
98. Rao, V.A., et al., *Phosphorylation of BLM, dissociation from topoisomerase IIIalpha, and colocalization with gamma-H2AX after topoisomerase I-induced replication damage.* Mol Cell Biol, 2005. **25**(20): p. 8925-37.
99. Shimura, T., et al., *Bloom's syndrome helicase and Mus81 are required to induce transient double-strand DNA breaks in response to DNA replication stress.* J Mol Biol, 2008. **375**(4): p. 1152-64.
100. Yamamoto, K., et al., *Fanconi anemia FANCG protein in mitigating radiation- and enzyme-induced DNA double-strand breaks by homologous recombination in vertebrate cells.* Mol. Cell. Biol., 2003. **23**: p. 5421-5430.
101. Larminat, F., et al., *Impairment of homologous recombination control in a Fanconi anemia-like Chinese hamster cell mutant.* Biol Cell, 2004. **96**(7): p. 545-52.
102. Niedzwiedz, W., et al., *The Fanconi anaemia gene FANCC promotes homologous recombination and error-prone DNA repair.* Mol Cell, 2004. **15**(4): p. 607-620.
103. Tischkowitz, M.D., et al., *Deletion and reduced expression of the Fanconi anemia FANCA gene in sporadic acute myeloid leukemia.* Leukemia, 2004. **18**: p. 420-425.
104. Howlett, N.G., et al., *The Fanconi anemia pathway is required for the DNA replication stress response and for the regulation of common fragile site stability.* Hum Mol Genet, 2005. **14**(5): p. 693-701.
105. Ohashi, A., et al., *Fanconi anemia complementation group D2 (FANCD2) functions independently of BRCA2- and RAD51-associated homologous recombination in response to DNA damage.* J. Biol. Chem., 2005. **280**(15): p. 14877-83.
106. Yang, Y.G., et al., *The Fanconi anemia group A protein modulates homologous repair of DNA double-strand breaks in mammalian cells.* Carcinogenesis, 2005. **26**(10): p. 1731-1740.
107. Hinz, J.M., et al., *The Fanconi anemia pathway limits the severity of mutagenesis.* DNA Repair (Amst), 2006. **5**(8): p. 875-84.
108. Ciccia, A., et al., *Identification of FAAP24, a Fanconi anemia core complex protein that interacts with FANCM.* Mol Cell, 2007. **25**(3): p. 331-43.
109. Mirchandani, K.D., R.M. McCaffrey, and A.D. D'Andrea, *The Fanconi anemia core complex is required for efficient point mutagenesis and Rev1 foci assembly.* DNA Repair (Amst), 2008. **7**(6): p. 902-11.

110. Sun, W., et al., *The FANCM ortholog Fml1 promotes recombination at stalled replication forks and limits crossing over during DNA double-strand break repair.* Mol Cell, 2008. **32**(1): p. 118-28.
111. Rothstein, R., B. Michel, and S. Gangloff, *Replication fork pausing and recombination or "gimme a break".* Genes Dev., 2000. **14**: p. 1-10.
112. Zheng, L., et al., *Disruption of the FEN-1/PCNA interaction results in DNA replication defects, pulmonary hypoplasia, pancytopenia, and newborn lethality in mice.* Mol Cell Biol, 2007. **27**(8): p. 3176-86.
113. Zou, Y., et al., *Functions of human replication protein A (RPA): from DNA replication to DNA damage and stress responses.* J. Cell. Physiol., 2006. **208**(2): p. 267-73.
114. Shimada, K., et al., *Ino80 chromatin remodeling complex promotes recovery of stalled replication forks.* Curr. Biol., 2008. **18**(8): p. 566-75.
115. Budzowska, M. and R. Kanaar, *Mechanisms of dealing with DNA damage-induced replication problems.* Cell Biochem. Biophys., 2009. **53**(1): p. 17-31.
116. Davies, S.L., P.S. North, and I.D. Hickson, *Role for BLM in replication-fork restart and suppression of origin firing after replicative stress.* Nat. Struct. Mol. Biol., 2007. **14**(7): p. 677-9.
117. Moldovan, G.L., B. Pfander, and S. Jentsch, *PCNA, the maestro of the replication fork.* Cell, 2007. **129**(4): p. 665-79.
118. Niimi, A., et al., *Regulation of proliferating cell nuclear antigen ubiquitination in mammalian cells.* Proc Natl Acad Sci U S A, 2008. **105**(42): p. 16125-30.
119. Cimprich, K.A. and D. Cortez, *ATR: an essential regulator of genome integrity.* Nat Rev Mol Cell Biol, 2008. **9**(8): p. 616-27.
120. McClendon, A.K., A.C. Rodriguez, and N. Osheroff, *Human topoisomerase IIalpha rapidly relaxes positively supercoiled DNA: implications for enzyme action ahead of replication forks.* J Biol Chem, 2005. **280**(47): p. 39337-45.
121. Wang, J.C., *Cellular roles of DNA topoisomerases: a molecular perspective.* Nat Rev Mol Cell Biol, 2002. **3**(6): p. 430-40.
122. Jiang, H.Y., et al., *Human cell DNA replication is mediated by a discrete multiprotein complex.* J Cell Biochem, 2002. **85**(4): p. 762-74.
123. Ward, I.M. and J. Chen, *Histone H2AX is phosphorylated in an ATR-dependent manner in response to replicational stress.* J. Biol. Chem., 2001. **276**(51): p. 47759-62.
124. Chanoux, R.A., et al., *ATR and H2AX cooperate in maintaining genome stability under replication stress.* J. Biol. Chem., 2008. **284**: p. 5994-6003.
125. Downey, M. and D. Durocher, *γH2AX as a checkpoint maintenance signal.* Cell Cycle, 2006. **5**(13): p. 1376-81.
126. Lundin, C., et al., *Different roles for nonhomologous end joining and homologous recombination following replication arrest in mammalian cells.* Mol. Cell. Biol., 2002. **22**(16): p. 5869-78.

127. Sharan, S.K., et al., *Embryonic lethality and radiation hypersensitivity mediated by Rad51 in mice lacking Brca2.* Nature, 1997. **386**: p. 804-810.
128. Lieber, M.R., et al., *Flexibility in the order of action and in the enzymology of the nuclease, polymerases, and ligase of vertebrate non-homologous DNA end joining: relevance to cancer, aging, and the immune system.* Cell Res, 2008. **18**(1): p. 125-33.
129. Wang, M., et al., *PARP-1 and Ku compete for repair of DNA double strand breaks by distinct NHEJ pathways.* Nucleic Acids Res, 2006. **34**(21): p. 6170-82.
130. Shimura, T., et al., *DNA-PK is involved in repairing a transient surge of DNA breaks induced by deceleration of DNA replication.* J Mol Biol, 2007. **367**(3): p. 665-80.
131. Miyoshi, T., J. Kanoh, and F. Ishikawa, *Fission yeast Ku protein is required for recovery from DNA replication stress.* Genes Cells, 2009. **14**(9): p. 1091-103.
132. Bryant, H.E., et al., *PARP is activated at stalled forks to mediate Mre11-dependent replication restart and recombination.* Embo J, 2009. **28**(17): p. 2601-15.
133. Robertson, H.M. and K.L. Zumpano, *Molecular evolution of an ancient mariner transposon, Hsmar1, in the human genome.* Gene, 1997. **205**(1-2): p. 203-17.
134. Cordaux, R., et al., *Birth of a chimeric primate gene by capture of the transposase gene from a mobile element.* Proc. Natl. Acad. Sci. USA, 2006. **103**: p. 8101-8106.
135. Liu, D., et al., *The human SETMAR protein preserves most of the activities of the ancestral Hsmar1 transposase.* Mol Cell Biol, 2007. **27**(3): p. 1125-32.
136. Hiom, K., M. Melek, and M. Gellert, *DNA transposition by the RAG1 and RAG2 proteins: a possible source of oncogenic translocations.* Cell, 1998. **94**(4): p. 463-70.
137. Miskey, C., et al., *The ancient mariner sails again: transposition of the human Hsmar1 element by a reconstructed transposase and activities of the SETMAR protein on transposon ends.* Mol Cell Biol, 2007. **27**(12): p. 4589-600.
138. Roman, Y., et al., *Biochemical characterization of a SET and transposase fusion protein, Metnase: its DNA binding and DNA cleavage activity.* Biochemistry, 2007. **46**(40): p. 11369-76.
139. Lee, S.H., et al., *The SET domain protein Metnase mediates foreign DNA integration and links integration to nonhomologous end-joining repair.* Proc. Natl. Acad. Sci. USA, 2005. **102**(50): p. 18075-80.
140. Williamson, E.A., et al., *Expression levels of the human DNA repair protein metnase influence lentiviral genomic integration.* Biochimie, 2008. **90**(9): p. 1422-6.
141. Zhang, X., et al., *Structural basis for the product specificity of histone lysine methyltransferases.* Mol Cell, 2003. **12**(1): p. 177-85.

142. Rea, S., et al., *Regulation of chromatin structure by site-specific histone H3 methyltransferases.* Nature, 2000. **406**(6796): p. 593-9.
143. Nakamura, T., et al., *ALL-1 is a histone methyltransferase that assembles a supercomplex of proteins involved in transcriptional regulation.* Mol Cell, 2002. **10**(5): p. 1119-28.
144. Xiao, T., et al., *Phosphorylation of RNA polymerase II CTD regulates H3 methylation in yeast.* Genes Dev., 2003. **17**: p. 654-663.
145. Krogan, N.J., et al., *Methylation of histone H3 by Set2 in Saccharomyces cerevisiae is linked to transcriptional elongation by RNA polymerase II.* Mol Cell Biol, 2003. **23**(12): p. 4207-18.
146. Williamson, E.A., et al., *The SET and transposase domain protein Metnase enhances chromosome decatenation: regulation by automethylation.* Nucleic Acids Res, 2008.
147. Wray, J., et al., *Metnase mediates resistance to topoisomerase II inhibitors in breast cancer cells.* PLoS One, 2009. **4**(4): p. e5323.
148. Wray, J., et al., *Metnase mediates chromosome decatenation in acute leukemia cells.* Blood, 2009. **114**(9): p. 1852-8.
149. Beck, B.D., et al., *Human Pso4 is a metnase (SETMAR)-binding partner that regulates metnase function in DNA repair.* J Biol Chem, 2008. **283**(14): p. 9023-30.
150. Hromas, R., et al., *The human set and transposase domain protein Metnase interacts with DNA Ligase IV and enhances the efficiency and accuracy of non-homologous end-joining.* DNA Repair (Amst), 2008.
151. Sandoval, J.A., R.J. Hickey, and L.H. Malkas, *Isolation and characterization of a DNA synthesome from a neuroblastoma cell line.* J Pediatr Surg, 2005. **40**(7): p. 1070-7.
152. Golding, S.E., et al., *Double strand break repair by homologous recombination is regulated by cell cycle-independent signaling via ATM in human glioma cells.* J. Biol. Chem., 2004. **279**(15): p. 15402-15410.
153. Anglana, M. and S. Bacchetti, *Construction of a recombinant adenovirus for efficient delivery of the I-SceI yeast endonuclease to human cells and its application in the in vivo cleavage of chromosomes to expose new potential telomeres.* Nucleic Acids Research, 1999. **27**(#21): p. 4276-4281.
154. Valerie, K., et al., *Improved radiosensitization of rat glioma cells with adenovirus-expressed mutant herpes simplex virus-thymidine kinase in combination with acyclovir.* Cancer Gene Ther, 2000. **7**(6): p. 879-84.
155. Liu, J., et al., *Inhibition of breast and brain cancer cell growth by BCCIPα, an evolutionarily conserved nuclear protein that interacts with BRCA2.* Oncogene, 2001. **20**: p. 336-45.
156. Miller, E.M., et al., *Mismatch repair by efficient nick-directed, and less efficient mismatch-specific mechanisms in homologous recombination intermediates in Chinese hamster ovary cells.* Genetics, 1997. **147**: p. 743-753.

157. Brenneman, M.A., et al., *XRCC3 is required for efficient repair of chromosome breaks by homologous recombination.* Mutat. Res., 2000. **459**: p. 89-97.
158. Allen, C., et al., *DNA-dependent protein kinase suppresses double-strand break-induced and spontaneous homologous recombination.* Proc. Natl. Acad. Sci. USA, 2002. **99**: p. 3758-3763.
159. Taghian, D.G. and J.A. Nickoloff, *Chromosomal double-strand breaks induce gene conversion at high frequency in mammalian cells.* Mol. Cell. Biol., 1997. **17**: p. 6386-6393.
160. Bergelson, J.M., et al., *Isolation of a common receptor for Coxsackie B viruses and adenoviruses 2 and 5.* Science, 1997. **275**(5304): p. 1320-3.
161. Parra, I. and B. Windle, *High resolution visual mapping of stretched DNA by fluorescent hybridization.* Nat Genet, 1993. **5**(1): p. 17-21.
162. Merrick, C.J., D. Jackson, and J.F. Diffley, *Visualization of altered replication dynamics after DNA damage in human cells.* J Biol Chem, 2004. **279**(19): p. 20067-75.
163. Seiler, J.A., et al., *The intra-S-phase checkpoint affects both DNA replication initiation and elongation: single-cell and -DNA fiber analyses.* Mol Cell Biol, 2007. **27**(16): p. 5806-18.
164. Arnaudeau, C., et al., *Inhibition of DNA synthesis is a potent mechanism by which cytostatic drugs induce homologous recombination in mammalian cells.* Mutat. Res., 2000. **461**: p. 221-228.
165. Arnaudeau, C., C. Lundin, and T. Helleday, *DNA double-strand breaks associated with replication forks are predominantly repaired by homologous recombination involving an exchange mechanism in mammalian cells.* J. Mol. Biol., 2001. **307**(5): p. 1235-1245.
166. Shao, R.G., et al., *Replication-mediated DNA damage by camptothecin induces phosphorylation of RPA by DNA-dependent protein kinase and dissociates RPA:DNA-PK complexes.* EMBO J., 1999. **18**: p. 1397-1406.
167. Liu, Q., et al., *Chk1 is an essential kinase that is regulated by Atr and required for the G(2)/M DNA damage checkpoint.* Genes Dev, 2000. **14**(12): p. 1448-59.
168. Zhao, H. and H. Piwnica-Worms, *ATR-mediated checkpoint pathways regulate phosphorylation and activation of human Chk1.* Mol Cell Biol, 2001. **21**(13): p. 4129-39.
169. Jiang, K., et al., *Regulation of Chk1 includes chromatin association and 14-3-3 binding following phosphorylation on Ser-345.* J Biol Chem, 2003. **278**(27): p. 25207-17.
170. Martin, S.A. and T. Ouchi, *Cellular commitment to reentry into the cell cycle after stalled DNA is determined by site-specific phosphorylation of Chk1 and PTEN.* Mol Cancer Ther, 2008. **7**(8): p. 2509-16.
171. Schwartz, M., et al., *Impaired replication stress response in cells from immunodeficiency patients carrying Cernunnos/XLF mutations.* PLoS One, 2009. **4**(2): p. e4516.

172. Shrivastav, M., et al., *DNA-PKcs and ATM co-regulate DNA double-strand break repair.* DNA Repair (Amst), 2009. **8**(8): p. 920-9.
173. Forsburg, S.L., *The MCM helicase: linking checkpoints to the replication fork.* Biochem. Soc. Trans., 2008. **36**(Pt 1): p. 114-9.
174. Bailis, J.M., et al., *Minichromosome maintenance proteins interact with checkpoint and recombination proteins to promote s-phase genome stability.* Mol Cell Biol, 2008. **28**(5): p. 1724-38.
175. Bryant, H.E., et al., *Specific killing of BRCA2-deficient tumours with inhibitors of poly(ADP-ribose) polymerase.* Nature, 2005. **434**(7035): p. 913-917.
176. Farmer, H., et al., *Targeting the DNA repair defect in BRCA mutant cells as a therapeutic strategy.* Nature, 2005. **434**(7035): p. 917-921.
177. Frouin, I., et al., *Human proliferating cell nuclear antigen, poly(ADP-ribose) polymerase-1, and p21waf1/cip1. A dynamic exchange of partners.* J Biol Chem, 2003. **278**(41): p. 39265-8.
178. Chuang, L.S., et al., *Human DNA-(cytosine-5) methyltransferase-PCNA complex as a target for p21WAF1.* Science, 1997. **277**(5334): p. 1996-2000.
179. Kedar, P.S., et al., *Direct interaction between mammalian DNA polymerase beta and proliferating cell nuclear antigen.* J Biol Chem, 2002. **277**(34): p. 31115-23.
180. Ducoux, M., et al., *Mediation of proliferating cell nuclear antigen (PCNA)-dependent DNA replication through a conserved p21(Cip1)-like PCNA-binding motif present in the third subunit of human DNA polymerase delta.* J Biol Chem, 2001. **276**(52): p. 49258-66.
181. Parker, A., et al., *Human homolog of the MutY repair protein (hMYH) physically interacts with proteins involved in long patch DNA base excision repair.* J Biol Chem, 2001. **276**(8): p. 5547-55.
182. Otterlei, M., et al., *Post-replicative base excision repair in replication foci.* Embo J, 1999. **18**(13): p. 3834-44.
183. Gary, R., et al., *The DNA repair endonuclease XPG binds to proliferating cell nuclear antigen (PCNA) and shares sequence elements with the PCNA-binding regions of FEN-1 and cyclin-dependent kinase inhibitor p21.* J Biol Chem, 1997. **272**(39): p. 24522-9.
184. Kanagaraj, R., et al., *Human RECQ5beta helicase promotes strand exchange on synthetic DNA structures resembling a stalled replication fork.* Nucleic Acids Res, 2006. **34**(18): p. 5217-31.
185. Yu, P., et al., *p15(PAF), a novel PCNA associated factor with increased expression in tumor tissues.* Oncogene, 2001. **20**(4): p. 484-9.
186. Scott, M., et al., *UV-induced binding of ING1 to PCNA regulates the induction of apoptosis.* J Cell Sci, 2001. **114**(Pt 19): p. 3455-62.
187. Banks, D., et al., *L2DTL/CDT2 and PCNA interact with p53 and regulate p53 polyubiquitination and protein stability through MDM2 and CUL4A/DDB1 complexes.* Cell Cycle, 2006. **5**(15): p. 1719-29.

188. Poot, R.A., et al., *The Williams syndrome transcription factor interacts with PCNA to target chromatin remodelling by ISWI to replication foci.* Nat Cell Biol, 2004. **6**(12): p. 1236-44.